Movement, Migration, and Melody: An interdisciplinary study of juvenile salmon ecology through otolith chemistry

A Dissertation
Presented in Partial Fulfillment of the Requirements for the
Degree of Doctor of Philosophy
with a
Major in Water Resources – Science & Management Option
in the
College of Graduate Studies
University of Idaho
by
Jensen C. Hegg

Major Professor: Brian P. Kennedy, Ph.D.
Committee Members: Elizabeth Cassel, Ph.D.; William Connor, Ph.D.;
Richard Zabel, Ph.D.
Department Administrator: Robert Heinse, Ph.D.

December 2017

Authorization to Submit Dissertation

This dissertation of Jensen C. Hegg, submitted for the degree of Doctor of Philosophy with a Major in Water Resources – Science & Management Option and titled “Movement, Migration, and Melody: An interdisciplinary study of juvenile salmon ecology through otolith chemistry," has been reviewed in final form. Permission, as indicated by the signatures and dates below, is now granted to submit final copies to the College of Graduate Studies for approval.

Major Professor: _____ Date: _____
Brian P. Kennedy

Committee Members: _____ Date: _____
Elizabeth J. Cassel

_____ Date: _____
William P. Connor

_____ Date: _____
Richard W. Zabel

Department Administrator:_____ Date: _____
Robert Heinse

Abstract

The movement of animals has important ecological consequences from the scale of the individual to the ecosystem. As populations move they exert important impacts on the ecology of the ecosystems they inhabit. Ultimately, the migratory movement of populations and the resulting large-scale effects are based on the movement of individuals, which are often influenced by conditions experienced at the individual scale. Understanding the relationship of individual movements to the temporal and spatial variation of conditions across the landscape, provides important insights on the ecology of populations. This dissertation focuses on the ecology of movement in juvenile fish populations using otolith microchemistry, the recovery of trace chemistry from the balance organs of fish, as an ecological tool to link detailed fish movement with population processes. The first chapter introduces the combined use of $^{87}Sr/^{86}Sr$ in otoliths, and the prediction of $^{87}Sr/^{86}Sr$ variation using geologic maps, to reconstruct the movements of goliath catfish in the Amazon basin, a species which undertake the longest freshwater migration on earth and whose migrations are poorly understood due to their scale and remote location. The remaining chapters focus on Snake River fall Chinook salmon, examining changes in the timing of juvenile outmigration which may be evolving due to environmental and anthropogenic influences. Chapter 2 examines the complexities in interpreting the transition from maternally derived to environmentally derived otolith chemistry in young juvenile salmon. Chapter 3 introduces a novel time-series statistical method to analyze fish movement, and compares it to a more standard multi-tracer approach. Chapter 4 combines the analysis methods from the prior chapters to build a mixed-effect model relating size at ocean entry to the effects of location, environment, and growth at multiple juvenile stages using a ten-year sample of returning adult salmon otoliths. Chapter 5 details the results of a collaborative, interdisciplinary experiment to test the preliminary use of data-to-sound sonification as a method for exploring otolith datasets.

Acknowledgements

Thanks to Dr. Brian Kennedy, and members of his Center for Integrative Fish Ecology and Ecosystem Studies lab for invaluable help in shaping this study. In particular Ellen Hamann, Emily Benson, Sam Bourret, and Jeff Reader provided a tremendous amount of time and effort in method development, and sample analysis.

This project would not have been possible without the lab undergraduates. Anna Miera deserves huge praise for her work in organizing the otolith database. Scott Bumpus and Earl Beasley provided critical early help. Kate Wilcox, Josie Greenwood, Avery King and Brandon Carman provided invaluable work on ICPMS data reduction.

In order of appearance, not importance; Rick Hartson, Chau Tran, Marius Myrvold, Bryce Oldemeyer, Jeff Caisman, Natasha Wingerter, Kat Gillies-Rector, and Austin Anderson all contributed work, and intellectual input, in framing this project.

Thanks to Paul Chittaro and Rich Zabel for their collaboration, as well as Debbie Milks, Billy Connor, Ken Tiffan, and Bill Arnsberg for their willingness to share their immense knowledge of Snake River fall Chinook salmon.

Thanks to Jeff Vervoort, Garrett Hart, and Charles Knaack in the Peter Hooper Geoanalytical Lab at Washington State University for their help in method development and keeping the machines running. Thanks to Scott Boroughs for his sharp eyes that saved a major portion of the final chapter.

Thanks to Alex Fremier and Jan Boll for their encouragement both to pursue work abroad as well as towards even greater interdisciplinarity. Thanks also to Jonathan Middleton and Ben Robertson for their musical collaboration, and immense knowledge base, in creating a compelling final chapter.

Funding for this research came from multiple sources including National Oceanic and Atmospheric Administration, Bonneville Power Association, National Science Foundation, U.S Geological Survey, and IBEST and the College of Natural Resources at University of Idaho. Thanks to One World Café for the office space and support of my habit, and my officemate Paul Anders for conversation and perspective.

Dedication

In memory of Robert Y. Tuttle, who embodied quiet perseverance
and problem solving,
usually only cussed in private,
and was a role model for me in this process
and in life.

In memory of Edith Hegg and Rev. Theodore Hegg,
who I'm sure would have been proud.

My son Berlyn Hegg, whose invitations to play
were most often respites and not distractions.

My wife Katie Cooper, who has supported me
with a surety I didn't always feel myself.

My parents Nancy and Mark Hegg,
who sacrificed to help me start this process
on the right foot.

My grandmother Doris Tuttle, whose help was invaluable at the start.
A woman who has always cut straight to the point,
she told me not to get married before I finished;
advice I promptly ignored,
which she hasn't seemed to mind.

Table of Contents

List of Tables

List of Figures

Chapter 1: Diverse Early Life-History Strategies in Migratory Amazonian Catfish: Implications for Conservation and Management

Published as:

Hegg, J. C., T. Giarrizzo, and B. P. Kennedy. 2015. Diverse Early Life-History Strategies in Migratory Amazonian Catfish: Implications for Conservation and Management. Plos One 10. DOI: 10.1371/journal.pone.0129697 (Creative Commons CC BY 4.0 Open Access)

Abstract

Animal migrations provide important ecological functions and can allow for increased biodiversity through habitat and niche diversification. However, aquatic migrations in general, and those of the world's largest fish in particular, are imperiled worldwide and are often poorly understood. Several species of large Amazonian catfish carry out some of the longest freshwater fish migrations in the world, travelling from the Amazon River estuary to the Andes foothills. These species are important apex predators in the main stem rivers of the Amazon Basin and make up the regions largest fishery. They are also the only species to utilize the entire Amazon Basin to complete their life cycle. Studies indicate both that the fisheries may be declining due to overfishing, and that the proposed and completed dams in their upstream range threaten spawning migrations. Despite this, surprisingly little is known about the details of these species' migrations, or their life history. Otolith microchemistry has been an effective method for quantifying and reconstructing fish migrations worldwide across multiple spatial scales and may provide a powerful tool to understand the movements of Amazonian migratory catfish. Our objective was to describe the migratory behaviors of the three most populous and commercially important migratory catfish species, Dourada (*Brachyplatystoma rousseauxii*), Piramutaba

(*Brachyplatystoma vaillantii*), and Piraíba (*Brachyplatystoma filamentosum*). We collected fish from the mouth of the Amazon River and the Central Amazon and used strontium isotope signatures ($^{87}Sr/^{86}Sr$) recorded in their otoliths to determine the location of early rearing and subsequent. Fish location was determined through discriminant function classification, using water chemistry data from the literature as a training set. Where water chemistry data was unavailable, we successfully in predicted $^{87}Sr/^{86}Sr$ isotope values using a regression-based approach that related the geology of the upstream watershed to the Sr isotope ratio. Our results provide the first reported otolith microchemical reconstruction of *Brachyplatystoma* migratory movements in the Amazon Basin. Our results indicate that juveniles exhibit diverse rearing strategies, rearing in both upstream and estuary environments. This contrasts with the prevailing understanding that juveniles rear in the estuary before migrating upstream; however it is supported by some fisheries data that has indicated the presence of alternate spawning and rearing life-histories. The presence of alternate juvenile rearing strategies may have important implications for conservation and management of the fisheries in the region.

Introduction

Animal migration provides many important ecological functions: they can be a stabilizing strategy in seasonal environments; offer transitory habitats for large populations; often transport materials across ecosystem boundaries; and may increase a regions biodiversity (Bauer and Hoye 2014). Large-scale migrations shed light on ecosystem connectivity across scales and can be used as a lens to understand broader behavioral responses to the environment and links to physical processes (Poiani et al. 2000, Webster et al. 2002, Bowlin et al. 2010). However, migrations worldwide are under threat from the alteration of migratory pathways, habitat loss, climatic changes and anthropogenic changes to the landscape (Wilcove and Wikelski 2008). In aquatic systems, changes in upstream land use and the placement of dams have had significant impacts on ecosystems and migrations worldwide (Rosenberg et al. 2000, Freeman

2003, Foley et al. 2005, Dudgeon et al. 2006, Tockner et al. 2011, Carpenter et al. 2011). This is particularly true for large migratory fish that are under threat in many of the world's largest river systems (Allan et al. 2005, Pikitch et al. 2005, Stone 2007). Despite this, many large migratory fish species are not well understood (Stone 2007).

Globally, dams and water resources challenges in the two largest rivers in China provide an example of the ongoing changes to large rivers and their effects on aquatic species, including sturgeon and paddlefish (Dudgeon 2011). In South America, transnational river systems and a lack of coordinated research of aquatic systems may result in losses to unspecified levels of biodiversity (Fearnside 2006, 2014, Finer and Jenkins 2012, Tavener 2012, Forero 2013). New dams present a unique challenge to migratory fish in the region. Because the young of many Amazonian species undergo a drifting larval stage, even if adults can pass above dams the lack of flow in reservoirs creates a barrier that drifting juveniles are unable to surmount on their way downstream (Pompeu et al. 2012).

Several species of Amazonian catfish in the genus *Brachyplatystoma* carry out some of the longest freshwater fish migrations in the world, travelling over 4,500 km from rearing areas in the Amazon estuary to spawning grounds in rivers in the foothills of the Andes (Barthem and Goulding 1997, Fabré and Barthem 2005, Petrere et al. 2005). These species largely inhabit whitewater and clearwater rivers (river classifications from Sioli (1956)) within the Amazon Basin (Junk et al. 2011), with rare reports in tannic blackwater rivers (Barthem and Goulding 1997). These catfish species are the only known organisms, terrestrial or aquatic, that require the entire length of the Amazon basin to complete their life cycle (Barthem and Goulding 1997). They are also one of the few apex predators in the pelagic and demersal zones of the largest Amazonian rivers, playing an important role in trophic dynamics and ecosystem functioning within the entire basin (Angelini et al. 2006). However, evidence indicates that the fisheries for the most populous species are in decline, potentially due to overfishing (Petrere et al. 2005, Córdoba et al. 2013). The reliance of these species on

headwater streams for spawning leaves adults and larva vulnerable to blocking of their migration paths by dams and their reservoirs (Barthem et al. 1991, Pompeu et al. 2012).

Surprisingly little is known about the life history of migratory Amazonian catfish given that the three most abundant *Brachyplatystoma* taxa support the largest fisheries in the Amazon Basin (Barthem and Goulding 1997, Fabré and Barthem 2005). Dourada (*Brachyplatystoma rousseauxii*) is a pelagic predator found throughout the whitewater and clearwater rivers of the Amazon and supports the largest fishery in the Amazon (Barthem et al. 1991, Angelini et al. 2006). Piramutaba (*Brachyplatystoma vaillantii*) make up a second large export fishery and are found almost exclusively in the Amazon River mainstem, whitewater tributaries, and the estuary (Godoy 1979, Barthem and Petrere Jr 1995, Jimenez et al. 2013). Piraíba (*Brachyplatystoma filamentosum*) is the largest of the migratory catfish, present in whitewater rivers throughout the Amazon basin. It is also the most locally exploited and least understood of these three species (Petrere et al. 2005). The expansive scale of the Amazon Basin, and the large size of the rivers these fish inhabit, have made tracking and reconstructing their movements very difficult (Godoy 1979). Our current understanding of the migratory behavior of migratory Amazonian catfish is based on fishing records (including the catch timing and size of fish across the Amazon basin) and a growing number of scientific sampling efforts (Barthem and Petrere Jr 1995, Barthem and Goulding 1997, Agudelo et al. 2000, Alonso and Fabré 2002, Pirker 2008, García Vásquez et al. 2009, Córdoba et al. 2013). After hatching in the upper reaches of the whitewater rivers originating in the Andes, larvae of these species drift downstream for two to four weeks before reaching the Amazon estuary. Juveniles rear in the estuary before commencing an upstream migration that coincides with the seasonal flood pulse. Genetic data indicate that dourada may home to natal tributaries in the basin to spawn (Batista and Alves-Gomes 2006, Carvajal 2013).

Otolith microchemistry has been an effective method for quantifying and reconstructing fish migrations worldwide across multiple spatial scales (Campana and Thorrold 2001, Kennedy et al. 2002, Hogan et al. 2007, Walther et al. 2011, Hamann

and Kennedy 2012, Hegg et al. 2013a, Collins et al. 2013, Garcez 2014). Strontium isotope ratio in particular has become a powerful tool for determining movement and location because it is not fractionated biologically. Thus, the signatures recorded in otoliths match the water through which fish pass (Kennedy et al. 1997, 2000, 2002, Barnett-Johnson et al. 2008, Hobson et al. 2010). Studies of geological weathering throughout the Amazon basin have provided detailed, multi-year records of micro-chemical and isotopic chemistry in the largest rivers of the basin. These data provide the required background sampling necessary to tie regional otolith signatures to geographic location (Gaillardet et al. 1997, Queiroz et al. 2009, Santos et al. 2013) (Fig 1A, Table 1). Recent studies have also shown the feasibility of predicting $^{87}Sr/^{86}Sr$ signatures of unknown watersheds using the geologic makeup of the basin, allowing researchers to characterize strontium signatures of unsampled areas (Bataille and Bowen 2012, Hegg et al. 2013a). These advances point to otolith microchemistry as a potentially powerful tool to understand the movements of Amazonian migratory catfish.

Our objective was to describe the migratory behaviors of large, migratory catfish in the Amazon River basin using otolith microchemistry. We focused our study on the three most populous and commercially important species in the Amazon Basin. We sought to determine the location of early rearing and subsequent movement in dourada, pirimutaba, and piraíba using samples collected from two, large fish markets at the mouth of the Amazon River and in the central Amazon. We determined the movement patterns over the lifetime of individual fish using laser ablation isotope mass spectrometry of their otoliths. Areas of stable signature were identified statistically throughout the chemical profile of the otolith, which were then classified to their location within the basin using discriminant function analysis. The discriminant function was created using a training set of $^{87}Sr/^{86}Sr$ samples from rivers throughout the Amazon basin. These samples were obtained from the geological literature. Where river $^{87}Sr/^{86}Sr$ values were unknown, we used established

relationships between surface water $^{87}Sr/^{86}Sr$ values and the age and composition of the underlying watershed geology to predict these signatures.

Ethical statement

Ethical approval was not required for this study, as all fish were collected as part of routine fishing procedures. Fish were sacrificed by the artisanal fishermen in Manaus and Belém using standard fisheries practices and donated to the authors.

No field permits were required to collect any samples from any location, since all samples derived from commercial catch. None of the species included in this investigation are currently protected or endangered. Therefore, no additional special permits were necessary. Permission to export the otolith samples was granted by the Brazilian Government with permit number: 116217 (MMA, IBAMA, CITES 09/01/2013).

Methods

Otolith Collection

In March 2012, a total of 24 paired lapillus otolith samples (16 pairs for dourada, 5 for piramutaba and 3 for piraíba) were collected from the two major fishing ports of Brazilian Amazonia, the cities of Manaus and Belém (Table 1 and Fig 1A). These cities are located 1,606 river kilometers apart. Manaus (03°05'39.60''S, 60°01'33.63''W), is the largest city in the central Amazon, located at the confluence of the whitewater Solimões River with the blackwater Negro River. Belém (01°27'18.04''S 48°30'08.90''W), is situated on the banks of the Amazon estuary and is the main landing port of large migratory catfishes fisheries in Brazil (Jimenez et al. 2013). Prior to otolith collection the total length (TL) and weight (W) of each fish was recorded: dourada: mean TL = 83.6 cm, mean W = 8.58 kg; piramutaba: mean TL = 67.6 cm, mean W = 3.34 kg; piraíba: mean TL =186.6 cm, mean W = 86.6 kg. Piramutaba were gutted prior to collection so weight was estimated using a length-to-weight ratio from Pirker (2001).

Fish collected from Manaus were captured in the mainstem Amazon River between the mouth of the Madeira River and Manaus as reported by the fisherman. Thus, we would expect the chemical signatures representing the end of the fish's life (signatures from the edge of the otolith) of fish caught in Manaus to represent signatures in the mainstem Amazon River or its tributaries upstream of the Madeira River. Fish collected in Belém were captured in the estuary between 60 km and 150 km from Belém according to the fisherman. The otolith edge chemistry of fish caught in Belém are therefore assumed to match the signature of the estuary, the lower Amazon tributaries, or the lower Amazon River mainstem. Because the $^{87}Sr/^{86}Sr$ signature can take days to weeks to equilibrate and accumulate enough material to reliably sample, it is possible that fish could exhibit signatures other than the location of capture if they had recently moved from a habitat with a different signature.

Otolith Analysis

The left lapillus otolith from each sample was prepared using standard methods of mounting, transverse sectioning with a high precision saw, and abrasive polishing to reveal the rings (Secor et al. 1991a, Pirker 2008) (Fig 2). If the left otolith was missing or unavailable the right otolith was used for analysis. Otoliths were then analyzed at the GeoAnalytical Laboratory at Washington State University using a Finnigan Neptune (ThermoScientific) multi-collector inductively coupled plasma mass spectrometer coupled with a New Wave UP-213 laser ablation sampling system (LA-MC-ICPMS). We used a marine shell standard to evaluate measurement error relative to the global marine signature of 0.70918 (Faure and Mensing 2004). Repeated analyses of a marine shell signature provided an average $^{87}Sr/^{86}Sr$ value of 0.70914 during the course of the study (N=22, St. Error=0.00002). The laser was used to ablate a sampling transect from the core of the otolith section to the edge (30 μm/s scan speed, 40 μm spot size, 0.262 s integration speed, ~7 J/cm). This resulted in a continuous time-series of $^{87}Sr/^{86}Sr$ data from the birth of the fish (core) to its death (edge) which was used for subsequent analysis. For more detailed methods see Hegg et. al (2013a). The asteriscus was used for one sample for which the lapilli were not

available; however, the strontium concentration was low and the unreliable results were not included.

Baseline Water Sampling and Prediction

Twenty-four water sampling points located throughout the Amazon River basin (Fig 1A) from three published studies provided baseline $^{87}Sr/^{86}Sr$ values for our study (Table 2 and Fig 3). Santos et al. (2013) provided thirteen samples from the Ore-HYBAM project (www.ore-hybam.org), a multi-year research effort with a comprehensive sampling design covering the mainstem Amazon River and all of the major tributaries above Obidos, Brazil. Nine additional samples from Gaillardet et al. (1997) covered the mainstem Amazon and the mouths of the major tributaries as far east as Santarem, Brazil. Finally, Queiroz et al. (2009) provided two samples from the Lower Solimões and Upper Purus Rivers. Our intention was to include samples that represented all major Amazon tributaries at a regional scale, while excluding smaller tributaries that were unlikely to provide long-term habitat for our study species. Smaller tributaries in the Amazon Basin have been shown to exhibit much different isotopic chemistry from their mainstem rivers (Queiroz et al. 2009). The scale and geologic heterogeneity of these smaller tributaries could jeopardize assignment accuracy (Hegg et al. 2013b).

The isotopic chemistry of a few significant locations were not available in the literature. Notably missing were samples from the mouth of the Amazon River, its tributaries below Obidos, and the Tocantins River which contributes to the estuary habitat of our study species. To account for the $^{87}Sr/^{86}Sr$ of these locations we used the relationship between the geologic makeup of a watershed and its $^{87}Sr/^{86}Sr$ signature to predict these points, following a similar regression approach to Hegg et al. (2013b). Watersheds were delineated in qGIS (http://www.qgis.org), an open-source geographic information system, using the GRASS analysis plugin, which contains advanced watershed analysis tools from the open-source GRASS GIS platform (http://grass.osgeo.org). All analysis layers were procured from open-access datasets. Water sampling points were manually digitized by the authors based on location

descriptions from Santos et al. (2013), Gaillardet et al. (1997), and Queiroz et al. (Queiroz et al. 2009). Topography layers were taken from the GTOPO30 dataset (USGS 1996) and stream courses from the HydroSHED dataset (Lehner et al. 2008). Geologic information came from the World Energy Assessment Geologic Map of the Amazon Region (USGS 1999).

We used geologic age as the primary candidate independent variables in our regression to predict the $^{87}Sr/^{86}Sr$ signatures for unsampled tributaries, along with very general intrusive and extrusive rock-type categories (Fig 1B). Our methods differed from Hegg et al. (2013b), who used rock type as the primary explanatory variable rather than age. We did this because the very generic designations of intrusive or extrusive rock available in our dataset were insufficient to provide explanatory power. The values for these candidate variables were calculated by converting the geologic age codes from the map attribute table to continuous variables using the mean age (Ma) of the geologic periods encompassed by each code using the International Chronostratigraphic Chart (Cohen et al. 2013). The percentage area of each rock age and type was then calculated within the watershed upstream of each $^{87}Sr/^{86}Sr$ sample point. The mean age of each watershed, weighted by area, was also included as a potential explanatory variable for the regression, leaving twenty-four potential explanatory variables for the regression.

Model selection used a genetic algorithm selection procedure in the {glmulti} package for R (Calcagno and Mazancourt 2010). We limited models to four terms to limit the number of potential models and included interaction terms. The genetic algorithm uses a search algorithm based on Darwinian natural selection, an efficient method for model optimization when the number of potential models is large, as was the case with our geologic data (Tang et al. 1996). Akaike's Information Criterion optimized for small datasets (AICc) was used as the optimization criteria for the genetic algorithm, a criterion that penalizes over-parameterization (Burnham and Anderson 2002). One third of the sample points were randomly selected as a validation set, withheld from the model selection procedure, and used to assess

prediction accuracy of the best model. The best model was then used to calculate the $^{87}Sr/^{86}Sr$ values for the unsampled points in the basin, using the geology upstream of these points.

Grouping of Distinguishable Watersheds

The water sample points were grouped into three distinguishable geographic regions using prior knowledge of the geography and geology of the watersheds (Table 1, Fig 1A, Fig 3). River basins that were geographically contiguous and broadly geologically and chemically similar were grouped. The Amazon River mainstem and western tributaries, all considered whitewater rivers (Junk et al. 2011), were grouped together due to the overwhelming influence of the Andes on their chemistry. The Beni-Madeira River and lower Negro River were grouped due to similar chemical signatures from a mix of upland mountainous geology and old, lowland, Amazon and Guyana shield geology. The Negro River, being blackwater, would not be expected to contain large numbers of our target species, while the whitewater Madeira is a known fishery (Barthem and Goulding 1997, Junk et al. 2011). The lower Amazon tributaries (below the Madeira River) were grouped due to the their similarly old, shield geologies resulting in high $^{87}Sr/^{86}Sr$ values. These rivers are all considered clearwater tributaries (Junk et al. 2011). These group assignments were then used as the training set, with $^{87}Sr/^{86}Sr$ as the predictor and group as the response, to create a quadratic discriminant function. This discriminant function was then used in the following section to classify the $^{87}Sr/^{86}Sr$ signatures recovered from fish otoliths to these three distinguishable river groups.

Determining Fish Movement and Location

The transect of $^{87}Sr/^{86}Sr$ values from the core to the rim of each otolith was analyzed using a PELT algorithm changepoint analysis (using the {changepoint} package in R (Killick and Eckley 2013)) to determine when the mean $^{87}Sr/^{86}Sr$ values changed to a new stable signature. This changepoint algorithm generated mean values and starting points for each stable region within the otolith transect using a penalty

value of 0.0001 (Killick et al. 2012). Each stable signature was assumed to correspond to movement into a new river signature, with the first stable signature corresponding to early rearing. In some cases the changepoint algorithm returned erroneous means for small portions of the signature, in locations were the means was obviously unstable. Such fragments were manually removed.

Stable otolith signatures were then classified to their likely location using the discriminant function developed from known and predicted water sampling points in the prior section. Because *a priori* probability of group membership was unknown, the prior probabilities for the discriminant function were set to be equal among groups. After classification, the results were plotted and the data were assessed to determine trends in early rearing and movement both within and among the three sampled species.

Results

Baseline Water Sampling and Prediction

The most parsimonious model without interaction terms explained ~80% of the variation in the data but provided an unreasonably high prediction for the mouth of the Amazon River. We had no direct evidence of significant interactions between geologic variables on strontium isotope ratio; however, we included interactions in a second model selection exercise in hopes of finding a parsimonious model that better fit the available data. We limited the maximum number of model terms to four to limit the number of potential models available from the twenty-four available variables plus interactions. This limit is reasonable since more terms would risk over parameterization given the number of observations used to build the model. Under these conditions the AICc model-selection algorithm selected three models that were greater than two AICc points superior to the next most parsimonious model. The top model,

$$^{87}Sr/^{86}Sr = (0.0263)Precambrian - (0.676)Precambrian{:}Tertiary - (0.0011)Mean\ Watershed\ Age^{(weighted\ by\ area)} + \varepsilon \quad (1)$$

explained 89% (Adjusted R^2) of the variation in the data, provided the best prediction residuals for the validation set, and resulted in a more reasonable prediction of the mouth of the Amazon. This equation was used to predict the $^{87}Sr/^{86}Sr$ signatures for the five unsampled watersheds.

Grouping of Distinguishable Watersheds

A quadratic discriminant function provided the best cross-validation error rate (3.6%) for discriminating all the watersheds into the three regions. One predicted value for the Madeira River was the lone misclassification from the validation set, being classified to the Lower Amazon Tributaries group. One sample from the Solimões River was dropped from the training set as an outlier (Table 2). The value for this site was unexplainably high in comparison to the multi-year samples above and below it on the river. While no explanation for this discrepancy was forthcoming from the original study, Bouchez et al. (2010) found that lateral heterogeneity in $^{87}Sr/^{86}Sr$ signatures can persist for long distances below confluences in the Solimões.

Determining Fish Movement and Location

Changes in $^{87}Sr/^{86}Sr$ ratio, indicating movement, were common across each of the three species. Movement between distinguishable river groups, as determined by discriminant function classification, was less frequent. Over 70% of dourada exhibited movement between stable signatures based on changepoint analysis, however only two (14%) showed movement between distinguishable river groups after discrimant function classification (Fig 4A). Sample BR24 started life in the Amazon Mainstem and Western Tributaries signature before moving to a signature consistent with the Lower Amazon Tributaries river group. Sample BR25 began life with a signature consistent with the Lower Amazon Tributaries river group, before moving twice to a signature

consistent with the Beni-Madeira and Lower Negro group with a small region consistent with the Amazon Mainstem and Western Tributaries river group.

Of five piramutaba, two (40%) were shown to move between stable signatures but none moved outside the Amazon Mainstem and Western Tributaries river group based on discriminant function classification (Fig 4B). Of the three piraíba samples two showed movement, both of which moved between the Beni-Madeira and Lower Negro River group and the Amazon Mainstem and Western Tributaries (Fig 4C).

Overall, these results indicated that the majority of fish begin life in the Amazon Mainstem and Western Tributaries signature, a signature which contains within it the estuary signature, the expected location of early rearing (Barthem and Goulding 1997). Our results were unable to distinguish the Amazon mainstem signature from that of the estuary, the expected location of early rearing. However, we would expect the signature to be intermediate between that of the signature of the Amazon River mouth and the global marine signature of 0.70918 resulting from the mixing of the two water bodies. The resulting estuary signature would be contained with the range of the Amazon Mainstem and Western Tributaries classification.

Conversely, some portion of fish begin life, and undergo some or all of their rearing, in signatures indicative of freshwater (Fig 4A, B and C). Sample BR25 (dourada) and BF1 (piraíba) were the two most obvious examples, starting life with signatures that correspond to the Beni-Madeira and Lower Negro and Lower Amazon Tributary signatures. Many of the fish that remained within the Amazon Mainstem and Western Tributaries river group began life with signatures > 0.71, significantly higher than the Mainstem Amazon River signatures (Table 2) and the global marine signature, and thus likely an upriver signature. Others (BR6, BR8, BV1, BF2) spent large portions of their lives in distinctly upriver environments.

Discussion

Understanding the migration ecology of Amazon catfish represents an opportunity to understand the large-scale ecosystem processes of long distance aquatic

migration in an intact, native fish population. These fish also represent an international conservation challenge, as their movements stretch across multiple national boundaries (Agudelo et al. 2000) and are potentially threatened by several hydropower projects (Fearnside 2006, 2014, Finer and Jenkins 2012, Tavener 2012). The first step in understanding these ecological processes, and their effects on the fishery, is a robust understanding of their migratory movements at a finer scale than is currently available from fisheries data.

Our results provide the first reported reconstruction of movements and migrations of individual *Brachyplatystoma* spp. in the Amazon Basin using chemical signatures from otoliths. Applying these techniques in this system appears promising for improving our understanding of the migratory movements of these species, which are currently understood only at the most basic level. While this work is preliminary, $^{87}Sr/^{86}Sr$ signatures appear capable of identifying large-scale fish movements at a meaningful spatial scale; between important river systems within the basin. Further, movement between areas with stable signatures can be observed within statistically distinguishable river groups, indicating that improved baselines and larger sample collections should allow greater resolution. Discrimination of fish location and movement may also be improved by applying multivariate analyses of elemental signatures in concert with $^{87}Sr/^{86}Sr$ signatures (Muhlfeld et al. 2012, Crook et al. 2013, Hughes et al. 2014).

We observed diversity in rearing location and behavior among a minority of individuals in each of the three species sampled using otolith $^{87}Sr/^{86}Sr$ movement reconstructions and discriminant function classification to location. For example, fish BR25 (a dourada caught in Manaus) appears to have spent most of its early life in areas with very high $^{87}Sr/^{86}Sr$ ratios assigned to the Lower Amazon Tributaries river group (Fig 4A). The chemical signatures of this fish indicate that rather than drifting to the estuary to rear, it spent the first third of its life in a lower tributary of the Amazon River before moving to a signature indicative of areas between the Madeira and Amazon Rivers, finally being caught near between Manaus and the mouth of the

Madeira (as reported by the fishermen who provided the samples in Manaus). Notably, the signatures appear to support the idea that this fish never traveled to the estuary. Fish BF1 (piraíba) also showed a significant length of freshwater rearing in a signature assigned to the Beni-Madeira and Lower Negro river group (Fig 4C).

Indeed, several additional dourada and piraíba, and one piramutaba all appeared to have spent significant time in $^{87}Sr/^{86}Sr$ signatures greater than 0.7100 (Fig 4A, B and C). This signature is higher than all but one location on the mainstem Amazon River and significantly higher than the accepted global marine signature of 0.70918 considering the analytical precision that is possible for otolith measurements. We would expect estuarian signatures to fall between the $^{87}Sr/^{86}Sr$ signature of the Amazon mouth and the global marine signature except very near the mouth of the Tocantins. The Tocantins signature is likely attenuated significantly by Amazon River water flowing through the Canal de Breves which noticeably muddies the water flowing from the Tocantins (Barthem and Goulding 1997). Further, the estuary signature should converge to the marine signature at relatively low salinities due to the much higher strontium concentration of the ocean (Hobbs et al. 2010). This indicates the possibility that a larger percentage of our samples may have reared upriver of the estuary as well, but our methods were unable to detect it.

Ecologically, the presence of upriver $^{87}Sr/^{86}Sr$ signatures during the rearing phase indicates that in some situations a rearing strategy that forgoes the high growth potential of the estuary may provide overall fitness benefits. This finding suggests that the life-history of these species is more complex than has been previously understood. The potential existence of a freshwater rearing life-history, based on evidence for alternative spawning periods in the upper reaches which do not fit the conventional estuary rearing model, was theorized by García Vasquez et al. (García Vásquez et al. 2009). This model is supported by evidence of young and immature fish present in the far western Amazon before and during the spawning season when the prevailing hypothesis would place these fish in the estuary (Agudelo et al. 2000, Alonso and Fabré 2002, Fabré and Barthem 2005).

Understanding the extent of diversity in life history strategies is critical for managing these little-studied native species, especially in habitats facing current and future perturbations. Variations in life history have been shown to affect recruitment, survival, and fisheries sustainability in other long-distance migratory fish (Hilborn et al. 2003, Winemiller 2005, Copeland and Venditti 2009). These species may home to their natal rivers, and sub-population structure and associated differences in life history may exist (Batista and Alves-Gomes 2006, Carvajal 2013), which may have important implications for planning and policy decisions related to dam placement and fishery management. For instance, fishing pressure in the estuary is high, potentially limiting juvenile escapement to upriver fisheries (Agudelo et al. 2000, Fabré and Barthem 2005). Freshwater rearing life-histories would avoid the high fishing pressures in the estuary, potentially increasing survival and providing important recruitment to upriver fisheries in the Western Amazon, fisheries which appear to be overfished (Sioli 1956, Barthem and Petrere Jr 1995, Fabré and Barthem 2005).

Dams in particular have been shown to decrease life-history diversity of other major migratory fish species, with consequences for their conservation and fisheries sustainability (Burke 2004, Beechie et al. 2006) and diverse source populations appear to provide resilient fisheries over time (Hilborn et al. 2003). So, the extent to which dams or other anthropogenic disturbances decrease the diversity of source populations in dourada, piramutaba, and piraíba could have adverse impacts on the sustainability of the fishery. The pace of dam building in the major Amazon Basin tributaries (Fearnside 2006, 2014, Finer and Jenkins 2012), the difficulty of providing significant fish passage in Amazonian rivers (Pompeu et al. 2012), and the known and suspected effects of dams on the migration of these migratory catfish species (Barthem and Petrere Jr 1995, de Mérona et al. 2001, Freeman 2003) increase the need to understand the details of their migration ecology. Only with detailed knowledge of *Brachyplatystoma* migration ecology can policymakers weigh the effects of dams on the sustainability of this important fishery.

Our study raises numerous important questions and opportunities for future research. While it is clear that water chemistry signatures for the Amazon basin can be classified into meaningful groups, such results do not necessarily translate into concrete interpretations of fish movement at anything but the largest of scales. Our understanding of the degree to which the movements and migrations of individual fish can be interpreted at the scale of the entire Amazon basin is in its infancy. At smaller spatial scales, many of the local tributaries to the major rivers of the Amazon basin exhibit vastly different signatures than those of the main channels, which reflect the headwater signature of the Andes or the Brazilian and Guyana Shield geology (Queiroz et al. 2009). Incomplete or slow mixing of different signatures, especially across muddy whitewater and tannic blackwater rivers, may occur over extended river distances, which may create unexpected intermediate signatures (Bouchez et al. 2010). Furthermore, our understanding of temporal variation associated with available empirical data is limited. Especially in the Amazon estuary, our understanding of the $^{87}Sr/^{86}Sr$ signatures in this seasonally dynamic environment are limited. Increased understanding of these estuarian signatures is critically important to understanding these species using otolith microchemistry studies. Our study species are thought to inhabit only the larger, mainstem tributaries, making large scale location classification useful. At smaller geographic scales additional ground truth sampling of fish and water chemistry is needed to constrain the scale at which movements and migrations can be accurately interpreted from otolith data. Otolith sampling across larger areas of the Amazon may also allow elemental ratios, which are fractionated biologically unlike $^{87}Sr/^{86}Sr$, to be used in addition to $^{87}Sr/^{86}Sr$ to improve location analysis.

Overall, this study highlights the feasibility and utility of the latest otolith chemistry techniques to greatly improve our understanding of the movements and ecology of these important native fishes throughout the entire Amazon basin. Recent declines in the fishery point to the necessity of conducting this research (JICA et al. 1998, Petrere et al. 2005, Córdoba et al. 2013). Migratory catfish in the Amazon Basin are several of only a few large, freshwater fishes worldwide that are not currently

imperiled due to anthropogenic changes to freshwater ecosystems (Allan et al. 2005). However, as fishing pressure increases, land use and forest clearing affect the river system, and dams threaten migration routes and access to critical habitats, these populations will likely be affected. The sustainability of these populations and the fisheries they support, especially across international borders, continues to depend on accurate population assessments of based on detailed knowledge of their behavior and ecology.

Tables

Table 1.1 *Brachyplaystoma* spp. sample information

Species	Sample Number	Location	Total Length (cm)	Weight (kg)
Brachyplatystoma rousseauxii *(dourada)*	BR1	Belém	75	8.00
	BR3	Belém	75	8.00
	BR6	Belém	75	8.00
	BR7	Belém	75	8.00
	BR8	Belém	75	8.00
	BR10	Belém	75	8.00
	BR12	Belém	75	8.00
	BR14	Belém	75	8.00
	BR16	Belém	75	8.00
	BR18	Belém	100	22.00
	BR19	Manaus	110	11.00
	BR21	Manaus	100	6.00
	BR23	Manaus	115	10.00
	BR24	Manaus	75	3.70
	BR25	Manaus	80	4.00
	BR26*	Manaus	-	-
Brachyplatystoma vaillanti *(piramutaba)*	BV1	Manaus	75	4.19°
	BV2	Manaus	70	3.38°
	BV3	Manaus	68	3.09°
	BV4	Manaus	65	2.68°
	BV5	Manaus	70	3.38°
Brachyplatystoma filamentosum *(piraíba)*	BF1	Belém	220	110.00
	BF3	Belém	250	130.00
	BF5	Belém	90	20.00

* Asterisci otolith. Analysis was excluded due to low Sr concentrations

° Weights are estimated from length-to-weight ratios

Fish were collected from two locations in the Brazilian Amazon; in the cities of Belém near the mouth of the Amazon River, and Manaus in the central Amazon Basin. Piramutaba were gutted prior to otolith collection. Their weights are estimated from a length-to-weight relationship from Pirker (Pirker 2001).

Table 1.2 - Isotopic and geologic makeup of major watersheds of the Amazon River basin

Sample Point Name (From Literature)	Literature Source	River	River Group Classification	$^{87}Sr/^{86}Sr$	St. Dev.	N	Geology Percent Area			Mean Age (Ma)
							Carboniferous	Tertiary	Precambrian	
Amazon 13	Gaillardet et al. 1997	Amazon	Wester Tributaries & Amazon Mainstem	0.710728	-	1	1%	47%	21%	409
Amazon 14	Gaillardet et al. 1997	Amazon	Wester Tributaries & Amazon Mainstem	0.71112	-	1	1%	47%	21%	409
Amazon 20	Gaillardet et al. 1997	Amazon	Wester Tributaries & Amazon Mainstem	0.711478	-	1	2%	42%	25%	429
Amazon 6	Gaillardet et al. 1997	Amazon	Wester Tributaries & Amazon Mainstem	0.709172	-	1	0%	60%	17%	407
Rio Madeira	Gaillardet et al. 1997	Lower Madeira	Beni-Madeira & Lower Negro	0.720036	-	1	2%	20%	30%	412
Rio Negro	Gaillardet et al. 1997	Lower Negro	Beni-Madeira & Lower Negro	0.716223	-	1	0%	21%	68%	1243
Rio Topajos	Gaillardet et al. 1997	Lower Topajos	Lower Amazon Tributaries	0.733172	-	1	10%	8%	48%	658
Rio Trombetas	Gaillardet et al. 1997	Lower Trombetas	Lower Amazon Tributaries	0.732295	-	1	3%	7%	78%	515
Uracara	Gaillardet et al. 1997	Lower Uracara	Lower Amazon Tributaries	0.723584	-	1	2%	19%	62%	558
Purus	Queiroz et al. 2009	Lower Purus	Wester Tributaries & Amazon Mainstem	0.711135	-	1	0%	92%	4%	564
Solimões*	Queiroz et al. 2009	Lower Solimões	Wester Tributaries & Amazon Mainstem	0.714461	-	1	0%	63%	1%	289
Atalaya	Santos et al. 2013	Upper Solimões	Wester Tributaries & Amazon Mainstem	0.70887	-	1	0%	20%	0%	331
Borba	Santos et al. 2013	Lower Madeira	Beni-Madeira & Lower Negro	0.71762	-	1	2%	20%	30%	412
Borja	Santos et al. 2013	Upper Solimões	Wester Tributaries & Amazon Mainstem	0.7085	-	1	0%	13%	0%	426
Caracarai	Santos et al. 2013	Upper Negro	Beni-Madeira & Lower Negro	0.72238	-	1	0%	0%	74%	1650
Francisco de Orellana	Santos et al. 2013	Upper Solimões	Wester Tributaries & Amazon Mainstem	0.70592	0.00037	26	0%	67%	10%	287
Itiatuba	Santos et al. 2013	Lower Tapajos	Lower Amazon Tributaries	0.72964	0.00587	27	10%	4%	51%	671
LaBrea	Santos et al. 2013	Lower Purus	Wester Tributaries & Amazon Mainstem	0.71012	-	1	0%	90%	6%	1126
Manacapuru	Santos et al. 2013	Lower Solimões	Wester Tributaries & Amazon Mainstem	0.70907	0.00025	38	0%	72%	2%	312
Obidos	Santos et al. 2013	Amazon	Wester Tributaries & Amazon Mainstem	0.71154	0.00053	46	1%	46%	23%	408
PortoVelho	Santos et al. 2013	Lower Madeira	Beni-Madeira & Lower Negro	0.71677	0.00073	9	3%	17%	22%	379
Ruranbaque	Santos et al. 2013	Upper Madeira	Beni-Madeira & Lower Negro	0.71730	0.00126	38	17%	13%	1%	433
Serrinha	Santos et al. 2013	Upper Negro	Lower Amazon Tributaries	0.73183	0.00737	16	0%	19%	80%	614
Tabitinga	Santos et al. 2013	Upper Solimões	Wester Tributaries & Amazon Mainstem	0.70881	0.00029	9	0%	75%	3%	200
Amazon Mouth (Predicted)	Predicted from regression	Amazon	Wester Tributaries & Amazon Mainstem	0.71625	0.00787°	-	2%	40%	29%	482
Jari (Predicted)	Predicted from regression	Lower Jari	Lower Amazon Tributaries	0.72928	0.00873°	-	0%	2%	89%	718
Paru (Predicted)	Predicted from regression	Lower Paru	Lower Amazon Tributaries	0.72703	0.00845°	-	1%	4%	78%	515
Tocantins (Predicted)	Predicted from regression	Lower Tocantins	Lower Amazon Tributaries	0.72683	0.00884°	-	13%	22%	36%	877
Xingu (Predicted)	Predicted from regression	Lower Xingu	Lower Amazon Tributaries	0.72633	0.00827°	-	2%	13%	70%	1091

* Outlier dropped from regression analysis

° Values are prediction intervals of the regression from Equation 1.

Strontium ratios were taken from water samples reported in the literature for locations throughout the Amazon Basin and used as baselines to determine the likely location of fish movement. These samples were classified to three statistically

distinguishable river group classifications using quadratic discriminant function analysis. Unsampled locations were predicted using geologic regression (Equation 1).

Figures

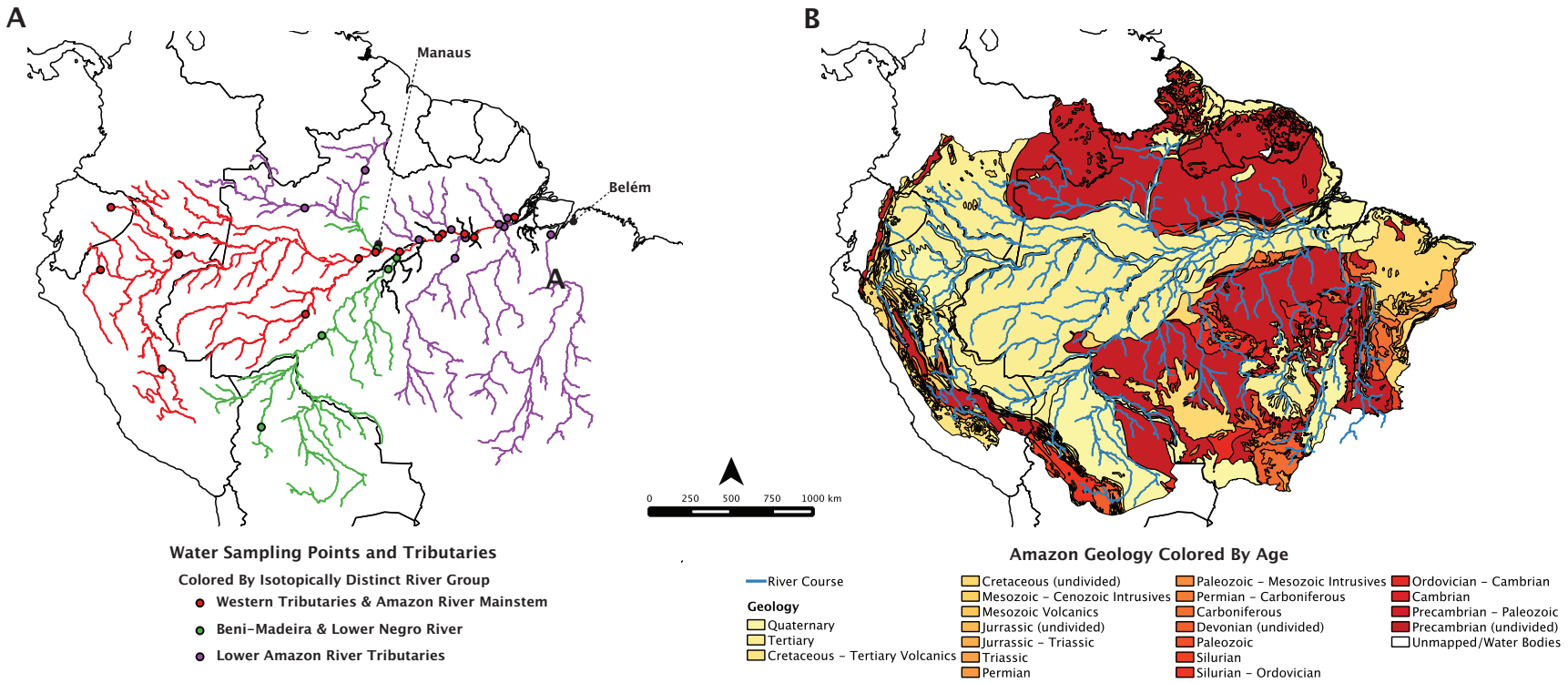

Figure 1.1 - Water sampling points and geology of the Amazon River basin

Maps show (A) the location of $^{87}Sr/^{86}Sr$ water samples within the Amazon River basin digitized by the authors from location descriptions in the literature (Gaillardet et al. 1997, Queiroz et al. 2009, Santos et al. 2013) and points predicted from

Equation 1. The geological age and composition of the basin (B) used to predict the $^{87}Sr/^{86}Sr$ signatures of unsampled watersheds is also shown. Maps created using USGS datasets (USGS 1996, 1999, Lehner et al. 2008)

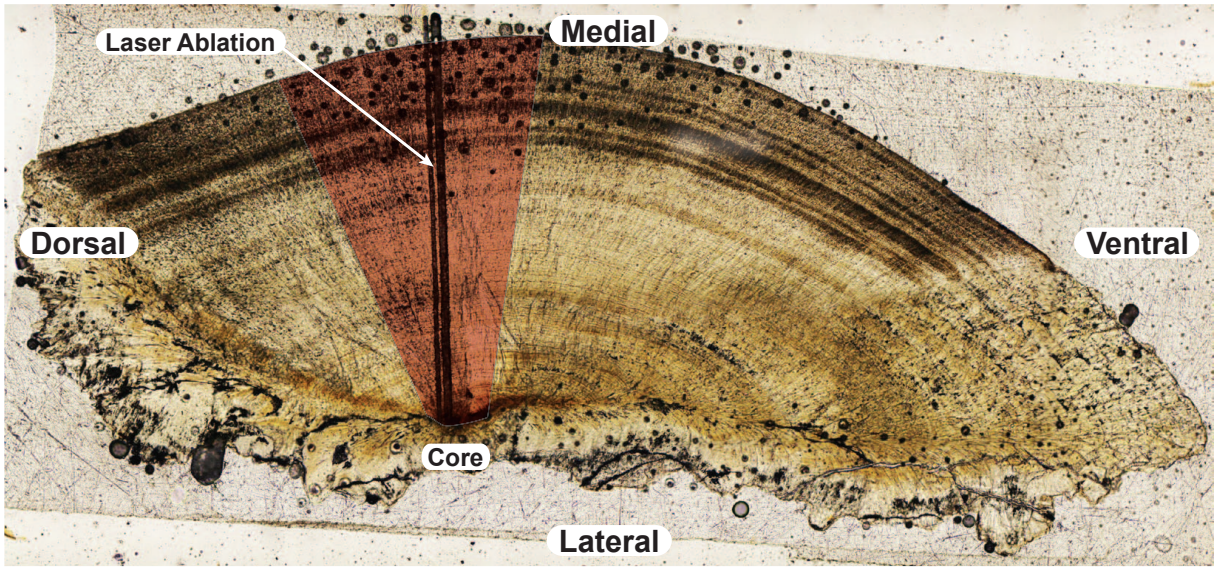

Figure 1.2 - Otolith sectioning and analysis

Representative transverse section from a dourada lapillus otolith showing the analysis area (in red) used for all otoliths with the laser-ablation tracks indicated. All analyses were performed approximately perpendicular to the growth rings.

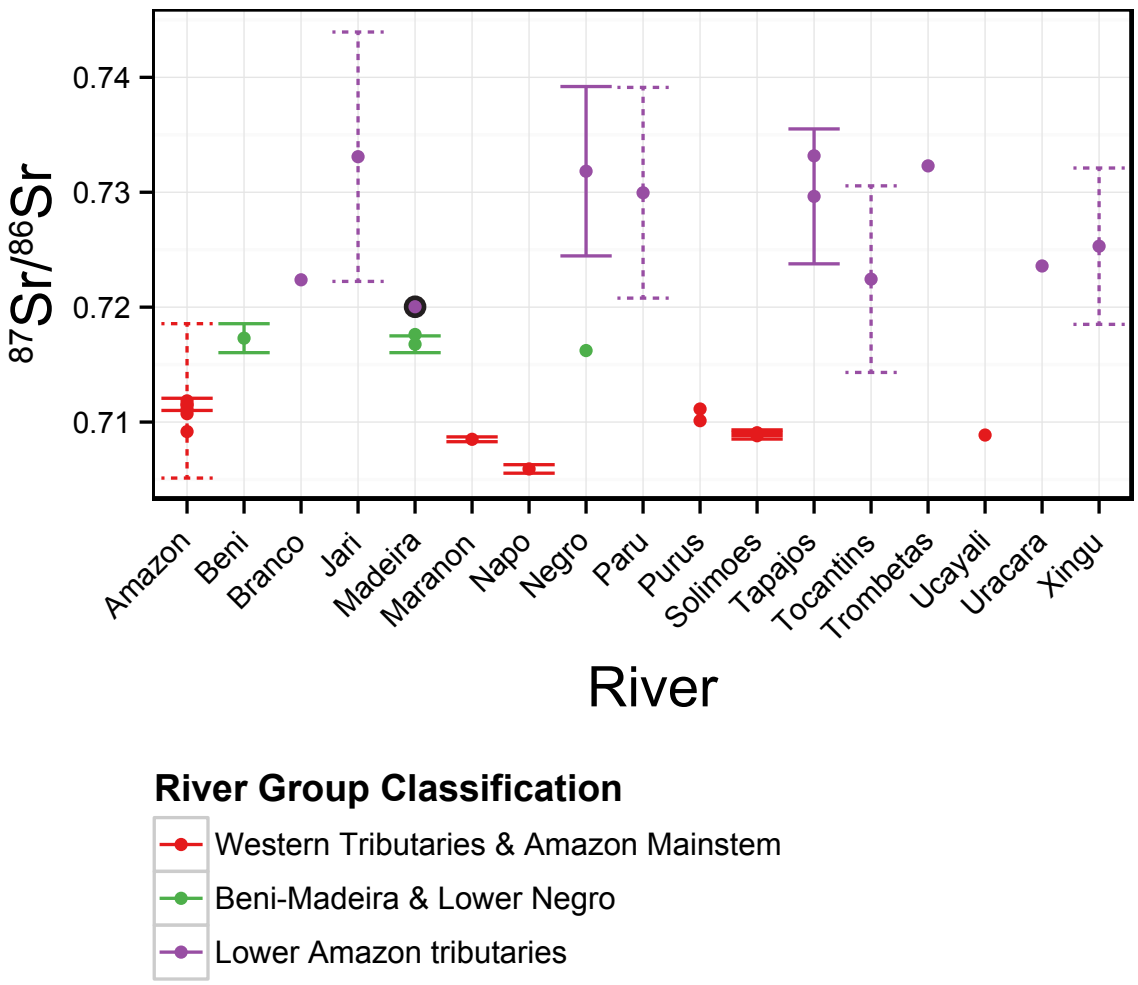

Figure 1.3 - River isotopic signatures throughout the Amazon River basin

Strontium ratio values (y-axis) for each sampled and predicted watershed (x-axis) in the current study. Color indicates the classification to three river groups using quadratic discriminant function analysis. Solid error bars indicate the standard deviation where samples were repeated over time (See Table 1 for sample sizes). Dashed error bars indicate the prediction intervals from the geologic regression (Equation 1) used to predict that point. Points bordered in black were misclassified during cross validation of the quadratic discriminant function.

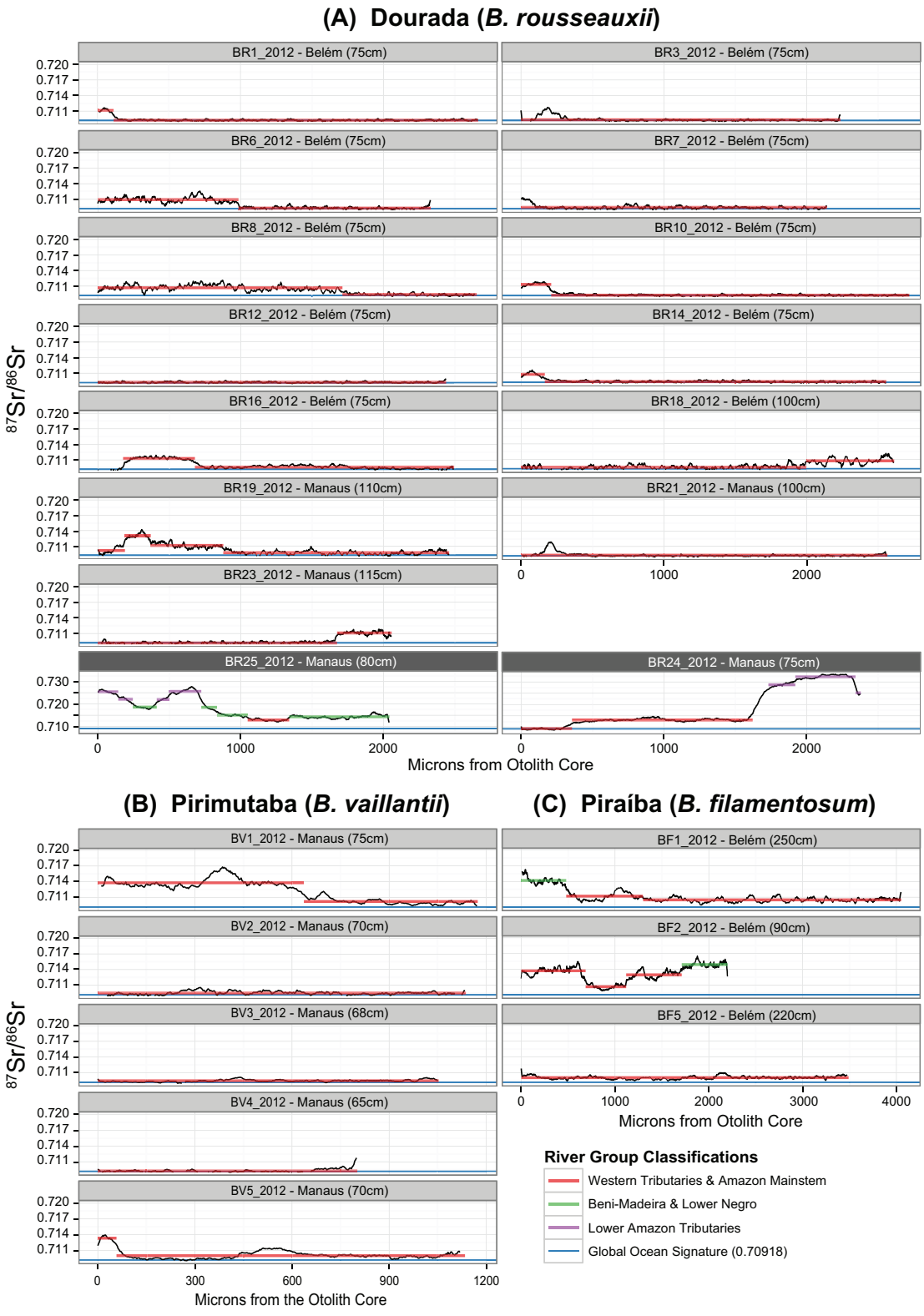
(A) Dourada (B. rousseauxii)
BR1_2012 - Belém (75cm)
BR3_2012 - Belém (75cm)
BR6_2012 - Belém (75cm)
BR7_2012 - Belém (75cm)
BR8_2012 - Belém (75cm)
BR10_2012 - Belém (75cm)
BR12_2012 - Belém (75cm)
BR14_2012 - Belém (75cm)
BR16_2012 - Belém (75cm)
BR18_2012 - Belém (100cm)
BR19_2012 - Manaus (110cm)
BR21_2012 - Manaus (100cm)
BR23_2012 - Manaus (115cm)
BR25_2012 - Manaus (80cm)
BR24_2012 - Manaus (75cm)
87Sr/86Sr
Microns from Otolith Core
(B) Pirimutaba (B. vaillantii)
(C) Piraíba (B. filamentosum)
BV1_2012 - Manaus (75cm)
BV2_2012 - Manaus (70cm)
BV3_2012 - Manaus (68cm)
BV4_2012 - Manaus (65cm)
BV5_2012 - Manaus (70cm)
BF1_2012 - Belém (250cm)
BF2_2012 - Belém (90cm)
BF5_2012 - Belém (220cm)
Microns from the Otolith Core
Microns from Otolith Core
River Group Classifications
Western Tributaries & Amazon Mainstem
Beni-Madeira & Lower Negro
Lower Amazon Tributaries
Global Ocean Signature (0.70918)

Figure 1.4 - Location classification of $^{87}Sr/^{86}Sr$ signatures in otolith transects

Plots show the variation in $^{87}Sr/^{86}Sr$ (y-axis) over the life of sampled fish, represented as distance from the otolith core in microns (x-axis). Horizontal colored lines indicate stable signatures identified using changepoint analysis, with colors representing inclusion in one of three statistically distinguishable river groups based on quadratic discriminant analysis. Fourteen samples of dourada (A) were collected in Belém and Manaus fish markets. Five samples of piramutaba (B) were collected in Manaus. Three samples of piraíba (C) were collected in Belém. Dark grey chart labels indicate a different y-axis scale was used to accommodate large variations in $^{87}Sr/^{86}Sr$. The x-axis scale differs for all fish depending on the width of the otolith, which varies based on age, growth and species-specific factors.

Chapter 2: All about my mother: the complexities of maternally derived chemical signatures in otoliths.

In Review with Canadian Journal of Fisheries and Aquatic Sciences.
Submitted August 17, 2017.

Abstract

Connecting maternal migratory behavior with the behavior and ecology of their progeny can reveal important details in the ecology of a population. One method for linking maternal migration to early juvenile life-history is through maternal chemistry recorded in otoliths. Despite the wide use of maternal signatures to infer anadromy, the duration and dynamics of maternal otolith signatures are not well understood. Shifts in the elemental concentrations and strontium isotope ($^{87}Sr/^{86}Sr$) chemistry in otoliths from juvenile Chinook salmon (*Oncorhynchus tshawytscha*) correlate with the timing of hatch and emergence respectively, indicating a chemical marker of these ontological stages. Additionally, analysis of maternal signatures show that maternally derived $^{87}Sr/^{86}Sr$ may be heavily affected by equilibration of the mother to freshwater, and in some circumstances the signature of the egg can shift significantly after being laid. These results provide guidance in separating maternal and juvenile signatures as researchers increasingly target early juvenile otolith chemistry. These results also caution against the use of $^{87}Sr/^{86}Sr$ alone as a marker of anadromy in populations with significant inland migrations.

Introduction

In many fish species migration is a facultative strategy, often encompassing various degrees of partial migration (Tsukamoto and Arai 2001, Secor and Kerr 2009, Chapman et al. 2011, Brodersen et al. 2014). Even within species and populations which are generally considered to be obligately migratory, the timing of migratory

movements can be quite diverse (Isaak et al. 2003, Burke 2004, Hegg et al. 2015a). In many cases life-history characteristics such as growth rate and propensity to migrate are heritable, and understanding their expression in the context of fitness necessitates linking parent and progeny (Stewart et al. 2006, Thériault et al. 2007, Liberoff et al. 2014, 2015, Waples et al. 2017). Further, maternal effects and conditions early in life can have large effects on adoption of particular strategies by individual fish (Taylor 1990, Morinville and Rasmussen 2003). However, it can be difficult without genetic parentage information to link the life-history of the mother to her progeny. Further, understanding behavior and the effects of environment on juvenile fish can be difficult in fish too small to apply tracking tags.

Otoliths provide a window into the link between mothers and progeny, as well as detailed juvenile information. An inner ear structure of bony fish, otoliths grow in size with the addition of daily layers of calcium carbonate (Campana and Thorrold 2001). These layers incorporate elements and isotopes which occasionally substitute into the calcium carbonate structure. Many of these are recorded in proportion to the water the fish inhabits, creating a temporal and spatial record throughout its life (Kennedy et al. 1997, Thorrold et al. 1998, Campana 2005). Numerous studies have reported the presence of a maternal chemical signature in the core of otoliths using various micro-chemical proxies, allowing researchers to infer some aspects of maternal location, spawning migration, and anadromy from their progeny (Kalish 1990, Volk et al. 2000, Miller and Kent 2009, Shippentower et al. 2011, Courter et al. 2013, Liberoff et al. 2015). At the same time, otoliths provide information on juvenile natal location, movement, growth and condition in the layers just outside the zone of maternal influence near the otolith core (Thorrold et al. 1998, Walther and Thorrold 2010, Hamann and Kennedy 2012, Hegg et al. 2013a, Schaffler et al. 2014, Shrimpton et al. 2014, Turner et al. 2015).

Despite the amount of available research using these adjacent areas of the otolith, Veinott et al. (2014) highlight variability in some core signatures and a lack of conclusive agreement on the markers of maternal signature and its duration. Further,

some assumptions of maternal chemical incorporation and duration in the otolith core is untested (Elsdon et al. 2008). Limburg et al. (2001) note that a lack of understanding of the duration of maternal signatures may affect their interpretation of Baltic sea trout which lack a freshwater phase. It is also unknown whether the maternal transition is related to underlying ontological changes in maturing fish which might provide further information on juvenile development. As the number of studies utilizing otolith chemistry to infer detailed juvenile movement patterns increase in frequency it is important to determine how to distinguish maternally-derived, versus environmentally-derived, chemical signatures of juvenile fish.

The maternal signature is retained in the otolith because the egg is provisioned using nutrients derived from the mother. The larva obtains all of its nutrients from the yolk sac until it commences feeding, which occurs shortly after hatching, at which point the larva begins significant chemical exchange with the surrounding water (Hayes et al. 1946). Therefore, as the otoliths develop prior to hatching, its isotopic signature should reflect that of the mother (Kalish 1990, Waite et al. 2008). If the mother has migrated from a location with a different micro-chemical signature her eggs will retain a chemical signature related to her past location, attenuated by the degree to which her body chemistry has equilibrated with the chemistry of the spawning stream (Volk et al. 2000, Bacon et al. 2004). This has also been demonstrated as a marking technique, by exposing mothers to known isotopic signatures prior to spawning (Thorrold et al. 2006, Woodcock et al. 2013, De Braux et al. 2014). This maternally derived chemical information recorded in the otolith can then be used to infer information about the maternal provenance or behavior.

The use of maternally-derived chemical signatures that allow for the identification of marine influence in fish been repeatedly demonstrated (Kalish 1990, Miller and Kent 2009, Liberoff et al. 2015). In most freshwater systems, the concentration of strontium (Sr) is much lower than that of the ocean, providing a large and predictable shift in Sr/Ca in dissolved ions that is conserved between anadromous and resident fish (Kraus and Secor 2004, Brown and Severin 2009). However,

examples exist showing that in some systems Sr/Ca is a poor indicator of ocean residence (Kraus and Secor 2004), that expected patterns of microchemical signatures of ocean residence can be population specific (Hamer et al. 2015), and that Sr/Ca ratios change in relation to the time females spend in freshwater and the difficulty of the migration (Donohoe et al. 2008).

It has also been demonstrated that maternal signatures are conserved in otolith $^{87}Sr/^{86}Sr$ signatures (Barnett-Johnson et al. 2008, Miller and Kent 2009, Hegg et al. 2013a). In contrast to Sr/Ca, however, the relationship between maternal $^{87}Sr/^{86}Sr$ values and juveniles is less well quantified. The assumption in anadromous species has been that $^{87}Sr/^{86}Sr$ maternal signatures follow the same mechanism as Sr/Ca, reflecting the global marine value of 0.70918 due to maternal investment in the yolk material (Courter et al. 2013). Several studies, however, have shown that migratory distance and migratory difficulty may influence the maternal $^{87}Sr/^{86}Sr$ signature (Volk et al. 2000, Bacon et al. 2004, Miller and Kent 2009). As more studies use $^{87}Sr/^{86}Sr$ as a marker of maternal anadromy (Courter et al. 2013, Hodge et al. 2016), it is necessary to understand the dynamics of maternal chemistry in the otolith core, as well as the migratory conditions under which the assumptions of maternal chemical influence hold.

Based upon a review of the otolith literature, the factors controlling the duration of the maternal signature have been largely unexplored. Many studies mention the need to avoid mistaking the period of maternal influence with the period of natal origin, or vice-versa (Barnett-Johnson et al. 2008, 2010, Donohoe et al. 2008, Hegg et al. 2013a). However, determining the end of maternal chemical influence on the otolith has largely been species- or population-specific. Further, the end of maternal influence is often determined subjectively or through associations with microstructural checks (Barnett-Johnson et al. 2008, Hegg et al. 2013a). Most studies of the microchemistry of the otolith core have focused on markers of the otolith primordium, rather than the extent of maternally derived influence, using various

microchemical ratios to calcium including barium (Ba/Ca), magnesium (Mg/Ca), and manganese (Mn/Ca) (Ruttenberg 2005, Macdonald et al. 2008).

Late season spawning Chinook salmon (*Oncorhynchus tshawytscha*) in the Snake River of Idaho provide an ideal population for examining the presence and duration of the maternal otolith signature. Females in this population are entirely anadromous and individuals migrate long distances (500-1000 kms) inland to spawn over a narrowly defined period in October and November (Garcia et al. 2005). Prior work has characterized the isotopic variation across spawning areas in the basin, indicating that juvenile signatures are significantly different between spawning areas and that $^{87}Sr/^{86}Sr$ and Sr concentration in freshwater habitats are significantly different from the marine signature (Hegg et al. 2013a). These factors provide both a range of freshwater strontium concentrations to interpret otolith signatures, as well as the migration distance required to explore the degree to which maternal marine signature varies from the global marine signature with inland migration.

This study used individual otolith transects from a collection of known-origin, juvenile Fall Chinook salmon from both wild and hatchery sources to quantify the duration and stability of maternal signatures in otoliths. This work also investigates the variability in these signatures that may be due to the equilibration of mothers to river-specific chemical signatures prior to spawning, as well as changes in the microchemistry of the egg after deposition in the redd. Given the inland location of the population we hypothesized that maternal $^{87}Sr/^{86}Sr$ signatures would reflect some degree of freshwater influence. We used a multi-tracer approach, including ratios of Sr/Ca, Ba/Ca, Mn/Ca, and Mg/Ca as well as $^{87}Sr/^{86}Sr$ to examine the presence and duration of the maternal signature on the otolith. Further, we explored whether changes in each tracer were simultaneous, and thus indicative of a single event, or if individual tracers may signal different ontological time-points in the early life of fish. First, using the suite of chemical signatures we determine the presence and duration of a maternal marine signature in individual juvenile otoliths. Finally, given the variability

we quantify in maternal signatures, we measure the spatial and temporal variability of maternal signatures across the study area.

Methods

Study System

Fall Chinook salmon in the Snake River are listed as threatened under the Endangered Species Act (Good et al. 2005). The population inhabits low-elevation, mainstem habitats of the Snake River and its tributaries. The majority of spawning occurs in the free flowing Snake River between Asotin, Washington and Hells Canyon dam and in the Clearwater River (Garcia et al. 2008). The main spawning areas in the Snake River are classified as "Upper", above the confluence with the Salmon River, and "Lower", in the free-flowing section below the Salmon River confluence to Asotin, WA. The watersheds of the basin are geologically heterogeneous with enough distinction to provide significant differences in water $^{87}Sr/^{86}Sr$ ratio between the major spawning reaches which can be used to classify fish to their natal location (Hegg et al. 2013a, 2013b). Adult salmon migrate a minimum of 750 km to the main spawning areas in the Snake and Clearwater Rivers above the town of Lewiston, ID. The watershed is heavily influenced by hydropower with eight downstream dams, four on the Columbia River and 4 on the Snake River, creating slow moving reservoir habitat downstream of Lewiston, ID.

The population is notable for a recent shift from a historically ubiquitous sub-yearling strategy, whereby individuals migrated shortly after emergence, toward a later, yearling strategy in response to anthropogenic changes to the river system (Connor et al. 2005, Williams et al. 2008). Studies have indicated that this change in juvenile life-history is likely heritable and under active selection in response to reservoirs and hydropower regulation which provide cool water opportunities during summer that did not exist historically (Williams et al. 2008, Waples et al. 2017). A separate study seeks to quantify the spatially explicit outmigration behaviors (Hegg et al. In prep). However, to accurately assess early life-history behaviors using chemical

reconstruction from otoliths, it is essential to determine the degree of maternal influences on the early chemistry of juvenile fish.

Background Water Sample Collection

Water samples were collected from 2008 through 2016 throughout the spawning range of Snake River Fall Chinook salmon to characterize the spatial and temporal variation in strontium isotopic chemistry within the basin (Figure 1). Samples were collected during baseflow periods in late summer and fall in all years to capture the most representative signature of water and rock interactions within each river. Starting in 2009, as resources permitted, samples were taken seasonally. Sampling began in the spring as soon as flows were safe to sample and included summer, and fall seasons to characterize the stability of the signatures. Additionally, in 2010, samples were taken in the Clearwater and Salmon Rivers at three periods encompassing the peak of the hydrograph to characterize seasonal variation observed in prior studies (Hegg et al. 2015b)

Samples were collected in acid cleaned 125ml HDPE bottles according to established protocol (Kennedy et al. 2000). Samples were analyzed for $^{87}Sr/^{86}Sr$ isotope ratios on a Finnigan MAT 262 Multi-Collector thermal ionization mass spectrometer (TIMS) as well as a Isotopix Phoenix TIMS. Throughout the research period, replicate analysis of the National Institute of Standards and Technology standard reference material (SRM-987) was used to determine the analytical error. The Finnegan MAT 262 yielded mean $^{87}Sr/^{86}Sr$ of 0.710231 (2SE = 0.000008, n=16), the Isotopix Phoenix yielded a mean $^{87}Sr/^{86}Sr$ of 0.710244 (2SE = 0.000001, n=89).

Fish and Otolith Collection

Wild juvenile fish (n=430) were captured using beach seines from spawning areas between the Snake and Clearwater Rivers as part of seasonal population surveys between April and August in years spanning 2007 to 2014 (Connor et al. 1998). Some of these fish (n=111) were PIT tagged, released, and recaptured at fish passage facilities at Lower Granite Dam on the Snake River during their downstream out-migration,

providing two known locations for these fish (tagging site and recapture site). Juvenile fish were also collected from the two hatcheries that produce Fall Chinook in the Snake River basin. Hatchery fish were collected from Lyons Ferry Hatchery in 2009 and 2011 (n=28), and from Nez Perce Tribal Hatchery in 2011 and 2012 (n=35).

Fish samples were kept frozen until otoliths could be removed through dissection. Otoliths were stored dry in polypropylene microcentrifuge tubes. Otoliths were then mounted on the sagittal plane on petrographic microscope slides using Crystalbond adhesive and ground by hand on fine grit Micromesh aluminum oxide sandpaper to reveal the otolith primordium and daily otolith increments. (Secor et al. 1991b, Hegg et al. 2013a).

Otolith Microchemical Analysis

Otoliths were analyzed for $^{87}Sr/^{86}Sr$ using a Finnigan Neptune (ThermoScientific) multi-collector inductively coupled plasma mass spectrometer coupled with a New Wave UP-213 laser ablation sampling system (LA-MC-ICP-MS). Analysis for trace element composition was conducted using an Element 2 (ThermoScientific) ICP-MS attached to the same laser ablation system. For each analysis method otoliths were analyzed using a transect moving from the edge of the otolith to the core. This transect was positioned approximately 90° from the sulcus on the dorsal side of the otolith to capture the area containing the clearest succession of rings from the edge to the core. The laser was set to ablate at a constant speed. For $^{87}Sr/^{86}Sr$ ratios the LA-MC-ICP-MS system was set to 10μm/second scan speed, 40μm laser spot size, and 0.262 second integration time. For trace element analysis, the LA-ICP-MS was set to scan at 10μ/second, 30μ laser spot size, and a 1 second sampling time. The trace element analysis included the elements calcium (Ca), strontium (Sr), barium (Ba), Magnesium (Mg), and Manganese (Mn).

Strontium ratio data was corrected based on the global marine signature for each analysis day using a marine shell standard (mean $^{87}Sr/^{86}Sr = 0.709186$, standard deviation = 0.000077, n=535). Elemental counts were corrected to the SRM 610 standard (Jochum et al. 2011) and corrected to calcium using a ten second, within-run

blank. Limits of detection (LOD) for each element were calculated as 3 X SD from the mean of the blank. Expressed as a ratio of elements to calcium resulted in detection limits of; Sr/Ca 0.029 $mm \bullet mol^{-1}$, Ba/Ca 0.023 $mm \bullet mol^{-1}$, Mn/Ca 0.031 $mm \bullet mol^{-1}$, and Mg/Ca 0.022 $mm \bullet mol^{-1}$.

The edges of the otolith were identified within the data using a CUSUM algorithm on Sr and Ca counts, then confirmed visually. Extraneous data was trimmed beyond the edge of the otolith before reversing the sequence to form a data transect from the core to the edge. The distance of each data point from the core, in microns, was calculated using the scan speed and integration/sampling time of the laser and ICP-MS software.

Statistical Analysis

Water chemistry and otolith data were aggregated into chemically distinguishable reaches as detailed by Hegg et al. (2013a) with the inclusion of two groups for hatchery signatures. One chemically distinguishable river group is made up of the Clearwater and Salmon Rivers (CWS). A second group is the Lower Snake River (LSK), which extends downstream from the confluence of the Snake and Salmon Rivers downstream to Asotin. A third group is the Upper Snake River (USK) consisting of the Snake River upstream of the confluence with the Salmon River to Hells Canyon Dam. Finally, the Grande Ronde, Imnaha, and Tucannon Rivers, comprise the fourth river group. Each of these rivers, flowing from the south, runs over the Columbia River basalts, a geological formation of flood basalts (referred to as CRB). Finally, Lyons Ferry Hatchery (LFH) and Nez Perce Tribal Hatchery (NPTH) made up two separate groupings. Hatchery fish were analyzed separately despite the inability to distinguish these groups using $^{87}Sr/^{86}Sr$ in the past (Hegg et al. 2013a). This was done with the hope that multi-tracer data would help to distinguish these groups, and because we expected early juvenile or maternal microchemistry might differ from wild fish.

Duration of Maternal Signature

Otolith transects were analyzed graphically to determine the location of a change between maternally derived and post-hatch chemistry. Strontium isotope ratio changes were gradual and were analyzed graphically and compared to results from the literature. Large, rapid, changes in elemental chemistry in the early otolith allowed for statistical confirmation of the location of chemical change. To confirm the identified location on the otolith did, in fact, represent a significant change in elemental signature, the mean signature from 100μm of otolith growth before the identified change was compared to the mean signature 100μm after, for all fish within each river group. This comparison was done using a two-sided, paired t-test assuming unequal variance ($\alpha = 0.05$) with Bonferroni correction for multiple comparisons. The chemical tracers that showed the most significant change across river groups were then used to develop a multivariate change-point algorithm to determine the otolith location of the maternal/natal change for individual fish.

We tested two change-point methods for their ability to identify the location of the maternal/natal chemical transition for individual otoliths. Both were applied to the data between 150μm and 350μm from the core of each otolith. The first 150μm was excluded so as to avoid the known peak in Mn/Ca near the core (Brophy et al. 2004, Ruttenberg 2005), while covering the location on the otolith where the presumed maternal/natal change occurs. The first change-point method tested was the multivariate {ecp} package for R, which used the three most significant elemental tracers from the paired t-test above (James and Matteson 2014). Additionally, we applied a univariate change-point algorithm from the {changepoint} package for R (Killick and Eckley 2013). This univariate approach used only the most significant chemical tracer from the prior paired t-test. The univariate change-point algorithm was applied using the "AMOC" (At Most One Change-point) procedure and an asymptotic penalty, for changes in both mean and variance.

Variation in Maternal Signature

To determine the degree to which maternal signatures vary we fit a linear model to the maternal $^{87}Sr/^{86}Sr$ signatures of all known juvenile fish and the known average $^{87}Sr/^{86}Sr$ of the river in which they were captured. Under the null hypothesis that all fish maintain an ocean signature we would expect the slope of this regression to be zero, with an intercept of 0.70918, the global ocean signature. A significant slope other than zero, with an intercept other than 0.70918 would indicate that maternal signatures vary with maternal equilibration to the spawning stream.

Stability of Maternal Signature

During the course of analysis, we noted that the mean $^{87}Sr/^{86}Sr$ in the early otolith (<150μm from the otolith core) of the CWS and NPTH groups appeared to differ. This was striking because contributing mothers of both groups inhabit similar water chemistries from the Clearwater River prior to spawning. Further, we noted that otolith chemistry during this early period appeared to change during development in both groups, with opposite slopes. Chemistry this early in the otolith is likely to reflect chemistry in the egg (Boyd et al. 2010), a period whose rate of chemical change has not been well studied and which some authors claim to be a closed system chemically and isotopically (Volk et al. 2000, Elsdon et al. 2008). To test for differences between these groups we tested the mean $^{87}Sr/^{86}Sr$ ratio between the CWS and NPTH groups using a two-sample t-test. To test for isotopic change within the egg during this isotopically "closed" period we also fit a linear model to the aggregate maternal data in each group to determine the presence and magnitude of change in the maternal signal.

To support our findings, we calculated expected changes in the $^{87}Sr/^{86}Sr$ ratios of the egg under seven scenarios of maternal equilibration and spawning water chemistry (Table 1). In these scenarios, we tested four different maternal equilibration chemistries; mothers equilibrated to the ocean, the Lower Snake River, the Clearwater River (as measured during Oct. & Nov.), and the observed signature at the otolith core (0μm) for known NPTH juveniles taken from the linear model above. For each of these maternal equilibration scenarios the change in $^{87}Sr/^{86}Sr$ was calculated assuming eggs

were laid into Clearwater River water, or into water similar to the well water used at NPTH. As a proxy for NPTH well water we used the signature for the Potlatch River, a nearby river which is representative of the low $^{87}Sr/^{86}Sr$ basalt signature of the area.

The signature observed in the core of NPTH otoliths represents an "intermediate" signature between the Lower Snake and the Clearwater Rivers, an indication that mothers may not be fully equilibrated to the Clearwater River signature at spawning. This "intermediate" signature provided a direct test of whether the changes we observed in the otoliths were supported by our calculations.

Calculations were based on two-component isotope mixing models including both concentration and isotope ratio differences (Faure and Mensing 2004 p. 350, equation 16.11). We calculated the expected change in $^{87}Sr/^{86}Sr$ during the first 80 hours after fertilization, when the egg takes on the majority of its external water (Loeffler and Løvtrup 1970). We then calculated the further change in $^{87}Sr/^{86}Sr$ due to the small amount of water exchange during the period from fertilization to hatch (0.33% of egg volume per day) as estimated by Loeffler and Løvtrup (1970). Calculations were based on values available from the literature. We used egg Sr concentration data for wild and hatchery steelhead from Kalish (1990), average egg volume in Atlantic salmon from Rombaugh and Garside (1982), and changes in Atlantic salmon egg volume over time from Leoffler and Løvtrup (1970). We assumed the number of days to hatch to be 73, the average for the Clearwater River in 2013 (Bill Arnsberg, Nez Perce Tribal Fisheries, pers. comm.).

Results

Duration of Maternal Signature

Graphical analysis of otoliths by known natal location indicated that changes occurred at consistent locations on the otolith for elemental ratios and $^{87}Sr/^{86}Sr$, regardless of river group. However, elemental ratios and $^{87}Sr/^{86}Sr$ did not change simultaneously. Instead $^{87}Sr/^{86}Sr$ exhibited changes at different locations on the otolith than elemental ratios.

Elemental ratios, particularly Mn/Ca and Ba/Ca, showed a marked change beginning at 225μm from the otolith core (Figure 2). These changes were less pronounced in fish from the hatchery.

Comparison of the 100μm segments on either side of 225μm using two-sided, paired t-tests assuming unequal variance ($\alpha = 0.05$) with Bonferroni correction showed that Mn/Ca was highly significant for all groups, while Ba/Ca was significant for all river groups except hatchery fish (Figure 3). Sr/Ca ratios were significantly different only for the USK and LSK groups and LFH. Mg/Ca ratios showed no significant differences.

Multivariate change-point analysis on Mn/Ca and Ba/Ca ratios using the {ecp} package did not provide consistent determination of the location of chemical change in individual otoliths. Similarly, univariate change-point analysis on Mn/Ca using the {changepoint} package resulted in inconsistent determination of the maternal/natal chemical shift at the individual level. Using a value of 225μm appeared to describe the location of the maternal/natal transition as well or better than change-point analysis. Individual variation in the magnitude of the chemical change, as well as data noise, was likely to blame for the difficulty in determining logical change-points at the individual level.

Plots of $^{87}Sr/^{86}Sr$ for each non-hatchery river group showed changes in the signature at approximately 150μm from the otolith core, as much as 100μm earlier than the location of chemical changes in the elemental ratios (Figure 4). Following the initial change in $^{87}Sr/^{86}Sr$ ratio after ~150μm the signature then began moving toward a second stable period near ~250-300μm. The signature for LFH was consistent throughout the life of the fish, with no distinct changes. Fish from NPTH began at a signature near 0.7096, before a sudden transition to a signature near 0.70918 around 150μm, before beginning near 300μm to move toward a signature near 0.7110 toward the end of their life.

Variation in Maternal Signatures

The regression of maternal signatures to the signatures of the rivers in which juveniles were captured resulted in a significant linear model ($p<0.00001$, $\alpha=0.05$) with the form,

$$Maternal\ ^{87}Sr/^{86}Sr\ =\ 0.2673 * Maternal\ ^{87}Sr/^{86}Sr + 0.5197$$

Both the slope and intercept terms were highly significant ($p<0.00001$, $\alpha=0.05$), providing support for the alternate hypothesis that maternal signatures are different from the ocean signature, and significantly influenced by the signature of the natal river.

Stability of Maternal Signatures

Despite mothers experiencing similar $^{87}Sr/^{86}Sr$ regimes, the maternal signatures of CWS and NPTH juveniles were significantly different prior to 150μm in a two-sample t-test ($p<0.00001$). CWS juveniles had a mean maternal $^{87}Sr/^{86}Sr$ signature of 0.7104, while NPTH juveniles had a mean maternal $^{87}Sr/^{86}Sr$ signature of 0.7096 (Figure 5A).

Maternal signatures in both groups also showed significant, but opposing, slopes and intercept values when a linear model was applied to the maternal data in each group, indicating changes in chemistry within the egg (Figure 5B). The linear model fit to Clearwater River juveniles returned an intercept of $^{87}Sr/^{86}Sr = 0.7101$ ($p=<0.00001$, $\alpha=0.05$) and a slope of .00000314 microns ($p=0.0016$, $\alpha=0.05$). Variability in the data was high ($R^2 = .0115$). Juveniles from NPTH were fit to a linear model with an intercept of $^{87}Sr/^{86}Sr = 0.7098$ ($p=<0.00001$, $\alpha=0.05$) and a slope of 0.00000236 microns ($p=0.0025$, $\alpha=0.05$). Variability in the NPTH juvenile data was also high ($R^2 = 0.0102$).

Our calculation of the expected change in egg maternal signatures indicated that $^{87}Sr/^{86}Sr$ can exhibit changes nearing 0.0001 between the time eggs are laid and when they hatch in some cases (Table 1). The degree of change was driven largely by

concentration differences, with mothers equilibrated to the high concentration of the ocean showing little change. The largest change in $^{87}Sr/^{86}Sr$ signature (0.00094) was seen for mothers equilibrated to the "intermediate" signature observed in NPTH fish, with eggs laid into NPTH well-water. This change, interestingly, is very similar to the significant difference (0.0009) between the mean $^{87}Sr/^{86}Sr$ maternal signatures of the Clearwater and NPTH groups above (Figure 5A). In this case, the egg changed its $^{87}Sr/^{86}Sr$ ratio by 0.00005 in the direction of the ambient water between initial swelling and hatch, supporting our observation of a slope in maternal signatures in Clearwater and NPTH juveniles (Figure 5B). In all cases approximately half of the $^{87}Sr/^{86}Sr$ ratio change occurred in the first 80 hours after hatch, with the subsequent change occurring slowly during the period after hatch, further supporting the observation of a slope in $^{87}Sr/^{86}Sr$ signature prior to 150μm in the otolith.

Discussion

Connecting maternal migratory behavior with the behavior and ecology of their progeny can reveal important details in the ecology of a population. In the case of fish, the maternally derived chemistry stored in the core of otoliths provides important clues about the behavior of mothers. This maternally derived chemistry has been particularly effective as a signature to identify ocean residence for partially migratory salmonid populations (Kalish 1990, Volk et al. 2000, Miller and Kent 2009, Shippentower et al. 2011, Liberoff et al. 2015). Recent work has extended this tool, using $^{87}Sr/^{86}Sr$ ratio to infer the degree of anadromy in multiple inland populations of steelhead (Courter et al. 2013). Additional studies have cited a period of maternal influence near the core of the otolith, however the duration and chemical makeup of this maternal signature is vague (Barnett-Johnson et al. 2008, Miller et al. 2011, Hegg et al. 2015b).

While the use of maternal Sr/Ca signature as a marker of anadromy has been validated (Kalish 1990, Zimmerman 2005), very little information is available regarding the duration of this maternal signature. Several elemental tracers have been

proposed as markers of the otolith core, including Ba/Ca and Mn/Ca, but the origin of these elevated elemental ratios may have more to do with juvenile ontogeny and formation of the core itself than maternal behavior (Brophy et al. 2004, Ruttenberg 2005). Whether these elemental systems change in concert with a single developmental stage, or whether there are asynchronous patterns of chemical changes during development has not been tested.

The hatching of juvenile fish or alternately, the moment of first exogenous feeding, is usually cited as the ontological event that precipitates a change between maternal and natal chemical signatures. The assumption made in most studies is articulated by Volk et al. (2000); that the egg makes up a closed system reflecting the chemistry of the mother during the time at which the eggs are sufficiently developed to close to outside chemical influence. Under this assumption, the juvenile otolith only begins to equilibrate to the external chemistry of the river after hatching when it begins to interact directly with the external environment. Some authors have extended the assumption to conclude that the equilibration of $^{87}Sr/^{86}Sr$ must be correlated to the first exogenous feeding (Barnett-Johnson et al. 2008).

Duration of the Maternal Signature

Our data indicate that Mn/Ca and Ba/Ca, and to a lesser degree Sr/Ca, appear to mark a sharp transition in the otolith chemistry of juvenile fish at 225μm from the otolith core. (Figure 2). The simultaneous changes in these elements argue for an underlying ontological change in the juvenile, however it is unclear whether this signals hatch, the onset of exogenous feeding, or another physiological or external driver. There is considerable individual variation in the magnitude and location of this change, however, making individual determination difficult and indicating that individual conditions may play a large role in this chemical change.

The results of our $^{87}Sr/^{86}Sr$ analysis show that in contrast to elemental signatures, $^{87}Sr/^{86}Sr$ ratios begin to change at 150μm from the otolith core (Figure 3). At this point the signature moves steadily toward the signature of the natal river, reaching a stable plateau between ~250μm and ~300μm depending on the population.

This change in signature is especially visible in juveniles from the CWS and CRB groups, natal locations with $^{87}Sr/^{86}Sr$ values far removed from the global marine signature.

The difference in the timing of change between elemental and $^{87}Sr/^{86}Sr$ isotopic ratios is interesting. Strontium ratios in our study begin to change at 150μm, ~75μm earlier than do elemental signatures (225μm). This distance corresponds to roughly 12 - 19 days, based on the range of known Chinook growth rates in the basin (Zabel et al. 2010). Further, experimental results indicate that otolith radius at emergence varies from 173μm to 259μm (Paul Chittaro, unpublished data). It is reasonable, based on this difference in timing, to assume that the shift in elemental ratios and $^{87}Sr/^{86}Sr$ are synchronized with different ontogenetic changes in the juvenile fish.

Since hatching represents the first time the egg is capable of a large degree of ion exchange with the surrounding water, the change in $^{87}Sr/^{86}Sr$ ratio at ~150μm likely represents hatching. Strontium and calcium uptake in juvenile fish begins to climb steadily after hatching, and experimental results indicate that it is possible to isotopically mark non-feeding salmonid fry using water spiked with ^{84}Sr (Hayes et al. 1946, Yamada and Mulligan 1987, De Braux et al. 2014). Further, between 30 and 83% of strontium is incorporated into the otolith from the surrounding water, enough to begin changing the $^{87}Sr/^{86}Sr$ signature once the fish begins exchanging ions directly with the surrounding water through its gills and endothelium (Hayes et al. 1946, Walther and Thorrold 2006).

Previous research indicates that the onset of exogenous feeding could be accompanied by a change in elemental ratios. Experimental evidence indicates that the rate of strontium intake increases to an even faster rate following first-feeding (Yamada and Mulligan 1987), and that magnesium concentration also increases 12-15 days after juveniles hatch (Hayes et al. 1946). The physiological changes that accompany the onset of exogenous feeding could change the regulation of these elements in relation to calcium within the fish's tissues, as well as changes related to the intake of food sources with differing concentrations of elements as compared to

that of the yolk sac. The microchemical change also broadly correlates with a first-feeding microstructural check at 235-240μm determined by Barnett-Johnson (2007) in Chinook salmon from California's Central Valley.

Taken together our data suggest that both elemental ratios and $^{87}Sr/^{86}Sr$ ratios provide information on maternally derived chemical influence on the otolith. However, the change from maternal to natal chemistry in $^{87}Sr/^{86}Sr$ and elemental data appear to correspond to different ontological stages. Changes in $^{87}Sr/^{86}Sr$ ratio appear to correspond to the hatching of the larval fish ~150μm, with equilibration continuing until sometime at, or soon after, the onset of exogenous feeding. Elemental ratios of manganese, barium, and strontium appear to reflect the onset of exogenous feeding at ~225μm with a more sudden shift to some equilibrium. While the equilibration of $^{87}Sr/^{86}Sr$ seems to coincide with the change in elemental data, we have no evidence to indicate that this is necessarily causal.

Variation in Maternal Signature

Although Sr/Ca in the core of the otolith can be used to determine maternal anadromy, long inland migrations may attenuate the ocean-derived maternal signature, resulting in variation in the maternal signature. Rieman et al. (1994) showed that Sr/Ca was an incomplete predictor of resident and anadromous maternal behavior in juveniles from a population of *O. nerka* in Idaho, 900km from the ocean. Bacon et al. (2004) found that inland populations in the Pacific Northwest had attenuated or nonexistent Sr/Ca and $^{87}Sr/^{86}Sr$ maternal signatures and Donohoe et al. (2008) showed that a metric of migratory difficulty could explain attenuation of the maternal signature.

This indicates that mothers who spend significant time in freshwater equilibrate to some degree to the freshwater chemistry along their migratory path and in the natal stream. This equilibration should also be reflected in maternally derived $^{87}Sr/^{86}Sr$ ratios. Our results show that maternal $^{87}Sr/^{86}Sr$ signatures of juvenile Snake River fall Chinook salmon do vary significantly from the global marine value (Figure 6). As might be expected, the maternal signatures vary in the direction of the water chemistry

of the natal stream, indicating a large degree of maternal equilibration not just to the mainstem river in which they reside for most of their upstream migration but to the spawning tributary itself. This is especially evident in fish captured from the Clearwater and Grande Ronde Rivers, spawning reaches whose $^{87}Sr/^{86}Sr$ signatures deviate considerably from the global marine signature, making these changes more apparent. This variation in maternal $^{87}Sr/^{86}Sr$ signatures indicates that for inland populations, maternal $^{87}Sr/^{86}Sr$ ratio does not correlate perfectly to marine residence of the mother.

This result, it seems, would argue that care should be taken in using $^{87}Sr/^{86}Sr$ as a marker of maternal anadromy. However, Courter et al. (2013) used $^{87}Sr/^{86}Sr$ to infer the production of anadromous juveniles in resident rainbow trout in the Yakima River, another inland system in the Columbia River basin with similar inland migration distances. Their success may indicate some degree of species or life-history specific retention of ocean signatures in spawning female salmon. However, without an understanding of these hypothetical species or life-history specific mechanisms, our results indicate caution in interpreting maternal $^{87}Sr/^{86}Sr$ signatures from the otoliths of populations with significant migration distances. This is particularly the case given that our results indicate that the $^{87}Sr/^{86}Sr$ signature of the egg can vary from that of the mother, and that the maternal signature may not be stable in all cases.

Stability of Maternal $^{87}Sr/^{86}Sr$ Signature

The apparent differences, and significant slope of change, in the maternal $^{87}Sr/^{86}Sr$ ratio of fish from the Clearwater River and NPTH groups challenge the assumption made in many studies that the egg is a closed system, reflecting only the chemical signature of the mother. Spawning females used as broodstock at NPTH are captured at Lower Granite dam and make up a random subsample of the run (Milks and Oakerman 2016). They are then transported to the NPTH complex where they are housed in Clearwater River water until they are spawned (Bill Arnsberg, Nez Perce Tribal Fisheries, pers. comm). Adults who spawn naturally in the Clearwater River move upstream past Lower Granite dam, through the remainder of the Snake River

and into the Clearwater River, spawning at a similar time. Thus, adults taken for broodstock at NPTH ultimately spend as much, or perhaps more, time exposed to Clearwater River water as adults who spawn naturally in the river. Despite this, the mean maternal signature of NPTH juveniles is significantly lower than that of juveniles originating in the Clearwater River (Figure 5A).

Because adult spawners experience similar water chemistries before spawning in both groups, the discrepancy in their progeny's maternal signature is best explained by changes in the isotopic signature of the egg after spawning. The eggs of the two groups of fish do experience different water chemistries between spawning and hatch, providing a mechanism for the observed difference in maternal $^{87}Sr/^{86}Sr$ if the egg takes up Sr from the surrounding water.

While NPTH adults are kept in Clearwater River water before spawning, spawned eggs are reared in a different water source. This water is a mix of water from the Clearwater River itself and a well drawing from an aquifer below the river which changes through the year. As the river level rises in the spring, the proportion of Clearwater River water increases (Bill Arnsberg, Nez Perce Tribal Fisheries, pers. comm.). The Potlatch River and Lapwai Creek, both nearby low-elevation streams influenced by the same basalt sources as the aquifer from which well water is taken, exhibit signatures of 0.7089 and 0.7068 respectively (Hegg, unpublished data). The mixing of low $^{87}Sr/^{86}Sr$ ratio water influenced by the Columbia River basalts, and the higher $^{87}Sr/^{86}Sr$ water from the Clearwater River which is influenced by older metamorphic rocks upstream, creates the characteristic movement from low $^{87}Sr/^{86}Sr$ ratio early in NPTH otoliths to higher $^{87}Sr/^{86}Sr$ signatures more reflective of the Clearwater River as fish age (Figure 3). Therefore, it is possible that the differing signatures of the water in which eggs at NPTH and in the Clearwater River incubate is responsible for the difference we observed in their maternal signatures.

The idea that the maternal signature of eggs might change seems to be in conflict with the idea that the egg is a closed system (Volk et al. 2000). It is also in contrast to several studies showing that the Sr/Ca chemistry of eggs does not change

(Waite et al. 2008, Gabrielsson et al. 2012), and that Sr/Ca signatures are inherited from mothers directly (Kalish 1990, Rieman et al. 1994). However, it should be kept in mind that these studies have been conducted in fish with relatively short spawning runs, whose strontium and calcium concentrations are relatively high compared to the freshwater signatures into which their eggs are laid. Isotope ratio mixing is highly dependent on the concentration of the sources being mixed (Faure and Mensing 2004). Therefore, it would require a relatively large amount of fresh water introduction into the egg to change either Sr/Ca or $^{87}Sr/^{86}Sr$ if the ocean-acquired maternal contribution is significantly elevated.

Salmon eggs do take in as much as 12-15% of their volume in water during the first hours after being laid, and external calcium is required during the process of water hardening, indicating that strontium would also be absorbed in proportion to its concentration in the water (Potts and Rudy 1969, Finn 2007). Further, the egg does not actively osmoregulate and continues to take on water at an approximate rate of $1/300^{th}$ of its mass per day (Loeffler and Løvtrup 1970). Recent research has shown that eggs can be successfully tagged using isotopes of strontium and barium during this initial uptake of water (De Braux et al. 2014, Warren-Myers et al. 2015). Thus, changes to the $^{87}Sr/^{86}Sr$ signature is possible in the hours after eggs are laid, and before the otolith is formed, creating a difference between the maternal signature of the juvenile otolith and the true maternal signature of its mother at the time the egg was laid. Further, under certain combinations of water and egg chemistry, the slow water exchange during development could create movement in the $^{87}Sr/^{86}Sr$ signature during the period between water-hardening and hatch, much as we observed in NPTH and Clearwater River juveniles.

Our calculations make clear that spawning females must equilibrate substantially to the concentration of freshwater before the $^{87}Sr/^{86}Sr$ signature of the egg could be changed by influx of freshwater (Table 1). The high concentration of Sr in ocean-equilibrated fish effectively buffers changes in $^{87}Sr/^{86}Sr$. But, for females that have substantially equilibrated to freshwater, our calculations show that the $^{87}Sr/^{86}Sr$

signature of the egg can change up to 0.00086 within the first 80 hours after being laid, and as much as 0.00091 by the time of hatch.

The largest calculated change between the mothers' signature and the signature of the egg at hatch was in the case testing NPTH equilibrated maternal signatures, with eggs laid into NPTH well water. In this case the signature changed significantly, and, it should be noted that this change is very close to the value of 0.0009 that we observed between the CWS and NPTH groups, an indication that our calculations are accurately representing the observed shift in $^{87}Sr/^{86}Sr$ for these fish.

Further, our data provide evidence that the signature of the egg can change significantly even after the initial hours of water-hardening. This is shown by the significant slopes of $^{87}Sr/^{86}Sr$ ratio during the maternal period in CWS and NPTH juveniles. Despite large amounts of individual variation, CWS and NPTH maternal signatures show highly significant slopes moving in the direction equilibration to the ambient water, a positive slope in CWS fish and a negative slope in NPTH juveniles (Figure 5B). This is further supported by our calculations showing that a change in $^{87}Sr/^{86}Sr$ ratio in the fourth digit, well within the analytical precision, could be expected in each case.

Conclusions

Maternally derived chemical signatures in fish otoliths, Sr/Ca in particular, have been instrumental in connecting maternal anadromy to the life-history of their progeny. More recently researchers have begun to infer anadromy from maternally derived $^{87}Sr/^{86}Sr$ signatures as well. Beyond determining maternal anadromy, as otolith studies examine ever more detailed early movement and life-stages of juvenile fish it is increasingly important avoid biasing our results by accidentally including maternally derived chemistry. Despite this need, there has been little understanding of when the influence of maternally derived chemistry ends on the otolith. Our study indicates that both elemental and $^{87}Sr/^{86}Sr$ ratios mark ontogenetic changes within larval fish. Further, these signals can be used to determine the end of maternal influence, and the beginning of signatures derived from the water of the natal location. However, our

results show that $^{87}Sr/^{86}Sr$ and elemental data are asynchronous, and likely signal two different ontogenetic changes in the developing fish. We believe it is likely that changes in $^{87}Sr/^{86}Sr$ signal hatching, while elemental signatures of Mn/Ca and Ba/Ca likely signal the onset of exogenous feeding. Further, our results indicate that as female spawners equilibrate toward freshwater microchemical concentrations, the $^{87}Sr/^{86}Sr$ signature of their eggs may shift after they are laid, and in some cases significant changes can occur. Thus, eggs may not directly reflect the maternal signature, complicating the use of $^{87}Sr/^{86}Sr$ as a method for determining maternal anadromy in inland populations with significant migrations. Further work is needed to verify the duration and stability of maternal signatures under varying elemental concentrations and signatures, and the relationship of elemental signatures to early ontological changes in larval fish.

Tables

Table 2.1 - Calculated change in $^{87}Sr/^{86}Sr$ in eggs between laying and hatch

The change in $^{87}Sr/^{86}Sr$ signature was calculated for six different scenarios of maternal equilibration and laying location. In the table strontium concentrations increase from top to bottom, and decrease from left to right. The largest changes within the egg were calculated for scenarios with low maternal concentration and high concentration in the surrounding water (grey outline). This indicates that concentration likely controls the change in strontium ratio of the egg. Calculations were based on sampled water chemistry and values from the literature. Strontium concentration in fish tissue was taken from Kalish et al. (1990), measured in ocean and freshwater reared steelhead. Changes were calculated for the first 80 hours, when the egg takes in the majority of external water, as well as the remaining 73 days of maturation (the average estimated days to hatch for Clearwater River juveniles in 2013). The furthest right-hand column represents the signature observed at the core of known NPTH juveniles, equilibrating to a signature similar to the well-water used to rear NPTH eggs.

Mother's signature (starting signature of egg)

High Concentration ⟶ Low Concentration

Signature of Surrounding Water (Low Conc. ⟵ High Conc.)	Ocean $^{87}Sr/^{86}Sr$ = 0.70918 Sr ppm = 4.73	Lower Snake River $^{87}Sr/^{86}Sr$ = 0.70956 Sr ppm = 0.88	Clearwater River $^{87}Sr/^{86}Sr$ = 0.71321 Sr ppm = 0.88	Observed signature of NPTH fish at 0µm $^{87}Sr/^{86}Sr$ = 0.70981 Sr ppm = 0.88
Potlatch River (similar to NPTH well water) $^{87}Sr/^{86}Sr$ = 0.70891 Sr ppm = 0.15	First 80h = 0.00000 To hatch = 0.00001 Total Δ = 0.00001	First 80h = -0.00003 To hatch =-0.00003 Total Δ = 0.00006	First 80h = -0.0002 To hatch = -0.0002 Total Δ = -0.00040	First 80h = -0.00086 To hatch = -0.00005 Total Δ = -0.00091
Clearwater River $^{87}Sr/^{86}Sr$ = 0.71321 Sr ppm = 0.03	First 80h = 0.00001 To hatch = 0.00001 Total Δ = 0.00002	First 80h = 0.00003 To hatch = 0.00004 Total Δ = 0.00007	N/A	First 80h = 0.00004 To hatch = 0.00003 Total Δ = 0.00007

Figures

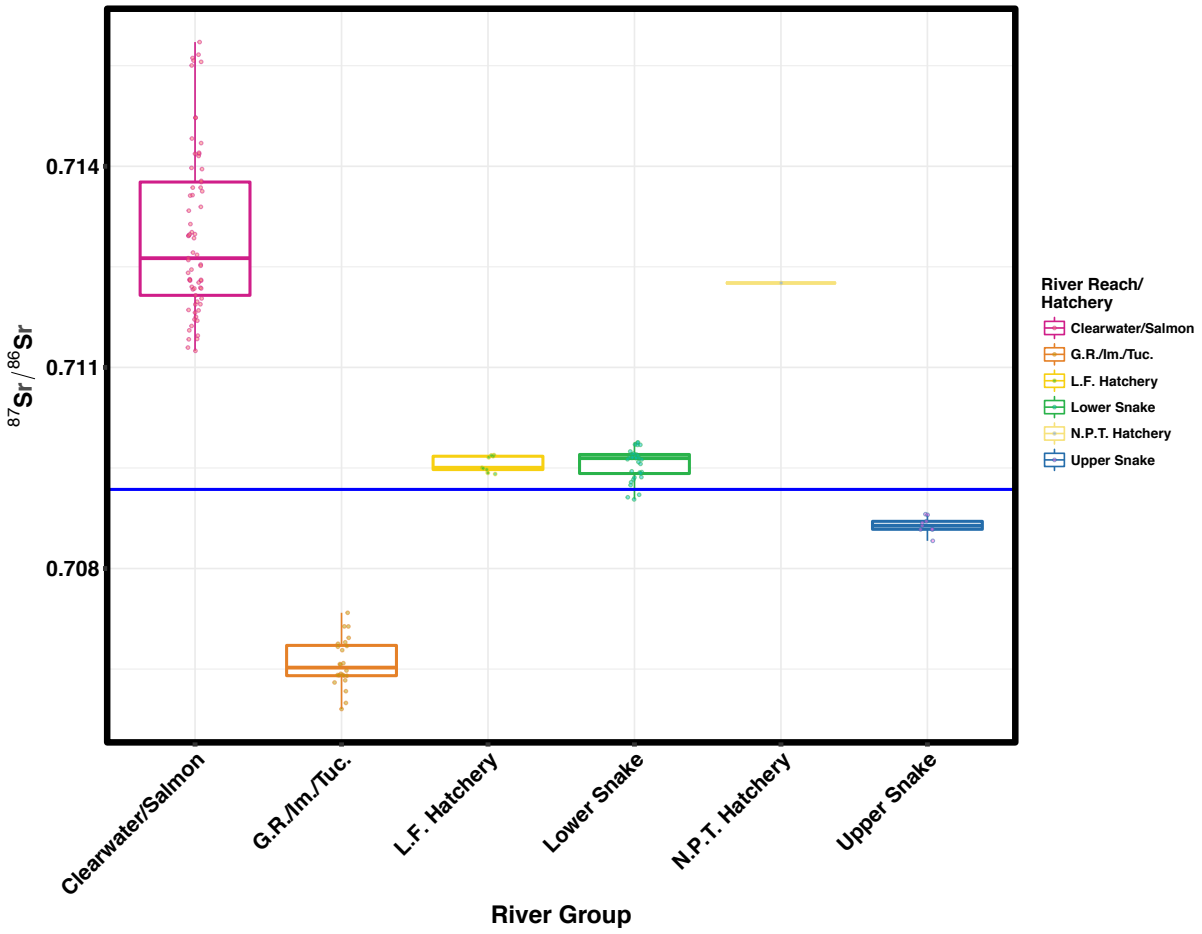

Figure 2.1 - Water $^{87}Sr/^{86}Sr$ Chemistry of the Study Area

Water samples of $^{87}Sr/^{86}Sr$ within the range of Fall Chinook salmon in the Snake River basin show distinct grouping between major river groups in the basin. Lyons Ferry Hatchery is located on the Lower Snake River. The Nez Perce Tribal Hatchery is located on the Clearwater River.

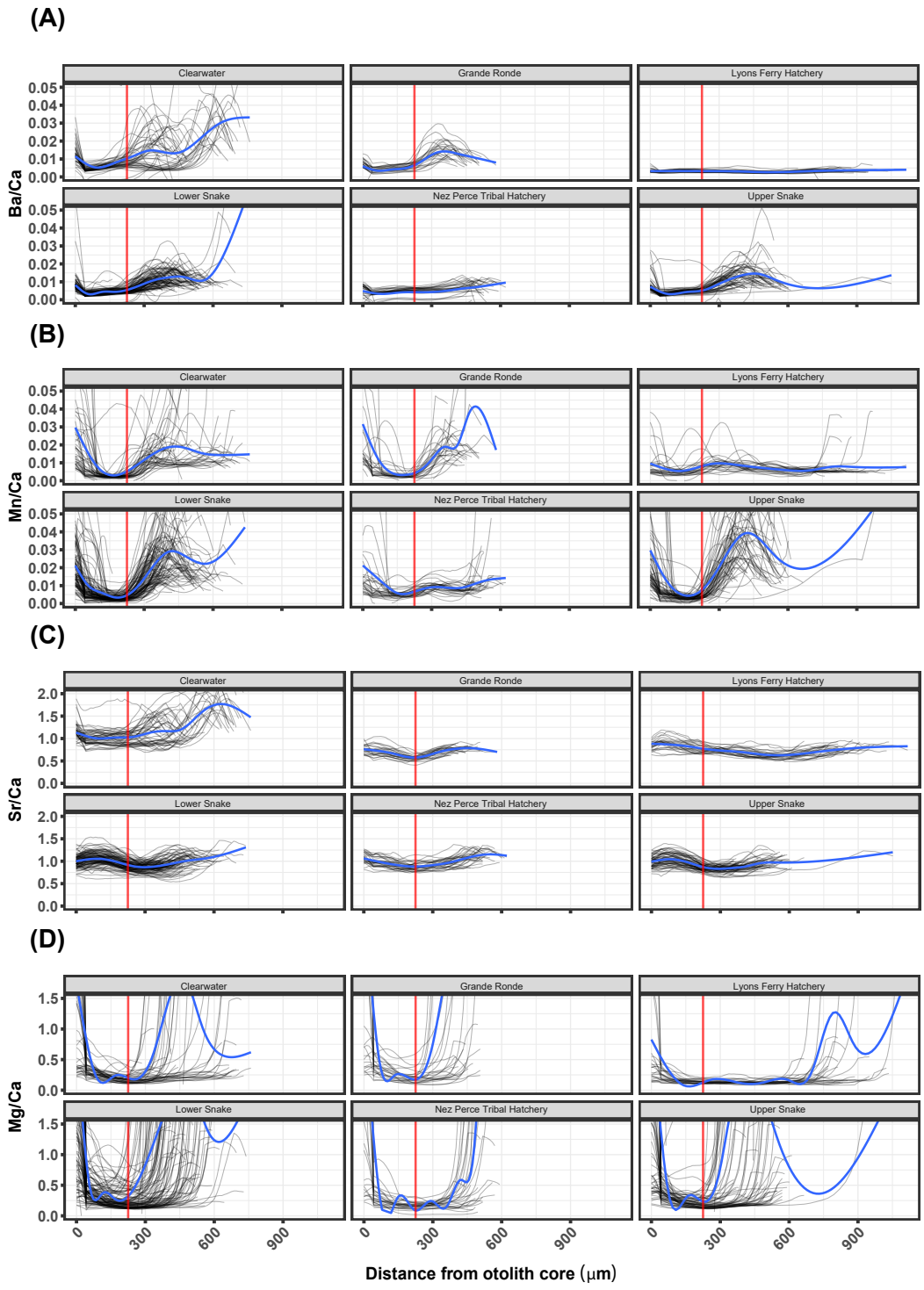

Figure 2.2 - Element to Calcium Ratios for Juvenile Fish from known locations

Plots of individual element to calcium ratios, plotted by river and hatchery grouping, show a shift in chemistry beginning at ~225µm from the otolith core (red

line). This shift is most apparent in Ba/Ca (A) and Mn/Ca (B), and less apparent in Sr/Ca (C) and Mg/Ca (D). Plots are smoothed with a 10-point moving average and exclude high values on the y-axis to maintain detail of the maternal/juvenile transition. Blue lines represent the smoothed average of all individual transects using a generalized additive model.

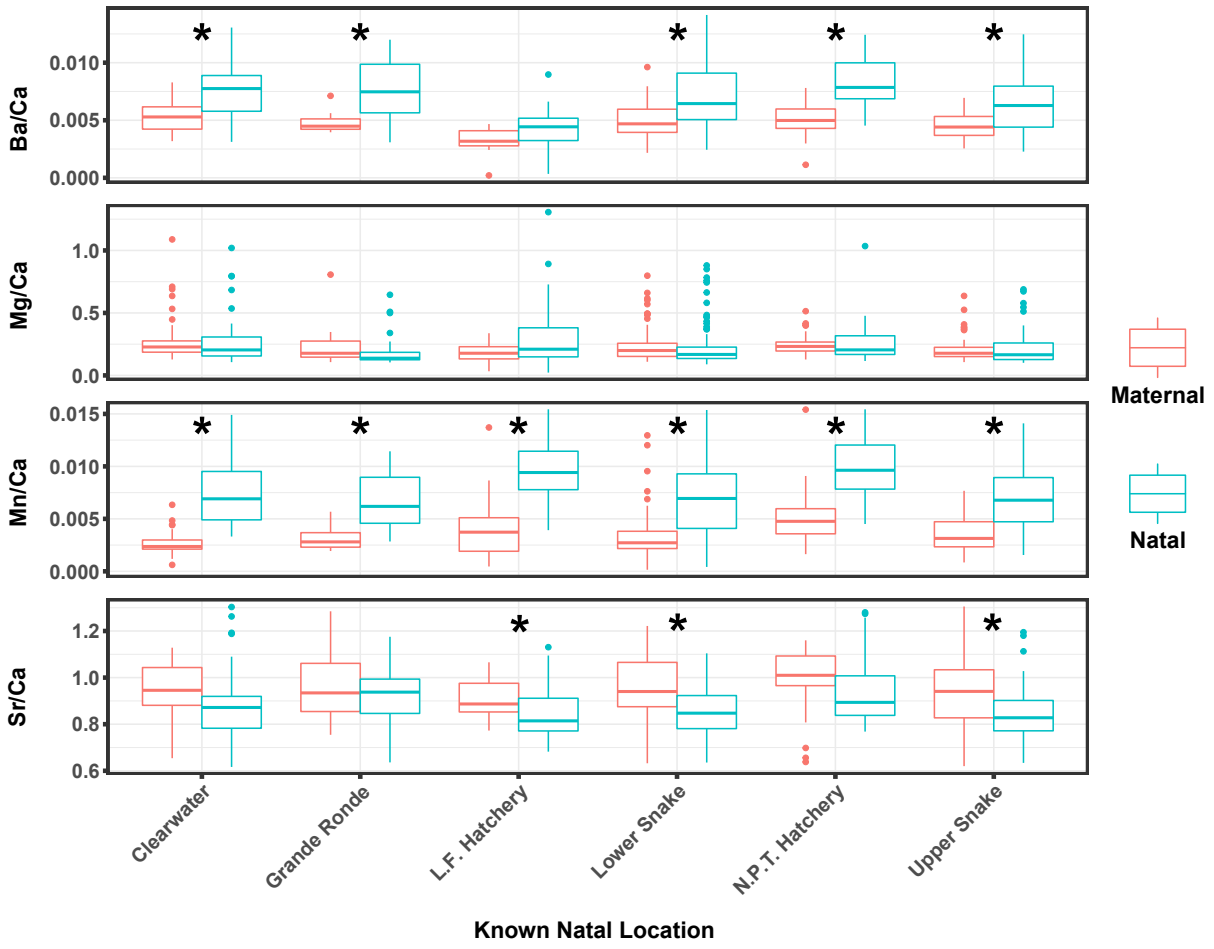

Figure 2.3 - Differences in elemental ratios of maternal vs. juvenile periods

Boxplots show the difference in elemental ratios 100µm before and after the 225µm otolith radius. Asterisks indicate cases in which maternal signatures (red) were significantly different than natal signatures (blue) based on paired t-tests with Bonferroni correction for multiple comparisons.

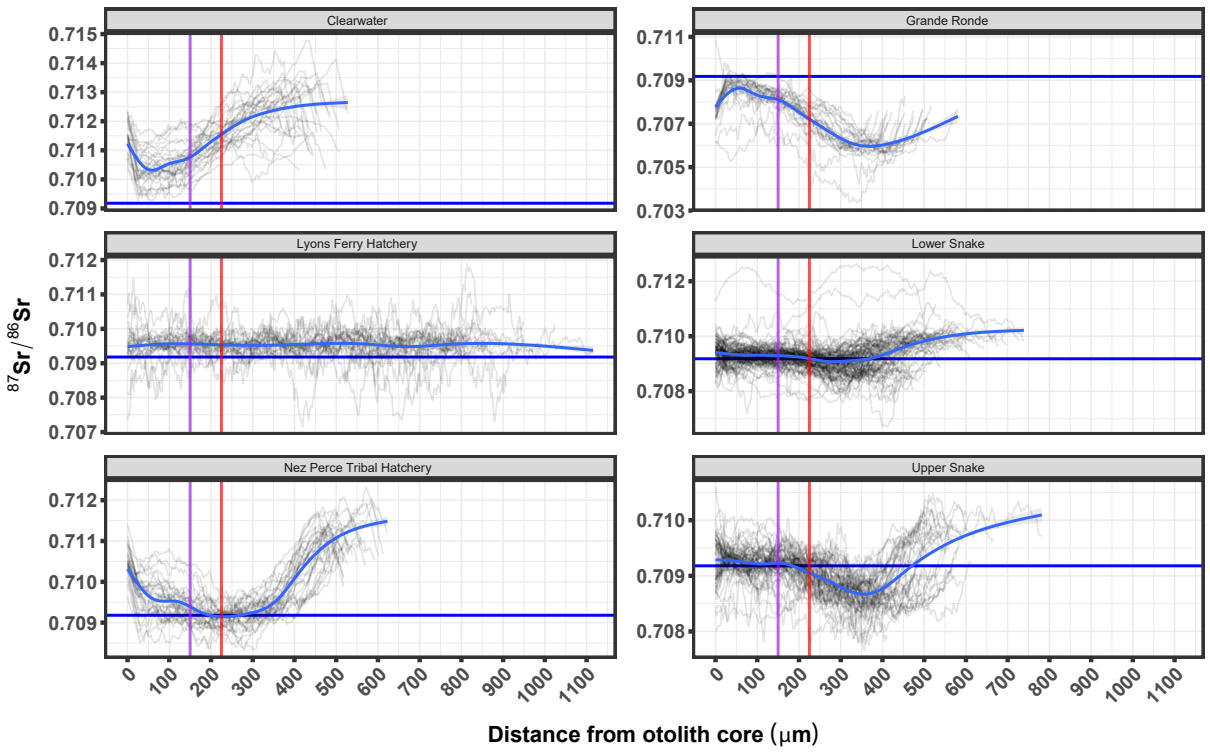

Figure 2.4 - Strontium isotope ratios ($^{87}Sr/^{86}Sr$) of individual fish from known locations

Plots of individual $^{87}Sr/^{86}Sr$ transects show a relatively stable period from the core of the otolith to ~150μm from the otoliths core (purple vertical line). After this point transects slowly equilibrate toward the expected $^{87}Sr/^{86}Sr$ value for their river group. Strontium ratio does not seem to change at 225μm (red vertical line) where elemental ratios show a change, indicating that $^{87}Sr/^{86}Sr$ may be recording a different ontological change within the developing fish. Fish from NPTH equilibrate toward an unknown well-water signature before moving upwards to signature reflecting the Clearwater river as river water is mixed with the hatchery well-water late in the season. Some late-season juveniles were removed from the Clearwater River plot for clarity (n=21) because their transects followed a pattern of movement that suggested hatchery origin and acclimation in unknown water sources. The global marine signature, 0.70918, is noted for reference (horizontal blue line).

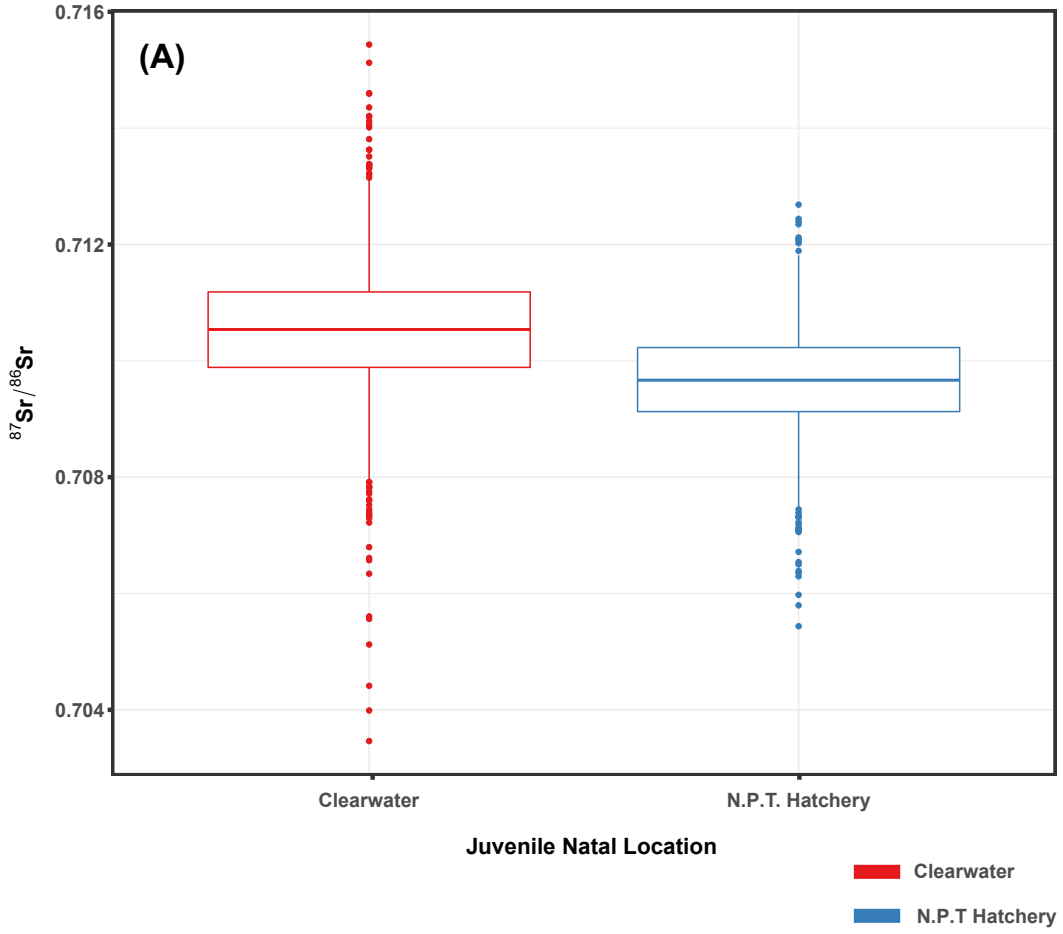
(A)
0.716
0.712
0.708
0.704
$^{87}Sr/^{86}Sr$
Clearwater
N.P.T. Hatchery
Juvenile Natal Location
Clearwater
N.P.T Hatchery

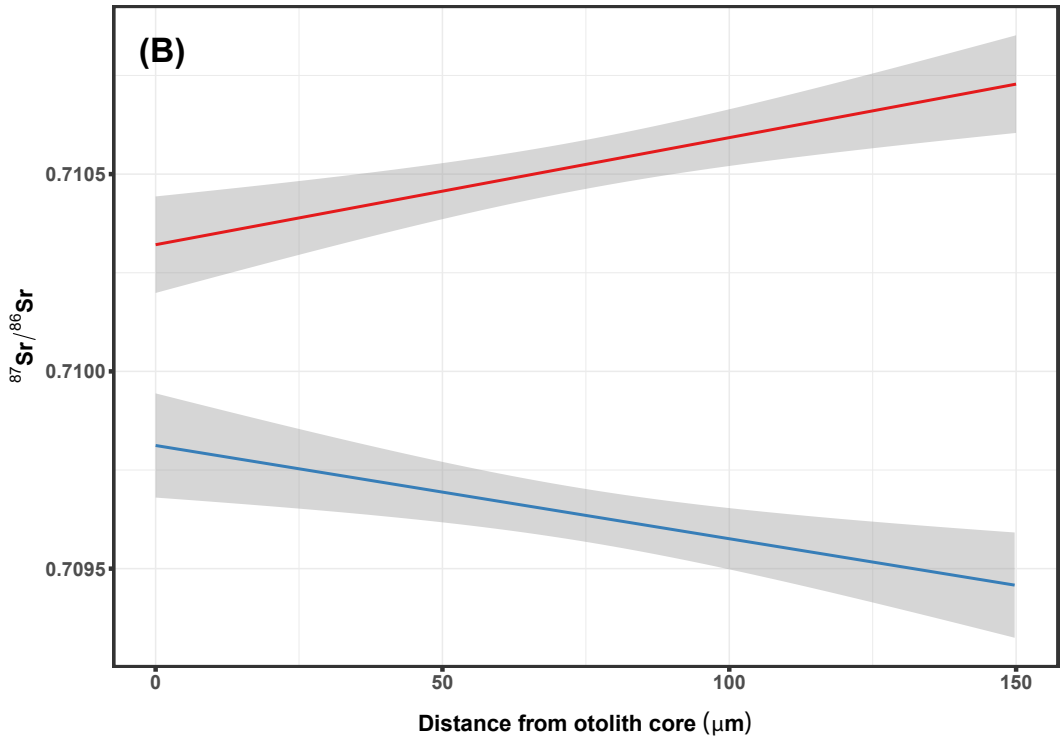
(B)
0.7105
0.7100
0.7095
$^{87}Sr/^{86}Sr$
0
50
100
150
Distance from otolith core (μm)

Figure 2.5 - Mean maternal signatures of hatchery and natural origin Clearwater juveniles

Despite NPTH adults being exposed to the same, or more, time in Clearwater River water, their progeny exhibit significantly lower $^{87}Sr/^{86}Sr$ maternal signatures (A) than juveniles spawned naturally in the Clearwater River (T-test, $p<0.0001$). Eggs at NPTH are reared in well-water, not Clearwater River water. Further, the maternal signatures of juveniles from each location exhibit significant slopes in the direction of the signature of their natal water sources, indicating equilibration of the egg signature before hatch (B). Dark blue lines represent the slope of the aggregate data, while thin lines represent individual fish.

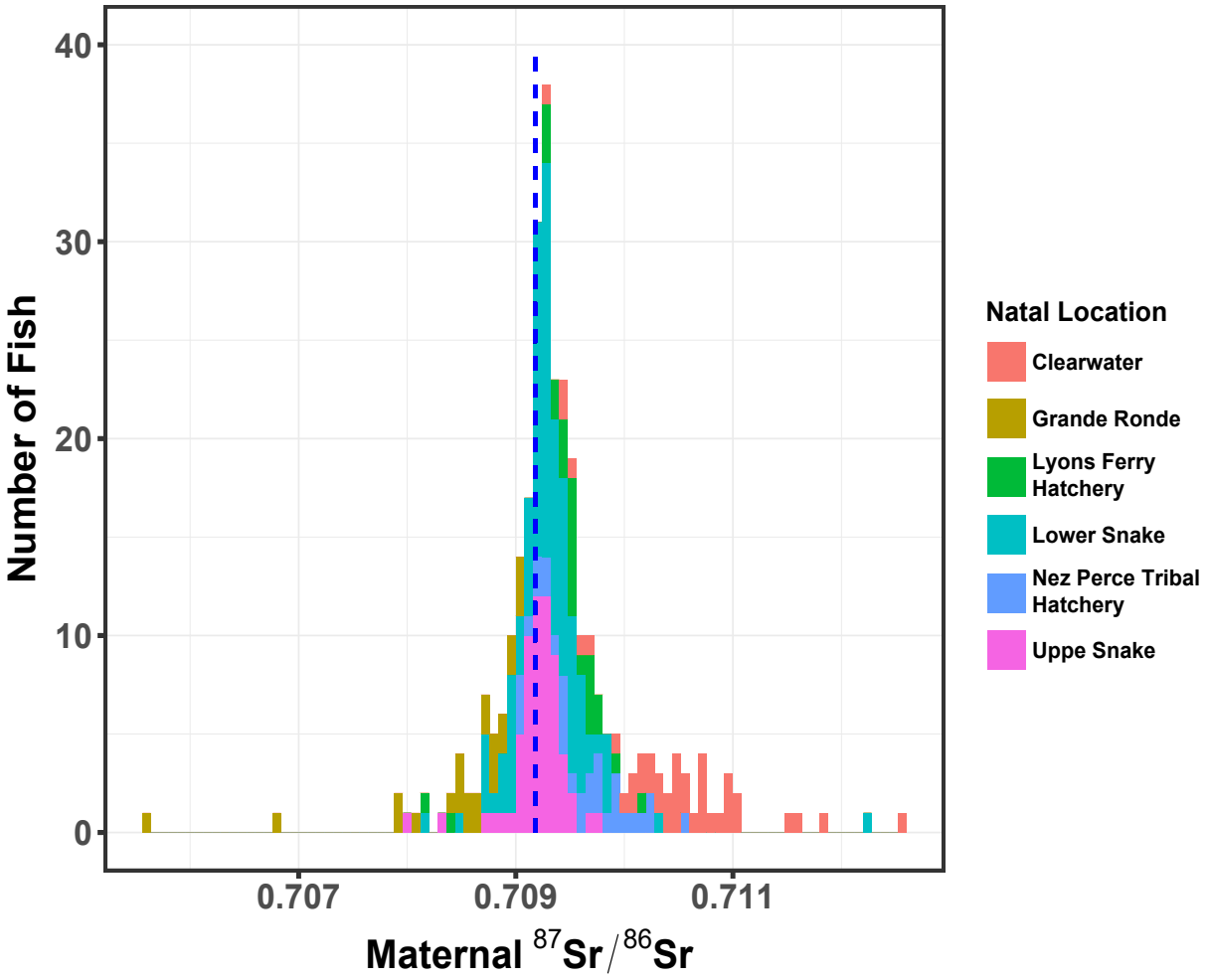

Figure 2.6 - Variation in Maternal $^{87}Sr/^{86}Sr$ signature

Maternal $^{87}Sr/^{86}Sr$ signatures of known origin juvenile fish vary significantly from the global marine value of 0.70918 (dotted line). Individual fish are colored by their known location, showing that maternal signatures vary in the direction of the water chemistry of the natal stream (Figure 1). Means for each group are; Clearwater (0.71050), Grande Ronde (0.70845), Lyons Ferry Hatchery (0.70946), Lower Snake (0.70931), Nez Perce Tribal Hatchery (0.70964), Upper Snake (0.70920).

Chapter 3: Let's Do the Time Warp Again: Non-linear time-series matching as a tool for mining temporally structured data in ecology

"The problem of aggregation and simplification is the problem of determining minimal sufficient detail... In so doing, we trade off the loss of detail or heterogeneity within a group for the gain of predictability; we thereby extract and abstract those fine-scale features that have relevance for the phenomena observed in other scales."

- Simon A. Levin (1992)

Abstract

Ecological patterns are often fundamentally chronological. Challenges exist, however, in generalizing this data from the scale of the individual or population to broad scale processes. Generalization of data inherently involves loss of detail. Temporal data in particular contains information not only in data values but in the temporal structure which is lost when these values are aggregated to provide point estimates. Dynamic Time Warping (DTW) is a measure of similarity which can be applied to compare two time-series, or any dataset which can be expressed sequentially, that which has become popular in computer science, voice recognition, economics and big-data analytics because of its ability to efficiently compare patterns in large time-series datasets despite temporal offsets that confound other time-series matching methods. As technological advances have increased the volume and detail available in small-scale ecological data DTW may be an attractive technique for analyzing this data while taking advantage of the increased information contained in these high resolution, temporal datasets. Accretionary biological material, such as tree rings, mussel shells or fish otoliths record valuable chemical information across the

lifetime of individuals. New technologies have dramatically increased the volume and detail of information contained in fish otoliths, but analysis techniques often do not take into account this newly uncovered data richness. In this study we compare the classification of natal origin and migrational movements of a threatened population of Chinook salmon using DTW and a more traditional discriminate-function based approach. Our objective was to test whether DTW of otolith data could reveal additional information regarding fish movement that could improve our classification over conventional techniques. Our results suggest that DTW is capable of detecting subtle behavioral patterns withing otolith datasets despite random asynchronous differences in the movement of individual fish. While DTW alone was unable to classify fish as consistently at traditional methods, it provided a powerful addition to discriminate function classification that was robust to behavioral factors that confounded the discriminate function alone.

Introduction

The study of ecology is fundamentally chronological, and the problems facing ecologists, and the data they collect, often reflects this temporal nature (Wolkovich et al. 2014). Populations rise and fall over years. Climate, predation, parasitism, and competition vary across time; affecting behavior, survival, and reproduction of populations. Consequently, researchers to construct ever more complex models to explain and predict these temporal dynamics. At the heart of these analyses is the necessity to translate data from small scales into meaningful metrics that can explain larger phenomenon, but doing so inevitably results in information loss (Levin 1992). As Levin shows, the generalization required to translate data to larger scales results in a loss of information through loss of detail and specificity. Time-series data in particular, contains information not just in the values of the data, but in the order of those values (Chatfield 2003, Cressie and Wikle 2011). Collapsing this data into discrete time-points, or overall descriptive statistics, removes temporal information, some of which may be more useful than we realize. New time-series analysis tools that have gained

prominence in other fields may allow more nuanced treatment of time-series data in ecology, decreasing the loss of information in time-series data due to aggregation.

The data "aggregation problem", information loss with increasing data simplification, is not new (Theil 1954). The name itself descends from a subfield spawned in economics to deal with the theoretical and practical effects of relating aggregate data to predictions of more specific economic indicators, and vice-versa (Orcutt et al. 1968, Wei 1979, Schlicht 1985, Chiappori and Ekeland 2011). It has also generated numerous publications in statistics (Clark and Avery 1976, Tiao and Wei 1976). This discussion has also appeared in ecology in terms of the predictive ability to model complex underlying dynamics with larger scale aggregate data (Costanza and Maxwell 1994, Syphard and Franklin 2004), and how to account for the error propagation that results from aggregating data across scales (Gardner et al. 1982).

Levin (1992) argues convincingly that simplifying data from the individual to the ecosystem scale should be done with the goal of thoughtfully preserving "minimal sufficient detail" to inform models at larger scales. However, as technology drives increases in the volume and richness of data at the individual and local scale (Hampton et al. 2009, Laurance et al. 2016), it is reasonable to assume that small-scale data may now contain more meaningful data with which to inform our models. Because so much of the data used by ecologists is temporal in nature, recent advances in time-series analysis techniques may allow researchers to take advantage of the increased data richness and structuring small scale temporal data, minimizing information loss due to aggregation.

Techniques for shape-based matching of time-series have improved greatly in recent years (Aghabozorgi et al. 2015, Sakurai et al. 2015). Comparison and clustering of time-series patterns has been an active area of research in speech recognition for many years (Myers and Rabiner 1981, Muda et al. 2010), followed closely by efforts in economics to forecast market movement based on known time-series patterns (Lee et al. 2012, Wang et al. 2012). However, the calculations needed to compare time series were, until relatively recently, prohibitively processor intensive. The boom in

computing power and the associated increase in the size of stored data has created a need for big-data analytical techniques to efficiently mine large amounts of time-series data and provide real-time information on its structure (Keogh and Pazzani 2000, Sakurai et al. 2015). At the same time, theoretical advances have dramatically decreased the processing time and efficiency for these calculation intensive methods. This has allowed them to be applied to even the biggest data questions, and analysis packages containing these routines are now available on multiple platforms (Rakthanmanon et al. 2012a, Gulzar 2015, Sarda-Espinosa 2017a).

One of the most popular time-series techniques is Dynamic Time Warping (DTW). DTW distance is a distance measure (similar to the familiar Euclidian or Mahalanobis distance measures) which describes the similarity of two time-series, or any dataset which can be expressed sequentially. It was first developed as a method to match sounds in speech recognition, where the speed and accent of speakers can vary despite the word or phrase being the same, creating phase shifts that are difficult to match using most distance metrics (Sakoe and Chiba 1978, Myers and Rabiner 1981). DTW excels at matching similar time series which vary temporally and has been shown to be highly efficient for classification of time series data (Al-Naymat et al. 2009, Rakthanmanon et al. 2012b).

The DTW distance describes the relative distance between two time-series based upon the amount of "warping" necessary to align them. An accessible and concise explanation is available in Ratanamahatana and Keogh (2004). Briefly, a matrix is created, in which each cell represents the distance needed to match each point in one time-series to the most similar point in the other, regardless of temporal location (Figure 1A). A dynamic programming algorithm is then applied to find the least-cost path across this matrix. In the case of two identical time-series the least cost path would be a perfect diagonal. For misaligned series, the algorithm matches each point to the closest point on the comparison time-series without regard to time, warping the temporal dimension to match the series (Figure 1B). The one-to-many point-matching determined by the dynamic programming step describes the path

through this matrix, called the warping path, needed to shift each point to align with the comparison series. The more warping needed to match the series, the overall departure from a perfect match, the further the series are from each other in DTW distance.

By calculating the DTW distance for all combinations of multiple time-series, the resulting DTW distances can be used within existing clustering and classification methods to determine similar groups of time-series (Mueen and Keogh 2016, Sarda-Espinosa 2017b). DTW clustering methods can then be extended to classification of new data through the use of "representative" time-series calculated for each cluster, known as centroids or prototypes. By calculating a centroid time-series for each cluster, new data can then be assigned based on the DTW distance of new data to the centroid of each cluster using nearest-neighbor classification, which has been shown to be very robust (Kate 2015). Numerous centroid calculation methods exist, from simple averaging to iterative barycenter averaging based on DTW distance, and fuzzy methods (Petitjean et al. 2011, Sarda-Espinosa 2017b).

The DTW calculation, with the requirement of multiple matrix calculations and dynamic programming optimizations is calculation intensive. To speed up the calculation, the distance matrix is often limited to a window surrounding the diagonal using various techniques, the most popular of which is the Sakoe-Chiba window (Sakoe and Chiba 1978). Further advances have allowed the process to be sped up even further, making accurate DTW searches of extremely large datasets possible (Al-Naymat et al. 2009, Rakthanmanon et al. 2012a).

Despite their increasing popularity in big-data mining (Keogh and Pazzani 2000, Sakurai et al. 2015), artificial intelligence & robotics (Xu et al. 2014, Cheng et al. 2015), economics (Lee et al. 2012, Wang et al. 2012), healthcare (Ortiz et al. 2016), and speech recognition (Pi-Yun Chen et al. 2015) fields these techniques are not well known in ecology. The few papers and preprints available from related fields are in animal-call recognition (an outgrowth of speech recognition); satellite imaging; agriculture; and identification of leaf shape, cetacean fins, or zebra fish movements

(Debeljak et al. 2010, Cope and Remagnino 2012, Stathopoulos et al. 2014, Tan et al. 2015, Jouary et al. 2016, Baumann et al. 2017, Weideman et al. 2017).

Over the same period that time-series clustering methods have matured, the microchemical analysis of accretionary biogenic materials has taken similarly large strides as an ecological tool (Campana 2005, Secor 2010). In particular, otolith microchemistry, the analysis of the trace element and isotopic chemistry recorded in the balance organs of bony fish, is an example of the dramatic increase in data richness of an individual-scale technology. The high temporal detail of data recorded in otoliths also makes them a promising example of how time-series methods could improve our ability to aggregate individual scale data, while conserving important small-scale detail, to better inform population-scale models.

With calcium carbonate rings laid down daily, the otolith is a natural temporal record (Campana and Neilson 1985). Otoliths record ambient chemistry which can reconstruct movement, life-history, and environmental information through the life of a fish with remarkable precision (Kennedy et al. 1997, 2002, Campana and Thorrold 2001, Hamann and Kennedy 2012). Improvements in instrumentation have decreased the necessary sample size, allowing for increasingly detailed continuous chemical transects (Hamann and Kennedy 2012, Hegg et al. 2015a), and full otolith chemical maps of the otolith (Limburg et al. 2013), tracing the life-history of a fish from birth to death. Studies now often including multiple chemical and isotopic tracers, each able to reconstruct different facets of the fish's life-history (Walther and Limburg 2012). These new techniques create information-rich, time-series data tracking the chemical profile of a fish from birth to death (Figure 2A).

While the resolution of data extracted from otoliths has increased dramatically, analysis techniques have not taken advantage of the increased information density of high-resolution time-series datasets. Most otolith studies are interested in the geochemistry of specific time-points in the life of the fish; e.g. maternal contributions, natal origins, nursery and rearing locations, or the timing of migration, for example. Therefore, the location of interest is located on the otolith and the corresponding data

is aggregated, creating a chemical index which can be analyzed as a discrete value, or a vector of values in the multivariate case (Barnett-Johnson et al. 2010, Hegg et al. 2013a, Garcez et al. 2014). While this is a valid approach, it risks ignoring or obscuring valuable information contained in the time-series itself.

Strontium isotope ratios ($^{87}Sr/^{86}Sr$) recovered from otolith transects can be considered a time-series, recording the chemical history of the fish from birth to death (Figure 1B). Understanding how this time-series is recorded in the otolith highlights the possible loss of information inherent in data aggregation. Sr isotope ratios are tied tightly to location and geology (Hegg et al. 2013b). Thus, the shape of an otoliths $^{87}Sr/^{86}Sr$ life-history transect describes movement between rivers with different isotopic signatures, and the time spent in each of these locations (Figure 1B). However, the curve is also the result of additional underlying processes which we often do not know. The slope of change between stable regions can change with the speed fish move between signatures or the differences in growth rates among individual, shrinking or stretching the time axis of the series (Figure 1B). Swimming speed, distance, or the need to equilibrate across salinity or temperature gradients are just a few examples. Similarly, concentration can buffer isotope ratio changes between two sources, changing the slope at which isotope ratio changes in the fish's tissue. Because the width of otolith rings correlates with growth, much like tree rings, periods of fast growth will be lengthened, while slow growth may be compressed. Seasonal changes in $^{87}Sr/^{86}Sr$ that occur in some river systems represent another underlying effect on the otolith transect. These effects can be numerous, and the underlying information contained in otolith transects can be significant. Using only local averages along this transect ignores potentially useful information contained in the temporal structure of the otolith time-series.

Otolith temporal data is just one example of ecological data for which DTW might be useful. Much of the small-scale data that ecologists collect has a temporal component; GPS or radio-telemetry data of tagged animals, mark-recapture data, population density, timing of spring leaf-out, all either are inherently temporal or

could be thought of as a time-series in some cases. Even genetics data can be coerced into a time-series format for use with time-series methods (Rakthanmanon et al. 2012b). In many of these cases it is useful to determine the similarity or difference between the structure of these data; for example, to classify streams by the characteristics of their hydrograph, or to track timing of phenology. Time-series clustering tools using distance measures such as k-shape distance (Paparrizos and Gravano 2015) or dynamic time warping (DTW) distance (Berndt and Clifford 1994) provide methods which can efficiently cluster similar time-series using all the information contained in the chronological structure of the data, avoiding some of the problems associated with data aggregation. These methods could potentially be useful in many ecological datasets, especially where temporal patterns must be grouped into related syndromes but natural variation in the temporal scale creates differences in frequency.

In this paper, we provide an example of how DTW can be used to determine natal origin and life-history from a large dataset of known-origin juvenile Chinook salmon otolith transect data. We demonstrate the ability of DTW to cluster fish using univariate $^{87}Sr/^{86}Sr$ data as well as multivariate data including elemental ratios. Next, we compare these results to a more conventional, model-based discriminate function analysis using aggregated multivariate data, and demonstrate how the two techniques could be paired to improve analysis. Finally, we discuss methods by which DTW, and similar time-series matching techniques, could be extended to classify life-history of unknown fish, irrespective of age or transect length. Finally, we discuss our results in the context of time-series data analysis in ecology more broadly.

Methods

Study Species

Snake River Fall Chinook salmon are a threatened population of fall spawning *Oncorhynchus tshawytscha* in the Snake River of Idaho, a major tributary to the Columbia River in the northwestern United States (Figure 3). The population is

notable for a recent shift in juvenile life-history strategy. Historically, the population spawned primarily in highly productive upstream habitats, with high summer temperatures selecting for a ubiquitous early outmigration strategy. The placement of eight downriver dams, as well as the loss of much of the most productive upstream spawning habitat by upstream hydropower dams, has resulted in major habitat changes during the last century. Management of outflows from another high-head dam on the Clearwater River, a major tributary and spawning area, have been used to create summer refugia for outmigrating salmon as well. These anthropogenic changes are thought to have driven a recent shift toward a later, yearling, outmigration strategy in a large proportion of the juvenile population. Further, recent research suggests that these changes are hereditary, indicating that these life-history shifts are an example of contemporary life-history evolution.

The geology of the major spawning tributaries is diverse both in age and rock type, creating significant differences in water chemistry (Hegg et al. 2013b). Ongoing water sampling throughout the basin has shown that $^{87}Sr/^{86}Sr$ signatures in the four main spawning areas of the basin are distinct (Hegg et al. *in review*), and that $^{87}Sr/^{86}Sr$ can be used to classify juvenile and adult fish to locations throughout the basin using otolith chemistry (Hegg et al. 2013a).

Otolith Collection and Analysis

The data used in this study consists of otoliths collected from known-origin, juvenile fall Chinook salmon from throughout their range in the Snake River basin. Juveniles were collected from three sources from 2009 to 2014 (n=376). Juveniles were sampled as a part of yearly beach-seine population surveys conducted by the United States Fish and Wildlife Service along the length of the free-flowing Snake River. In these surveys fish were sacrificed and collected each year at sites in the Upper and Lower sections of the Snake River, as well as from the Grande Ronde River. Some fish were tagged with passive integrated transponder (PIT) tags and released, then recaptured weeks to months later based upon their sorted PIT tag code at Lower Granite dam, the first dam fish encounter on their path downstream. Additional

samples were provided yearly by the Nez Perce Tribe Department of Fisheries Resource Management based upon similar beach-seine sampling on the Clearwater River. Juvenile samples were also obtained from the two major hatcheries in the basin, Lyons Ferry Hatchery and Nez Perce Tribal Hatchery.

Sampled fish were frozen until sagittal otoliths could be removed. Otoliths were stored dry in 1.5ml microcentrifuge tubes. Samples were then prepared for chemical analysis using established methods (Secor et al. 1991a, Hegg et al. 2013a). The left sagittal otolith was mounted on glass microscopic slides and polished in the sagittal plane, using fine grit sandpaper to reveal the core. In the case of a missing otolith or a failed preparation, the right otolith was used.

Otoliths were then analyzed for $^{87}Sr/^{86}Sr$ isotope ratios and trace elemental signatures using a New Wave UP-213 laser ablation sampling system coupled with two different mass spectrometer systems. Elemental ratios of calcium (Ca), strontium (Sr), barium (Ba), Magnesium (Mg), and Manganese (Mn) were sampled on a ThermoScientific Element 2 inductively coupled plasma mass spectrometer (ICP-MS), while $^{87}Sr/^{86}Sr$ was measured on a ThermoScientific Finnigan Neptune multicollector ICP-MS (MC-ICP-MS). On each system the otolith was sampled using a continuous transect from the otolith edge to its core, positioned approximately 90˚ from the otolith sulcus on the dorsal side. For $^{87}Sr/^{86}Sr$ isotope analyses using LA-MC-ICP-MS, the laser was set to 10μm/second scan speed with a 40μm spot size, and data was recorded with a 0.262 second integration time. For trace element analysis, the laser was set to scan at 10μm/second, with a 30μm spot size, and the ICP-MS software was set to a 1 second sampling time.

Strontium ratio data was corrected based on the global marine signature for each analysis day using a marine shell standard (mean $^{87}Sr/^{86}Sr$ = 0.709186, standard deviation = 0.000077, n=535). Elemental counts were corrected to the SRM 610 standard (Jochum et al. 2011) and corrected to calcium using a ten second, within-run blank. Limits of detection (LOD) for each element were calculated as 3 X SD from the mean of the blank. Expressed as a ratio of elements to calcium resulted in detection

limits of; Sr/Ca 0.029 mm•mol^{-1}, Ba/Ca 0.023 mm•mol^{-1}, Mn/Ca 0.031 mm•mol^{-1}, and Mg/Ca 0.022 mm•mol^{-1}.

The edges of the otolith were located within the data using a CUSUM algorithm, then checked visually. After isolating the otolith data, the sequence was reversed, and micron distances from the core were calculated based on laser speed and sampling time, to create a core-to-edge chemical transect. Elemental ratios were used to standardize $^{87}Sr/^{86}Sr$ distance so that both transects reflected the same distance across the otolith.

Multivariate Discriminate Function Classification

A model-based discriminant function was created to classify fish to known location. The goal was to develop a robust classification which can than later be applied to unknown adult fish to inform ecology and management of the population. Past efforts using univariate $^{87}Sr/^{86}Sr$ have been unable to distinguish hatchery origin individuals or reservoir movement (Hegg et al. 2013a). The addition of additional chemical tracers, however, has allowed us to separate hatchery origin fish, as well as movement into reservoir habitat, using a multiple tracer approach that includes elemental ratios of Sr/Ca, Ba/Ca, Mn/Ca, and Mg/Ca (Chapter 2, *in review*).

Within our dataset, juveniles were assigned to a known origin based on the location at which they were captured. Juveniles which were captured and sacrificed during beach seine sampling early in the season were considered to have a natal location of the river reach in which they were captured; the Upper Snake River (USK), the Lower Snake River (USK), the Clearwater River (CWS), or the Grande Ronde River (GR). These categories match earlier work which show that these locations are chemically distinguishable (Hegg et al. 2013a, 2013b). Some juveniles captured during early season beach seine sampling were tagged with a passive integrated transponder (PIT) tag and released. These fish were subsequently captured when their tag was detected at Lower Granite dam. These juveniles were then assigned a second known location in Lower Granite Reservior (LGR). Juveniles obtained from Lyons Ferry

Hatchery (LFH) and Nez Perce Tribal Hatchery (NPTH) were assigned to these natal locations respectively.

Understanding downstream passage through the reservoirs is important for constraining life-history diversity, yet prior studies using only $^{87}Sr/^{86}Sr$ had been unable to determine reservoir residence. Therefore, a downstream category was created for fish captured at Lower Granite Dam (LGR) to attempt to classify this downstream location. Some of these fish were captured in upstream natal reaches, PIT-tagged, released, and recaptured as they passed the dam. Therefore, it was possible for a fish to have both a known natal location and a known downstream location. Some fish were caught in the dam forebay as a part of prior studies and their natal location was not known, although their migration timing suggested Clearwater River origin. These fish were assigned only a known downstream location of LGR and were not analyzed for natal location.

Prior work has shown that maternal effects in the early otolith of Snake River Fall Chinook equilibrate to the chemistry of the natal stream between 250-300μm (Hegg et. al, *in review*) Therefore, we defined the natal location as the period between 300μm and 400μm from the core of the otolith. The mean of each isotopic and elemental signature within these boundaries were taken, creating a five-element vector of natal value representing the natal chemical signature for each fish.

Fish arriving at Lower Granite Dam can be moving downstream quickly. Therefore, we averaged the signatures from the outer 50μm from the edge of these otoliths in order to minimize error due to the equilibration from upstream signatures. Otoliths which reflected an $^{87}Sr/^{86}Sr$ signature far removed from that of LGR were assumed to be fast moving migrants, fish moving too fast to have equilibrated to the surrounding water. In cases where $^{87}Sr/^{86}Sr$ ratios were anomalous, and transects indicated that a fish had not equilibrated to the location it was caught, it was removed to maintain a consistent training set for the discriminant function.

Classifying fish to location was done using a model-based discriminant function using $^{87}Sr/^{86}Sr$, Sr/Ca, Ba/Ca, Mn/Ca, and Mg/Ca as independent variables and known

location as the classifier. We used the {mclust} package (version 5.2) for R to build the discriminant function (Fraley and Raftery 2007, Scrucca et al. 2016). This model-based approach uses BIC to determine the best model fit, while enabling variable variance and direction between groups, and does not require a prior probability of group assignment. The dataset was randomly split into a training set (80%) and test set (20%), with the training set used to construct the discriminate function. Related river reaches were combined successively in cases where significant misclassification occurred between them until an acceptable misclassification rate was achieved. The final discriminate function was then applied to the test-set to quantify its performance on unknown data.

Dynamic Time Warping Cluster Analysis

Time series clustering using DTW distance was used to identify groups of similar fish based on the shape of their otolith transects. Clustering was performed for two subsets of the otolith dataset. First, otoliths were clustered using DTW on the univariate $^{87}Sr/^{86}Sr$ transects alone. Second, multivariate DTW clustering was performed on the full multivariate chemical dataset which included $^{87}Sr/^{86}Sr$, Sr/Ca, Ba/Ca, Mn/Ca, and Mg/Ca transects. For each set clustering was performed using both hierarchical and partitional clustering methods to compare the utility of these two clustering methodologies. The partitional and hierarchical clustering results for both the univariate and multivariate datasets were then compared to the classifications of the model-based discriminate function.

Hierarchical clustering was accomplished using the base clustering algorithm in R applied within the {dtwclust} package (Sarda-Espinosa 2017b). Hierarchical clustering groups data based on similarity, grouping data into clusters which are subsequently combined at higher levels of the hierarchical structure (Murtagh and Contreras 2017). In the base R implementation this is accomplished through an agglomerative clustering algorithm which builds clusters by agglomerating similar clusters moving upwards in the hierarchy. Clusters can then be defined by “cutting” the dendrogram at a given height within the hierarchy to separate clusters. This is

perhaps best understood in ecology in terms of a dendrogram of species in evolutionary biology. Partitional approaches do not impose a hierarchical structure and instead partition the data into a pre-assigned number of clusters by optimizing cluster membership based on the distance criteria (Nagpal et al. 2013). Partitional clustering was accomplished using a custom implementation within the {dtwclust} package (Sarda-Espinosa 2017b)

Prior to clustering a centered, 20-point, rolling average was used to smooth all otolith transects. Transects were then re-interpolated to a length of 200 cells, which allows faster calculation through the implementation of lower bounds, without a loss of matching ability (Al-Naymat et al. 2009). A 10% Sakoe-Chiba window was employed to decrease processing effort and limit potentially erroneous warping (Sakoe and Chiba 1978, Ratanamahatana and Keogh 2004). The resulting distance matrix was then clustered using standard hierarchical and partitional clustering algorithms (Sarda-Espinosa 2017a, 2017b).

Clustering was exploratory, and the number of groups were not forced to conform to those of the known origin fish. This was done to investigate whether DTW, using the additional temporal data in the chemical transect, was capable of distinguishing additional life-history complexity. Hierarchical clusters were defined using simple dendrogram cutting where possible, however in cases with complex nested clustering we employed dynamic tree cutting methods from the {dynamicTreeCut} package for R (Langfelder et al. 2008). The goal, in all cases, was to minimize the number of clusters while maintaining clusters which were easily interpretable based on the known-origin of the fish within each cluster.

Combining DTW with Discriminate Function Analysis

In cases where the discriminant function was unable to separate groups of fish from known locations we tested the ability of DTW to separate these confounded groups. We applied partitional clustering using a 10% Sakoe-Chiba window and Keogh lower bounds to the $^{87}Sr/^{86}Sr$ transects of training-set otoliths from the confounded

groups in the DFA analysis. The number of clusters was set equal to the number of confounded groups. Cluster prototypes were determined using the partitioning around medoids, or PAM, method. We then predicted the cluster membership of the test-set otoliths within the same confounded groups using nearest-neighbor classification, to test the stability of these cluster results to unknown data. Comparison to known water chemistry from Hegg et al. (*in* review) was used to evaluate the veracity of this group membership.

Results

Multivariate Discriminate Function Analysis

Initial data exploration indicated that the LGR group, as expected, contained a number of juvenile fish whose signatures had not equilibrated and instead reflected signatures of upstream habitats (n=22). Additionally, the LSK group contained one fish caught in the Lower Snake River and later at LGR which exhibited a very high, Clearwater River signature. These fish were removed to provide a robust training set, under the assumption that adult fish would exhibit a clear signature in these locations, having not been captured and sacrificed. (Figure 2)

Additionally, a group of anomalous life history transects were identified in the CWS group which did not appear to conform to the known signatures through which a Clearwater origin fish would experience, nor did they match the expected patterns or signatures seen in NPTH fish. All of these fish began with a presumed maternal $^{87}Sr/^{86}Sr$ signature near 0.711, followed by a pronounced decrease to 0.70918, followed by a sharp rise 0.712 and above. All of these fish were captured late in the year and could potentially be unmarked hatchery juveniles, Spring Chinook from upriver populations which were erroneously included in the sample, or an unknown source. To avoid biasing our CWS training set these fish were excluded (n=25).

Despite removal of these obviously anomalous fish, there was significant overlap in the $^{87}Sr/^{86}Sr$ signatures between the USK and LSK groups. Many LSK fish appeared, subjectively, to have originated in the USK and moved very early to the LSK

downstream. Evidence of this type of early movement has been observed in the population (Ken Tiffan, USGS, unpublished data). However, without evidence to clearly identify these potentially early-moving juveniles they were kept within their known-origin groupings.

Model based clustering resulted in a model with variable, ellipsoidal and diagonal variance structures for each group. The initial classification attempt resulted in large misclassification errors between the LSK and USK groups. The USK and LSK groups were subsequently combined and the classification was run again. This final training set classification resulted in an absolute training error of 3.6% (n=298), with a 10-fold cross-validation error rate of 12.8% (SE = 3.3%). Classification of the test set (n=74) resulted in an overall classification error rate of 12.2%. (Table 1)

Dynamic Time Warping Analysis

Univariate Hierarchical Clustering

Univariate, hierarchical clustering of DTW distance for $^{87}Sr/^{86}Sr$ otolith transects resulted in a complex dendrogram (Figure 4A). Cutting this dendrogram at a height of 0.395 resulted in three large clusters and one bifoliate branch. This cluster solution effectively separated all of the CRB juveniles, as well as the majority of juveniles originating in the CW system. It results, however, in a single large (n=260) cluster with complex structure, containing a mix of LSK, USK and hatchery origin juveniles. Dynamic tree cutting algorithms did not result in easily interpretable results for the univariate, hierarchical dendrogram.

To explore the structure of this larger branch we re-clustered only the fish assigned to this cluster (Figure 4B). Simple cutting of the dendrogram, in this case, did not provide easily interpretable clusters due to the nested structure. Using dynamic tree cutting with a minimum group size of 30 and the highest setting of "deep cut," which controls the number of cuts high in the dendrogram, returned six clusters (Figure 4C). This cluster result separated NPTH hatchery fish into their own cluster

(cluster 4), as well as fish of CW origin (cluster 6). Separation of LFH hatchery fish was less successful (cluster 1 & 5), and failed to separate USK and LSK juveniles.

Univariate Partitional Clustering

Univariate, partitional clustering of juvenile $^{87}Sr/^{86}Sr$ transects began with six groups, the same as the number of groups in the multivariate discriminant function. This clustering solution resulted in significant overlap and appeared to be unstable, with repeated runs resulting in very different clusters. Clustering with ten groups appeared to result in more repeatable clusters, while separating fish into meaningful clusters. Partional clustering uses random starting values and each run can converge differently. The results reported here used a seed of 7629, which was representative of the majority of clustering outcomes using a 10% Sakoe-Chiba window and the Keogh et al. (2009) lower bound.

This cluster solution effectively separates hatchery fish into their own clusters (clusters 1 & 2, Figure 5). It also cleanly separates fish from the Grande Ronde river, with 100% of these fish being clustered together (cluster 9). Fish of CW origin are split between three clusters (clusters 4, 7 & 8). The remaining clusters are split between fish of USK and LSK origin.

The clusters containing CW fish are interesting, particularly cluster 4 (Figure 5). The Clearwater origin fish in this cluster correspond to the group of anomalous signatures which were removed from the multivariate discriminate function. The shape of these transects is clearly different than those of the other two clusters of CW fish, indicating a different location or a different life-history from other CW fish. The similarity to several NPTH fish classified to the same group supports the idea that these are fish from NPTH which were caught unknowingly. Further, the fish in this cluster were all captured late in 2014 due to high flows, which increases the chances that hatchery juveniles would be included in sampling.

The chief difference in shape between cluster 4 fish and those from NPTH seems to be a higher signature in the otolith near the core. Under the assumption that this group is unknowingly captured NPTH fish, this indicates that some NPTH fish

may inherit a much higher maternal signature. This is possible, as previous research has shown that the maternal signature of eggs at NPTH can change significantly due to the mix of well-water and river-water used within the hatchery, and the speed of maternal migration may change from year to year which could affect maternal signature (Donohoe et al. 2008, Hegg et al. *in review*).

Clusters 7 and 8 appear to separate CW fish largely based on subtle differences in the upward-trending $^{87}Sr/^{86}Sr$ characteristic of CW fish. Cluster 8 is interesting due to the many fish captured at LGR with unknown natal-origin which are included in this cluster. Although their origin is unknown these fish were collected by USGS in 2012 in the Lower Granite forebay and the collection notes include, "Unknown origin. Likely from Clearwater but could be hatchery or natural." This provides evidence that the DTW algorithm is able to successfully match these fish despite the change in transect shape due to movement into the lower $^{87}Sr/^{86}Sr$ signature of LGR.

Clusters 5 and 6 support the finding from the multivariate DFA that USK and LSK fish are confounded, due to early movement (Figure 5). However, the predominant shapes in each of these groups indicates the possibility that DTW can be used to separate the two groups. Water data indicates that the signatures of USK and LSK reaches are distinguishable (Hegg et al. 2015b, Hegg et al. *in review*). We should expect USK fish to exhibit a $^{87}Sr/^{86}Sr$ signature lower than the global marine average (0.70918) after the end of the maternal signature (150μm), while fish of LSK origin should have a signature slightly higher than the global marine average. Fish from the USK which subsequently move downstream into the LSK or LGR should show a shift upward in $^{87}Sr/^{86}Sr$ toward this new signature. Cluster 5 shows this movement from a lower signature toward a signature more indicative of LSK or LGR. The majority of fish in cluster 6 remain in a USK-like $^{87}Sr/^{86}Sr$ signature, indicating that many of the fish which were caught in the LSK may have been recent migrants from the USK which had not equilibrated. Clusters 3 and 10 have shapes indicative of fish which originated in the LSK, however the presence of USK fish does indicate some degree of overlap in signature between these groups.

Multivariate Hierarchical and Partitional Clustering

The results of multivariate DTW clustering was unsuccessful using both hierarchical and partitional methods, using various window constraints and internal distance functions. Results tended to cluster CW and GR fish together, and other clusters were often nonsensical. This could be due to the fact that element-to-calcium data contains less location-specific data but the algorithm weights it equally to $^{87}Sr/^{86}Sr$, which has a much greater geochemical link to location and movement.

Combining DTW with Discriminate Function Analysis

The USK and LSK groups from the discriminate function were confounded, resulting in the combination of these groups into a single group representing the entire Snake River above the reservoirs. Partitional clustering of this confounded group in the training-set used for discriminate function classification resulted in one cluster of 50 fish with 70% of fish originating in the LSK (48% captured in LSK, 32% caught in the LSK and re-captured at LGR, 4% from the USK and 16% originating in LSK and recaptured at LGR). The second cluster of 62 fish contained a majority (58%) of fish originating in the USK (40% captured in LSK, 2% caught in the LSK and re-captured at LGR, 42% from the USK and 16% originating in LSK and recaptured at LGR) (Figure 6).

Predicting the cluster location of the confounded group of the test-set resulted in fifteen fish being classified to cluster 1, the cluster containing a majority of USK fish. Ten fish were classified to cluster 2, containing the majority of LSK fish. (Figure 6)

Comparison of the clusters to the range of $^{87}Sr/^{86}Sr$ signatures in water collected from the USK and LSK reaches supports the contention that the two groups are separated by river reach (Figure 6). Previous research shows that juvenile fish in this population equilibrate to the ambient river signature at ~250µm from the otolith core (Hegg et al. 2013a, Hegg et al. in review). Cluster 1 shows this equilibration from a maternal signature above 0.70918 to a signature reflective of the USK reach between ~250µm - 450µm before moving to a higher signature as they commence downstream movement. Cluster 2, on the other hand, shows that the majority of fish equilibrating to a signature reflective of the USK group. The transects classified from the test-set

generally follow the same behavior, with fish being classified to USK equilibrating to a signature representative of the USK water samples and fish classified to LSK representative of the LSK signature. The LSK group does include some notable exceptions, fish captured in USK and re-catpured at LGR, whose shape was matched to the LSK cluster and whose $^{87}Sr/^{86}Sr$ signature appears to be closer to the USK signature.

Discussion

Finding analysis methods that best "extract and abstract those fine-scale features that have relevance for the phenomena observed in other scales," is important for maintaining parsimony as well as accuracy in ecology (Levin 1992). To do this ecologists must balance the loss of data inherent in the "aggregation problem", with the level of generalization required of their problem. While many methods exist for analyzing time-series and sequential datasets, DTW is unique in its ability to quickly, and accurately, compare time-series with few assumptions and without requiring significant transformation of the raw data (Mueen and Keogh 2016, Bagnall et al. 2016). Since so much of the ecological data collected across multiple ecological scales is temporal or sequentially structured, DTW may be a useful tool to extract maximal information from datasets by leveraging the structured nature of time-series data. Despite this, DTW is not a well-known technique within the ecological community.

Our results, using otolith chemical transects as an example dataset, indicate that DTW clustering can distinguish important groupings in in geochemical transitions identified from temporal otolith life-history data, and may be useful for other ecological datasets. DTW was very sensitive to life-history differences recorded in otolith transects, with univariate $^{87}Sr/^{86}Sr$ data capable of classifying fish by location in ways broadly comparable to traditional discriminant function techniques. However, the interpretability of the results was highly dependent on the cluster method that was chosen, and there were important differences between the classification ability of discriminate function analysis and DTW clustering in grouping fish by location.

The results of model-based discriminate function analysis show that the traditional approach, aggregating data into a mean from the natal period on the otolith, is effective (Table 1). However, the inability of the multivariate discriminate function to classify juveniles from the USK and LSK reaches of the Snake River provides an interesting example of the loss of information due to aggregation. Since the water signatures between the two reaches are significantly different over multiple years of sampling (Hegg et al. 2013a, Chapter 2 *in review*), we would expect the natal signatures of the fish to reflect this. However, the evidence of early-moving juveniles from field sampling indicates that fish may be moving downstream prior to even the earliest field sampling, and are therefore identified as LSK when in fact they are recent migrants from the upstream USK reach. Using only an average of the chemistry from the natal period on the otolith creates an accurate point-estimate of natal signature, but removes information from the entire otolith transect which might be useful in determining whether this hypothesized early movement is, in fact, the case.

Initial partitional clustering appeared to cluster USK and LSK fish in ways that indicated that DTW may be able to disentangle these two confounded groups. Clusters 5, 6 and 10 seem to be made up primarily of a mix of fish from the USK and LSK groups, but the shape of their transects is very different (Figure 5). Water sampling data shows that the USK and LSK $^{87}Sr/^{86}Sr$ signatures fall on opposite sides of the global marine signature of 0.70918 (Chapter 2, Figure 2.1) making the global marine signatures a convenient marker for visual comparison between the two groups. Cluster 6 is made up primarily of fish whose signature begins below the global marine signature, similar in value to the water samples in the USK reach (Chapter 2, Figure 2.1). In contrast, fish in cluster 10 have signatures which largely remain above the global marine average, the range of the LSK reach (Chapter 2, Figure 2.1). Cluster 5 contains fish whose signatures begin within the range of the USK, before moving upward, moving into range of the LSK reach. In fact, many of the fish in clusters 5 were captured at Lower Granite dam after being initially tagged in the Upper Snake, and

those fish whose signatures move above the global marine signature in cluster 6 originated in the USK reach (Figure 5). These results seem to indicate that partitional DTW clustering is clustering fish into meaningful groups based on the temporal structure of their $^{87}Sr/^{86}Sr$ transect data.

Partitional DTW clustering to the full transects of the fish data used to build the discriminate function, excluding all but fish assigned to the combined USK/LSK group, split the fish into two groups. The makeup of these groups appear to conform to expectations we might expect if the DTW clustering were separating the two groups based on true natal origin. One group largely contained fish with natal signatures (signatures 150μm < 250μm) within the range of the USK $^{87}Sr/^{86}Sr$ water signatures (Figure 6). The majority of these fish were captured in the USK (58%). The second cluster contains some fish whose natal signature appeared to overlap the USK, but the majority of fish appeared to have natal signatures within the range of the $^{87}Sr/^{86}Sr$ signature of water from the LSK. In this group 80% of the fish had been captured in the LSK. When these groups were used to perform nearest-neighbor classification on the test-set used to test the multivariate discriminate function the resulting classifications appeared to conform to the same patterns, indicating a robust classification (Figure 6).

Since the USK and LSK locations are sequentially located on the river (Figure 3), and juveniles do not move upstream for appreciable distances, this cluster result makes sense. If fish are moving downstream prior to sampling we would expect more USK fish to be misclassified as LSK because they are moving downstream into the LSK and are caught there, hence the lower percentage of known USK fish in the perported USK cluster. Similarly, LSK fish cannot move upstream to develop a USK signature, so we should expect the percentage of correctly classified known-origin fish to be higher as we observed.

Thus, although the evidence is circumstantial, our results indicate that the DTW clustering algorithm is successfully separating USK and LSK based on their behavior, using the differences in their chemical time-series as a whole as the measure

of difference rather than a point-average. In other words, using the temporal structure of the univariate $^{87}Sr/^{86}Sr$ otolith transect, DTW appears to be capable of aggregating complex, individual otolith data into general natal-origin classifications in ways that point-average methods of the univariate and multivariate data cannot.

However, the results of DTW clustering of the juvenile otolith data differ markedly based on the clustering method used, and results were often not easily comparable to results based on the discriminate-function. Hierarchical clustering was capable of readily distinguishing fish from the CWS and LGR groups (Figure 4A, however the complex clustering structure of cluster 1 made it very difficult to interpret the clustering of hatchery fish from NPTH and LFH, as well as USK and LSK fish (Figure 4B & C).

As with hierarchical clustering, the partitional method accurately clustered GR fish into their own unique cluster. Partitional clustering also separated both LFH and NPTH fish into their own clusters with relatively high specificity. Fish from the CWS group were split into three clusters (Figure 5, Clusters 4, 7, and 8,). Cluster 7 was defined by the lack of downstream movement, with most fish having been captured in the CWS reach. Cluster 8 contained a majority of CWS fish who has subsequently moved to LGR before capture. Interestingly, cluster 4 contains CWS fish which were excluded while building the model-based discriminate function (Chapter 2) because they were assumed to be NPTH fish captured accidentally, Spring Chinook which were erroneously included, or Fall Chinook juveniles from an unknown source (Figure 5). The ability to discriminate subsets of fish based on their prior movements, and to identify unknown patterns, is further evidence of the ability of DTW-based methods to provide additional detail which cannot be easily aggregated from a simple average.

However, these clustering results are only interpretable in the context of our prior discriminate function. Time warping techniques may identify subtle differences in datasetes that are not easily interpretable in an ecological context without significant prior knowledge of the system in question. Thus, the advantages of DTW as an analytical tool might be most apparent when combined with existing analysis

techniques. In the case of the data presented here, discriminant function analysis excels at pinpointing fish location based on the extremely accurate means that can be aggregated from the natal signature, but this aggregation is foiled by fish from the USK and LSK because behavioral clues within the temporal structure of their otolith data is lost when data is aggregated into natal averages. DTW, because of its use of the entire time-series, is able to distinguish the behavioral differences that appear to separate these fish, differences which the prevailing analysis methods miss.

The possibilities of DTW extend beyond the methods presented here. While our analysis is limited to clustering short time-series with equal lengths, DTW is capable of more flexible pattern matching. For example, by opening the constraint that the time-series be of the same length it is possible to search for short, prototype time-series within longer series (Tormene et al. 2009). In the data presented here, this would make it possible to search for specific short-term behaviors, perhaps transitions between specific rivers, within the longer transects of adult fish. In other contexts this could be used to identify specific hydrological events within many years of hydrograh data, or specific patterns of phenology across years or across a landscape. This "open-ended" method has been successfully used to classify human movements in post-stroke physical therapy, to identify human heartbeat arrhythmias within a full day of ECG data, and to quickly find short DNA segments within trillions of basepairs (Tormene et al. 2009, Rakthanmanon et al. 2012a).

The ways in which DTW data is pre-processed can improve results. Mueen and Keogh (2016) highlight the fact that data normalization and pre-processing can have large effects on the efficiency and accuracy of DTW. The same authors also state that multivariate DTW can be difficult without a very careful approach to understanding how tightly correlated the variables are. Our own multivariate DTW clustering attempt, which was largely uninterpretable, may be an example of this. We know that $^{87}Sr/^{86}Sr$ is much more closely related to fish location than element-to-calcium ratios, which means that the series are likely loosely coupled, rather than tightly correlated. Our poor outcome with multivariate data may be more indicative of the relationships

within the data, and the specific DTW method used to compute the multivariate distances, than DTW itself. The success of univariate DTW using $^{87}Sr/^{86}Sr$ does, however, highlight how well DTW works even with univariate data.

Overall, our data provide an example of only one use of DTW on ecological time-series data. While examples exist, the ecological community has not adopted these techniques to the degree of other fields. However, despite persistent myths (Ratanamahatana and Keogh 2004), the methods are fast and accurate in comparison to other time-series clustering and classification methods (Rakthanmanon et al. 2012a, Mueen and Keogh 2016). Further, DTW implementations are available on multiple popular analytical tools and programming languages including R, Python, Java and SAS (Leonard and Wolfe 2001, Salvador and Chan 2007, Albanese and Visintainer 2012, Gulzar 2015). Analysis of ecological data is always a balance between detail and parsimony, but DTW provides an additional tool for ecologists to maximize the information extracted from their data when interpreting ecological phenomenon.

Tables

Table 3.1 – Classification accuracy of discriminate function training set

		Observed					
		CWS	CRB	LFH	LGR	NPTH	USK/LSK
Predicted	CWS	64	0	0	0	0	0
	CRB	0	21	0	0	0	0
	LFH	0	0	19	0	2	0
	LGR	2	0	0	60	0	9
	NPTH	2	0	2	0	21	5
	USK	0	0	0	2	1	92

Figures

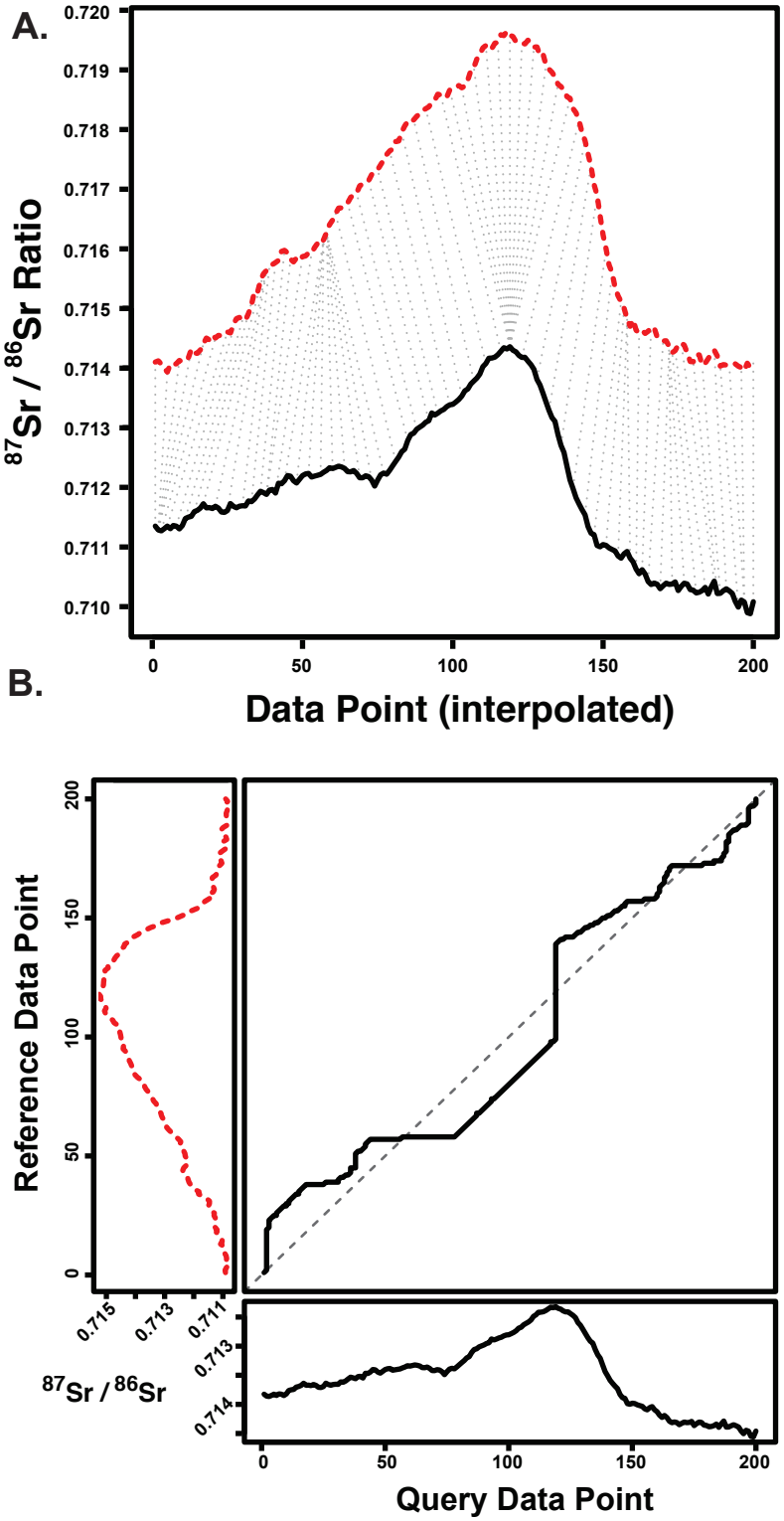
A.
0.720
0.719
0.718
0.717
0.716
0.715
0.714
0.713
0.712
0.711
0.710
87Sr / 86Sr Ratio
0
50
100
150
200
B.
Data Point (interpolated)
Reference Data Point
200
150
100
50
0
0.715
0.713
0.711
87Sr / 86Sr
0.713
0.714
0
50
100
150
200
Query Data Point

Figure 3.1 – Dynamic time warping distance and sequence matching

Two otolith $^{87}Sr/^{86}Sr$ transects of two fish caught in the LGR reach of the Snake River are shown. Dynamic Time Warping computes the amount of warping on the temporal (x) axis needed to optimally align two series (**A**). Dotted grey lines show matching points along these series computed by DTW (a subsample of matching points are shown and transects are offset by 0.004 to improve clarity). DTW was performed using a 20% Sakoe-Chiba window, resulting in the optimal warping path (**B**) shown between the two time-series.

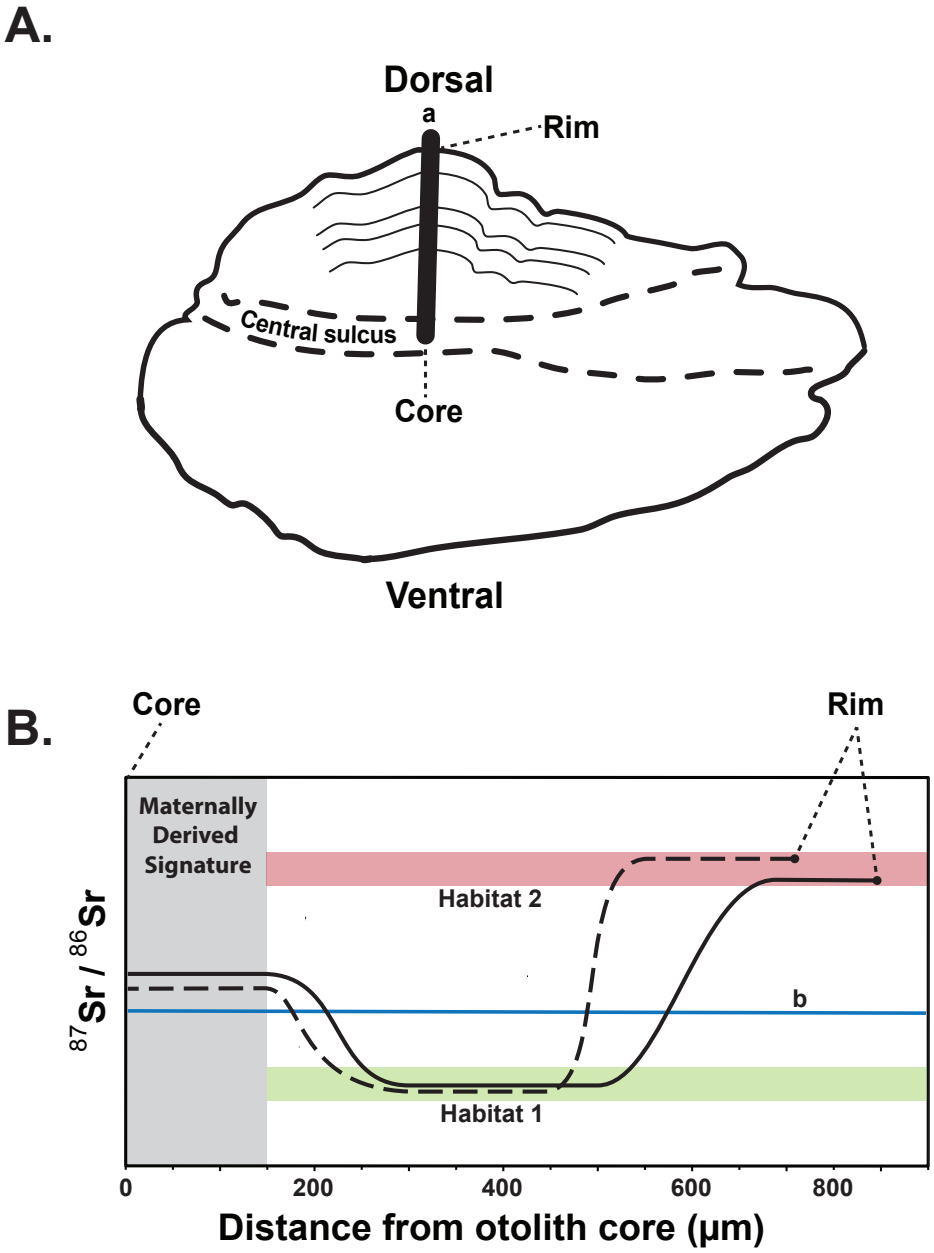

Figure 3.2 – Otolith analysis and temporal phase shifts in otolith data

Otoliths (**A**) form from a central core, with rings of calcium carbonate deposited daily much like the rings of a tree. To reconstruct the chemistry within these rings (**a**) a laser is used to ablate sample from the core (birth) to the rim (death), which is subsequently analyzed. This analysis creates a temporally structured dataset for each fish, representing the chemistry of the rivers they inhabited. These otolith chemical

transects (**B**) are represented with microns from the core of the otolith on the temporal (x) axis. Otolith $^{87}Sr/^{86}Sr$ transects for two hypothetical fish inhabiting the same two habitats, but exhibiting different life histories, are shown (solid and dashed black lines). Movement decisions (and growth, which changes the width of deposited rings) change the distance on the otolith represented by a given habitat signature. The speed of movement, and the speed of chemical equilibration between two habitats can also change the slope of the $^{87}Sr/^{86}Sr$ curve as the fish moves between habitats. Thus, the otolith transects for fish which experienced the same habitats are phase-shifted on the temporal axis. DTW excels at matching these types of phase-shifted datasets. The global marine $^{87}Sr/^{86}Sr$ signature is shown (b) for reference.

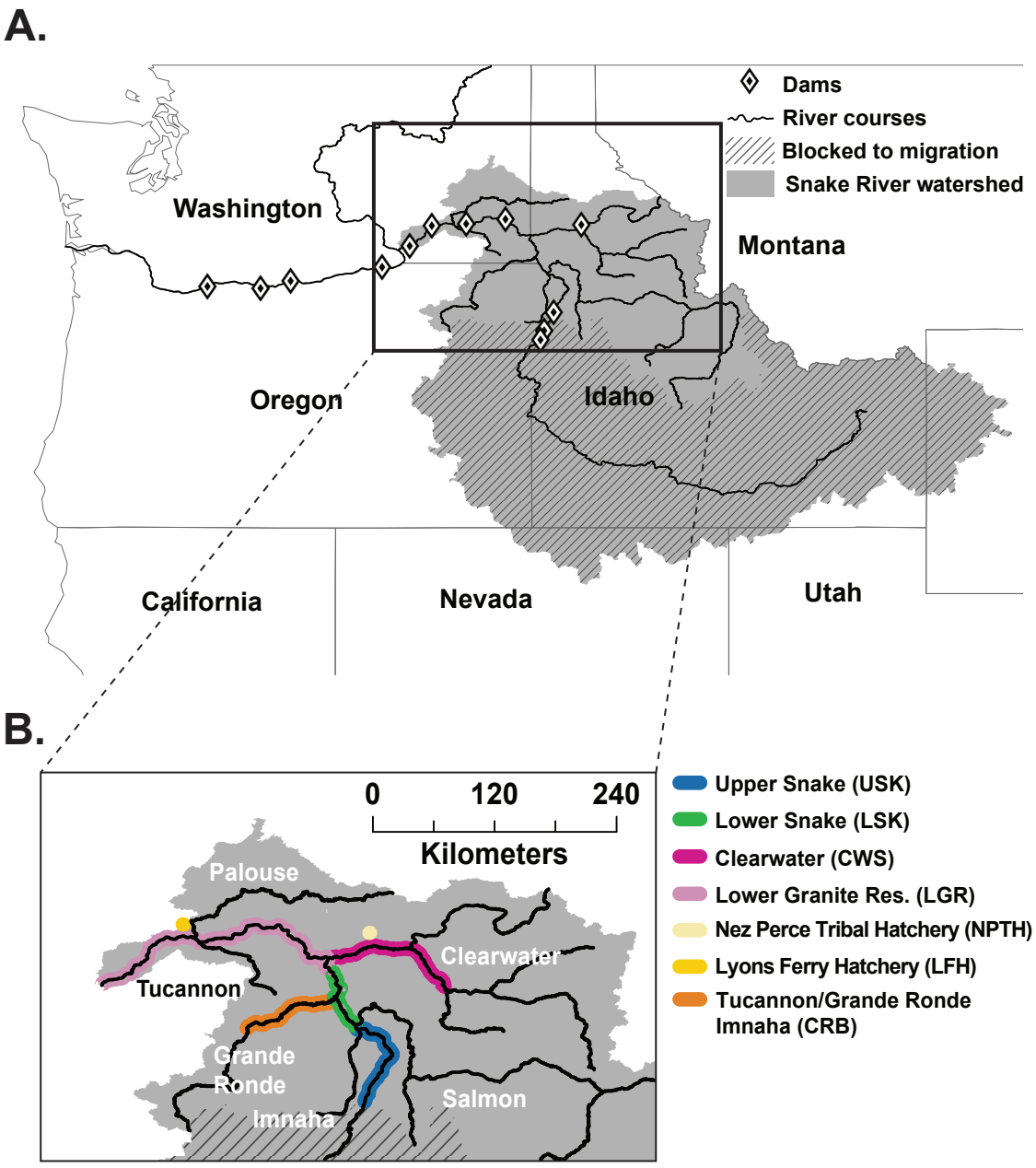
A.
Dams
River courses
Blocked to migration
Snake River watershed
Washington
Montana
Oregon
Idaho
California
Nevada
Utah
B.
0
120
240
Kilometers
Palouse
Clearwater
Tucannon
Grande
Ronde
Imnaha
Salmon
Upper Snake (USK)
Lower Snake (LSK)
Clearwater (CWS)
Lower Granite Res. (LGR)
Nez Perce Tribal Hatchery (NPTH)
Lyons Ferry Hatchery (LFH)
Tucannon/Grande Ronde
Imnaha (CRB)

Figure 3.3 – Spawning areas of Snake River fall Chinook salmon

Snake River fall Chinook salmon inhabit the Snake River (**a**) in the US States of Idaho, Washington and Oregon. The population is blocked from spawning above Hells Canyon Dam, and must pass 8 downriver dams on the Snake and Columbia Rivers to reach the ocean. The extent of spawning for known origin fish in our study (**b**) are highlighted. The Tucannon, Grande Ronde, and Salmon Rivers were not sampled for juveniles and produce a very small percentage of the wild fish in the basin.

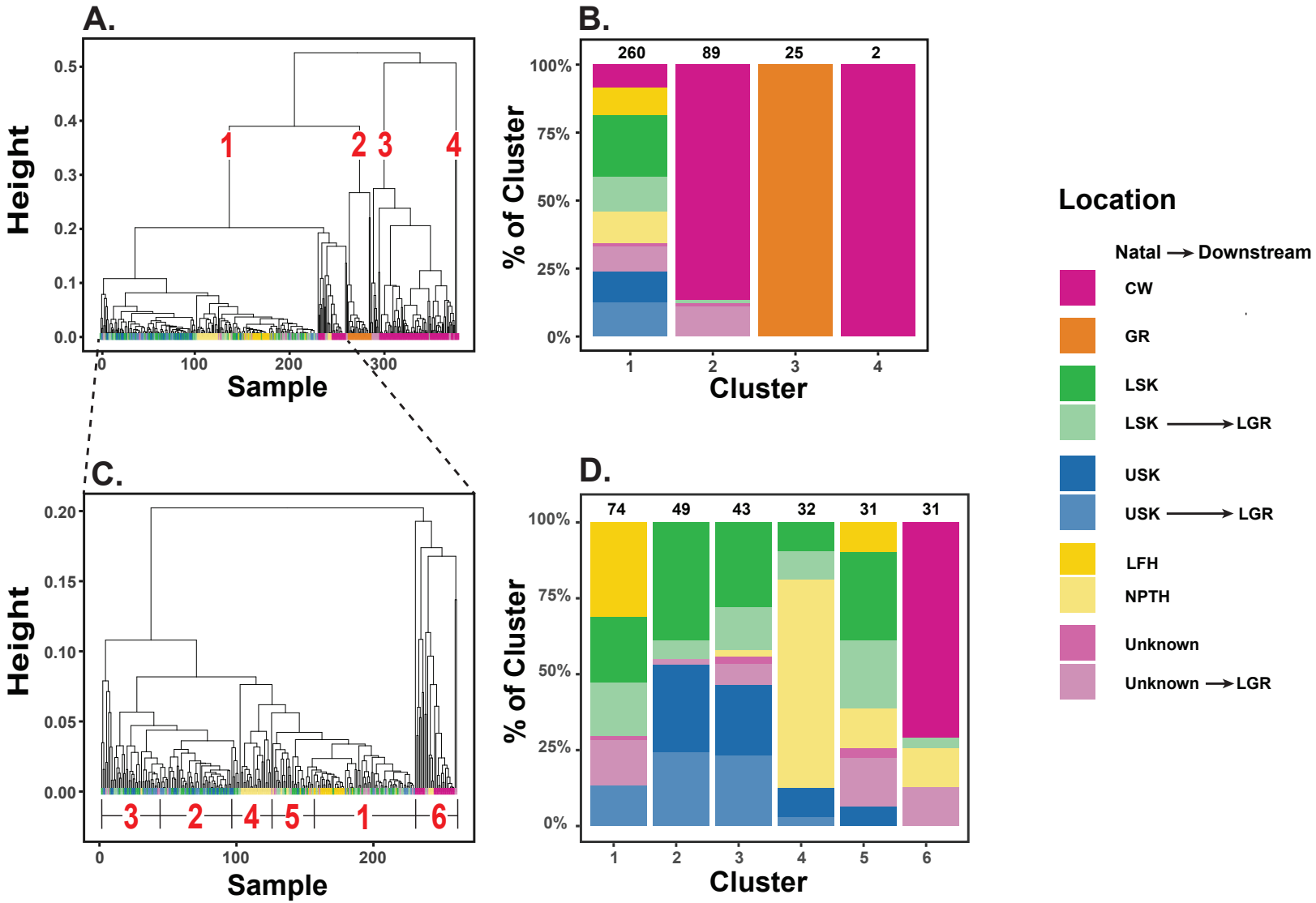
A.
Height
0.5
0.4
0.3
0.2
0.1
0.0
1
2
3
4
0
100
200
300
Sample
B.
% of Cluster
100%
75%
50%
25%
0%
260
89
25
2
1
2
3
4
Cluster
C.
Height
0.20
0.15
0.10
0.05
0.00
3
2
4
5
1
6
0
100
200
Sample
D.
% of Cluster
100%
75%
50%
25%
0%
74
49
43
32
31
31
1
2
3
4
5
6
Cluster
Location
Natal → Downstream
CW
GR
LSK
LSK → LGR
USK
USK → LGR
LFH
NPTH
Unknown
Unknown → LGR

Figure 3.4 – Hierarchical DTW clustering results

Hierarchical clustering of known-origin juvenile otolith transects resulted in a dendrogram (**A**) which, when cut at a height of 0.385, created four clusters. Clusters 2 and 3 (**B**) successfully clustered CWS and CRB juveniles, with a single bifoliate branch made up of CWS fish. Cluster 1 contained complex sub-structure. Re-clustering of cluster 1 as a single subset of the full dataset (**C**) and dynamic tree cutting resulted in six clusters (colored). The results of this clustering where mixed (**D**), with CWS and LFH juveniles being the most consistently grouped.

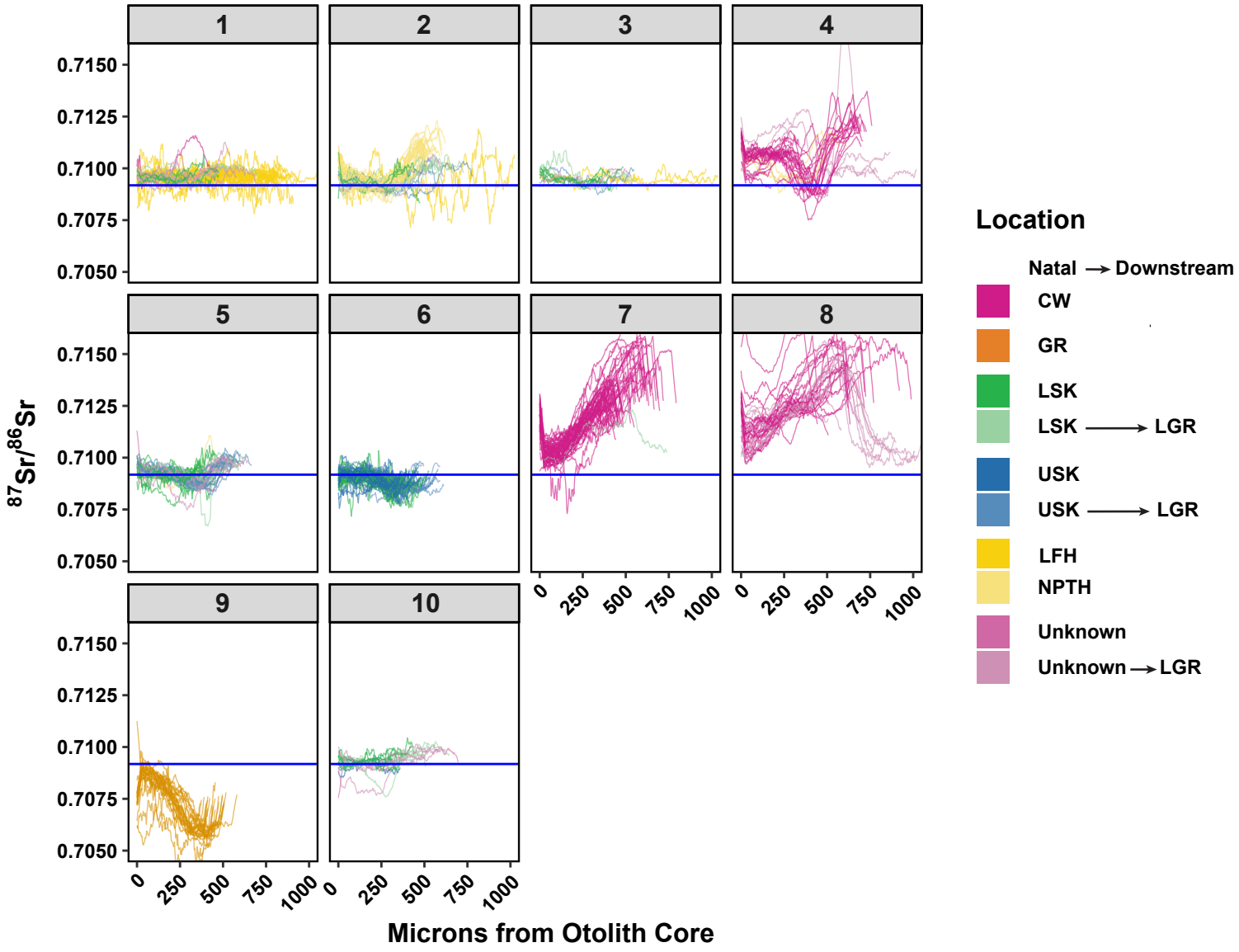
1
2
3
4
5
6
7
8
9
10
0.7150
0.7125
0.7100
0.7075
0.7050
0
250
500
750
1000
$^{87}Sr/^{86}Sr$
Microns from Otolith Core
Location
Natal → Downstream
CW
GR
LSK
LSK → LGR
USK
USK → LGR
LFH
NPTH
Unknown
Unknown → LGR

Figure 3.5 – Partitional DTW clustering results

Partitional clustering of known-origin juvenile otoliths with 10 clusters resulted in the most consistent clustering results. Clustering resulted in clusters which sub-divided the known classifications as determined by the known capture locations of juveniles but resulted in identifiable and meaningful clusters which separated hatchery fish (Clusters 1&2), fish from the CWS reach (Clusters 4, 7&8), LSK and USK reaches (Clusters 5, 6 & 10), and the GR (cluster 9).

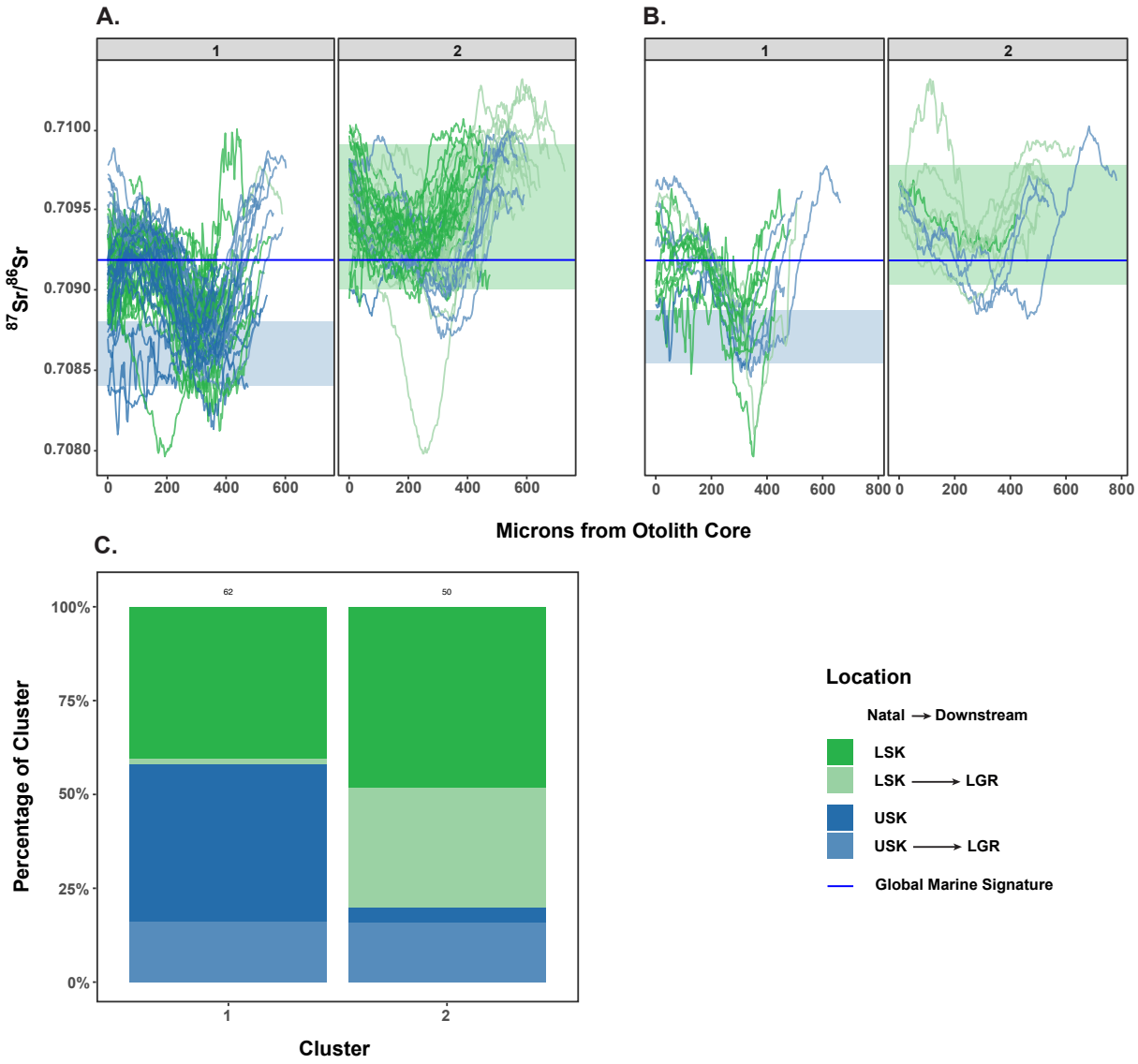
A.
B.
1
2
0.7100
0.7095
0.7090
0.7085
0.7080
$^{87}Sr/^{86}Sr$
0
200
400
600
800
Microns from Otolith Core
C.
62
50
100%
75%
50%
25%
0%
Percentage of Cluster
Cluster
Location
Natal → Downstream
LSK
LSK → LGR
USK
USK → LGR
Global Marine Signature

Figure 3.6 – Partitional DTW clustering to separate confounded USK and LSK groups

DTW clustering appears to separate the confounded USK and LSK groups which are confounded in the model-based discriminate function analysis using data from the test set used to create the discriminate function (**A**). Cluster 1 appears to contain mostly fish with a natal signature (~250-400μm from the otolith core) representative of the range of sampled water chemistry of the USK reach (light blue bar), While Cluster 2 appears to contain fish with signatures representative of the sampled water chemistry of the USK reach (light green bar). Test set data classified by nearest-neighbor classification (**B**) show similar separation of clusters. The majority of fish (**C**) in Cluster 1 (69%) were caught in the USK reach, while the majority of Cluster 2 (80%) were caught in the LSK reach.

Chapter 4: Abiotic and biotic effects on successful life history strategies under variable environmental conditions

Abstract

Early life events can shape the trajectory of individual life history with consequences for future survival and fitness. At the individual scale life history plasticity allows animals to respond across a gradient of external conditions to optimize their fitness. The range of life history variation within a population provides resilience in the form of a portfolio effect, as conditions favor different strategies under changing conditions. Environmental conditions are inherently variable in space and time across a populations range, which requires an understanding of life history variation that is spatially and temporally explicit. Climate change and anthropogenic impacts further shift the timing of environmental events and the conditions experienced by individuals across space. The timing of juvenile migration to the ocean has shown recent shifts within a population of Chinook salmon (*Oncorhynchus tshawytscha*) in the Snake River in the Northwestern United States. These shifts are spatially correlated among spawning areas and thought to be linked to spatial differences in temperature and the effects of dams. Evidence also indicates that this shift in migration strategy may be an example of rapid life-history evolution. Using a dataset spanning ten years of otoliths from returning adult otoliths we related the size of fish at ocean entry to the environmental conditions and growth experienced within each spawning area during their juvenile phase. We used a linear mixed modelling approach combined with location and movement information recovered using multi-tracer otolith microchemistry analysis of individual otoliths. Growth was also recovered from a second dataset of juvenile otoliths captured at known locations throughout the basin. Our findings indicate that delayed migration, as evidenced by longer residence within the Snake River, is correlated with larger sizes at ocean entry. Ocean entry size in the Snake River was affected by the interaction of location with high and low flow years, with fish in the Snake River entering the ocean at the largest

sizes during low flow years, with high flow years sharply decreasing the ocean entry size. The trajectory of late juvenile growth had an important positive effect on ocean entry size, indicating that growth within the reservoir system plays in important role in ocean entry size, despite research indicating that food resources are generally poorer than in riverine habitat.

Introduction

Events during the early life of individuals are often related to critical developmental events, and thus can affect the future trajectory of an individual's life history (Lindström 1999, Metcalfe and Monaghan 2001). Even in relatively long-lived species bird and mammal species with complex life-histories, early growth has been shown to affect survival and ultimate fitness (Lindström 1999). The same is true in insects and crustaceans, with early nutritional and environmental constraints affecting eventual reproduction, sex specific fitness, and resistance to starvation (Giménez and Torres 2004, De Block and Stoks 2005). Similarly, a one-week difference in emergence timing in Atlantic Salmon (*Salmo salar*) can translate into a one-year difference in the timing of ocean migration through a complex interplay of environment, social dominance, and developmental decision windows (Huntingford et al. 1990, Metcalfe and Thorpe 1992, Metcalfe et al. 1995).

Life history plasticity allows individuals the opportunities to respond to the tradeoffs in growth, survival, and resource allocation that these variable conditions create (Gotthard and Nylin 1995, Nylin and Gotthard 1998). These conditions vary both spatially and temporally across the landscape, the life history strategies employed to respond to them are inherently spatial and temporally distributed as well (Brommer 2000).

At the population level, this diversity of life-history response across time and space creates a portfolio effect of population dynamics (Hilborn et al. 2003, Schindler et al. 2010, 2015, Greene et al. 2010). As conditions change this "portfolio" of existing life-history strategies and plastic reaction-norms at the level of the individual provide

resilience for populations under a variety of conditions. Within this variation across the population, life history strategy as well as plasticity are under selection, with species evolving life history traits and plastic responses in reaction to changes in the balance of selective pressures on the population (Gotthard and Nylin 1995, Ghalambor et al. 2007, 2015, Buczkowski 2010).

Climate change and anthropogenic impacts create the possibility for demonstrable changes in the relevant timing and magnitude of many environmental processes influencing life history responses (Walther et al. 2002, Parmesan 2006, Wolkovich et al. 2014). For fish on the west coast of North America the alteration of snow melt and streamflow under climate change predictions, that tend towards lower summer flows and higher summer maximum temperatures, creates myriad temporal changes across the spatial extent of many aquatic species (Wenger et al. 2011, Isaak et al. 2012). Habitat fragmentation and the changes in species composition imposed by anthropogenic changes can also alter the mix of spatial and temporal environment (Dynesius et al. 1994, Haddad et al. 2015). Understanding how populations respond to these changes is critical to understanding their response and persistence, especially as the loss of life-history diversity has been implicated in the weakening of the portfolio effect for West Coast salmon (Moore et al. 2010, Carlson and Satterthwaite 2011, Griffiths et al. 2014).

The performance of a life-history strategy can be defined by the relative fitness of those individuals in the population that expressed it. Summed across generations, this performance provides insight into how a particular strategy was able to balance the tradeoffs in resource allocation presented by their environment in order to reproduce (Stearns 1989). For species whose generation time spans several years and/or that travel large distances through multiple environments, connecting juvenile strategy to eventual fitness can be quite challenging. Furthermore, for semelparous organisms with these characteristics, directly linking lifetime fitness to strategy assumes that environmental heterogeneity is at least as predictable today as it has been in the landscape under which historical selection has occurred. Linking life history

strategies to fitness are typically answered at the population level, or fitness is measured by proxy with the assumption that metrics such as body condition are reflective of future fitness. However, proxies of fitness across individual and population scales do not always match and proxies at one life stage may not reflect fitness in future stages (Brommer et al. 2004, Wilder et al. 2016). Population level studies are often limited in their ability to link successful strategies to the smaller-scale, spatially and temporally explicit conditions that influence life-history across life-stages (Clutton-Brock and Sheldon 2010).

Understanding the link between strategy at earlier life stages and eventual fitness in a spatial and temporally explicit context may provide important insights into life-history evolution and species persistence. Especially as climate change and habitat fragmentation alter the balance of selective pressures across multiple life stages, the historically optimal strategies at one life stage may no longer provide selective advantage throughout the life-cycle. Understanding the limits of population responses to the changing selective landscape, the degree to which evolutionary responses are possible, and the interplay of plasticity and evolution on fitness, are both of intellectual interest ecologically as well as important in the context of conservation (Nylin and Gotthard 1998, Crozier et al. 2008, Hutchings 2011).

Snake River fall Chinook salmon provide a compelling study system for examining life-history variation, and life-history evolution, within a spatially and temporally explicit context. This population historically exhibited a consistently early juvenile outmigration strategy, likely selected for by high growth potential and high summer temperatures that selected against juveniles remaining in the river (Connor et al. 2016). The construction of dams has fragmented and reduced their range, while simultaneously changing flow and temperature regimes across their range. Juveniles in the population have relatively recently begun to exhibit an alternate outmigration strategy in which juveniles remain in the reservoirs throughout the summer, remaining as long as the following spring (Connor et al. 2005). Evidence indicates that this change is spatially correlated, with cooler spawning areas producing the majority of

late migrating fish, and late migrating fish making up a large proportion of adults returning to spawn (Connor et al. 2002, Hegg et al. 2013a). Recent evidence indicates that this change in migratory strategy includes a hereditary component and may be an example of evolution in response to the changes in their habitat (Williams et al. 2008, Waples et al. 2017).

For juvenile salmon, the size of outmigration is a balance between the increased probability of survival in downstream habitats that size provides and the growth opportunity that ocean entry affords (Mangel and Satterthwaite 2008, Satterthwaite et al. 2009). For Fall Chinook salmon, under historical conditions summer survival would have been limited by temperature and therefore the balance presumably favored fast growth and early outmigration. In contrast, the recent shift toward delayed "yearling" outmigration is thought to be a response to later hatch dates and lower growth rates in the Clearwater river (Waples et al. 2017). While these fish may experience slower or delayed initial growth, their delayed outmigration can result in juveniles leaving the basin at significantly larger sizes (~100mm greater) than their "subyearling" counterparts, having grown over the winter in reservoir habitat (Connor et al. 2005). The size at which fish outmigrate and enter the ocean is correlated with their survival (Zabel and Williams 2008, Satterthwaite et al. 2012), and therefore this difference in size may be one reason for the evidence of higher survival in yearling fish.

Our interests in the relating the variability of wild salmon life history strategies to environmental conditions and, ultimately the fitness consequences is hindered by our inability to track individuals across their entire lifetime. Otoliths, the inner ear organ of bony fish, grow through the accretion of a new layer of calcium carbonate every day (Campana 1983) like a tree the width of these rings is correlated with somatic growth and can be used to reconstruct growth history (Campana and Thorrold 2001). As well, trace amounts of elements and isotopes substitute into the calcium carbonate matrix in proportion to their concentration in the environment, providing a temporal record of the chemical properties associated with each life stage (Thorrold et al. 1998, Kennedy et al. 2000). Because many of these trace chemicals are tightly coupled to the

geology of watersheds, $^{87}Sr/^{86}Sr$ in particular (Kennedy et al. 1997, Hegg et al. 2013b, Bataille et al. 2014), the location of fish can be reconstructed throughout their life based upon the sampled chemical and isotopic variation across their range (Kennedy et al. 2002, Barnett-Johnson et al. 2008, Limburg et al. 2013). Efforts to apply the otolith microchemistry techniques to this population of have successfully describe variation in juvenile life-history patterns with a high degree of spatial and temporal resolution (Hegg et al. 2013a, 2013b, Hegg et al. Chapters 1, 2 & 3).

This technique allows for the reconstruction of movement in the juvenile phase in adult fish which have successfully returned to spawn, as well as juveniles across the range (Hegg et al. 2013a). This provides an opportunity to link location-specific growth from otoliths, and abiotic variables experienced at earlier life-stages, to the strategies employed by successful spawners across a range of years. In essence, allowing for the ability to examine the norms of reaction across space and time within the population under a range of environmental conditions.

Our overarching objective was to correlate ten years of variation in 1) environmental conditions in mainstem spawning rivers (flow and temperature), 2) individual growth (both as a function of location and relative size), and 3) behaviors in term of dispersive movements before smoltification, to the timing of ocean entry for wild population of Columbia River salmon. Based upon a population of naturally spawned, unmarked adult Snake River fall Chinook salmon that represented a period of ten hatch years (2002 – 2012), we used established variation in chemical and isotopic signatures, to reconstruct spatially explicit patterns in natal origin, outmigration strategy and outmigration timing. Known origin, tagged individuals sampled as juveniles permitted us to unequivocally link microchemical patterns to rearing areas in the basin. These juvenile samples were also used to estimate location-specific growth and to relate fish size to otolith radius. Otolith microchemistry and microstructure of returning adults permitted us to determine natal location, downstream movements within the Snake River, and the length of fish at ocean entry. We used a large sample of known-origin juveniles to link otolith chemistry to location.

Variables affecting the size of returning adult fish during their juvenile entry into the ocean were associated to juvenile environmental conditions using linear mixed-effects models to partition the variance between natal location and hatch-year. We utilized a multi-model inference approach to determine the factors that most strongly affect juvenile outmigration life-history strategies that are represented in successfully returning adult fish.

Methods

Study Population

The Snake River is the largest tributary to the Columbia River in the Northwestern United States (Figure 1). The Snake River basin extends throughout the state of Idaho, with its headwaters in the Teton mountain range in Wyoming and parts of the basin extending into Nevada and Utah. The Snake River flows into the Columbia River in South-Central Washington State. Starting in 1958 and ending in 1975 construction of hydropower dams in the Columbia and Snake Rivers, which provide a navigable shipping channel to Lewiston, Idaho, 751km inland, created significant anthropogenic impacts on the river system (Waples et al. 1991). This network of slack water reservoirs impounds natural flows to the town of Asotin, WA at the entrance to Hells Canyon on the Snake River. Fish passage is blocked above Hells Canyon Dam in the Upper Snake River.

Snake River fall Chinook salmon, a threatened population of fall returning Chinook salmon (*Oncorhynchus tshawytscha*) utilize the free-flowing, mainstem rivers above the reservoirs to spawn (Waples et al. 1991, Good et al. 2005). The most productive spawning areas for this population historically were located above Hells Canyon between Shoshone Falls and the Burnt River which is now inaccessible due to Hells Canyon Dam (Connor et al. 2002). While growth opportunity in these aquifer moderated habitats was, spawning areas and downstream reaches could reach lethal or sub-lethal temperatures in the summer months (Connor et al. 2016). This is thought to have selected for a nearly universal ocean-type life history strategy, with juveniles

moving downstream to the ocean by the summer of their first year (Connor et al. 2005, Waples et al. 2017).

The current population (Figure 1) spawns in the Snake River below Hells Canyon dam and above the confluence of the Salmon River, known as the Upper Snake River spawning area, and the Lower Snake River spawning area from the Salmon River to Asotin, WA. The third major spawning area is in the main stem of the Clearwater River, as well as smaller populations in the Grande Ronde, Imnaha, and Tucannon Rivers (Waples et al. 1991, Good et al. 2005). Juveniles from these spawning areas move downstream, utilizing shallow water habitat along the reservior margins before moving to pelagic habitat as summer progresses (Connor et al. 2003b, Tiffan and Connor 2012). Cool water from Dworshak Reservoir on the Clearwater River is used to moderate summer reservoir temperatures and increase survival of migrating juvenile salmon in the reservoirs (Connor et al. 1998, 2003b) and pelagic juvenile fall Chinook salmon utilize the temperature gradient with depth to thermoregulate (Tiffan et al. 2009).

Recently, the timing of juvenile outmigration has shifted from the historical early outmigration toward a mixture of early- and late-migrating juveniles, with some juveniles remaining in the Snake River until the next spring (Connor et al. 2005). This behavior is thought to be related to cooler temperatures in the extant spawning areas (Connor et al. 2002), with larger numbers of late-migrating juveniles originating in the Clearwater than from spawning areas in the Upper and Lower Snake Rivers (Hegg et al. 2013a). Recent work has indicated that this shift in outmigration strategy is likely linked to heritable factors and that this shift is an example of recent evolution in response to the anthropogenic effects of the dams (Williams et al. 2008, Waples et al. 2017). This shift in life-history strategies has been accompanied by earlier movement from riverine to reservoir habitats, with one study indicating density-dependent processes may be moving the population toward more historical outmigration timing as populations have increased over the last twenty years (Connor et al. 2013).

Flow, Temperature, and Hatch Date

Stream flow and temperature data was obtained for each of the hatch years represented in our fish samples. These flow and temperature datasets were then used to calculate descriptive flow and temperature metrics used as predictor variables in our subsequent model.

Daily flow for the Snake and Clearwater Rivers was obtained from the USGS National Water Information System (https://waterdata.usgs.gov/nwis). Flow for the USK reach was obtained from the USGS site at Hells Canyon Dam (site# 13290450). Flow for the LSK reach was obtained from the USGS site at Anatone, WA (site# 13334300). The CW reach flow was obtained from the USGS site at Spalding, ID (site# 13342500). Daily flow for the LGR reservoir section was queried from the Fish Passage Center (http://www.fpc.org/river/flowspill/FlowSpill_Query.html) as total discharge for Lower Granite dam.

Daily average temperature for the USK and LSK sections was obtained from data collected cooperatively by US Fish and Wildlife Service and Idaho Power. Daily average temperature data for the CW reach was taken from records at the Spalding gauge. Temperature for LGR was queried from USGS site on the right bank below Lower Granite Dam (site# 13343595).

Temperature data was used to calculate the hatch date of fall Chinook salmon redds in each reach according to the metric proposed by Connor et. al (Connor et al. 2003a). Mean daily temperature (°C) for each year and location in our sample were summed cumulatively from November 1st until cumulative degrees reached 1066°C. The date at which cumulative temperature surpassed this threshold was considered the mean hatch date for that year and location.

Temperature during incubation, as well as within the context of juvenile bioenergetics has been shown to affect the growth and persistence of salmonids (Merz and Vanicek 1996, Myrick and Cech, Jr. 2000, Nislow et al. 2000), and limits the habitat available to Snake River fall Chinook salmon (McCullough 1999, Connor et al. 2003a). Therefore, three additional temperature metrics were calculated which we

hypothesized may affect the growth or life-history of juvenile fall Chinook salmon and ultimately affect ocean entry timing. The first was the maximum temperature attained for each location and year. As well, we calculated the accumulated degrees from January 1st to August 1st as a measure of the overall temperature regime during the juvenile phase. As a more specific indicator of temperature regime during the active phase of the juvenile life cycle we calculated the cumulative degrees from the calculated hatch date to July 1st when fish begin to move in large numbers past Lower Granite dam (Tiffan and Connor 2012).

Flow has been found to affect the survival of redds, as well as affecting survival and downstream movement decisions in juvenile salmon (Stevens and Miller 1983, Cunjak et al. 1998, Lawson et al. 2004). To capture the effects of flow variation on juvenile salmon life history we calculated four descriptive metrics of flow for each reach and year. The first was the volume of the maximum flow, which in the Snake is generally in the early Spring as the system is snowmelt dominated. The date of this maximum flow event was also calculated. Finally, we calculated the volume and date corresponding to the center of timing (CT) for the year's flow, the volume at which 50% of the yearly flow has passed. This metric has been shown to summarize both yearly flow, as well as the timing of flow in terms of early snowmelt events and the amount of precipitation which falls as rain versus snow (Regonda et al. 2005, Wenger et al. 2010).

Finally, we utilized these abiotic metrics to classify flow in each of our study reaches into distinguishable water-year regimes. This was done using model based clustering in the {mclust} package for R (Scrucca et al. 2016). The variables used to classify stream flow regimes were the cumulative temperature between Jan 1st and August 1st, the maximum flow volume, the date of maximum flow, and the day of CT for each year. Clusters were limited to 5, with unconstrained shape, direction and variance. The number of optimal clusters in each reach was determined based on the lowest BIC score. The results of this clustering were then used to partition available juvenile growth into water-year groups below.

Otolith Collection and Preparation

Otolith samples were taken from both adult and juvenile fish. Adult samples (n=591) were trapped upon their return to Lower Granite Dam as a part of broodstock collections, transported to Lyons Ferry Hatchery, and otoliths were collected after fish were spawned (Milks and Oakerman 2016). Otoliths were collected from all presumed-wild adult fish (fish which did not have a hatchery implanted coded-wire tag, adipose fin clip, or other marking identifying them as hatchery origin) between 2006 and 2013. Scale aging was completed on all collected fish to determine their hatch year. Not all hatchery fish are tagged with a coded-wire, passive integrated transponder (PIT), or adipose fin clip, which required the identification of hatchery and wild fish using otolith chemistry described below.

Samples from return years 2006-2010 were likely biased toward Clearwater origin adults due to the use of scale-based hatchery-wild classification which was later found to be inaccurate (Deborah Milks, WDFW, *personal communication*). During these years otoliths were only analyzed for those fish designated as wild-origin from their scales. This was discontinued when it was discovered that the scale-based classification was ineffective. The effectiveness of scale-based designation of hatchery and wild fish was different for yearling and subyearling fish. The technique was found to be most effective for late-outmigrating yearling fish, meaning that a higher percentage of yearling fish were retained in our sample while a lower percentage of subyearlings were retained. As previous work has shown (Connor et al. 2005, Hegg et al. 2013a), these strategies are spatially correlated, with more fish exhibiting a yearling strategy in the Clearwater River. The end result was a bias of unknown magnitude toward fish from the Clearwater in our sample set.

Juvenile fish were captured as a part of ongoing beach-seine population surveys in the Snake, Clearwater, and Grande Ronde Rivers (n=376, hatch years 2010-2014). A subsample of these juveniles were PIT tagged and recaptured when they passed Lower Granite dam. Samples were also collected from both hatcheries in the basin as described in Hegg et al. (Chapter 2, *in review)*. A subsample of these fish (n=97) were

analyzed for growth below. An additional sample of juvenile fish (n=79, hatch years 1993,1994, 2007, 2008) captured at Lower Granite dam were analyzed for growth. Additionally, the otolith radius of a smaller sample of fish (n=17) captured in the Columbia River and in the ocean near the mouth of the Columbia River and confirmed to be Snake River Fall Chinook based on genetic data, were included as endmembers in the calculation of fork length from otolith radius below (Sagar et al. 2013). The fork length (mm) of all fish was recorded.

Otoliths were mounted and prepared as described in Hegg et al. (Hegg et al. 2013a) based on established techniques (Campana and Neilson 1985, Secor et al. 1991a). Briefly, otoliths were mounted on glass microscope slides using heat-set adhesive, then ground on the sagittal plane using a lapping wheel and increasingly fine grit silicon dioxide sandpaper until the core and rings were visible in the region 90° from the otolith sulcus on the dorsal side. Analysis for chemical composition and growth were carried out on this region for all analyses.

Otolith Microchemistry

Otolith microchemistry was analyzed for each adult otolith using laser ablation inductively coupled plasma mass spectrometry (LA-ICP-MS) as described in Hegg et al. (Chapter 2 & 3). Analysis was performed to determine $^{87}Sr/^{86}Sr$ as well as a suite of four elemental ratios of Calcium (Strontium, Barium, Manganese, and Magnesium). Microchemistry was analyzed along a transect from the core of the otolith to its edge (Figure 2), creating a continuous chemical time-series from the birth of the fish (core) to its death (edge). The length of each transect was calculated based on the laser scan speed (10μm/second) and instrument integration time. Distances were corrected to the elemental scan and, in the case of otoliths measured for growth, the length was corrected based on the otolith radius measured in Image Pro software described in the next section.

Growth and Length Analysis

Somatic growth was measured in juvenile otoliths using digital images taken with a Zeiss Axio Scope A1 microscope and a Leica DFC450 digital camera. Juvenile otoliths were imaged at 20X magnification and images were measured using Image Pro software (version 7.0; MediaCybernetics©). Contiguous, visible rings were measured in microns from the core of the otolith, as was the otolith radius at the edge of the otolith.

Otolith increment-width was converted to fish fork-length through by creating a linear regression between otolith width (μm) and measured fork length (mm) for each fish in the sample set (Figure 3), plus the fish collected downstream from the Columbia River and Ocean near the mouth of the Columbia. This relationship was then used to convert otolith increment width to growth in millimeters per day based on the fact that each increment is equivalent to one day of growth.

Growth data was determined for three periods (early, middle, and late growth) of juvenile growth based on results of beach seine sampling. Early growth was defined as growth prior to 65mm of fish length, which is roughly equivalent to the end of the natal period from Hegg et al. (Chapter 2, *in review*). Middle growth was defined as growth greater than or equal to 65mm and less than 95mm fork length. Late growth was defined as any growth greater than or equal to 95mm. The cutoff between middle and late growth was set to approximate the length of fish during the peak day of beach seine capture, assuming that the decrease in capture after this date was due to downstream migration to the reservoir.

The mean early, middle, and late growth within each river reach and water-year (as calculated in the 'Flow, Temperature and Hatch Date' section above), was then applied to adult samples from each location and water year. As well the trajectory of growth, whether growth rate was increasing or decreasing during each period, was determined by fitting a linear regression to each growth period, for each juvenile sample and retaining the slope coefficient of this model. A mean of the resulting slopes was then taken for each growth period, within each reach and water-year, and

matched to adult otoliths with hatch years corresponding to the same water-year regime.

Natal Location, Downstream Movement and Ocean Entry

The natal location of adult fish, whose provenance was unknown, was determined using the methods from Hegg et al. (Chapter 2, *in review*). A 100μm period on the otolith after the end of maternal influence (between 300-400μm) was classified to location using the model based discriminate function developed by Hegg et al. This discriminate function classified otoliths to a natal location of the Clearwater (CW), Snake River (SK), Lower Granite Reservoir (LGR), Lyons Ferry Hatchery (LFH), or Nez Perce Tribal Hatchery (NPTH). Because we expected the timing of hatchery fish to vary due to unmeasured factors within the hatchery we excluded fish classified to a natal origin of LFH or NPTH from further analysis.

The model-based discriminate function was unable to separate fish from the two Snake River reaches, despite the significant chemical differences between these reaches (Hegg et al. 2013a), due to early movement of juvenile fish. To separate these two groups, we used the Dynamic Time Warping (DTW) method developed by Hegg et al. (Chapter 2 in prep, Sarda-Espinosa 2017a) which evidence indicated was able to distinguish these populations using nearest neighbor classification to the time warping clusters. To classify adult otoliths using this method the first 500 microns of the $^{87}Sr/^{86}Sr$ transects of fish classified to the SK group were extracted (equivalent to the average length plus one standard deviation of the juvenile otoliths used to create the DTW clusters). These transects were smoothed using a 20-point moving average and reinterpolated to 200 cells before being classified to the USK or LSK cluster using nearest neighbor DTW classification. The locations of these fish were then updated based on the DTW classification results.

Additionally, the discriminate function classification for the Clearwater River included some fish with $^{87}Sr/^{86}Sr$ signatures well below the signatures recorded in the Clearwater based on water sampling (Chapter 2, *in review*), and in fact lower than all but the Grande Ronde, Imnaha, and Tucannon Rivers, which have the lowest $^{87}Sr/^{86}Sr$

signature in the basin (Figure 2.1). Additionally, the $^{87}Sr/^{86}Sr$ signatures of some fish classified to the Lower Snake River were much higher than signatures recorded from water sampling. This is likely due to the fact that the discriminate function is not weighted between chemical variables. However, $^{87}Sr/^{86}Sr$ in otoliths is tightly tied to the water signature, making these outlying classifications impossible. Therefore, we filtered the Clearwater group for any fish with a signature below 0.7077, well below that of the Upper Snake River according to water sampling. These fish were re-classified to the Grande Ronde. We similarly filtered the Lower Snake River group such that any fish with a natal $^{87}Sr/^{86}Sr$ signature above 0.7103 was reclassified as Clearwater.

We determined each downstream movement using a changepoint algorithm applied to each otolith transect (Killick and Eckley 2013, Hegg et al. 2015a). The penalty value was set at 0.00005 which appeared to balance the number of changepoints and the sensitivity to chemical changes using an elbow plot (Killick et al. 2012). Each of the identified changepoints was then classified to location using the model-based discriminate function used to classify fish to natal location. When sequential changepoints were classified to the same river reach the changepoints were collapsed into a single movement. The number of changepoints after the end of the natal period (>400μm) was determined for each fish, as well as the fork-length at each downstream movement.

We determined the size of each fish at ocean entry using the increase in ^{88}Sr intensity due to the increase in strontium concentration in ocean water (Hegg et al. 2013a) as well as the convergence of the $^{87}Sr/^{86}Sr$ signature to the global marine $^{87}Sr/^{86}Sr$ signature of 0.70918 (Faure and Mensing 2004). We defined the point of ocean entry as the distance from the otolith core at which the ^{88}Sr intensity had peaked and the $^{87}Sr/^{86}Sr$ signature had visually converged to the global marine signature. The increase in ^{88}Sr intensity at ocean entry was marked when a ten-point running mean increased to greater than 2 standard-deviations from a ten-point rolling mean lagged ten points behind. The ocean entry location was then refined visually

based on the criteria above. Initial ocean entry determinations were all checked by a single master reader to ensure consistency. This location on the otolith was then converted to fork length (mm) using the regression equation developed in the previous section.

Modelling Ocean Entry Timing

To relate ocean entry size to the abiotic and biotic variables of flow, temperature, growth and movement we developed a linear mixed effect model with a nested random effects structure using the {lme4} package for R (Bolker et al. 2009, Gałecki and Burzykowski 2013, Bates et al. 2015). River reach was used as the first random effect, with water-year or hatch-year as a nested random effect. We used likelihood ratio tests to determine significance of fixed effects as well as the fit of random intercept and random slope models after fixed effects were selected.

The selection of fixed effects was done using a multi-model approach since the importance of the potential variables on ocean entry size was unknown. We used the {glmulti} model selection package for R to perform model selection based on minimizing AICc (Calcagno and Mazancourt 2010). We did not include higher level interactions in the selection procedure. The genetic algorithm selection procedure within {glmulti} was used to converge on the best model since the number of potential models was large. The genetic algorithm was run twice for each potential model to ensure that the parameter space was effectively searched and to minimize the chances of converging to local optima.

The AICc metric is sensitive to sample size, however growth data was not available for all adult samples. Therefore, model selection was completed for two datasets, a full dataset including abiotic variables and the number of post-natal downstream movements, and a subset that included only the adults for which growth data was available.

Results

Flow, Temperature and Hatch Date

The Lower Snake River had the earliest mean date of the yearly maximum flow event, averaging the first week of May (Julian Day 127 ±29), as well as the earliest CT date (142 ±14), but also displayed the most variability in the timing of both events (Table 1). Flow timing was latest in Lower Granite Reservoir and also was the least variable (varying by less than a week in both maximum flow timing and CT). This is expected as the flow is highly controlled through Lower Granite Dam. The Upper Snake River and Clearwater River maintained similar mean maximum flow dates, in mid- and late-May respectively.

The Clearwater, as expected from prior research (Connor et al. 2002, 2003a), was the coolest river in terms of its mean maximum temperature (18 ±3°C) over the study period (Table 1). The other three reaches having a mean maximum temperature of 23°C, near the thermal limit for Chinook salmon juveniles (McCullough 1999). The Clearwater River, in keeping with its cooler water, also showed the slowest accumulation of thermal units, with mean accumulated degrees of only 623°C (±224°C) for the period between hatching and July 1st. However, the variability in accumulated temperature was also approximately double that of the other three reaches.

The slower accumulation of temperature in the Clearwater resulted in the latest and most variable mean hatch date, May 12th (Julian Day 132 ±14), across the years represented in the study. Hatch date in the Upper and Lower Snake River averaged as much as a month earlier, at 104 (± 9) and 110 (±10) Julian days respectively. Hatch date was late in Lower Granite Reservoir (Julian Day 119 ±4), however there is no spawning within the impounded section of the river.

The results of cluster analysis on temperature and flow metrics resulted in remarkably consistent results across each river reach. The model-based clustering algorithm consistently identified models including three clusters as the top model using BIC model selection, except in Lower Granite Reservoir were only two clusters

were identified (Figure 3). These clusters were consistently separated by the maximum yearly flow, with high volume flow, mid-volume and low volume years separating into distinct water-year clusters with the other variables helping to define the separation. Therefore we utilized these three water-year designations (high cfs, middle cfs, and low cfs) as a metric to describe the general water-year patterns within the basin in subsequent modeling and growth analysis.

Otolith Microchemistry

Microchemistry was taken for each juvenile and adult otolith in the sample set, excluding fish used solely for growth captured in the Columbia River and Ocean and Snake River fall Chinook juveniles captured in 1993, 1994, 2007, 2008. The detailed results of this analysis are contained in Hegg et al. (Chapter 2, *in review*). A total of fifteen (15) adult fish were removed from analysis due to poor strontium intensity resulting in wide variation in $^{87}Sr/^{86}Sr$ signatures within the otolith.

Strontium $^{87}Sr/^{86}Sr$ data was corrected based on the global marine signature for each analysis day using a marine shell standard (mean $^{87}Sr/^{86}Sr$ = 0.709186, standard deviation = 0.000077, n=535). Elemental counts were corrected to the SRM 610 standard (Jochum et al. 2011) and also corrected to calcium using a ten second, within-run blank. Limits of detection (LOD) for each element were calculated as 3 X SD from the mean of the blank. Expressed as a ratio of elements to calcium resulted in detection limits of; Sr/Ca 0.029 $mm \bullet mol^{-1}$, Ba/Ca 0.023 $mm \bullet mol^{-1}$, Mn/Ca 0.031 $mm \bullet mol^{-1}$, and Mg/Ca 0.022 $mm \bullet mol^{-1}$.

Growth and Length Analysis

The otolith radius for each fish measured for growth, as well as juvenile fish captured in the Columbia River and Ocean, were regressed against their measured fork-length at capture (Figure 4). This resulted in a linear relationship of the form,

$$Fork\ Length = 0.1995 \bullet Otolith\ Radius - 12.3152$$

whose intercept ($p=0.00017$) and slope ($p<0.00001$) terms were both significant. The overall model was also significant ($p<0.00001$) and explained 89.2% of the variation in the data (adjusted R^2). This otolith radius to fork-length relationship was then used to convert measured otolith growth to fish fork length, and to the length of each individual at the point that ocean entry was determined using $^{87}Sr/^{86}Sr$ and ^{88}strontium intensity.

Growth rate and trajectory varied both between river reaches and between growth periods (Table 1). Mean growth rate was highest in the late growth period (fork-length > 95mm), varying between 0.877mm/day in the Clearwater and 1.47mm/day in Lower Granite Reservoir. Growth trajectory was highest for Clearwater fish across all growth periods, with the highest trajectory (0.035mm/day) in the middle period. Trajectory was flat to slightly negative (-0.005mm/day) in Lower Granite during early and middle periods, with the highest growth trajectory in the late growth period (0.012mm/day). In contrast the Lower Snake River showed highest trajectory in the early period (0.015mm/day) with flat growth in the middle period and negative growth in the late growth period (-0.004 mm/day). The Upper Snake River also maintained high trajectories, ranging from 0.010 mm/day in the early period to 0.031mm/day in the late growth stage.

When separated by water-year and river reach, mean growth rate maintained the trend of increasing growth rate from early to late growth periods. Growth trajectory was markedly lower in mid-cfs water years, with growth increasing at the highest rate in all reaches during the early period, middle period growth nearly flat and late growth periods having negative growth trajectories in all but the Clearwater.

This trend was reversed in low-cfs years with trajectories averaging 0.004mm/day across the Clearwater, Upper and Lower Snake reaches during the early and middle growth period (no growth was available for Lower Granite Reservoir during low-cfs years). However, the late growth period showed high increases in growth with growth rate increasing by between 0.044 and 0.063mm/day.

During high cfs water-years Lower Granite reservoir showed low growth trajectories, with negative early growth (-0.005mm/day), nearly flat growth in the middle period (0.002mm/day) and late growth at 0.012mm/day. The Clearwater, in contrast, showed low early growth trajectory (0.002mm/day) increasing to 0.054mm/day during the middle period and then decreasing to 0.022mm/day during the late period. The Lower Snake River showed its highest growth during the early period (0.019mm/day) decreasing to 0.006mm/day in the middle period. The Upper Snake showed similar early growth the Lower Snake reach during this period (0.018mm/day), increasing to 0.035mm/day during the middle period of growth. No growth data was available for the late period in high cfs years for the Upper and Lower Snake Reaches.

Natal Location, Downstream Movement and Ocean Entry

Classification to natal location using discriminant function analysis, followed by DTW re-calssification of fish classified to the Snake River, and subsequent filtering of Clearwater and Lower Snake groups resulted in 219 fish classified to the Clearwater River, 78 fish classified to the Lower Snake River, 48 classified to the Upper Snake, and 38 fish classified as early-moving juveniles with a natal signature in Lower Granite Reservior. One hundred and seventy-two fish were classified to a natal origin in the Snake River by their otolith chemistry using the model-based discriminant function. Of the fish classified to the Snake River by the model-based discriminant function 65% were re-classified to the Lower Snake river by subsequent DTW classification.

Returning adult fish originating in the Clearwater River were the largest at ocean entry as juveniles across all years (Figure 5A). In general fish size at ocean entry showed a decreasing trend within river reaches in response to water-year, with fish entering the ocean at increasingly smaller sizes during middle-cfs and high-cfs water years.

The majority of fish (212, 54%) did not show an additional downstream movement after their natal location based on changepoint analysis. An additional 124 fish (32%) exhibited only 1 additional downstream movement after their natal location.

Fish with two or more distinguishable downstream movements prior to ocean entry were rare with 37 having two distinguishable movements (9.4%), 11 exhibiting three movements (2.8%) and 7 exhibiting 4 downstream movement (1.7%).

Adult fish originating in the Clearwater River entered their first new downstream habitat at the largest size as compared to the other river reaches (Figure 5B). Overall the length of the first changepoint exhibited a decreasing relationship within each river reach in response to water year, with fish leaving their natal location at smaller sizes in higher flow volume water-years.

Modelling Ocean Entry Timing

The first model selection was performed to determine the most likely fixed effects for a random-intercept model with water-year as a nested fixed effect within river reach fit to the full dataset (only abiotic temperature and flow variables and the number of downstream movement for each fish were included as the potential fixed effects). The genetic algorithm explored 30,000 models in across two runs of 150 generations and 160 generations. Both model selection runs converged on the same top model within 30 generations but continued exploring the parameter space until the change in average AICc was less than .2 between generations. The combined results of these model selection runs resulted in 9 models within two AICc points of the top model (Table 2). Across all of the investigated models the number of downstream movements and the date of maximum flow were the most important, appearing in more than 80% of the top models (Figure 6A, Table 3). The yearly median flow volume also appeared in nearly 80% of the top models. The model with the lowest AICc score took the form,

Ocean Entry Length (mm) = Median flow volume + Date of maximum flow + Maximum temperature + Cum. temperature (Jan. 1 – Aug. 1) + Number of Downstream Movements

with the random effect of river reach explaining 458mm (±21.4 SD) of the variance in ocean entry length and the nested fixed effect of water-year within river

reach explaining 74mm (±8.3 SD). Residual variance unexplained by the fixed effects structure was 1055mm (±32.5 SD). The q-q plot of residuals did not indicate significant deviations from the assumption of heteroskedasticity.

Likelihood ratio tests between models with and without each fixed effect in the top model indicated marginal support for the cumulative temperature between Jan 1st and Aug. 1st ($p=0.065$). The number of downstream movements was highly significant ($p<0.0001$), as was the median flow volume ($p<0.0001$). The date of maximum yearly flow ($p=0.02$) and maximum yearly temp ($p=0.02$) showed more moderate but still significant support.

Random-intecept models fit to the subset of fish for which growth data was available resulted in zero variance for the water-year term, indicating lack of support for nested fixed effects structure. Thus, model fitting was conducted with only river reach as a random effect. The genetic algorithm converged on the top model between ~30 generations in both runs but continued for 240 and 270 generations respectively, surveying 51,000 potential models. The resulting combined model selection results contained 11 models within two AICc points of the top model (Table 3). The trajectory of late period growth, the number of downstream movements, and the date of maximum flow were included in all top models (Figure 6B, Table 4), with the date and volume of median flow, as well as the maximum yearly temp being included in ~60% of the top models.

The top model was nearly a full AICc point from the next best model (0.96 ΔAICc). The form of the top model was,

$$\textit{Ocean Entry Length (mm)} = \textit{Median flow volume} + \textit{Date of Median Flow} + \textit{Maximum temperature} + \textit{Number of Downstream Movements} + \textit{Late Growth Trajectory}$$

with the random effect of location explaining 862.1mm of the variance in the data (±29.36 SD) with residual variance of 1093.3mm (±33.07mm). Late growth trajectory, the number of downstream movements, and the date of maximum yearly

flow were all highly significant ($p<0.0001$ for all). The volume of the median yearly flow was also highly significant ($p=0.0008$). The maximum yearly temperature ($p=0.02$) and the date of median yearly flow ($p=0.0169$) were slightly less significant but still supported. Plotting of residuals indicated no significant deviations from the assumption of heteroscedasticity.

In both models as the number of downstream movements recorded beyond the natal reach increased the size of ocean entry increased, with a marginal increase of approximately 20mm in fork-length between fish with no additional movements compared with those having 4 recorded movements (Figure 7). The later the Julian day of the maximum flow event, the larger fish were at ocean entry (~70mm across the range of the data), while their size decreased with increasing volume of these maximum flow events by approximately 40mm across the range of the data. Fish size increased with maximum yearly temperature by between ~30-40mm across the range of the data in both models. Increasing volume of the median flow event also had a large negative effect of between ~50mm and ~70mm across the range of the data in both models.

In the top model using the full dataset, ocean entry length decreased in warmer years, with cumulative degrees between January 1st and August first decreasing size at ocean entry by 40mm across the range of the data (Figure 7A).

In the model fit to the subset data the timing of the median flow event decreased ocean entry size by ~30mm (Figure 7B) as median yearly flow varied from Julian day 125 (May 5) to 165 (June 14). As the trajectory of late period growth increased from ~0.03mm/day to ~0.09mm/day the size of fish at ocean entry increased by 50mm with all other factors held constant.

The model fit to the full data indicated that fish from LGR entered the ocean at the largest overall size, with fish from the CW only 1mm smaller. Fish from the LSK were estimated to enter the ocean on average 5mm smaller in size. Fish from the USK, in contrast, were estimated to enter the ocean 37mm smaller than those from LGR. However, the interaction of the random effects of river reach and water-year indicated

a large effect of water-year on ocean entry (Figure 8). In low volume water-years the model indicated large ocean entry for LSK and USK reaches. However, in mid- and high-cfs water-years the size of ocean entry in these reaches declined markedly. In contrast, the model predicted an increase in ocean entry size with increasing flow volume water-years. The CW reach was largely unchanged across water-years, with the highest ocean entry predicted in mid-cfs water-years.

The model fit to a subset of data indicated that fish in the LGR entered the ocean at the largest average size, with the CW reach only 5mm smaller on average. The LSK reach was on average 18mm smaller than LGR at ocean entry, while ocean entry for fish of USK origin was 59mm shorter.

Discussion

The conditions an animal experiences as a juvenile can have significant effects on future life stages (Lindström 1999). At the individual level an animal's response to these conditions during critical early life stages can determine its survival and fitness, with ultimate implications for population structure and dynamics (Metcalfe et al. 1995, Giménez and Torres 2004). Climatic shifts or anthropogenic changes to habitat can change the timing, location, and degree of both abiotic and biotic conditions, potentially shifting the fitness consequences associated with life-history decisions that an organism makes. These changes may also shift the selective pressures exerted on the life history strategies expressed in the population, resulting in changes in life-history strategies and the potential for evolutionary change (Reznick and Ghalambor 2001, Ghalambor et al. 2015). Further, the ability of populations to withstand changes in conditions across their range may lie in the buffering ability of life-history diversity available within the population (Greene et al. 2010).

For juvenile salmon decisions associated with particularly migratory behaviors have fitness consequences. Generally, fast, early growth is correlated with early outmigration, while larger size is correlated with higher survival (Randall et al. 1987, Thorpe and Metcalfe 1998, Zabel and Williams 2008). Since entry into the ocean

provides substantial growth opportunity the rewards of early ocean entry are large, but first a fish must also survive the journey. Therefore, fish must optimize the size at which they move downstream and enter the ocean to both maximize their size while also maximizing their growth potential between freshwater and ocean environments. At the same time, if the timing of thresholds for migration are not met this can delay migration substantially (Metcalfe et al. 1995)

Historically, Snake River fall Chinook salmon exhibited an early outmigration strategy (Connor et al. 2016). Presumably, growth potential was high enough to confer adequate survival while high summer temperatures were a risk to survival that precluded overwintering in the Snake River. However, recent changes in the basin have been hypothesized to shift many of the environmental conditions that juvenile fall Chinook salmon experience in the Snake River. The timing of flow events is heavily regulated in the Upper Snake River, while new reservoir habitats with a new balance of prey exist downstream (Tiffan and Connor 2012, Tiffan et al. 2014). Further, summer flow augmentation is used to cool the reservoirs during the period of peak temperatures to increase juvenile salmon survival (Connor et al. 2003b). All of these changes have been implicated in the changes observed in the timing of juvenile outmigration, with the conclusion that the balance of the growth/size tradeoff has shifted toward selection for a later outmigration strategy which incurs more growth in fresh water (Connor et al. 2005, Williams et al. 2008, Waples et al. 2017).

Effect of Location

Our modeling examines the potential drivers of this tradeoff, taking into account the correlation between location and environmental conditions which may affect the timing of outmigration. Both models indicate that between 34% and 44% of the variance in ocean entry size can be explained by location and water-year alone. In both models the CW exhibits the largest outmigration size, along with fish from LGR, despite the hatch date in the Clearwater being significantly later. This is consistent with observations that the majority of late-outmigrating juveniles originate in the CW reach, presumably holding over to compensate for late hatch date (Connor et al. 2005,

Hegg et al. 2013a). The larger size at ocean entry for fish assigned to LGR as their natal location is not as clear.

No spawning occurs in the reservoir habitat, so fish assigned to this location originate in other locations. They are assigned to LGR because they move before their natal signature has stabilized, and therefore their first natal signature reflects their entry into LGR rather than their true natal origin. Being early movers we would expect these fish to be faster growing and more likely to reach the size threshold for migration. However, Tiffan et al. (2014) also provide evidence that prey quality in the reservoir habitat is lower than in the free-flowing river, which could hinder growth in these fish and therefore delay their migration.

The nested model fit to the full dataset also indicates that the water-year, as defined by our cluster analysis of abiotic factors, has some effect on ocean entry size. The most significant of these effects is in fish from the two Snake River reaches. Low water years push the LSK, and to a lesser degree the USK, toward larger ocean entry size (Figure 8). However, during higher flow years the size of fish at ocean entry is pushed as much as 20mm smaller by this combination of abiotic conditions. At the same time, fish in LGR increase in ocean entry timing while fish in the Clearwater are largely unaffected by water-year. The reasons for these relationships is unclear. It does, however, indicate that outmigration strategy may be responding to more complex tradeoffs across the basin.

Despite these relationships, the association between ocean-entry size and outmigration from the Snake River are not necessarily directly linked. Juveniles leaving the Snake River at smaller sizes could compensate for growth through extending their downriver or estuary residence, confounding the relationship. We do not see chemical evidence of significant residence or growth in the Columbia River, whose signatures are significantly higher than the Snake River and would therefore be distinguishable (Barnett-Johnson et al. 2010). Based upon our analyses, we are unable to chemically distinguish estuary residence, so it is very possible that estuary growth could be contributing to the residual variance of the model.

Effects of environment and growth

Despite this, the high importance of the number of downstream movements as a fixed effect across both fitted models suggests that residence time in the Snake River is significant to ocean entry size with an overall positive relationship between distinguishable downstream movements and size at ocean entry (Tables 2&3, Figure 6).

The number of movements that the changepoint algorithm detects is a function of the length and stability of the signature. Fish that move very quickly through distinct downstream reaches are less likely to develop a distinguishable signature due to the time it takes for water chemistry and otolith to equilibrate (Bath et al. 2000, Walther and Thorrold 2006). Likewise, fish whose growth is slow in a new habitat will develop a shorter signature for that habitat as the width of daily growth increments is shorter, potentially limiting the ability to detect that movement with the changepoint algorithm. Fish with more distinguishable changepoints are spending enough time in these environments to develop a distinguishable signature. For these reasons, a higher number of detectable downstream movements can be viewed a reflection of the amount of time a fish has spent within the Snake River system. This additional time spent in the Snake River system translates to larger ocean entry in surviving adult fish in our data, which fits the hypothesis that delayed outmigration may confer selective advantage (Zabel and Williams 2008, Waples et al. 2017).

The apparent importance of late growth trajectory as a fixed effect (Table 3, Figure 6B), offers potentially interesting insights into the drivers of outmigration timing. Our defined "growth trajectory" measures the increase or decrease in growth rate during defined growth period, regardless of mean growth. The slope of this change in growth rate reflects both the trend within a single location, but also the shift in growth potential as a fish moves from a location with low growth potential to one with higher potential (positive slope), or from locations with high growth potential to low (negative slope). The late growth period was defined as the size at which beach-seine

sampling peaks in the upper reaches and fish begin moving downstream. Therefore, the slope of the late growth period likely reflects, to some degree, the relative growth potential of the riverine habitat and the reservoir.

The slope of late growth trajectory can, under this assumption, be interpreted as an indication of whether the reservoir provides a relatively improved growth potential compared to the riverine environment experienced by any individual fish. When growth conditions in the reservoir are good this may provide an advantage to those individuals who spend extra time utilizing that growth, moving to the ocean at a larger size with higher survival. Thus, conditions within the reservoir habitat may play an important role in the decision to delay outmigration.

The correlation between outmigration size and late growth trajectory is only apparent in adult fish from the LSK and USK reaches. Juveniles from the CW reach showed little effect of late growth trajectory (correlation = 0.012). In contrast fish from LSK show the highest correlation between ocean entry size and late growth trajectory (0.47), with fish originating in the USK showing a lower correlation (0.21). These trajectories are driven by higher ocean entry sizes and higher late-growth trajectories in low volume water-years. This indicates that the importance of reservoir growth opportunity may be more important during low water years. For fish originating in the CW reach this does not necessarily negate the potential importance of late growth trajectory but that it is important across a variety of conditions.

The effect of flow and temperature, while consistent across both models, is more difficult to link to outmigration timing. Increasing ocean entry size with increasing maximum temperature (Figure 7) indicates a straightforward positive relationship of higher growth with higher temperatures, an expected relationship for ectotherms. However, the negative relationship between ocean entry size and cumulative temperature is difficult to explain. Futher, cumulative temperature can be less important than the timing of that accumulation (Steel et al. 2012), which complicates its interpretation. The same is true for the conflicting effects of the date of maximum flow and the date of median flow.

These seemingly conflicting effects could be related to several potential un-modelled variables within our dataset. Our data includes only surviving fish, and therefore does not reflect the potential variability of life-histories that survive to exit the Snake River. Survival is also correlated with ocean-entry size, along with the other variables in our model. So, the direction of effects could, for example, relate to hidden effects of survival that serve to increase or decrease the size at ocean entry in our sample but do not relate directly to juvenile conditions. As well, the model does not explicitly account for the difference in size between fish which delay outmigration, and those which do not, because timing of ocean entry is unknown. Thus, it is difficult to apportion the effects on size which apply to yearling and subyearling migration strategies beyond their known correlation with natal location. Therefore, care should be taken in the interpretation of fixed effects, as they cannot be unequivocally linked to events during the juvenile stage.

Overall, our results suggest that juvenile ocean entry size in returning adult fish is affected by spatially explicit conditions across the basin. Our data supports prior findings that fish from the CW, despite later hatch dates, outmigrate at larger sizes. Further, our model supports the contention that additional time spent in the Snake River, the observed "yearling" life history strategy, is correlated with this ocean entry size in surviving adult fish. Further, our results indicate that flow conditions may create unexpected tradeoffs in life-history strategies within the Snake River which appear to shift the size of ocean entry and may affect life history strategy.

While this study provides insight into the spatial effects of environment on juvenile migration strategy, further work is needed to clarify the specific drivers of migration strategy within the Snake River beyond large scale indicators of flow and temperature. As well, linking the full range of life history strategies exhibited in the Snake River over the same range of conditions to those which finally return to spawn would be helpful in understanding the sources of mortality within the lifecycle. Finally, improving our ability to link individual growth within the reservoir system to

migration strategy across a range of conditions may provide a clearer picture of the role of late stage growth in juvenile Snake River fall Chinook salmon.

Tables

Table 4.1 – Descriptive statistics of adult otoliths

	Natal Location				
	Clearwater River	**Lower Granite Reservoir**	**Lower Snake River**	**Upper Snake River**	**units**
Hatch Year		**Sample Size (Water-Year)**			
2002	5 (high)	0 (low)	1 (low)	0 (low)	-
2003	7 (middle)	3 (high)	4 (high)	0 (mid)	-
2004	21 (high)	3 (low)	2 (low)	0 (low)	-
2005	23 (low)	11 (low)	8 (low)	4 (mid)	-
2006	21 (mid)	1 (high)	3 (high)	3 (high)	-
2007	54 (low)	10 (low)	3 (low)	6 (low)	-
2008	43 (high)	5 (high)	16 (mid)	21 (low)	-
2009	24 (mid)	1 (low)	22 (mid)	4 (mid)	-
2010	18 (high)	3 (high)	19 (high)	7 (high)	-
2011	3 (high)	1 (high)	0 (high)	3 (high)	-
		Mean (SD)			
Ocean Entry Length	185 (± 37)	173 (± 41)	168 (± 36)	143 (± 30)	mm
Growth					
Early Trajectory	0.013 (±0.014)	-0.005 (±0.000)	0.015 (±0.004)	0.010 (±0.006)	mm/day
Middle Trajectory	0.035 (±0.028)	0.002 (±0.000)	0.005 (±0.002)	0.014 (±0.016)	mm/day
Late Trajectory	0.016 (±0.018)	0.012 (±0.000)	-0.004 (±0.042)	0.031 (±0.025)	mm/day
Early Growth	0.783 (±0.043)	0.888 (±0.000)	0.752 (±0.069)	0.796 (±0.102)	mm/day
Middle Growth	0.872 (±0.089)	1.205 (±0.000)	0.871 (±0.032)	0.956 (±0.066)	mm/day
Late Growth	0.877 (±0.163)	1.467 (±0.000)	0.981 (±0.048)	1.037 (±0.060)	mm/day
Predicted Hatch Date	132 (± 14)	119 (± 4)	104 (± 9)	110 (± 10)	Julian Day
Accum. Deg. (Jan. 1 - Aug.1)	2,204 (±341)	2,754 (±183)	2,922 (± 59)	2,946 (± 82)	°C
Accum. Deg. (Hatch - July 1)	623 (±224)	856 (± 75)	1,075 (±116)	1,028 (±119)	°C
Yearly Maximum Temperature	18 (± 3)	23 (± 2)	23 (± 1)	23 (± 0)	°C
Maximum Flow	69,039 (±36,965)	145,855 (±44,237)	81,940 (±47,971)	73,706 (±29,173)	$m^3 \cdot sec^{-1}$
Maximum Flow Date	135 (± 18)	140 (± 9)	127 (± 29)	139 (± 16)	Julian Day
Yearly Median Flow Volume	2.66 (±1.49)	5.86 (±1.33)	3.84 (±1.90)	3.69 (±0.80)	$m^3 \cdot 10^{11}$
Timing of Median Yearly Flow (CT)	146 (± 9)	149 (± 7)	142 (± 14)	145 (± 12)	Julian Day

Table 4.2 – Table of top models for full dataset (within 2 AICc points from top model)

Rank	Fixed Effect Model Terms	AICc	ΔAICc
1	Median Flow (cfs) + Date of Max. Flow + Max. Temperature + Cum. Temperature (Jan.1-Aug.1) + Number of Downstream Movements	3873.60	0.00
2	Water Year + Median Flow (cfs) + Date of Max. Flow + Number of Downstream Movements	3874.47	0.87
3	Water Year + Median Flow (cfs) + Date of Max. Flow + Max. Temperature + Cum. Temperature (Jan.1-Aug.1) + Number of Downstream Movements	3874.54	0.93
4	Water Year + Median Flow (cfs) + Date of Max. Flow + Max. Temperature + Cum. Temperature (Jan.1-Aug.1) + Cum. Temperature (Hatch-July 1) + Number of Downstream Movements	3875.03	1.42
5	Median Flow (cfs) + Date of Max. Flow + Max. Temperature + Cum. Temperature (Jan.1-Aug.1) + Cum. Temperature (Hatch-July 1) + Number of Downstream Movements	3875.04	1.43
6	Median Flow (cfs) + Date of Max. Flow + Number of Downstream Movements	3875.07	1.47
7	Median Flow (cfs) + Max. Flow + Date of Max. Flow + Max. Temperature + Cum. Temperature (Jan.1-Aug.1) + Number of Downstream Movements	3875.08	1.48
8	Median Flow (cfs) + Date of Max. Flow + Date of Median Flow + Max. Temperature + Cum. Temperature (Jan.1-Aug.1) + Number of Downstream Movements	3875.32	1.72
9	Max. Flow + Date of Max. Flow + Number of Downstream Movements	3875.37	1.76
10	Hatch Date + Median Flow (cfs) + Date of Max. Flow + Max. Temperature + Cum. Temperature (Jan.1-Aug.1) + Number of Downstream Movements	3875.58	1.98

Table 4.3 – Table of top models for growth subset of data (within 2 AICc points from top model)

Rank	Fixed Effect Model Terms	AICc	ΔAICc
1	Median Flow (cfs) + Date of Max. Flow + Date of Median Flow + Max. Temperature + Number of Downstream Movements + Late Growth Trajectory	3155.08	0.00
2	Median Flow (cfs) + Maximum Flow Volume (cfs) + Date of Max. Flow + Date of Median Flow + Max. Temperature + Number of Downstream Movements + Late Growth Trajectory	3156.04	0.96
3	Median Flow (cfs) + Date of Max. Flow + Date of Median Flow + Max. Temperature + Number of Downstream Movements + Late Growth Trajectory + Early Growth Mean	3156.30	1.22
4	Median Flow (cfs) + Date of Max. Flow + Date of Median Flow + Max. Temperature + Cum. Temperature (Jan.1- Aug.1) + Number of Downstream Movements + Late Growth Trajectory	3156.38	1.30
5	Median Flow (cfs) + Date of Max. Flow + Date of Median Flow + Max. Temperature + Number of Downstream Movements + Late Growth Trajectory + Middle Growth Mean	3156.56	1.48
6	Median Flow (cfs) + Date of Max. Flow + Date of Median Flow + Max. Temperature + Number of Downstream Movements + Late Growth Trajectory + Late Growth Mean	3156.60	1.52
7	Median Flow (cfs) + Max. Flow (cfs) + Date of Max. Flow + Date of Median Flow + Max. Temperature + Number of Downstream Movements + Late Growth Trajectory + Middle Growth Mean	3156.98	1.90
8	Hatch Date + Median Flow (cfs) + Date of Max. Flow + Date of Median Flow + Max. Temperature + Cum. Temperature (Jan.1 – Aug.1) + Number of Downstream Movements + Late Growth Trajectory	3156.98	1.90
9	Median Flow (cfs) + Date of Max. Flow+ Date of Median Flow + Max. Temperature + Number of Downstream Movements + Early Growth Trajectory + Late Growth Trajectory	3157.03	1.95
10	Median Flow (cfs) + Date of Max. Flow + Date of Median Flow + Max. Temperature + Cum. Temperature (Hatch – July.1) + Number of Downstream Movements + Late Growth Trajectory	3157.05	1.97
11	Hatch Date + Median Flow (cfs) + Date of Max. Flow + Date of Median Flow + Max. Temperature + Number of Downstream Movements + Late Growth Trajectory	3157.07	1.99
12	Median Flow (cfs) + Date of Max. Flow + Date of Median Flow + Max. Temperature + Number of Downstream Movements + Middle Grwoth Trajectory + Late Growth Trajectory	3157.08	2.00

Table 4.4 – Coefficients for Top Models

Random Effect Level	Fixed Effects						
Model fit to full dataset (nested random effects of River Reach and Water Year)							
River Reach	Intercept (mm)	Median Flow (cfs)	Date of Max. Flow (Julian Day)	Max. °C	Cum. °C (Jan.1-Aug1)	Number of Downstream Movements	
CW	159.34	-5.68E-06	0.22	4.21	-0.03	10.55	
GR	112.93	-5.68E-06	0.22	4.21	-0.03	10.55	
LGR	160.17	-5.68E-06	0.22	4.21	-0.03	10.55	
LSK	155.33	-5.68E-06	0.22	4.21	-0.03	10.55	
USK	123.21	-5.68E-06	0.22	4.21	-0.03	10.55	
Water Year:River Reach							
low-cfs:CW	142.59	-5.68E-06	0.22	4.21	-0.03	10.55	
low-cfs:GR	141.54	-5.68E-06	0.22	4.21	-0.03	10.55	
low-cfs:LGR	140.27	-5.68E-06	0.22	4.21	-0.03	10.55	
low-cfs:LSK	154.78	-5.68E-06	0.22	4.21	-0.03	10.55	
low-cfs:USK	148.84	-5.68E-06	0.22	4.21	-0.03	10.55	
mid-cfs:CW	145.16	-5.68E-06	0.22	4.21	-0.03	10.55	
mid-cfs:GR	140.26	-5.68E-06	0.22	4.21	-0.03	10.55	
mid-cfs:LSK	133.93	-5.68E-06	0.22	4.21	-0.03	10.55	
mid-cfs:USK	138.68	-5.68E-06	0.22	4.21	-0.03	10.55	
high-cfs:CW	141.62	-5.68E-06	0.22	4.21	-0.03	10.55	
high-cfs:GR	140.03	-5.68E-06	0.22	4.21	-0.03	10.55	
high-cfs:LGR	147.04	-5.68E-06	0.22	4.21	-0.03	10.55	
high-cfs:LSK	140.02	-5.68E-06	0.22	4.21	-0.03	10.55	
high-cfs:USK	135.99	-5.68E-06	0.22	4.21	-0.03	10.55	

Random-intercept model fit to subset of data with growth (Random effect of River Reach)

River Reach	Intercept (mm)	Median Flow (cfs)	Date of Max. Flow	Max. Temp.	Date of Median Flow	Number of Downstream Movements	Late Growth Trajectory
CW	164.14	-6.40E-06	0.49	2.47	-0.56	13.88	393.43
GR	99.12	-6.40E-06	0.49	2.47	-0.56	13.88	393.43
LGR	167.14	-6.40E-06	0.49	2.47	-0.56	13.88	393.43
LSK	149.31	-6.40E-06	0.49	2.47	-0.56	13.88	393.43
USK	108.48	-6.40E-06	0.49	2.47	-0.56	13.88	393.43

Figures

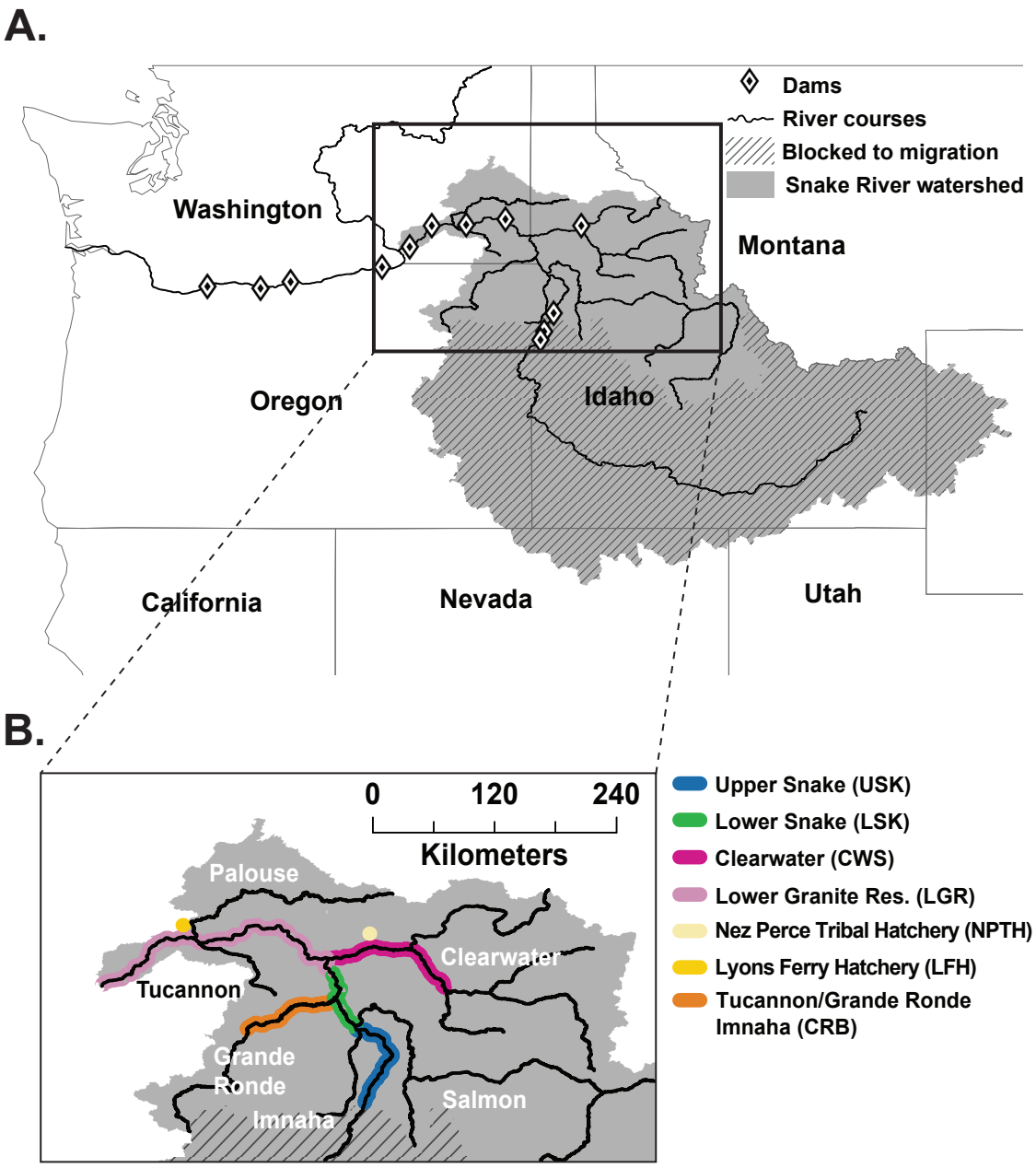
A.
Dams
River courses
Blocked to migration
Snake River watershed
Washington
Montana
Oregon
Idaho
California
Nevada
Utah
B.
0
120
240
Kilometers
Palouse
Clearwater
Tucannon
Grande
Ronde
Imnaha
Salmon
Upper Snake (USK)
Lower Snake (LSK)
Clearwater (CWS)
Lower Granite Res. (LGR)
Nez Perce Tribal Hatchery (NPTH)
Lyons Ferry Hatchery (LFH)
Tucannon/Grande Ronde
Imnaha (CRB)

Figure 4.1 – Snake River Basin

The Snake River is a tributary to the Columbia River in the Northwestern United States (**a**). Its basin is primarily within the states of Idaho, Washington and Oregon. Upstream passage of salmon is blocked by dams in Hells Canyon, with 8 downriver dams along the migration path to the ocean. The range of Snake River fall Chinook salmon (**b**) is divided into Upper (USK) and Lower (LSK) Snake River spawning reaches, the Clearwater River (CW), and smaller spawning populations in the Grande Ronde, Imnaha, and Tucannon Rivers. Two hatcheries contribute to the populations, Lyons Ferry Hatchery (LFH) and Nez Perce Tribal Hatchery (NPTH). No spawning occurs in the impounded reach above Lower Granite dam to the river mouth (LGR).

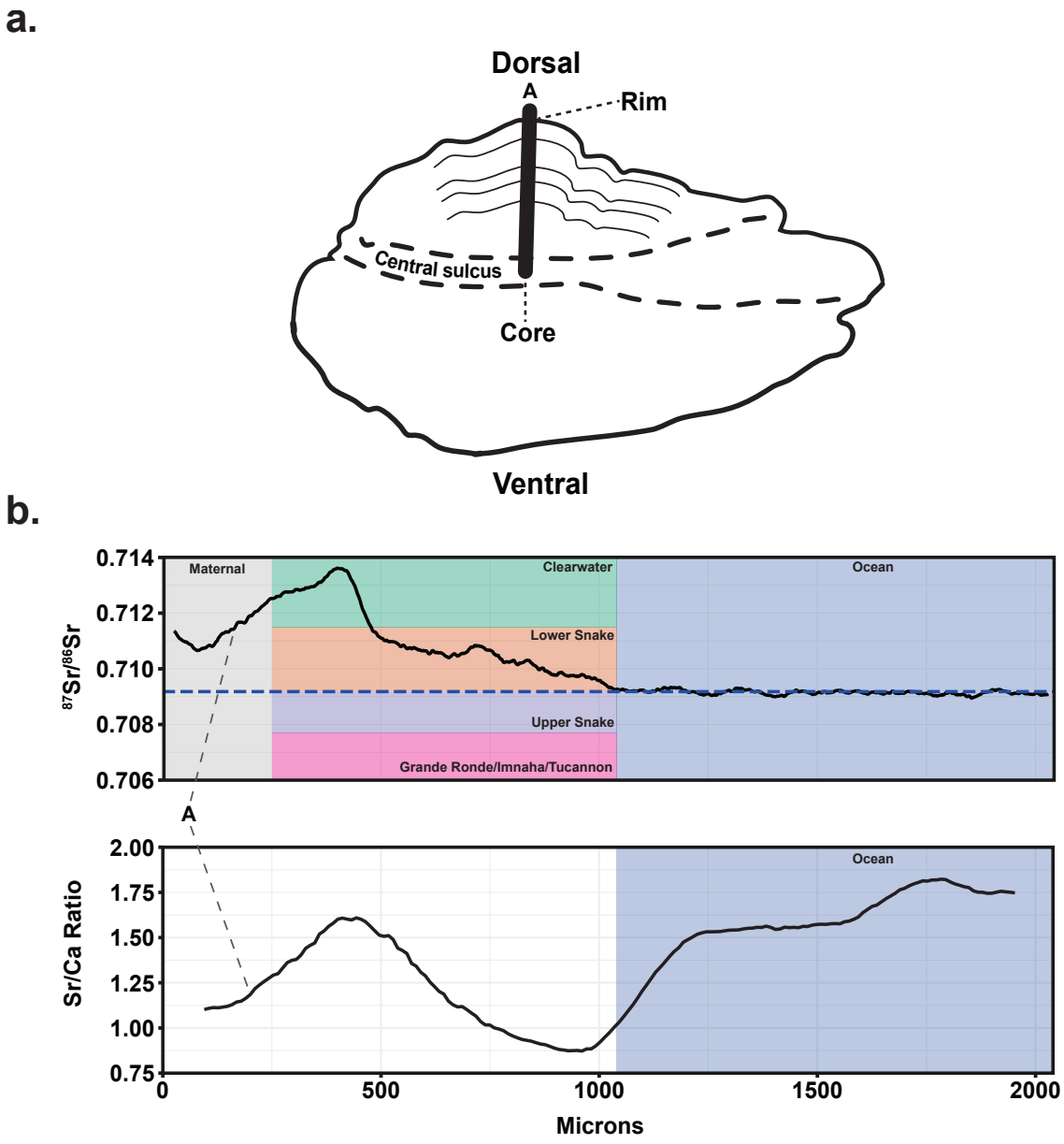

Figure 4.2 – Otolith Analysis

Otoliths, a balance organ in bony fish, grow in sequential, daily layers of calcium carbonate (**a**). Recovery of the chemical signatures recorded in these rings requires polishing until the central core and rings are visible. A laser is then used to ablate material (**A**) in a line perpendicular to the otolith sulcus on the dorsal side. This ablated material is analyzed using inductively couples plasma mass spectrometry, resulting in a chemical record across the otolith (**b**). The ratio and concentration of

these elements and isotopes can then be used to determine the location of a fish at different time points throughout its life.

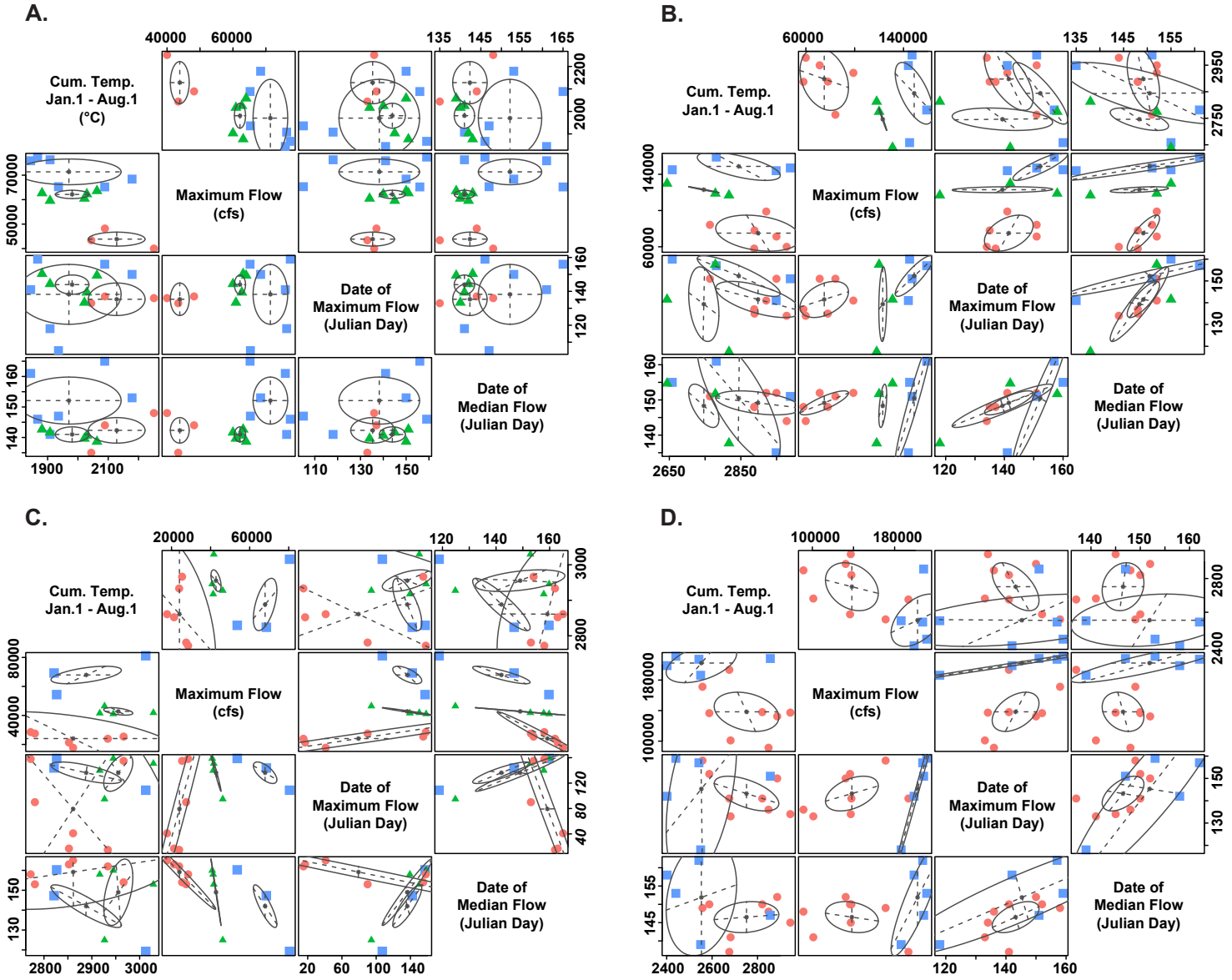
A.
Cum. Temp. Jan.1 - Aug.1 (°C)
Maximum Flow (cfs)
Date of Maximum Flow (Julian Day)
Date of Median Flow (Julian Day)
B.
Cum. Temp. Jan.1 - Aug.1
Maximum Flow (cfs)
Date of Maximum Flow (Julian Day)
Date of Median Flow (Julian Day)
C.
Cum. Temp. Jan.1 - Aug.1
Maximum Flow (cfs)
Date of Maximum Flow (Julian Day)
Date of Median Flow (Julian Day)
D.
Cum. Temp. Jan.1 - Aug.1
Maximum Flow (cfs)
Date of Maximum Flow (Julian Day)
Date of Median Flow (Julian Day)

Figure 4.3 – Clustering to determine flow and temperature regimes

Plots show the model based clustering results of clustering abiotic factors into "water year" flow/temperature regimes. Clusters were determined by maximizing BIC. The Clearwater (**A)**, Lower Snake (**B**), and Upper Snake (**C**) resolved to three clusters most clearly delineated by the maximum recorded flow (cfs). Lower Granite reservoir (**D**) resolved to two clusters. High volume (cfs) water years are shown in blue, middle volume water years are shown in green, low volume water years are shown in red.

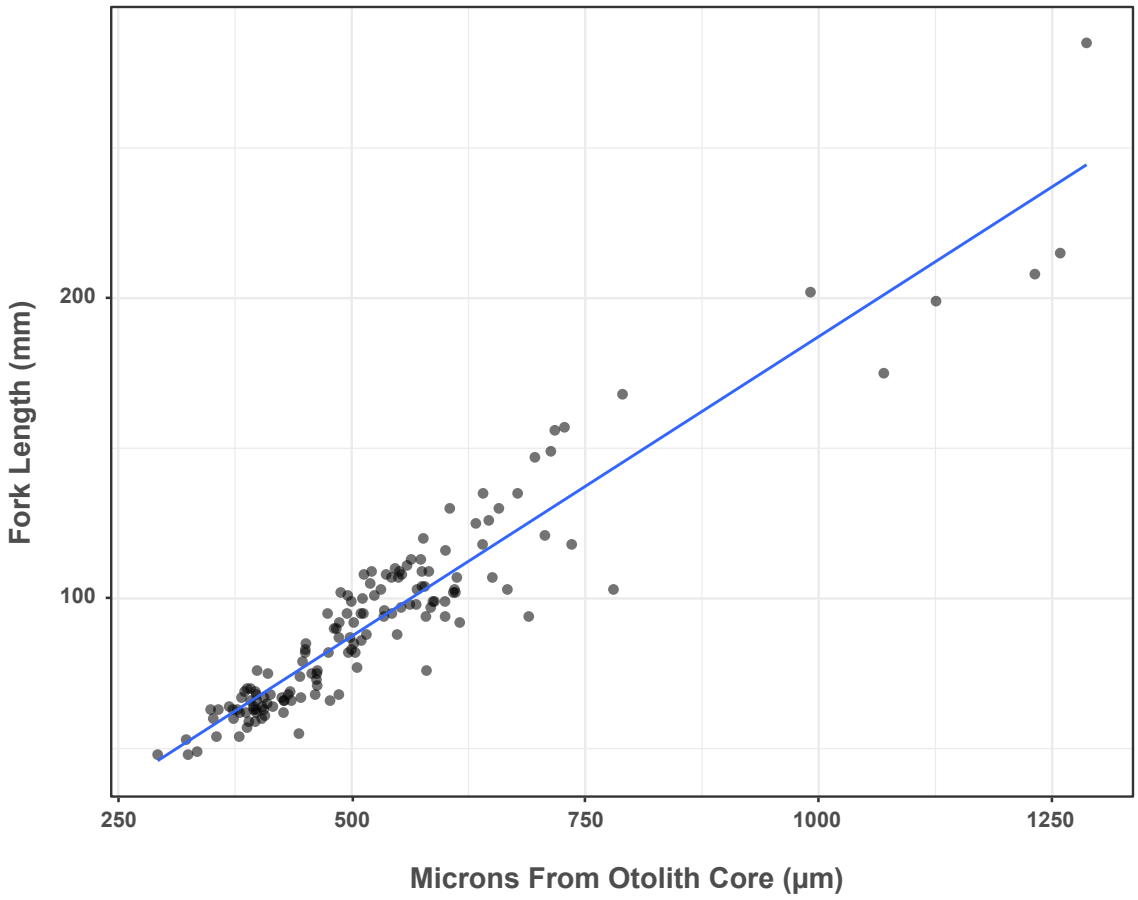

Figure 4.4 – Otolith radius to fork-length relationship

The relationship between otolith radius (µm) and fork length (mm) for juvenile fish captured at locations throughout the basin and after early ocean entry.

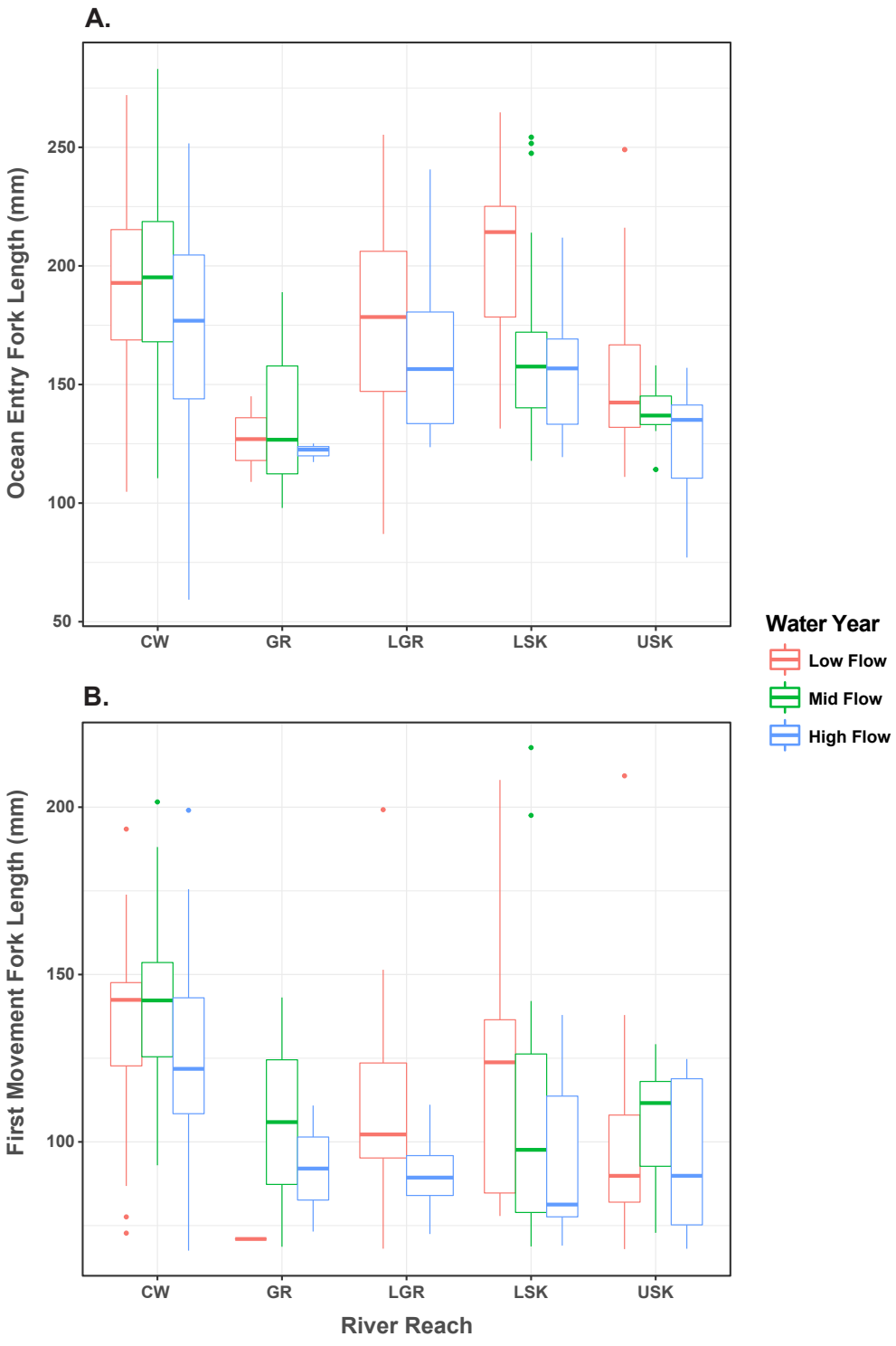
A.
Ocean Entry Fork Length (mm)
250
200
150
100
50
CW
GR
LGR
LSK
USK
B.
First Movement Fork Length (mm)
200
150
100
CW
GR
LGR
LSK
USK
River Reach
Water Year
Low Flow
Mid Flow
High Flow

Figure 4.5 – Size at ocean entry and first downstream movement

This plot shows juvenile fork length at ocean entry (**A**) and first downstream movement into a chemically distinguishable reach (**B**) for juvenile Fall Chinook salmon originating in each of the spawning reaches of the Snake and Clearwater Rivers. Results are displayed by water-year as determined by cluster analysis of flow and temperature data.

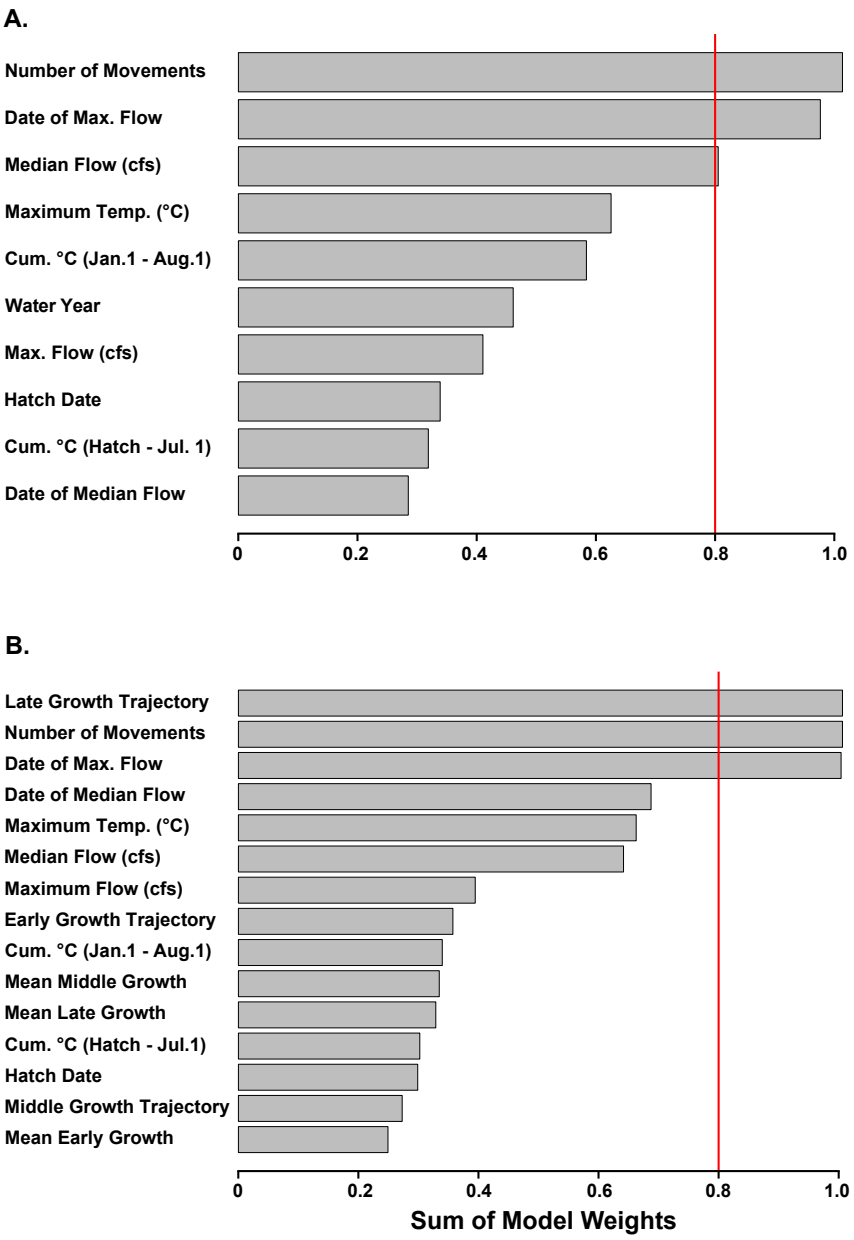

Figure 4.6 – Variable Selection

The importance of model fixed effects for a model fit using the full dataset (**a**, n=391) shows the importance of the degree of early downstream movement, as well as flow and temperature on ocean entry timing. A model fit with a subset of the data (n=239) for which growth information was available (**b**) shows the additional importance of late growth trajectory (>90mm fork length) in determining ocean entry timing.

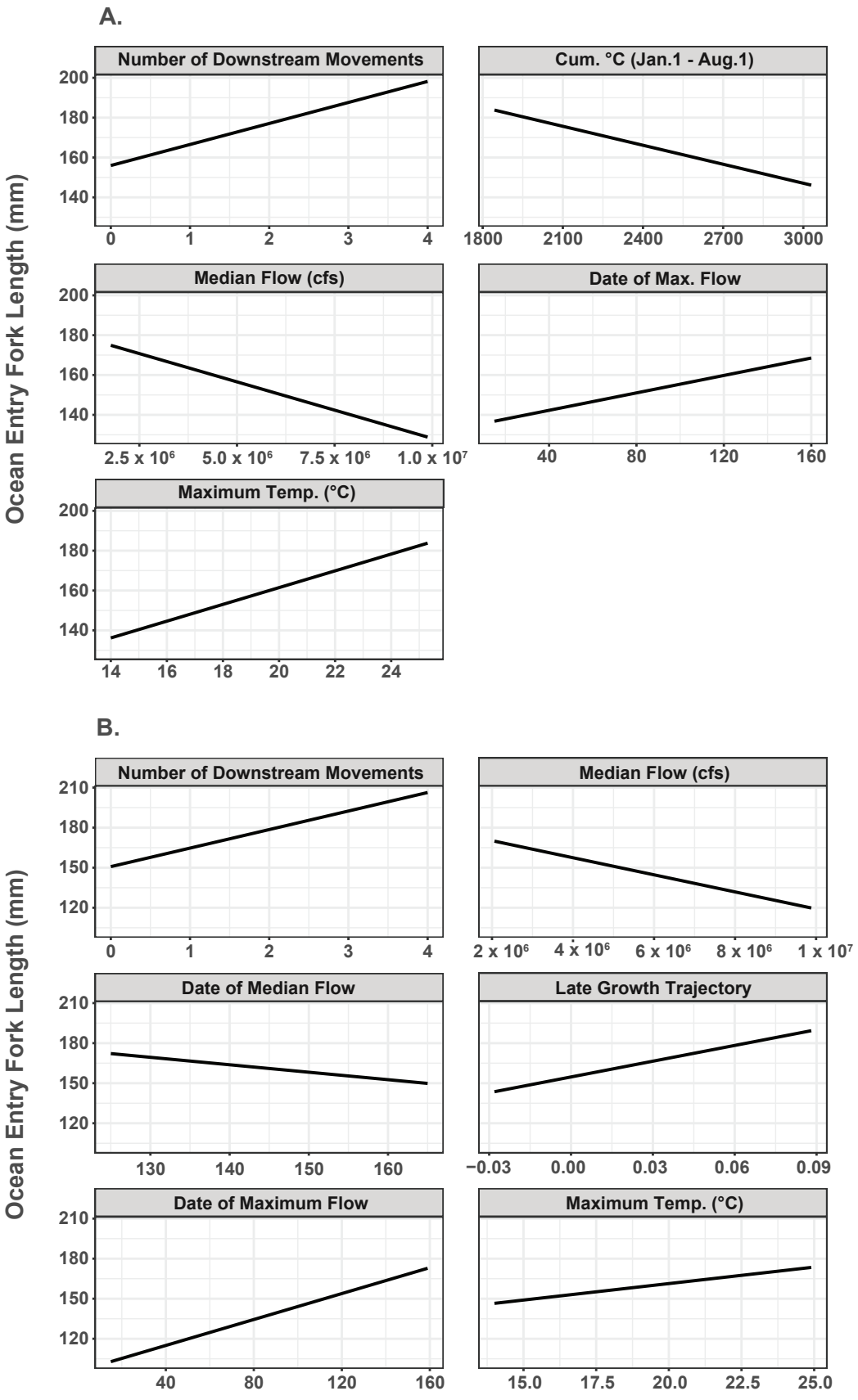
A.
Ocean Entry Fork Length (mm)
Number of Downstream Movements
Cum. °C (Jan.1 - Aug.1)
Median Flow (cfs)
Date of Max. Flow
Maximum Temp. (°C)
B.
Ocean Entry Fork Length (mm)
Number of Downstream Movements
Median Flow (cfs)
Date of Median Flow
Late Growth Trajectory
Date of Maximum Flow
Maximum Temp. (°C)

Figure 4.7 – Marginal effects of fixed effects

Plots of marginal effects (all other effects set to mean), showing the effect of each fixed effect on ocean-entry timing for models fit to the full sample (**A**), and to the subsample for which growth information was available (**B**).

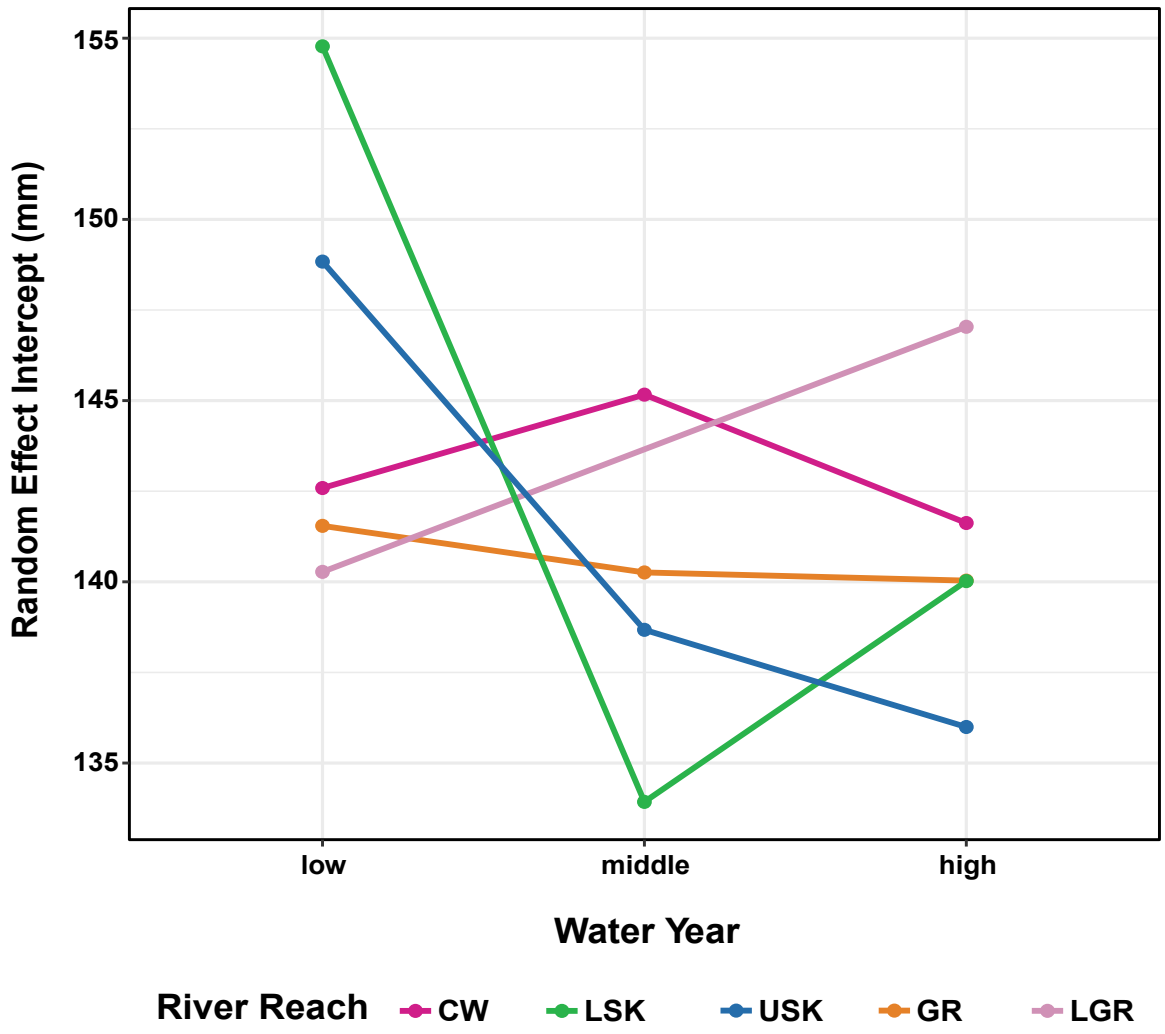

Figure 4.8 – Interaction of River Reach and Water-Year on Ocean Entry Size

The interaction of random effects of river reach and water-year affect the relative size of fish from the USK and LSK reaches, with low water years increasing the size of Snake River fish compared to those from the CW. The trend is opposite for fish assigned a natal location in the LGR reach.

Chapter 5: The Sound of Migration: Exploring data sonification as a means of interpreting multivariate salmon movement datasets

Accepted with minor revision in Heliyon. (Submitted June 28, 2017)

Abstract

The migration of Pacific salmon is an important part of functioning freshwater ecosystems, but as populations have decreased and ecological conditions have changed, so have migration patterns. Understanding how the environment, and human impacts, change salmon migration behavior requires observing migration at small temporal and spatial scales across large geographic areas. Studying these detailed fish movements is particularly important for one threatened population of Chinook salmon in the Snake River of Idaho whose juvenile behavior may be rapidly evolving in response to dams and anthropogenic impacts. However, exploring movement data sets of large numbers of salmon can present challenges due to the difficulty of visualizing the multivariate, time-series datasets. Previous research indicates that sonification, representing data using sound, has the potential to enhance exploration of multivariate, time-series datasets. We developed sonifications of individual fish movements using a large dataset of salmon otolith microchemistry from Snake River Fall Chinook salmon. Otoliths, a balance and hearing organ in fish, provide a detailed chemical record of fish movements recorded in the tree-like rings they deposit each day the fish is alive. This data represents a scalable, multivariate dataset of salmon movement ideal for sonification. We tested independent listener responses to validate the effectiveness of the sonification tool and mapping methods. The sonifications were presented in a survey to untrained listeners to identify salmon movements with increasingly more fish, with and without visualizations. Our results showed that untrained listeners were most sensitive to transitions mapped to pitch and timbre. Accuracy results were non-intuitive; in aggregate, respondents clearly identified

important transitions, but individual accuracy was low. This aggregate effect has potential implications for the use of sonification in the context of crowd-sourced data exploration. The addition of more fish, and visuals, to the sonification increased response time in identifying transitions.

Introduction

Pacific salmon migration provides important inputs to the freshwater ecosystems, affecting nutrient cycling and biodiversity in the areas where they spawn (Gende et al. 2002, Healey 2009, Carlson et al. 2011). Despite this, the combined effects of overfishing, hydropower, and other anthropogenic changes have caused large declines in salmon migrations, particularly in the Columbia River basin in the Northwestern United States (Ruckelshaus et al. 2002, Good et al. 2005). Management and conservation of these salmon species requires a detailed understanding of their migration incorporating both temporal detail and large spatial extent. The resulting data is complex and multivariate, and new tools may help researchers understand and explore this data. Sonification is a data representation method that uses sound instead of visualizations to represent data . When data is mapped to sound in a pleasing way, the human mind can intuitively process the sound to discover trends or features that may be important to researchers (Barrass and Kramer 1999, Hermann et al. 2011).

Many traditional methods of studying fish movement lack the temporal and spatial resolution to study salmon movement both at the fine scales at which important effects occur and across the large spatial extent of the migration. Fish ear stones, called otoliths, provide one method for collecting detailed movement data across the span of salmon migration. Otoliths are a balance and hearing organ in the inner ear of fish. Otoliths grow through the addition of daily rings of calcium carbonate, similar to the growth of tree rings (Campana and Neilson 1985, Campana 2005). Each stream a fish travels through has a different chemical signature, and otoliths record this chemistry in their daily growth rings. Measuring the chemistry in these otolith rings, it is possible to reconstruct the location and timing of the

movements a fish makes throughout its life (Kennedy et al. 1997, 2002, Thorrold et al. 1998).

For migratory fish, and especially salmon, this technique is a powerful, but data intensive, way of studying the ecological implications of movements and migration for species under protected status or that otherwise cannot be handled physically for manual tagging (Hamann and Kennedy 2012, Hegg et al. 2013a, 2015a). These chemical signatures record the time a juvenile salmon spends in each freshwater habitat, from the location where it hatched, to each new river it enters on its way downstream, to its entry into the ocean (Kennedy et al. 2002, Walther et al. 2008, Hegg et al. 2013a).

Reconstructing the movements of a large number of salmon presents challenges for perception and analysis due to the difficulty in visualizing the multivariate time-series datasets. The ability to interpret datasets visually begins to degrade relatively quickly with additional data streams or dimensions (Tufte 2001, Ware 2004). For salmon populations, the variation in movement timing within the population is particularly difficult to analyze statistically, despite our ability to collect and analyze large datasets. In this regard otolith microchemistry data shares the same issues of other big data problems: that our ability to collect, store, model, and analyze large amounts of data requires concurrent advances in analysis, communication and interpretation of these complex datasets (Overpeck et al. 2011, Wong et al. 2012, Keefe and Isenberg 2013).

In contrast to visualization, hearing is inherently multidimensional (Moore 1995) and the human ability to interpret nuanced changes in pattern, and especially timing, in audio signals is striking (Fitch and Kramer 1994, Moore 1995, Kramer et al. 2010, Neuhoff 2011). This is exemplified by the so called, “cocktail party problem,” the observation that human hearing is remarkably capable of disentangling many simultaneous channels of sonic input to focus only on a sound of interest (McDermott 2009). This indicates that multivariate data, and time-series data in particular, is especially suitable to exploration and interpretation using data sonification and

auditory display (Kramer et al. 2010). However, no definitive sonification model for this purpose exists, as the theory and best-practices for creating effective sonifications is still under active development (De Campo 2007, Hermann et al. 2011, Walker and Nees 2011).

Understanding the timing of large numbers of salmon movements is particularly important in one population of Fall Chinook salmon in the Snake River in the northwestern United States. Recent evidence indicates that the timing of ocean migration in juveniles of this population may be evolving due to human induced changes in the river system (Williams et al. 2008, Waples et al. 2017 in press). Migration in these fish has changed from exclusively early outmigration in their first summer (sub-yearling) historically, to a mix of migration timings that includes fish which enter the ocean the following spring (yearling) (Connor et al. 2005). Since the selective pressures driving this evolution are likely different in locations across the basin it is important to understand the timing at which sub-populations of fish decide to move downstream to each new habitat (Connor et al. 2002, Hegg et al. 2013a). Sonification of this data has the potential to provide a method to quickly explore temporal details of movement timing which would normally require detailed statistical analysis to uncover. As a multivariate, time-series dataset it is also an ideal candidate to explore elements of sonification design. This is particularly true because the temporal complexity of the dataset can be scaled through addition or subtraction of the data from individual fish.

The field of sonification has resulted in exciting recent advances for data exploration (Dombois 2002, Loeb and Fitch 2002, Ballora et al. 2004, Khamis et al. 2012), which often requires an understanding of how listeners perceive important changes in the data (Barrass and Kramer 1999, Ware 2004, Flowers 2005, De Campo et al. 2006, Hermann et al. 2011). Although sonification can be paired with visuals in interactive displays, it is often unclear to what degree simultaneous visualization improves listener accuracy in interpretation of sonifications (Rabenhorst et al. 1990, Minghim and Forrest 1995, Hermann and Hunt 2005). Further, understanding of how

users respond to the addition of aural complexity, and its effect on the ability of listeners to identify important changes in the data is an open question as most sonifications are limited to a relatively few data streams (Ferguson et al. 2011). The complexity of listener responses is one reason for the recommendation that sonification researchers should validate their work with perceptual surveys (Kramer et al. 2010). In the case of otolith microchemistry, the data provided a scalable, multivariate dataset upon which to test listener responses to layers of sonification complexity, with and without visualizations.

Using a sonification of multivariate salmon movement data and naïve listeners, we tested for generalizable trends in the ability of listeners to identify changes in an increasingly complex dataset. Our study was based on a sonification model developed by the authors through an iterative, interdisciplinary process with the goal of creating a useful, and aesthetically interesting, data exploration tool. The sonification used five chemical tracers relevant to fish location; strontium isotope ratio ($^{87}Sr/^{86}Sr$), and ratios of elemental strontium (Sr), barium (Ba), magnesium (Mg) and manganese (Mn) to calcium (Ca). These data were mapped to pitch, timbre and stereo-location with the intention of creating clear transitions in fish location as well as aesthetically interesting harmonic and timbral effects.

This study had three objectives. The first was to quantify the specific sonic elements that can provide effective markers of data transitions that reflect salmon movements between habitats. Untrained respondents were tested on a suite of four sonic markers and two negative controls to test the hypothesis that pitch and timbre would be the most effective indicators of transition. Our second objective was to test the ability of respondents to identify known transitions within multivariate fish-otolith sonifications of increasing complexity. We hypothesized that respondent accuracy would decrease with increasing sonification complexity. Finally, we tested whether the addition of a simultaneous visualization of the data improved respondent accuracy as complexity increased. We hypothesized that respondent accuracy would be unchanged, based on recent results from Bywater and Middleton (2016) who found

that a high percentage of users can perceive similarities between line graphs and corresponding sonifications based mainly on data-to-pitch mapping.

Methods

Salmon Movement Data

The data used to create the sonifications were taken from a dataset of threatened Fall Chinook salmon in the Snake River in the northwestern United States (Hegg et al. 2013a). Juvenile movement timing is important to ecologists and managers because recent evidence suggests that the population may be evolving novel migration patterns in response to dams and other anthropogenic affects across their habitat (Williams et al. 2008, Waples et al. 2017 pre-print).

The dataset consisted of isotopic and micro-chemical data from forty-five adult salmon otoliths within a larger dataset collected by Hegg et al. (Hegg et al. 2013a). Hegg et al. showed that river location can be reliably determined through the natal, rearing and overwintering phases of the juvenile outmigration using linear discriminant function classification of $^{87}Sr/^{86}Sr$ ratio. This discriminant function analysis was used to provide location information to the sonification. In addition to the $^{87}Sr/^{86}Sr$ isotopic signature, the sonification utilized four elemental signatures expressed as a ratio with calcium; Sr/Ca, Ba/Ca, Mg, and Mn. Trace amounts of these elements replace calcium in the calcium carbonate matrix of the otolith as a function of both the dissolved concentration of these elements in the water the fish inhabits and the bioregulation within the body. The data is expressed as a ratio of the abundance of each element in comparison to calcium, the element they substitute for in the otolith matrix (e.g. - Sr/Ca).

Analysis of otolith data using LA-ICP-MS is done by moving a laser across the surface of the otolith from the core to the edge, ablating small amounts of otolith material which is drawn into the mass spectrometer and analyzed in sequence (e.g. Hegg et al. 2015a). Therefore, the data consists of measurements of each isotopic and elemental ratio in increasing distance from the core of the otolith. This results in a

temporal record of the life of the fish, with the core representing birth and the edge representing the death of the fish after returning to spawn. The microns from the core represent the relative time within the life of the fish. (Figure 1)

Sonification Design

The sonification design was based on an interdisciplinary working process between a scientist and two composers, with the objective of meaningfully representing juvenile salmon movement as sound (Robertson et al. 2015). Within the resulting sonification (Audio File 1), the distance from the otolith core, measured in microns, represents time, from the start of the file to its end. Across this timeline various life stages were mapped to changes in overall amplitude, with important temporal markers, including birth, the end of maternal influence, and death, acting as breakpoints within these overlapping envelopes. For each fish the end of maternal chemical influence on the developing otolith was considered to be 250μm (Barnett-Johnson et al. 2008), representing an initial crescendo, with the amplitude ascending at a consistent rate towards a steady value that is sustained until the death of that individual, which begins a sudden decrescendo into silence. During simultaneous playback of all fish (tutti), the sound of each fish (soli) in each watershed are cumulative, giving the listener an indication of the how many salmon are currently active within a given watershed or marine system.

For each fish the sonification mapped strontium isotope ratios to audio parameters associated with spatial orientation, distance, and passage between specific river or marine systems. At the foundation of this model is the ability for the listener to recognize discrete entrances or exits of individuals through one of four chemically distinct river groups within the Snake River watershed defined by Hegg et al. (2013a): the Lower Snake River, the Upper Snake River, the Clearwater/Salmon Rivers, and the Grand Ronde/Imnaha/Tucannon Rivers, as well as the Pacific Ocean. The $^{87}Sr/^{86}Sr$ signatures unique to these locations are ranges defined by the group boundaries of the discriminate function used by Hegg et al. (2013a), so that as a fish's otolith signature crosses this group boundary its location changes instantaneously (Table 1, Figure 1).

Therefore, $^{87}Sr/^{86}Sr$ ratio was mapped to discrete, nearly instantaneous changes in pitch at these transition points, indicating the passage of salmon from one river system into another.

Passage between river locations was further punctuated by applying a percussive envelope to each sounding sine tone, creating a sudden, bell-like, audio marker of the transition between habitats. This envelope utilizes a sharp attack (5 milliseconds), a brief decay (100 milliseconds), a sustained amplitude 6dB lower than the peak value, and a release time of 400 milliseconds. Following the onset of each envelope, the corresponding pitch is sustained at a significantly lower amplitude until another habitat change occurs or the lifecycle of the fish concludes.

All mapped pitches originate from sinusoidal waveforms whose frequencies are derived from whole-number ratios. This system of integral tuning, or *just intonation*, create intervallic structures between simultaneously sounding individual fish which form cohesive chordal structures. As these structures often stem from high-order partials, resultant harmonies display distinctly rich microtonal qualities that often deviate from standard musical temperament.

Beyond mapping fish location to pitch, the sonification algorithm also used $^{87}Sr/^{86}Sr$ thresholds to mapped fish to a generalized geographic location within the stereo field. In this way, each fish changed location in relation to the listener as it moved downstream as if the listener were located at the confluence of the Snake and Columbia River (46.233° North Latitude) and facing toward the geographic center of the basin. Latitude ranges for each river group was estimated using the USGS Streamer tool (http://water.usgs.gov/streamer/web/) based on spawning distributions from Garcia et al. (2008). Each fish, at each point during the sonification, was then stochastically assigned a stereo location within the latitude range of the river in which it was assigned (Table 1). To maintain a consistent perception of loudness across the stereo field, a constant-power panning algorithm is employed.

To supplement this spatial model and suggest proximity to the listener, reverberation was applied in linear proportion to each fish's virtual location in relation

to the listener's virtual location, at the Snake and Columbia Rivers. A greater proportion of reverberation was used to suggest greater distance from the listener, while a direct, unaffected signal indicated proximity.

In addition to strontium isotope signatures, the intensity of Sr/Ca ratios were used to determine entry into the ocean, due to the sharp increase in Sr/Ca associated with entry into salt water. Entry into the ocean was defined as a stable, 20-point moving average of $^{87}Sr/^{86}Sr$ within +/- 0.0004 of the global marine value (0.70918) as well as Sr/Ca values between 0.9478 < 1.1609 (Figure 1).

Entry into the Pacific Ocean is heard as a distinctive transformation of spectral quality as spectral bandwidth is broadened and the perception of a single, center pitch is progressively obscured by an increased noise bandwidth, creating a wash of sound rather than the more pure tone of freshwater residence. This timbral change was accomplished using a modified amplitude modulation synthesis in which the audio output is interpolated between a sinusoidal waveform reflecting frequency value of the previously occupied freshwater system and a random-amplitude carrier waveform ("rand~" object in the programming language, Max/MSP). As chemical signatures indicative of entry into the Pacific Ocean begin to stabilize, the random-amplitude waveform is modulated by a steady, 440 Hertz sine wave. Meanwhile, the frequency of the carrier waveform is mapped to a transitional range of Sr/Ca intensity values (0.947882 < 1.160923) using a linear-scaling function.

Minimum and maximum output for this function vary between 50 and 400 Hertz. However, as Sr/Ca values recorded in the study occasionally exceed 2.55, intermodulation effects resulting from higher frequency outputs may be heard as momentary spikes in noise bandwidth, booming noises during the ocean phase. From an aural perspective, the associative qualities and continuum of "pure" to "noisy" timbres generated by this modified form of AM synthesis illustrate variation in the character of environments encountered during out-migration.

Perceptual Survey

In order to test the integrity of the sonification model, a perceptual survey was created using sonifications of three individual fish from the larger sonification, as well as six short synthesizer clips. Each fish originated in one of three natal locations as defined by the discriminate function analysis in Hegg et al. (Hegg et al. 2013a); the Upper Snake River (fish 5132), Clearwater River (fish m2742), and Imnaha/Grande Ronde/Tucannon Rivers (fish 3354). All fish then moved to the Lower Snake River during the rearing phase, followed by entry into the ocean. Thus, each fish had two major sonic transitions during its life. All otolith sonifications were limited to 1522μm, the shortest of the three otoliths, and the time span of the sonifications was set to 1 minute and 30 seconds. Each fish was recorded individually, after which the files were combined in open source Audacity audio editing software (www.audacityteam.com). Known fish movements were determined from the discriminate function analysis in Hegg et al. (2013a) and the timing of each location change for individual fish was determined by the author using a stopwatch.

The survey also included a set of shorter sound clips used as controls, which were based on granular syntheses similar in timbral richness to the sonifications. Positive controls represented sonic transitions in left-to-right stereo panning (Audio File 2), adding a pitch (Audio File 3), adding a new timbre (Audio File 4), and increasing volume (Audio File 5). The two negative controls consisted of steady random static (Audio File 6) and a clip with randomly intermittent sounds over a steady bass tone (evoking a vibrato-like sound, Audio File 7). (Table 2)

The survey was designed and built in Flash 3.0 using Adobe Animate software (Adobe.com) and administered via computer (Hegg et al. 2017). All listening was done through headphones. All sounds were accompanied by a counter showing the seconds elapsed in the right-hand corner of the screen. Sounds were also accompanied by a progress bar showing the remaining length of the clip, with the exception of sounds with visual displays. In these cases the visualizations indicated the progress of the sonification with a clear beginning and end point. Visualizations were animated as

sparse graphs of the raw $^{87}Sr/^{86}Sr$ data (absent x and y value labels and using an aggressive 30-point moving average smoother) such that they revealed themselves in time with the sonification so that respondents were not able to look forward in the visualization to anticipate transitions.

Respondents were allowed to proceed through the survey at their own pace, with sounds only starting once respondents clicked to start the sound. Responses were recorded on a paper datasheet (Hegg et al. 2017). Respondents were first asked to rate their level of training in Music and Math or Science as these relate to data analysis (none, up to one year, or more than 1 year). The survey then proceeded to a listening section made up of the controls using sounds based on granular synthesis. For each trial respondents answered "yes" or "no" to the same question, "Do you perceive a transition in the sound." The answers were recorded after listening to each clip, and participants were offered only one listening experience per trial. At the end of the control section respondents were then counseled on the survey's new method for identifying transitions in longer clips, in real-time, using a push-button training clicker (www.starmarkacademy.com). Respondents were asked to depress the clicker button at the moment they identified a transition in the sound, at which point the test administrator would record the seconds elapsed on the datasheet.

Questions using the sonification data proceeded from a single fish, to the addition of a second fish, to the addition of a third fish. Questions 7-9 were accompanied by a progress bar serving as the only visual aid. Questions 10-12 repeated the same sequence of sonifications, with the inclusion of animated visualizations, proceeding from a single fish (Video 1), to two fish (Video 2), and three fish (Video 3).

At the end of the survey respondents were asked four questions related to their experience taking the survey, with space given for a long-form answer. The questions were:

1. Comment on your ability to identify transitions in the short, sound only clips.
2. Comment on your ability to identify transitions in the longer, sound only clips.
3. Comment on the effect of the visuals in identifying transitions in the sound clips

4. Comment on your ability to identify transitions as more sounds were added to the clips.

Survey respondents were intentionally left untrained as to what constituted a "transition" in the sound. Advertisement for the survey did indicate that the sounds were derived from salmon, however details were only given after the testing if respondents were interested.

All surveys were administered by Dr. Jonathan Middleton and a graduate assistant at Eastern Washington University between January 25th and February 24th of 2017. This survey was granted exemption from federal regulations for the protection of human subjects (under CFR Title 45, Part 46.101(b)(1-6) by the Institutional Review Board for Human Subjects Research at Eastern Washington University (Review HS-5155). University of Idaho also provided an exemption under CFR Title 45, part 46.101(b)(2,4) (protocol 17-080).

Data Analysis

Data analysis proceeded along three main hypotheses, one for each section of the survey. The first hypothesis was that respondents would positively identify each of the four positive control sound clips as transitions, while failing to identify the negative controls as transitions. This was tested using Fisher's Exact test of independence with post-hoc pairwise comparison with Bonferroni correction.

The second hypothesis was that survey respondents could identify the transitions in the sonifications in real-time. Since clicker responses exhibited a time-delay we calculated accuracy based on an envelope between the actual transition and the end of the estimated response delay. This response delay was calculated based on the peak center and variance of aggregate responses of all the survey responses for each question. We used R package {mclust} to identify the unique density peaks in the aggregate data using BIC model selection to identify the number of clusters (limited to between 5 and 20) and whether those clusters had equal or variable variance. This

resulted in a mean and variance for each estimated response group within the aggregate data.

The peaks directly following a known transition were identified as “correct” response peaks and the envelope for correct responses for each known transition was calculated from their mean and variance. The “correct” window was calculated as the number of seconds between the known transition to three standard deviations to the right of the following peak center. This, theoretically, encompasses 99.9% of the responses within the response peak. In cases where the cluster model picked wide variance we decreased this window to two or one standard deviations to avoid including data from nearby response peaks.

Respondents were only given one “correct” response within that window so that responses were not biased towards respondents who clicked many times. In cases where a respondent clicked multiple times within the “correct” envelope the response closest in time to the cluster peak center was chosen as the correct response. Response accuracy was then calculated as the number of correct clicks for each question divided by the total clicks the respondent made during the duration of that question. We tested the hypothesis that respondents could identify transitions by comparing response accuracy to 50%, the expected response accuracy in the case of random responses.

The third hypothesis was that visualizations would have no effect on the ability of respondents to correctly identify transitions. We analyzed the response accuracy between questions containing visuals and those without, paired by the number of fish used in the sonification, to determine if there was a difference in response accuracy using Chi-squared test of independence.

In addition to hypothesis testing we analyzed the aggregate data to understand the response delay and variance as the complexity of the sonification increased.

Data was analyzed in R version 3.3.2 (https://cran.r-project.org) and RStudio version 1.0.44 (https://www.rstudio.com).

Results

The control questions showed clear differences in respondents' determination of a transition between negative and positive controls (Table 2). Respondents (n=35) identified a transition in the two negative controls at lower rates (Static = 8.57%, Random Intermittent = 34.29%) than for the positive controls. Respondents identified transitions in the positive controls at high rates, ranging from 82.86% for the Crescendo control to 100% for the Pitch control. A chi-square test of independence over the responses to all control questions indicated a significant difference in responses ($p=2.2 \times 10^{-16}$, $\alpha = 0.05$). Pairwise comparisons of each control using Holm's correction for multiple comparisons showed that the static control was significantly different from all the positive controls (adj. $p \leq 2.9 \times 10^{-8}$ in all cases) but not from the intermittent negative control (adj. $p = 0.14$). The Random Intermittent control was also significantly different from all the positive controls (adj. $p \leq 0.0008$ or less in all cases).

Density estimation of the aggregate responses for the sonification questions using the {mclust} package identified the best fit models to include clusters of variable variance in all cases. The algorithm identified 6 clusters for both questions with a single fish sonification (questions 7 and 10) and different numbers for all the other questions: question 8 (11 clusters), question 9 (13 clusters), question 11 (9 clusters), and question 12 (10 clusters). To avoid models which conflated response peaks the available models were limited to greater than five clusters and up to 20. In the case of question 12 the minimum model was increased to 8 to avoid extremely wide variance clusters (see Figure 2).

The cluster centers directly following a known sound transition were identified and the envelope for correct answers was defined from the point of the known transition to three standard deviations to the right of the associated peak center (Figure 2). For some questions the peaks defined by {mclust} had wide variance and the number of standard deviations were adjusted to avoid classifying obviously different peaks as correct. This was done for question 8 (4^{th} peak, 2 st. dev.), question

11 (4th peak, 2 st. dev.), question 9 (4th peak, 2 st. dev.), question 12 (2nd, 4th & 5th peaks, 1 st. dev.; 6th peak, 2 st. dev).

The models identified several clusters in the period from 70 seconds to the end of the sonification, as well as a cluster at 63 seconds, which were not correlated with known salmon movement locations (Figure 2). These peaks corresponded to a series of loud booming sounds generated by chemical changes occurring after the fish entered the ocean. These are also the most obvious example of the additional complexity, beyond simple movement data, that was incorporated into the sonification.

Correct responses were calculated for each question using the envelope criteria established from the cluster model. The percentage of correct answers were calculated in aggregate for each question, as well as for individual respondents. The aggregate frequency of correct and incorrect responses was compared for question pairs with the same number of fish, with and without visualizations, using chi-squared test for independence. None of the response rates were significantly different between the question pairs ($p \leq 0.91$ for all tests). The number of correct responses increased with the number of fish included in the sonification. Questions with one fish (questions 7 and 10), with and without visuals, had a 43.5% and 45.8% accuracy, respectively. Questions with two fish (questions 8 and 11), with and without visuals, had an accuracy rate of 54.5% and 52.9% respectively. Questions with three fish (questions 9 and 12), with and without visuals, had an accuracy rate of 52% and 46% respectively. Individual accuracy ranged from 0% to 100% across questions 7 through 12, with a mean individual accuracy ranging from 40.5% on question 10 to 16.6% on question 12.

The response delay was also analyzed, using the difference in time between the known transitions and their associated cluster mean from the {mclust} results. The response delay increased from a minimum of 1.2 seconds with one fish and no visuals (question 7), to a maximum of 2.1 seconds with three fish with visuals (question 12). Both response delay and the variance in those responses increased as more fish were added (Table 2, Figure 3).

No difference was seen between individual accuracy and the amount of musical or math and science training of respondents.

All raw data is available in an online data repository (Hegg et al. 2017, http://dx.doi.org/10.17632/7sk82n38sh.2).

Discussion

Human hearing is particularly adept at determining changes in pattern and timing within incoming temporal data streams. In contrast to visual representations of multivariate data, which are limited by the number of available dimensions as well as the ability to interpret large numbers of time-series in one visualization, sonification has the potential to provide a method for display and exploration of high-dimensional time series datasets which may be faster and more intuitive for identifying timing shifts within large datasets (Barrass and Kramer 1999, Kramer et al. 2010).

Kramer et al. (2010), in their report on the status of the field of sonification, identify the need to understand the additive effects of multiple data streams on listener understanding and memory load as a central question. The movement data available from salmon otolith microchemistry studies provides an ideal dataset for the study and development of useful sonification methods. This data is temporal in nature, with discrete changes in chemistry relating directly to easily interpretable movements in individual fish. Since otolith data are inherently multivariate and scalable, each individual fish can be represented by multiple, simultaneous, chemical data streams while the entire dataset can be scaled by adding additional fish. This scalability and temporal nature lend themselves to auditory display, which relies on the ability of the human ear to interpret temporal patterns (Walker and Nees 2011). This relates to an important ecological question in salmon populations: how individual movement decisions scale to the population level. Our study indicates that sonification could provide a method for data exploration and communication of results on its own or as a complement to traditional statistical methods and visualizations.

In our survey respondents were able to identify transitions in several sonic elements with a high degree of accuracy, and to distinguish transitions from random noise (Table 2). In particular, our results indicate that pitch and timbre are the most easily recognized sonic transitions, with volume and panning transitions being recognized slightly less often. This indicates that our naïve participants fall within the expectations of previous research showing that pitch and timbre are effective, and often used, mappings (Neuhoff 2011, Dubus et al. 2013).

Another interesting finding from our control responses is that the degree of granularity in random noises appear to determine whether participants view them as random, or as transitions. The intermittent and static negative controls were not significantly different, however, higher numbers of respondents identified the intermittent control as a transition. This may indicate that the more granular random noises become in a sonification the more likely people may be interpret them as transitions. Similarly, the more complex, and thus seemingly chaotic or random a sonification becomes, the more likely listeners might be to identify random noises as transitions.

Overall the control results argue for parsimony in sonification designs. If the most important data streams within a multivariate dataset are known *a priori* they should be mapped to pitch and timbre given the sensitivity of listeners to transitions in these sonic elements. Further, if the sonification is being developed for exploration of unknown data, attempts should be made to avoid random, granular fluctuations in the data that might be interpreted as important transitions.

Our results indicate interesting interactions between sonification complexity, listener response latency, and accuracy. Most sonification experiments have focused on individual accuracy metrics to interpret whether listeners are able to interpret the contents of the sonification (Schuett and Walker 2013). Sonification complexity has also been cited as a limiting factor in the utility of sonifications (Box and Group 2002, Pauletto and Hunt 2005). In our tests, individual accuracy was relatively low, and highly variable (Figure 4). This lack of individual accuracy contrasts with the fact that

the control data shows that listeners could distinguish transitions with a high degree of accuracy.

The sonifications themselves were complex; utilizing pitch, timbre and stereo location within the data streams for each individual fish. Thus, without training, listeners may have been identifying transitions in other sonic elements which were not counted as "correct." Despite this, there is evidence to indicate that most listeners were identifying the intended transitions. Respondents who clicked fewer times tended to have higher accuracy rates (Figure 4), indicating that they were identifying the intended transitions and ignoring other sonic changes. Respondents who clicked more often had lower accuracy rates, however, this is likely due to a dilution effect. Those who clicked more often still largely identified the appropriate transitions in addition to other perceived transitions which were not counted as correct.

This leads to the non-intuitive conclusion that although individual accuracy may be low, the natural ability of naïve listeners to identify transitions in pitch and timbre can be useful in aggregate. In essence, our data suggest that untrained listeners were able to "crowd source" the location of sonic transitions in complex, multivariate datasets. The most complex sonifications showed increased variation in individual accuracy (three-fish, no visuals) and a decrease in overall accuracy (three fish, with visuals), indicating that this "crowd sourcing" ability may be limited by complexity.

Decreases in aggregate accuracy with increasing sonification complexity may be explained due to the time it took for respondents to identify a transition. Schuett et al. (2013) argued that response latency indicates the ability of listeners to process sonification information. Response delay increased in our study as more fish were added (Figure 3), indicating that the additional complexity required more processing time before respondents identified a transition.

The inclusion of visuals resulted in further increases in response time across all levels of sonification complexity (Table1, Figure 3). The majority of listeners reported that visuals were either unhelpful or even detrimental to interpretation of the audio:

"[Visuals were] distracting because I wasn't quite sure what to focus on."

"Watching the visuals was more of a distraction. I decided to just focus on the listening and just watch for fun."

Several respondents provided feedback that indicated that the visualizations clashed with the audio:

"I did not feel the visuals correlated with the sound clips."

"The visuals almost were tricky because they made it look like there were more transitions than I heard."

"The visuals don't necessarily match up with the transitions as far as I could tell."

These expressed challenges could be interpreted as the result of an additional data stream which increased processing time, however, the numerous responses indicating that the sound and audio did not match up may indicate another problem. Neuhoff (2011) discusses how visual and audio cues can interact, and that mismatched audio and visual can cause the listener to focus on one stream or the other. The fact that so many respondents felt the visuals did not match the audio indicates some degree of this "ventriloquist effect" in our results that may have increased response time due to increased confusion or switching from audio to visual cues.

Conclusions The results of our perceptual testing demonstrate the extent to which sonification could serve as a tool to explore salmon movement in otolith datasets. Even untrained listeners were very sensitive to sonic transitions in pitch and timbre, indicating that sonification can be used to understand fish movement between habitats. Respondents tended to over-report transitions, however, leading to low individual accuracy. This tendency to over-report may be alleviated through listener training in the future. The promise of sonification for otolith migration studies is that

these methods may lead to more easily interpreted trends in large, population-level time-series data, with less required training than visual data (Loeb and Fitch 2002, Ballora et al. 2004, Khamis et al. 2012). Therefore, future work should focus on determining listeners' ability to interpret movement patterns in larger otolith datasets, and tailoring sonifications for this purpose.

Beyond salmon migration, this work has implications for crowd-sourced data exploration in complex datasets. Crowdsourcing scientific data is increasingly used successfully to explore large datasets which cannot be analyzed computationally (Gura 2013, Bonney et al. 2014). The ability of naïve listeners, in aggregate, to identify potentially interesting trends using sonification could be used to improve citizen-science initiatives, or enable effective public outreach for projects based on complex data. However, in developing sonifications, our data indicate that simplicity should be the goal, with an attention to limiting chaotic intermittent sounds and mapping the data of interest to pitch and timbre when possible. Further, our data indicate that the identification of transitions within an auditory display is slowed as complexity increases, which may limit a listener's ability to interpret the sonification. This effect may be overcome by slowing the data stream to allow more processing time between transitions, or by increasing listener training. More work is needed, however, to understand how data complexity affects respondent's ability to process and correctly respond to sonification, and to develop strategies to improve individual perception through sonification design.

Tables

Table 5.1 - Summary of Sonification Parameters

River System	$^{87}Sr/^{86}Sr$ Range	Pitch Ratios	Frequency—Hertz	Note Values	Latitude Range	Azimuth Angle
Grande Ronde/ Imnaha/ Tucannon	<= 0.70772	35/32 35/16 35/8 35/4	120.3125 240.625 481.25 962.5	B2 -45 cents B3 -45 cents B4 -45 cents B5 -45 cents	45.863°N. <46.080° N.	6.97° <16.9°
Upper Snake	0.70772 < 0.70919	5/1 15/2 10/1	550 825 1100	C#5 -14 cents G5 -12 cents C#6 -14 cents	45.245°N. <45.856° N.	44.8° >17.0°
Lower Snake	0.70919 <= 0.71149	1/2 3/4 1/1 3/2 2/1	55 82.5 110 165 220	A1 E2 +2 cents A2 E3 +2 cents A3	45.856°N. <46.708° N.	17.0° >45.0°
Clearwater	>0.71149	11/4 11/2 45/8 11/1 45/4	302.5 605 618.75 1210 1237.5	D#4 -49 cents D#5 -49 cents D#5 -10 cents D#6 -49 cents D#6 -10 cents	45.830°N <46.417° N.	18.4° >17.4°

Table 5.2 - Summary of perceptual survey questions

Description of questions used in perceptual survey of salmon otolith chemistry sonification. Letters indicate significantly different groups among the control responses.

Question #	Description	Type	Visuals	Mean Accuracy	Mean Response Delay (seconds)
1	Static	Control	No	8.6% [a]	-
2	Left-Right Panning	Control	No	85.7% [b]	-
3	Pitch	Control	No	100% [b]	-
4	Random intermittent	Control	No	34.3% [a]	-
5	Timbre	Control	No	97.1% [b]	-
6	Crescendo	Control	No	82.9% [b]	-
7	1-Fish	Experimental	No	43.5%	1.47
8	2-Fish	Experimental	No	54.5%	1.53
9	3-Fish	Experimental	No	40.5%	2.10
10	1-Fish	Experimental	Yes	45.8%	1.64
11	2-Fish	Experimental	Yes	52.9%	1.86
12	3-Fish	Experimental	Yes	16.6%	2.41

Figures

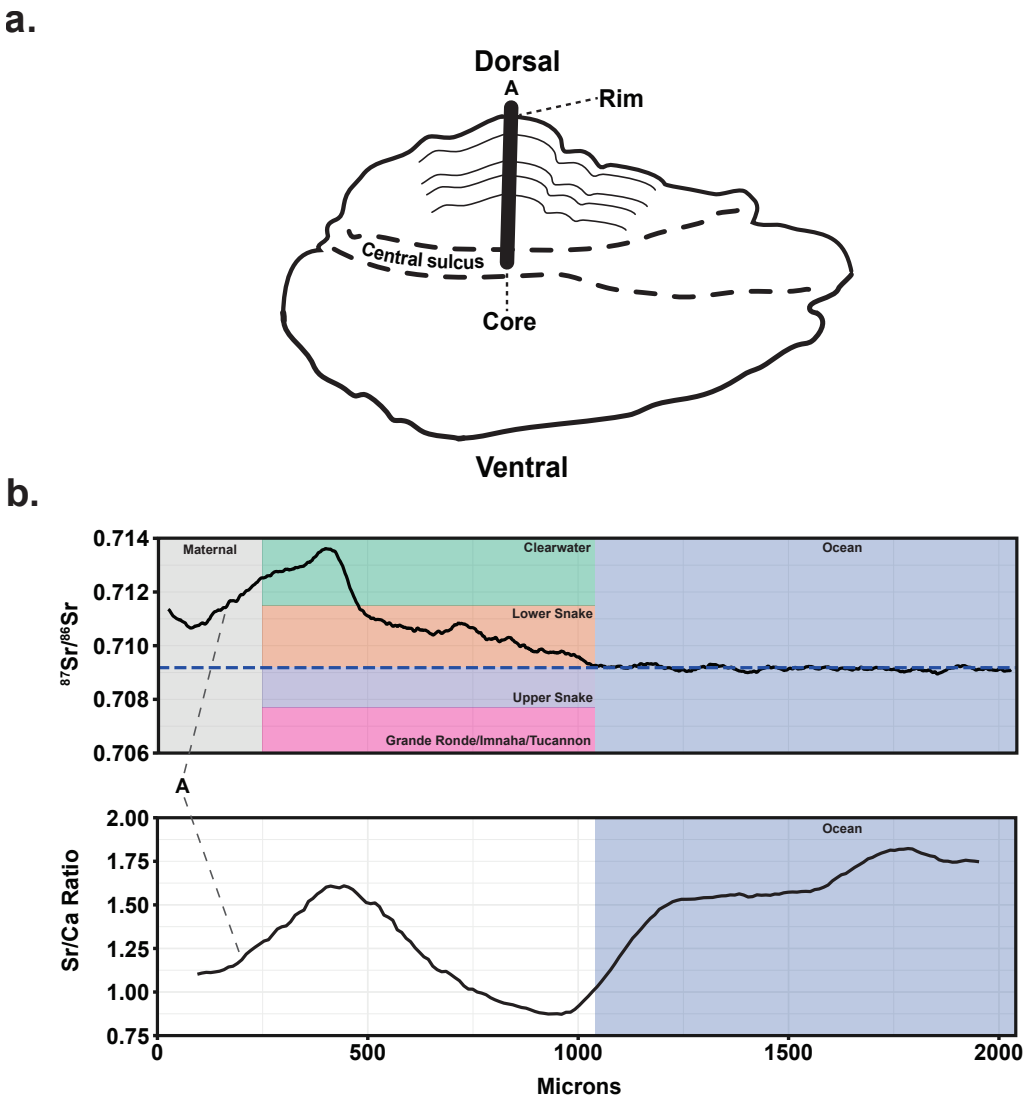

Figure 5.1 - Otolith Data collection

Otoliths are polished along the saggital plane to uncover the rings (a). Polishing is stopped with the core is visible. Otolith chemistry is then analyzed by ablating a transect across the otolith from the otolith core to its rim (A). As the laser moves across the otolith, ablated material is swept into the Inductively coupled plasma mass spectrometer (ICP-MS), ionized, and the ratio of isotopes and elements contained in the sample is measured. The resulting data (b) shows the changes in chemical values

(A) from the birth of the fish (0μm) to its death (the edge of the otolith and end of the data). Changes in $^{87}Sr/^{86}Sr$ indicate movements between locations with distinct chemistry (b).

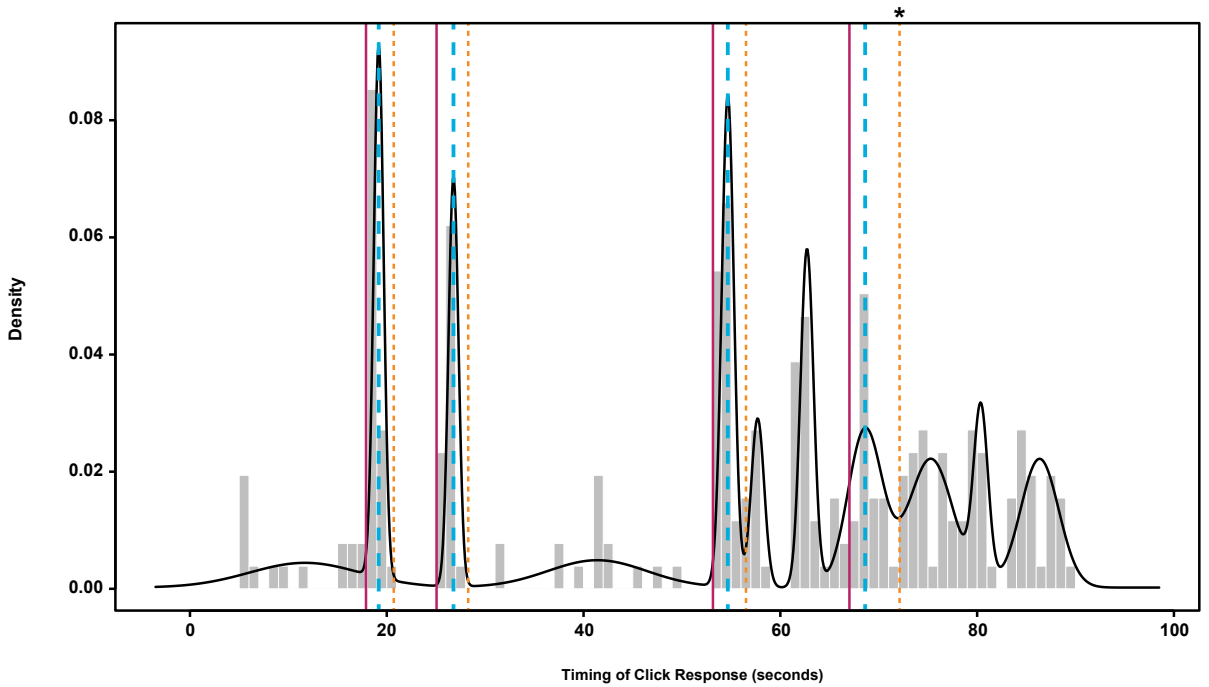

Figure 5.2 - Determining Correct Response Envelopes

Model based clustering analysis was used to determine density peaks in the aggregate response data for each question (black line). Grey bars indicate the number of responses at that time point. Peak centers (light blue, dashed lines) directly following a known transition (red lines) were identified. The variance of these peaks was used to calculate the right-hand boundary for correct responses, defined as three standard deviations to the right of the peak center (orange, dashed lines). In some cases, the number of standard deviations was decreased to avoid including following data peaks (* denotes peak constrained to 1-st. dev).

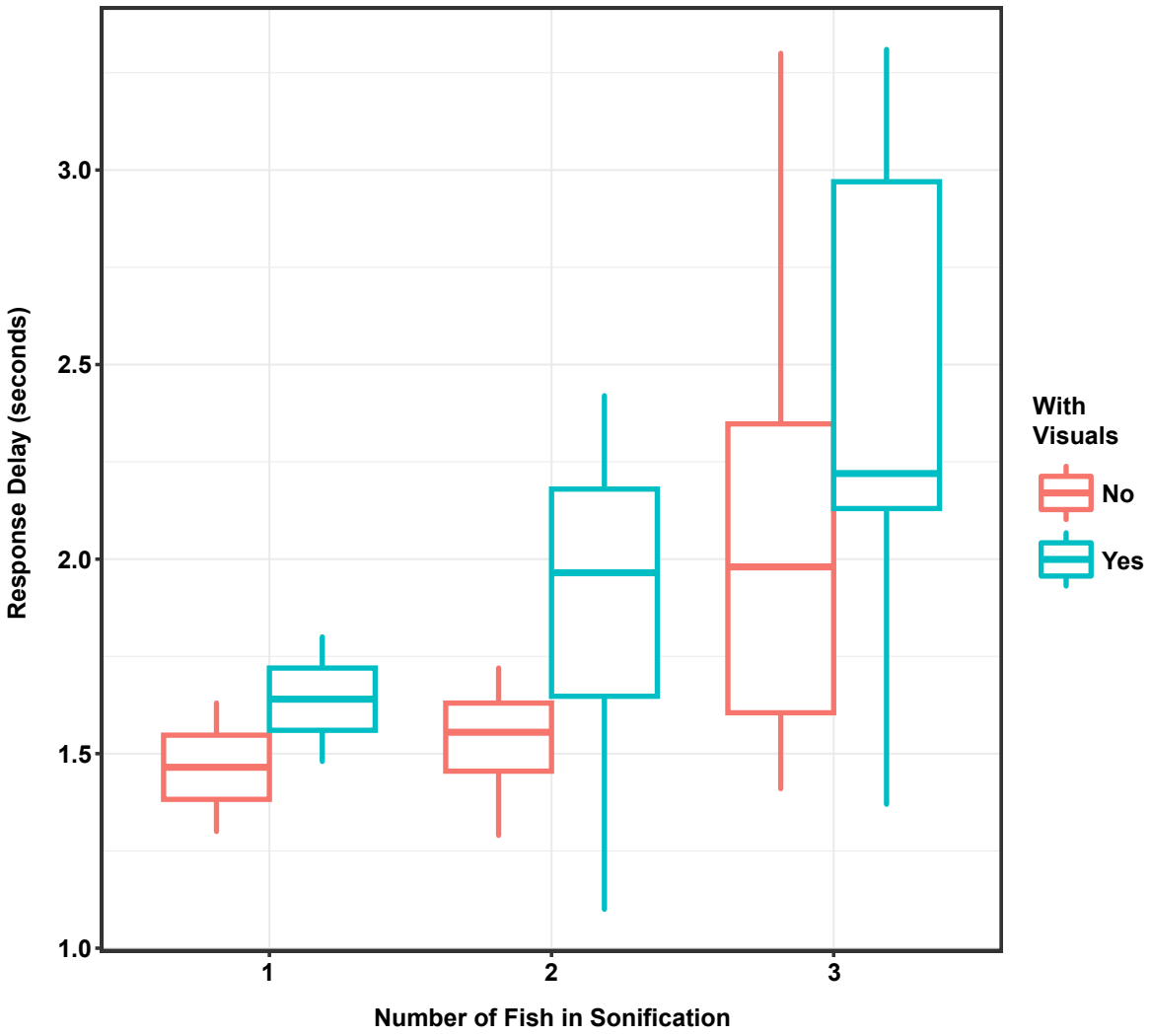

Figure 5.3 - Response delay with Increasing Numbers of Fish

The response delay of respondents was calculated for each question. Delay time, as well as the variance of that delay, increased as the number of sonified fish increased. Delay was lower throughout the survey for questions without visuals (red) than for questions that included visuals (blue).

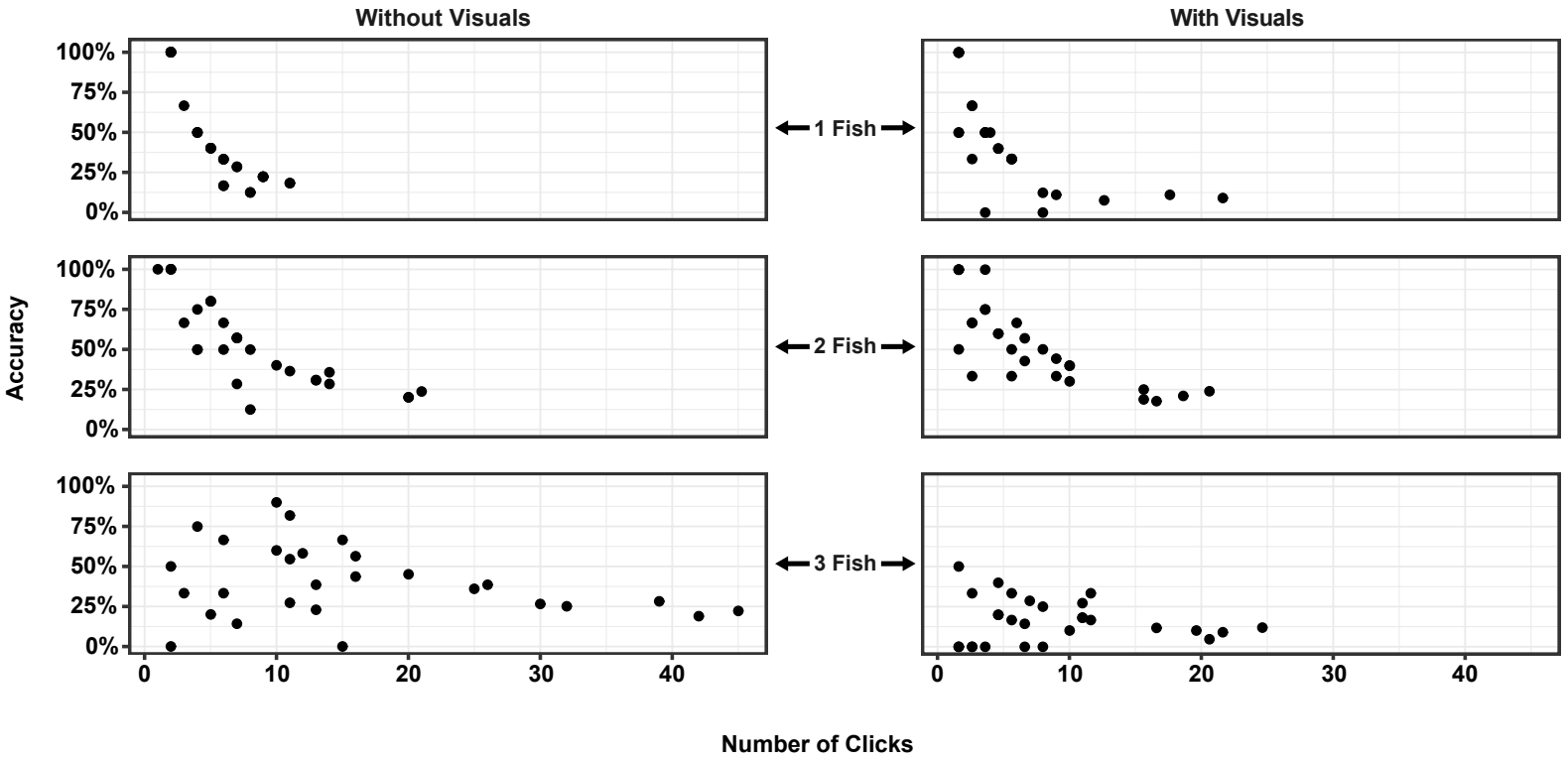

Figure 5.4 - Accuracy of individual responses by number of responses

The accuracy of individual respondents for each survey question (black dots) shows that accuracy decreases with an increased number of clicks, as expected. Some respondents were very selective in their determination of transitions, while others identified many transitions. This pattern holds for questions with one and two fish included in the sonification, with and without visuals. However, the addition of a third fish shows much more variation in accuracy, indicating a limit to the complexity at which respondents could accurately identify individual transition points.

References Cited

Aghabozorgi, S., A. Seyed Shirkhorshidi, and T. Ying Wah. 2015. Time-series clustering - A decade review. Information Systems 53:16–38.

Agudelo, E., Y. Salinas, C. L. Sanchez, D. L. Munoz-Sosa, J. C. Alonso, M. E. Arteaga, O. J. Rodriguez, N. R. Anzola, L. E. Acosta, M. Nunez, and H. Valdes. 2000. Bagres de la Amazonia Colombiana: un Recurso sin Fronteras. Editorial Scripto Ltda., Santa Fé de Bogota D.C., Columbia.

Al-Naymat, G., S. Chawla, and J. Taheri. 2009. SparseDTW: A novel approach to speed up dynamic time warping. Conferences in Research and Practice in Information Technology Series 101:117–127.

Albanese, D., and R. Visintainer. 2012. mlpy: Machine Learning Python. arXiv:1–4.

Allan, J. D., R. Abell, Z. Hogan, C. Revenga, B. W. Taylor, R. L. Welcomme, and K. Winemiller. 2005. Overfishing of Inland Waters. BioScience 55:1041.

Alonso, J. C., and N. N. Fabré. 2002. Padrão espaço-temporal da estrutura populacional e estado atual de exploração pesqueira da dourada Brachyplatystoma flavicans, Castelnau, 1855 (Siluriformes: Pimelodidae), no sistema estuário-Amazonas-Solimões. Universidade Federal do Amazonas, Manaus.

Angelini, R., N. N. Fabrè, and U. L. Silva-jr. 2006. Trophic analysis and fishing simulation of the biggest Amazonian catfish. Journal of Agricultural Research 1:151–158.

Bacon, C. R., P. K. Weber, K. A. Larsen, R. Reisenbichler, J. A. Fitzpatrick, and J. L. Wooden. 2004. Migration and rearing histories of chinook salmon (Oncorhynchus tshawytscha) determined by ion microprobe Sr isotope and Sr/Ca transects of otoliths. Canadian Journal of Fisheries and Aquatic Sciences 61:2425–2439.

Bagnall, A., A. Bostrom, J. Large, and J. Lines. 2016. The Great Time Series Classification Bake Off: An Experimental Evaluation of Recently Proposed Algorithms. Extended Version. arXive.

Ballora, M., B. Pennycook, and P. Ivanov. 2004. Heart Rate Sonification : A New Approach Medical Diagnosis. Leonardo 37:41–46.

Barnett-Johnson, R., C. B. Grimes, C. F. Royer, and C. J. Donohoe. 2007. Identifying the contribution of wild and hatchery Chinook salmon (Oncorhynchus tshawytscha) to the ocean fishery using otolith microstructure as natural tags. Canadian Journal of Fisheries and Aquatic Sciences 64:1683–1692.

Barnett-Johnson, R., T. E. Pearson, F. C. Ramos, C. B. Grimes, and R. B. MacFarlane. 2008. Tracking natal origins of salmon using isotopes, otoliths, and landscape geology. Limnology and Oceanography 53:1633–1642.

Barnett-Johnson, R., D. J. Teel, and E. Casillas. 2010. Genetic and otolith isotopic markers identify salmon populations in the Columbia River at broad and fine geographic scales. Environmental biology of fishes 89:533–546.

Barrass, S., and G. Kramer. 1999. Using sonification. Multimedia Systems 7:23–31.

Barthem, B., M. Ribeiro, and M. Petrere. 1991. Life strategies of some long-distance migratory catfish in relation to hydroelectric dams in the Amazon Basin. Biological conservation 55:339–345.

Barthem, R. B., and M. Petrere Jr. 1995. Fisheries and population dynamics of Brachyplatystoma vaillantii (Pimelodidae) in the Amazon Estuary. Pages 329–340*in* N. B. Armantrout and R. Wolotira, editors.Proceedings of the World Fisheries Congress, Theme 1. Condition of the World's Aquatic Habitats. Oxford and IBH Publishing Co. Pvt. Ltd., New Delhi, India.

Barthem, R., and M. Goulding. 1997. The Catfish Connection: Ecology, Migration, and Conservation of Amazon Predators. Page Biology and resource management in the tropics. Columbia University Press, New York.

Bataille, C. P., and G. J. Bowen. 2012. Mapping 87Sr/86Sr variations in bedrock and water for large scale provenance studies. Chemical Geology 304:39–52.

Bataille, C. P., S. R. Brennan, J. Hartmann, N. Moosdorf, M. J. Wooller, and G. J. Bowen. 2014. A geostatistical framework for predicting variations in strontium concentrations and isotope ratios in Alaskan rivers. Chemical Geology 389:1–15.

Bates, D., M. Mächler, B. Bolker, and S. Walker. 2015. Fitting Linear Mixed-Effects Models Using **lme4**. Journal of Statistical Software 67:1–48.

Bath, G. E., S. R. Thorrold, C. M. Jones, S. E. Campana, J. W. McLaren, and J. W. H. Lam. 2000. Strontium and barium uptake in aragonitic otoliths of marine fish. Geochimica et Cosmochimica Acta 64:1705–1714.

Batista, J. S., and J. A. Alves-Gomes. 2006. Phylogeography of Brachyplatystoma rousseauxii (Siluriformes - Pimelodidae) in the Amazon Basin offers preliminary evidence for the first case of "homing" for and Amazonian migratory catfish. Genetics and Molecular Research 5:723–740.

Bauer, S., and B. J. Hoye. 2014. Migratory Animals Couple Biodiversity and Ecosystem Functioning Worldwide. Science 344:54–54(8).

Baumann, M., M. Ozdogan, A. D. Richardson, and V. C. Radeloff. 2017. Phenology from Landsat when data is scarce: Using MODIS and Dynamic Time-Warping to combine multi-year Landsat imagery to derive annual phenology curves. International Journal of Applied Earth Observation and Geoinformation 54:72–83.

Beechie, T., E. Buhle, M. Ruckelshaus, A. Fullerton, and L. Holsinger. 2006. Hydrologic regime and the conservation of salmon life history diversity. Biological Conservation 130:560–572.

Berndt, D. J., and J. Clifford. 1994. Using dynamic time warping to find patterns in time series. Pages 359–370KDD workshop.

De Block, M., and R. Stoks. 2005. Fitness Effects from Egg to Reproduction: Bridging the life history transition. Ecology 86:185–197.

Bolker, B. M., M. E. Brooks, C. J. Clark, S. W. Geange, J. R. Poulsen, M. H. H. Stevens, and J.-S. S. White. 2009. Generalized linear mixed models: a practical guide for ecology and evolution. Trends in Ecology & Evolution 24:127–135.

Bonney, R., J. L. Shirk, T. B. Phillips, A. Wiggins, H. L. Ballard, A. J. Miller-Rushing, and J. K. Parrish. 2014. Citizen science: Next steps for citizen science. Science 343:1436–1437.

Bouchez, J., E. Lajeunesse, J. Gaillardet, C. France-Lanord, P. Dutra-Maia, and L. Maurice. 2010. Turbulent mixing in the Amazon River: The isotopic memory of confluences. Earth and Planetary Science Letters 290:37–43.

Bowlin, M. S., I.-A. Bisson, J. Shamoun-Baranes, J. D. Reichard, N. Sapir, P. P. Marra, T. H. Kunz, D. S. Wilcove, A. Hedenström, C. G. Guglielmo, S. Åkesson, M. Ramenofsky, and M. Wikelski. 2010. Grand challenges in migration biology. Integrative and comparative biology 50:261–79.

Box, P. O., and F.-N. Group. 2002. EXPERIMENTAL COMPARISON OF COMPLEX AND SIMPLE SOUNDS IN MENU AND HIERARCHY SONIFICATION Juha Marila Visual Communications Laboratory. Engineering:2–6.

Boyd, J. W., E. W. Oldenburg, G. A. McMichael, M. Dell, and T. Schadt. 2010. Color Photographic Index of Fall Chinook Salmon Embryonic Development and Accumulated Thermal Units. PLoS ONE 5:e11877.

De Braux, E., F. Warren-Myers, T. Dempster, P. G. Fjelldal, T. Hansen, and S. E. Swearer. 2014. Osmotic induction improves batch marking of larval fish otoliths with enriched stable isotopes. ICES Journal of Marine Science 71:2530–2538.

Brodersen, J., B. B. Chapman, P. A. Nilsson, C. Skov, L. A. Hansson, and C. Brönmark. 2014. Fixed and flexible: Coexistence of obligate and facultative migratory strategies in a freshwater fish. PLoS ONE 9:e90294.

Brommer, J. E. 2000. The evolution of fitness in life - history theory. Biol. Rev 75:377–404.

Brommer, J. E., L. Gustafsson, H. Pietiäinen, and J. Merilä. 2004. Single-generation estimates of individual fitness as proxies for long-term genetic contribution. The American naturalist 163:505–17.

Brophy, D., T. E. Jeffries, and B. S. Danilowicz. 2004. Elevated manganese concentrations at the cores of clupeid otoliths : possible environmental , physiological , or structural origins. Marine Biology 144:779–786.

Brown, R. J., and K. P. Severin. 2009. Otolith chemistry analyses indicate that water Sr:Ca is the primary factor influencing otolith Sr:Ca for freshwater and diadromous fish but not for marine fish. Canadian Journal of Fisheries and Aquatic Sciences 66:1790–1808.

Buczkowski, G. 2010. Extreme life history plasticity and the evolution of invasive characteristics in a native ant. Biological Invasions 12:3343–3349.

Burke, J. L. 2004. Life histories of juvenile chinook salmon in the Columbia River estuary: 1916 to the present. Oregon State University.

Burnham, K. P., and D. R. Anderson. 2002. Model selection and multimodel inference: a practical information-theoretic approach. Springer Verlag.

Bywater, R. P., and J. N. Middleton. 2016. Melody discrimination and protein fold classification. Heliyon 2.

Calcagno, V., and C. de Mazancourt. 2010. glmulti: an R package for easy automated model selection with (generalized) linear models. Journal of Statistical Software 34.

Campana, S. E. 1983. Feeding periodicity and the production of daily growth increments in otoliths of steelhead. Can. J. Zool 61.

Campana, S. E. 2005. Otolith science entering the 21st century. Marine and Freshwater Research 56:485–496.

Campana, S. E., and S. R. Thorrold. 2001. Otoliths, increments, and elements: keys to a comprehensive understanding of fish populations? Canadian Journal of Fisheries and Aquatic Sciences 58:30–38.

Campana, S., and J. Neilson. 1985. Microstructure of fish otoliths. Canadian Journal of Fisheries … 42:1014–1032.

De Campo, A. 2007. TOWARD A DATA SONIFICATION DESIGN SPACE MAP. Pages 342–347Proceedings of the 13th International Conference on Auditory Display. Montreal, Canada.

De Campo, A., C. Dayé, C. Frauenberger, K. Vogt, A. Wallisch, and G. Eckel. 2006. SONIFICATION AS AN INTERDISCIPLINARY WORKING PROCESS. Pages 28–35Proceedings of the 12th International Conference on Auditory Display. London, UK.

Carlson, S. M., T. P. Quinn, and a P. Hendry. 2011. Eco-evolutionary dynamics in Pacific salmon. Heredity 106:438–47.

Carlson, S. M., and W. H. Satterthwaite. 2011. Weakened portfolio effect in a collapsed salmon population complex. Canadian Journal of Fisheries and Aquatic Sciences 68:1579–1589.

Carpenter, S. R., E. H. Stanley, and M. J. Vander Zanden. 2011. State of the World's Freshwater Ecosystems: Physical, Chemical, and Biological Changes. Annual Review of Environment and Resources 36:75–99.

Carvajal, F. 2013, January 18. Phylogeny and population genetics of the fish performing the largest migratin known in freshwater, the Amazonian catfish "Brachyplatystomarousseauxii" : revelations from the upper Madera Basin. Montpellier 2.

Chapman, B. B., C. Brönmark, J. Å. Nilsson, and L. A. Hansson. 2011. The ecology and evolution of partial migration. Oikos 120:1764–1775.

Chatfield, C. 2003. The Analysis of Time Series: An Introduction. 6th edition. Taylor & Francis, Boca Raton, FL.

Cheng, H., Z. Dai, Z. Liu, and Y. Zhao. 2015. An image-to-class dynamic time warping approach for both 3D static and trajectory hand gesture recognition. Pattern Recognition 55:137–147.

Chiappori, P. A., and I. Ekeland. 2011. New Developments in Aggregation Economics.

Clark, W. A. V, and K. L. Avery. 1976. The Effects of Data Aggregation in Statistical Analysis. Geographical Analysis VIII:429–438.

Clutton-Brock, T., and B. C. Sheldon. 2010. Individuals and populations: The role of long-term, individual-based studies of animals in ecology and evolutionary biology.

Cohen, K. M., S. Finney, and P. L. Bibbard. 2013. International Chronostratigraphic Chart. International Commission on Stratigraphy.

Collins, S. M., N. Bickford, P. B. McIntyre, A. Coulon, A. J. Ulseth, D. C. Taphorn, and A. S. Flecker. 2013. Population Structure of a Neotropical Migratory Fish: Contrasting Perspectives from Genetics and Otolith Microchemistry. Transactions of the American Fisheries Society 142:1192–1201.

Connor, W., H. Burge, and D. Bennett. 1998. Detection of PIT-tagged subyearling chinook salmon at a Snake River dam: implications for summer flow augmentation. North American Journal of … 18:530–536.

Connor, W. P., B. D. Arnsberg, J. A. Chandler, T. D. Cooney, P. A. Groves, J. A. Hesse, G. W. Mendel, D. J. Milks, D. W. Rondorf, S. J. Rosenberger, M. L. Schuck, K. F. Tiffan, R. S. Waples, and W. Young. 2016. A Retrospective (circa 1800 – 2015) on the Abundance , Spatial Distribution , and Management of Snake River Basin Fall Chinook. Portland, OR.

Connor, W. P., H. L. Burge, R. Waitt, and T. C. Bjornn. 2002. Juvenile life history of wild fall Chinook salmon in the Snake and Clearwater rivers. North American Journal of Fisheries Management 22:703–712.

Connor, W. P., C. E. Piston, and A. P. Garcia. 2003a. Temperature during Incubation as One Factor Affecting the Distribution of Snake River Fall Chinook Salmon Spawning Areas. Transactions of the American Fisheries Society 132:1236–1243.

Connor, W. P., J. G. Sneva, K. F. Tiffan, R. K. Steinhorst, and D. Ross. 2005. Two alternative juvenile life history types for fall Chinook salmon in the Snake River basin. Transactions of the American Fisheries Society 134:291–304.

Connor, W. P., K. F. Tiffan, J. M. Plumb, and C. M. Moffitt. 2013. Evidence for Density-Dependent Changes in Growth, Downstream Movement, and Size of Chinook

Salmon Subyearlings in a Large-River Landscape. Transactions of the American Fisheries Society American Fisheries Society 142:1453–1468.

Connor, W., R. Steinhorst, and H. Burge. 2003b. Migrational behavior and seaward movement of wild subyearling fall Chinook salmon in the Snake River. North American Journal of Fisheries Management 23:414–430.

Cope, J., and P. Remagnino. 2012. Classifying Plant Leaves from Their Margins Using Dynamic Time Warping. Pages 258–267Advanced Concepts for Intelligent Vision Systems. Springer, Berlin, Heidelberg.

Copeland, T., and D. A. Venditti. 2009. Contribution of three life history types to smolt production in a Chinook salmon (Oncorhynchus tshawytscha) population. Canadian Journal of Fisheries and Aquatic Sciences 66:1658–1665.

Córdoba, E. A., Á. Viviana, J. León, C. A. Bonilla-Castillo, M. P. Junior, M. Peláez, and F. Duponchelle. 2013. Breeding , growth and exploitation of Brachyplatystoma rousseauxii Castelnau , 1855 in the Caqueta River , Colombia. Neotropical Icthyology 11:637–647.

Costanza, R., and T. Maxwell. 1994. Resolution and predictability: An approach to the scaling problem. Landscape Ecology 9:47–57.

Courter, I. I., D. B. Child, J. A. Hobbs, T. M. Garrison, J. J. G. Glessner, S. Duery, and D. Fraser. 2013. Resident rainbow trout produce anadromous offspring in a large interior watershed. Canadian Journal of Fisheries and Aquatic Sciences 70:701–710.

Cressie, N., and C. K. Wikle. 2011. Statistics for Spatio-Temporal Data. Page Wiley Series on Probability and Statistics. First edition. John Wiley & Sons, Inc., Hoboken, NJ.

Crook, D. A., J. I. Macdonald, D. G. McNeil, D. M. Gilligan, M. Asmus, R. Maas, J. Woodhead, and B. Gillanders. 2013. Recruitment sources and dispersal of an invasive fish in a large river system as revealed by otolith chemistry analysis. Canadian Journal of Fisheries and Aquatic Sciences 70:953–963.

Crozier, L. G., A. P. Hendry, P. W. Lawson, T. P. Quinn, N. J. Mantua, J. Battin, R. G. Shaw, and R. B. Huey. 2008. Potential responses to climate change in organisms with complex life histories: evolution and plasticity in Pacific salmon. Evolutionary Applications 1:252–270.

Cunjak, R. A., T. D. Prowse, and D. L. Parrish. 1998. Atlantic salmon (*Salmo salar*) in winter: "the season of parr discontent"? Canadian Journal of Fisheries and Aquatic Sciences 55:161–180.

Debeljak, M., G. R. Squire, D. Kocev, C. Hawes, M. W. Young, and S. Džeroski. 2010. Analysis of time series data on agroecosystem vegetation using predictive clustering trees. Ecological Modelling 222:2524–2529.

Dombois, F. 2002. Auditory seismology on free oscillations, focal mechanisms, explosions and synthetic seismograms. ... of the 2002 International Conference on Auditory ...:1–4.

Donohoe, C. J., P. B. Adams, and C. F. Royer. 2008. Influence of water chemistry and migratory distance on ability to distinguish progeny of sympatric resident and anadromous rainbow trout (Oncorhynchus mykiss). Canadian Journal of Fisheries and Aquatic Sciences 1075:1060–1075.

Dubus, G., R. Bresin, D. Calvet, C. Vallée, and B. Shneiderman. 2013. A Systematic Review of Mapping Strategies for the Sonification of Physical Quantities. PLoS ONE 8:e82491.

Dudgeon, D. 2011. Asian river fishes in the Anthropocene: threats and conservation challenges in an era of rapid environmental change. Journal of fish biology 79:1487–524.

Dudgeon, D., A. H. Arthington, M. O. Gessner, Z.-I. Kawabata, D. J. Knowler, C. Lévêque, R. J. Naiman, A.-H. Prieur-Richard, D. Soto, M. L. J. Stiassny, and C. a Sullivan. 2006. Freshwater biodiversity: importance, threats, status and conservation challenges. Biological reviews of the Cambridge Philosophical Society 81:163–82.

Dynesius, M., C. Nilsson, M. Dynesius, and C. Revenga. 1994. Fragmentation and flow regulation of river systems in the northern third of the world. Science (New York, N.Y.) 266:753–62.

Elsdon, T. S., B. K. Wells, S. E. Campana, B. M. Gillanders, C. M. Jones, K. E. Limburg, D. H. Secor, S. R. Thorrold, B. D. Walther, and H. R. Barnes. 2008. Otolith chemistry to describe movements and life-history parameters of fishes: Hypotheses, assumptions, limitations and inferences. Pages 297–330Oceanography and Marine Biology: an annual review, vol 46.

Fabré, N. N., and R. B. Barthem. 2005. O manejo da pesca dos grandes bagres migradores: Piramutaba e Dourada no Eixo Solimões-Amazonas. Page (M. L. Ruffino, Ed.). ProVárzea/Ibama, Manaus, Amazonas, Brazil.

Faure, G., and T. M. Mensing. 2004. Isotopes: principles and applications. John Wiley & Sons Inc.

Fearnside, P. M. 2006. Dams in the Amazon : Belo Monte and Brazil's Hydroelectric Development of the Xingu River Basin. Environmental Management 38:16–27.

Fearnside, P. M. 2014. Impacts of Brazil's Madeira River Dams: Unlearned lessons for hydroelectric development in Amazonia. Environmental Science & Policy 38:164–172.

Ferguson, S., W. L. Martens, and D. Cabrera. 2011. Statistical sonification for exploratory data analysis. Pages 175–196*in* J. Neuhoff, editor.The Sonification Handbook. Logos-Verlag, Berlin.

Finer, M., and C. N. Jenkins. 2012. Proliferation of hydroelectric dams in the Andean Amazon and implications for Andes-Amazon connectivity. PloS one 7:e35126.

Finn, R. N. 2007. The physiology and toxicology of salmonid eggs and larvae in relation to water quality criteria. Aquatic Toxicology 81:337–354.

Fitch, W. T., and G. Kramer. 1994. Sonifying the body electric: Superiority of an auditory over a visual display in a complex, multivariate system. Pages 307–326*in* J. Repcheck, editor.Santa Fe Institute in the Sciences of Complexity-Proceedings Volume 18 Volume 18. Addison-Wesley Publishing Co.

Flowers, J. H. 2005. THIRTEEN YEARS OF REFLECTION ON AUDITORY GRAPHING : PROMISES , PITFALLS , AND POTENTIAL NEW DIRECTIONS. Pages 406–409 Eleventh Meeting of the Internationsal Conference on Auditory Display. Limerick, Ireland.

Foley, J. A., R. DeFries, G. P. Asner, C. Barford, G. Bonan, S. R. Carpenter, F. S. Chapin, M. T. Coe, G. C. Daily, and H. K. Gibbs. 2005. Global consequences of land use. Science 309:570.

Forero, J. 2013, February 9. Power-hungry Brazil builds dams, and more dams, across the Amazon. The Washington Post. Washington, DC.

Fraley, C., and A. E. Raftery. 2007. Bayesian regularization for normal mixture estimation and model-based clustering. Journal of Classification 24:155–181.

Freeman, B. J. F. 2003. Ecosystem-Level Consequences of Migratory Faunal Depletion Caused by Dams. American Fisheries Society Symposium 35:255–266.

Gabrielsson, R. M., J. Kim, M. R. Reid, C. H. Stirling, M. Numata, and G. P. Closs. 2012. Does the trace element composition of brown trout Salmo trutta eggs remain unchanged in spawning redds? Journal of Fish Biology 81:1871–1879.

Gaillardet, J., B. Dupre, C. J. Allegre, and P. Négrel. 1997. Chemical and physical denudation in the Amazon River Basin. Chemical Geology 142:141–173.

Gałecki, A., and T. Burzykowski. 2013. Linear Mixed-Effects Model. Pages 245–273Linear Mixed-Effects Models Using R. Springer, New York, NY.

Garcez, R. C. S. 2014. Composição Química de Otólitos de Tucunaré (Chicla temensis Humbolt, 1821) como Marcadores Ambientais em Populações de Lagos de Várzea e Igapó (Amazonas - Brazil). INSTITUTO NACIONAL DE PESQUISAS DA AMAZÔNIA - INPA.

Garcez, R. C. S., R. Humston, D. Harbor, and C. E. C. Freitas. 2014. Otolith geochemistry in young-of-the-year peacock bass Cichla temensis for investigating natal dispersal in the Rio Negro (Amazon - Brazil) river system. Ecology of Freshwater Fish:n/a-n/a.

Garcia, A. P., S. Bradbury, B. D. Arnsberg, and P. A. Groves. 2008. Fall Chinook Salmon Spawning Ground Surveys in the Snake River Basin Upriver of Lower Granite Dam, 2007 Annual Report.

Garcia, A. P., S. Bradbury, B. D. Arnsberg, S. J. Rocklage, and P. A. Groves. 2005. Fall Chinook salmon spawning ground surveys in the Snake River basin upriver of Lower Granite Dam, 2004. 2004 Annual Report to Bonneville Power Administration. Project:3.

García Vásquez, A., J.-C. Alonso, F. Carvajal, J. Moreau, J. Nuñez, J.-F. Renno, S. Tello, V. Montreuil, and F. Duponchelle. 2009. Life-history characteristics of the large Amazonian migratory catfish Brachyplatystoma rousseauxii in the Iquitos region, Peru. Journal of fish biology 75:2527–51.

Gardner, R. H., W. G. Cale, R. V. O. ' Neill, and A. R. V O 'neill. 1982. Robust Analysis of Aggregation Error. Ecology 63:1771–1779.

Gende, S. M., R. T. Edwards, M. F. Willson, and M. S. Wipfli. 2002. Pacific salmon in aquatic and terrestrial ecosystems. BioScience 52:917–928.

Ghalambor, C. K., K. L. Hoke, E. W. Ruell, E. K. Fischer, D. N. Reznick, and K. A. Hughes. 2015. Non-adaptive plasticity potentiates rapid adaptive evolution of gene expression in nature. Nature 525:372–375.

Ghalambor, C. K., J. K. McKay, S. P. Carroll, and D. N. Reznick. 2007. Adaptive versus non-adaptive phenotypic plasticity and the potential for contemporary adaptation in new environments. Functional Ecology 21:394–407.

Giménez, K. A., and G. Torres. 2004. Linking life history traits in successive phases of a complex life cycle: effects of larval biomass on early juvenile development in an estuarine crab, Chasmagnathus granulata. Oikos 104:570–580.

Godoy, M. P. 1979. Marcação e migração de piramutaba Brachyplatystoma vaillanti (Val., 1840. na Bacia Amazonica (Pará e Amazonas), Brasil (Pisces, Nematognathi, Pimelodidae). Boletim de Faculdade de Ceincias do Pará, Belém 11:3–21.

Good, T. P., R. S. Waples, and P. Adams. 2005. Updated status of federally listed ESU's of West Coast salmon and steelhead. Page (U. S. D. of Commerce, Ed.) NOAA Technical Memorandum NMFS-NWFSC-66. NOAA.

Gotthard, K., and S. Nylin. 1995. Adaptive Plasticity and Plasticity as an Adaptation: A Selective Review of Plasticity in Animal Morphology and Life History. Oikos 74:3–17.

Greene, C. M., J. E. Hall, K. R. Guilbault, and T. P. Quinn. 2010. Improved viability of populations with diverse life-history portfolios. Biology letters 6:382–6.

Griffiths, J. R., D. E. Schindler, J. B. Armstrong, M. D. Scheuerell, D. C. Whited, R. A. Clark, R. Hilborn, C. A. Holt, S. T. Lindley, J. A. Stanford, and E. C. Volk. 2014. Performance of salmon fishery portfolios across western North America. Journal of Applied Ecology 51:1554–1563.

Gulzar, H. M. 2015, June 15. Comprehensive Python module for computing and visualizing dynamic time warping alignment: DTWPy. University of Stavanger, Norway.

Gura, T. 2013. Citizen science: amateur experts. Nature 496:259–261.

Haddad, N. M., L. A. Brudvig, J. Clobert, K. F. Davies, A. Gonzalez, R. D. Holt, T. E. Lovejoy, J. O. Sexton, M. P. Austin, C. D. Collins, W. M. Cook, E. I. Damschen, R. M. Ewers, B. L. Foster, C. N. Jenkins, A. J. King, W. F. Laurance, D. J. Levey, C. R. Margules, B. A. Melbourne, A. O. Nicholls, J. L. Orrock, D.-X. Song, and J. R. Townshend. 2015. Habitat fragmentation and its lasting impact on Earth's ecosystems. Science Advances 1:e1500052–e1500052.

Hamann, E. J., and B. P. Kennedy. 2012. Juvenile dispersal affects straying behaviors of adults in a migratory population. Ecology 93:733–740.

Hamer, P., A. Henderson, M. Hutchison, J. Kemp, C. Green, and P. Feutry. 2015. Atypical correlation of otolith strontium : Calcium and barium : Calcium across a marine-freshwater life history transition of a diadromous fish. Marine and Freshwater Research 66:411–419.

Hampton, S. E., C. A. Strasser, J. J. Tewksbury, W. K. Gram, A. E. Budden, A. L. Batcheller, C. S. Duke, and J. H. Porter. 2009. Big data and the future of ecology Data-intensive Science: A New Paradigm for Biodiversity Studies. bioscience 11:156–162.

Hayes, F. R., D. A. Darcy, and C. M. Sullivan. 1946. Changes in the Inorganic Contituents of Developing Salmon Eggs. Journal of Biological Chemistry 163:621–632.

Healey, M. C. 2009. Resilient salmon, resilient fisheries for British Columbia, Canada. Ecology and Society 14:2.

Hegg, J. C., T. Giarrizzo, and B. P. Kennedy. 2015a. Diverse Early Life-History Strategies in Migratory Amazonian Catfish: Implications for Conservation and Management. Plos One 10.

Hegg, J. C., T. Giarrizzo, and B. P. Kennedy. 2015b. Diverse Early Life-History Strategies in Migratory Amazonian Catfish: Implications for Conservation and Management. bioRxiv (in-review, PloS One) pre-print:1–37.

Hegg, J. C., B. P. Kennedy, P. M. Chittaro, and R. W. Zabel. 2013a. Spatial structuring of an evolving life-history strategy under altered environmental conditions. Oecologia 172:1017–1029.

Hegg, J. C., B. P. Kennedy, and A. K. Fremier. 2013b. Predicting strontium isotope variation and fish location with bedrock geology: Understanding the effects of geologic heterogeneity. Chemical Geology 360–361:89–98.

Hegg, J. C., J. Middleton, B. L. Robertson, and B. Kennedy. 2017. Salmon Otolith Sonification Perceptual Survey Dataset. Mendeley Data v2.

Hermann, T., and A. Hunt. 2005. An Introduction to Interactive Sonification. IEEE multimedia 12:20–24.

Hermann, T., A. Hunt, and J. G. Neuhoff. 2011. The Sonification Handbook. Page (T. Hermann, A. Hunt, and J. G. Neuhoff, Eds.). Logos-Verlag, Berlin.

Hilborn, R., T. P. Quinn, D. E. Schindler, and D. E. Rogers. 2003. Biocomplexity and fisheries sustainability. Proceedings of the National Academy of Sciences of the United States of America 100:6564–8.

Hobbs, J. A., L. S. Lewis, N. Ikemiyagi, T. Sommer, and R. D. Baxter. 2010. The use of otolith strontium isotopes (87Sr/86Sr) to identify nursery habitat for a threatened estuarine fish. Environmental Biology of Fishes 89:557–569.

Hobson, K. A., R. Barnett-Johnson, and T. Cerling. 2010. Using isoscapes to track animal migration. Pages 273–298Isoscapes: understanding movement, pattern, and process on Earth through isotope mapping. Springer Verlag.

Hodge, B. W., M. A. Wilzback, W. G. Duffy, R. M. Quinones, and J. A. Hobbs. 2016. Life history diversity in Klamath River steelhead. Transactions of the American Fisheries Society 145:227–238.

Hogan, Z., I. G. Baird, R. Radtke, and M. J. Vander Zanden. 2007. Long distance migration and marine habitation in the tropical Asian catfish, Pangasius krempfi. Journal of Fish Biology 71:818–832.

Hughes, J. M., D. J. Schmidt, J. I. Macdonald, J. A. Huey, and D. A. Crook. 2014. Low interbasin connectivity in a facultatively diadromous fish: evidence from genetics and otolith chemistry. Molecular ecology 23:1000–13.

Huntingford, F. A., N. B. Metcalfe, J. E. Thorpe, W. D. Graham, and C. E. Adams. 1990. Social dominance and body size in Atlantic salmon parr, Salmo solar L. Journal of Fish Biology 36:877–881.

Hutchings, J. a. 2011. Old wine in new bottles: reaction norms in salmonid fishes. Heredity 106:421–37.

Isaak, D. J., R. F. Thurow, B. E. Rieman, and J. B. Dunham. 2003. Temporal variation in synchrony among Chinook salmon (Oncorhynchus tshawytscha) redd counts from a wilderness area in central Idaho. Canadian Journal of Fisheries and Aquatic Sciences 60:840–848.

Isaak, D. J., S. Wollrab, D. Horan, and G. Chandler. 2012. Climate change effects on stream and river temperatures across the northwest U.S. from 1980–2009 and implications for salmonid fishes. Climatic Change 113:499–524.

James, N. A., and D. S. Matteson. 2014. ecp: An R Package for Nonparametric Multiple Change Point Analysis of Multivariate Data. JSS Journal of Statistical Software 62.

JICA, I. Japan International Cooperation Agency: Sanyo Techno Marine, IBAMA, and Japan. 1998. The fishery resources study of the Amazon and Tocantins river mouth areas in the Federative Republic of Brazil: final report. Tokyo.

Jimenez, E. A., M. A. Filho, and F. L. Frédou. 2013. Fish Bycatch of the Laulao catfish Brachyplatystoma vaillantii (Valencienes, 1840) Trawl Fishery in the the Amazon Basin. Brazilian Journal of Oceanography 61:129–140.

Jochum, K. P., U. Weis, B. Stoll, D. Kuzmin, Q. Yang, I. Raczek, D. E. Jacob, A. Stracke, K. Birbaum, D. A. Frick, D. Günther, and J. Enzweiler. 2011. Determination of reference values for NIST SRM 610-617 glasses following ISO guidelines. Geostandards and Geoanalytical Research 35:397–429.

Jouary, A., G. Sumbre, E. Normale, and S. Erieure. 2016. Automatic classification of behavior in zebrafish larvae. BioRxiv.

Junk, W. J., M. T. F. Piedade, J. Schöngart, M. Cohn-Haft, J. M. Adeney, and F. Wittmann. 2011. A Classification of Major Naturally-Occurring Amazonian Lowland Wetlands. Wetlands 31:623–640.

Kalish, J. M. 1990. Use of Otolith Microchemistry to Distinguish the Progeny of Sympatric Anadromous and Non-anadromous Salmonids. Fisheries Bulletin 88:657–666.

Kate, R. J. 2015. Using dynamic time warping distances as features for improved time series classification. Data Mining and Knowledge Discovery 30:283–312.

Keefe, D. F., and T. Isenberg. 2013. Reimagining the Scientific Visualization Interaction Paradigm. Computer 46:51–57.

Kennedy, B. P., J. D. Blum, C. L. Folt, and K. H. Nislow. 2000. Using natural strontium isotopic signatures as fish markers: methodology and application. Canadian Journal of Fisheries and Aquatic Sciences 57:2280–2292.

Kennedy, B. P., C. L. Folt, J. D. Blum, and C. P. Chamberlain. 1997. Natural isotope markers in salmon. Nature 387:766–767.

Kennedy, B. P., A. Klaue, J. D. Blum, C. L. Folt, and K. H. Nislow. 2002. Reconstructing the lives of fish using Sr isotopes in otoliths. Canadian Journal of Fisheries and Aquatic Sciences 59:925–929.

Keogh, E. J., and M. J. Pazzani. 2000. Scaling up dynamic time warping for datamining applications. Pages 285–289Proceedings of the sixth ACM SIGKDD international conference on Knowledge discovery and data mining. ACM Press, New Yok, NY.

Khamis, H., A. Mohamed, S. Simpson, and A. McEwan. 2012. Detection of temporal lobe seizures and identification of lateralisation from audified EEG. Clinical neurophysiology : official journal of the International Federation of Clinical Neurophysiology 123:1714–20.

Killick, R., and I. A. Eckley. 2013. Changepoint: An R Package for changepoint analysis. R package version 0.6, URL http://CRAN.R-project.org/package=changepoint:1–15.

Killick, R., P. Fearnhead, and I. Eckley. 2012. Optimal detection of changepoints with a linear computational cost. Journal of the American … 107:1–25.

Kramer, G., T. Bonebright, and J. H. Flowers. 2010. Sonification Report : Status of the Field and Research Agenda, Report prepared for the National Science Foundation by members of the International Community for Auditory Display.

Kraus, R. T., and D. H. Secor. 2004. Incorporation of strontium into otoliths of an estuarine fish. Journal of Experimental Marine Biology and Ecology 302:85–106.

Langfelder, P., B. Zhang, and S. Horvath. 2008. Defining clusters from a hierarchical cluster tree: the Dynamic Tree Cut package for R. Bioinformatics 24:719–720.

Laurance, W. F., F. Achard, S. Peedell, and S. Schmitt. 2016, September 1. Big data, big opportunities. Frontiers in Ecology and the Environment 14:347.

Lawson, P. W., E. A. Logerwell, N. J. Mantua, R. C. Francis, and V. N. Agostini. 2004. Environmental factors influencing freshwater survival and smolt production in Pacific Northwest coho salmon (*Oncorhynchus kisutch*). Canadian Journal of Fisheries and Aquatic Sciences 61:360–373.

Lee, S. J., K. J. Oh, and T. Y. Kim. 2012. How many reference patterns can improve profitability for real-time trading in futures market? Expert Systems with Applications 39:7458–7470.

Lehner, B., K. Verdin, and A. Jarvis. 2008. New global hydrography derived from spaceborne elevation data. Eos 89:93–94.

Leonard, M., and B. Wolfe. 2001. Mining Transactional and Time Series Data Data Mining and Predictive Modeling. Data Mining and Predictive Modeling:1–26.

Levin, S. A. 1992. The Problem of Pattern and Scale in Ecology: The Robert H. MacArthur Award Lecture. Ecology 73:1943–1967.

Liberoff, A. L., J. A. Miller, C. M. Riva-Rossi, F. J. Hidalgo, M. L. Fogel, M. A. Pascual, and K. Tierney. 2014. Transgenerational effects of anadromy on juvenile growth traits in an introduced population of rainbow trout (Oncorhynchus mykiss). Canadian Journal of Fisheries and Aquatic Sciences 71:398–407.

Liberoff, A. L., A. P. Quiroga, C. M. Riva-Rossi, J. A. Miller, and M. A. Pascual. 2015. Influence of maternal habitat choice, environment and spatial distribution of juveniles on their propensity for anadromy in a partially anadromous population of rainbow trout (Oncorhynchus mykiss). Ecology of Freshwater Fish 24:424–434.

Limburg, K. E., T. A. Hayden, W. E. Pine, M. D. Yard, R. Kozdon, and J. W. Valley. 2013. Of travertine and time: Otolith chemistry and microstructure detect provenance and demography of endangered humpback chub in Grand Canyon, USA. PLoS ONE 8:e84235.

Limburg, K. E., P. Landergren, L. Westin, M. Elfman, and P. Kristiansson. 2001. Flexible modes of anadromy in Baltic sea trout: making the most of marginal spawning streams. Journal of Fish Biology 59:682–695.

Lindström, J. 1999, September 1. Early development and fitness in birds and mammals. Elsevier Current Trends.

Loeb, R. G., and W. T. Fitch. 2002. A Laboratory Evaluation of an Auditory Display Designed to Enhance Intraoperative Monitoring. Anesth. Analg. 94:362–368.

Loeffler, C. A., and S. Løvtrup. 1970. Water Balance in the Salmon Egg. Journal of Experimental Biology 52:291–298.

Macdonald, J. I., J. M. G. Shelley, and D. a. Crook. 2008. A Method for Improving the Estimation of Natal Chemical Signatures in Otoliths. Transactions of the American Fisheries Society 137:1674–1682.

Mangel, M., and W. H. Satterthwaite. 2008. Combining proximate and ultimate approaches to understand life history variation in salmonids with application to fisheries, conservation, and aquaculture. Bulletin of Marine Science 83:107–130.

McCullough, D. A. 1999. A review and synthesis of effects of alterations to the water temperature regime on freshwater life stages of salmonids, with special reference to chinook salmon. Page Water Resources. U. S. Envi.

McDermott, J. H. 2009. The cocktail party problem. Current biology : CB 19:R1024–R1027.

de Mérona, B., G. Mendes dos Santos, and R. Goncçalves de Almeida. 2001. Short term effects of Tucuruí Dam (Amazonia, Brazil) on the trophic organization of fish communities. Biology of Fishes 60:375–392.

Merz, J. E., and D. C. Vanicek. 1996. Comparative feeding habits of juvenile Chinook salmon, steelhead, and Sacremento squawfish in the lower American River, California. California Fish and Game 82.4:149–159.

Metcalfe, N. B., and P. Monaghan. 2001. Compensation for a bad start: Grow now, pay later?

Metcalfe, N. B., A. C. Taylor, and J. E. Thorpe. 1995. Metabolic rate, social status and life-history strategies in Atlantic salmon. Animal Behaviour 49:431–436.

Metcalfe, N. B., and J. E. Thorpe. 1992. Early predictors of life-history events: the link between first feeding date, dominance and seaward migration in Atlantic salmon, Salmo salar L. Journal of Fish Biology 41:93–99.

Milks, D., and A. Oakerman. 2016. Lyons Ferry Hatchery Evaluation Fall Chinook Salmon Annual Report: 2014. Olympia, WA.

Miller, J. A., V. L. Butler, C. A. Simenstad, D. H. Backus, A. J. R. Kent, and B. Gillanders. 2011. Life history variation in upper Columbia River Chinook salmon (Oncorhynchus tshawytscha): a comparison using modern and~ 500-year-old archaeological otoliths. Canadian Journal of Fisheries and Aquatic Sciences 68:603–617.

Miller, J. A., and A. J. R. Kent. 2009. The determination of maternal run time in juvenile Chinook salmon (Oncorhynchus tshawytscha) based on Sr/Ca and 87Sr/86Sr within otolith cores. Fisheries Research 95:373–378.

Minghim, R., and A. R. Forrest. 1995. An Illustrated Analysis of Sonification for Scientific Visualisation. Pages 110–117Vis '95 Proceedings of the 6th Conference on Visualization. IEEE Computer Society Washington, DC, USA.

Moore, B. C. J., editor. 1995. Hearing (Google eBook). Academic Press, San Diego, CA.

Moore, J. W., M. McClure, L. A. Rogers, and D. E. Schindler. 2010. Synchronization and portfolio performance of threatened salmon. Conservation Letters 3:340–348.

Morinville, G. R., and J. B. Rasmussen. 2003. Early juvenile bioenergetic differences between anadromous and resident brook trout (Salvelinus fontinalis). Canadian Journal of Fisheries and Aquatic Sciences 60:401–410.

Muda, L., M. Begam, and I. Elamvazuthi. 2010. Voice recognition algorithms using Mel frequency cepstral coefficient (MFCC) and dynamic time warping (DTW) techniques. JOURNAL OF COMPUTING 2:2151–9617.

Mueen, A., and E. Keogh. 2016. Extracting Optimal Performance from Dynamic Time Warping. Pages 2129–2130Proceedings of the 22nd ACM SIGKDD International Conference on Knowledge Discovery and Data Mining - KDD '16. ACM Press, New York, New York, USA.

Muhlfeld, C. C., S. R. Thorrold, T. E. McMahon, B. Marotz, and B. Gillanders. 2012. Estimating westslope cutthroat trout (Oncorhynchus clarkii lewisi) movements in a river network using strontium isoscapes. Canadian Journal of Fisheries and Aquatic Sciences 69:906–915.

Murtagh, F., and P. Contreras. 2017. Algorithms for hierarchical clustering: an overview, II. Wiley Interdisciplinary Reviews: Data Mining and Knowledge Discovery 7:e1219.

Myers, C. S., and L. R. Rabiner. 1981. A Comparative Study of Several Dynamic Time Warping Algorithms for Connected Word Recognition. Bell System Technical Journal 60:1389–1409.

Myrick, C. A., and J. J. Cech, Jr. 2000. Temperature influences on California rainbow trout physiological performance. Fish Physiology and Biochemistry 22:245–254.

Nagpal, A., A. Jatain, and D. Gaur. 2013. Review based on data clustering algorithms. Pages 298–3032013 IEEE CONFERENCE ON INFORMATION AND COMMUNICATION TECHNOLOGIES. IEEE.

Neuhoff, J. G. 2011. Perception, cognition and action in auditory displays. Pages 63–85*in* T. Hermann, A. Hunt, and J. G. Neuhoff, editors.The Sonification Handbook. Logos Verlag, Berlin.

Nislow, K. H., C. L. Folt, and D. L. Parrish. 2000. Spatially Explicit Bioenergetic Analysis of Habitat Quality for Age-0 Atlantic Salmon. Transactions of the American Fisheries Society 129:1067–1081.

Nylin, S., and K. Gotthard. 1998. Plasticity in life-history traits. Annual Review of Entomology 43:63–83.

Orcutt, G. H., H. W. Watts, and J. B. Edwards. 1968. Data aggregation and information loss. American Economic Review 58:773–787.

Ortiz, J. J. G., C. P. Phoo, and J. Wiens. 2016. Heart Sound Classification Based on Temporal Alignment Techniques. Computing in Cardiology 43:589–592.

Overpeck, J. T., G. a Meehl, S. Bony, and D. R. Easterling. 2011. Climate data challenges in the 21st century. Science (New York, N.Y.) 331:700–2.

Paparrizos, J., and L. Gravano. 2015. k-Shape: Efficient and Accurate Clustering of Time Series. Pages 1855–1870Proceedings of the 2015 ACM SIGMOD International Conference on Management of Data. Melbourne, Victoria, Australia.

Parmesan, C. 2006. Ecological and evolutionary responses to recent climate change. Annual Revue of Ecology Evolution and Systematics 37:637–669.

Pauletto, S., and A. Hunt. 2005. A comparision of audio & visual analysis of complex time-series data sets. Proceedings of the 11th International Conference on Auditory Display (ICAD2005):175–181.

Petitjean, F., A. Ketterlin, and P. Gançarski. 2011. A global averaging method for dynamic time warping, with applications to clustering. Pattern Recognition 44:678–693.

Petrere, M., R. B. Barthem, E. A. Córdoba, and B. C. Gómez. 2005. Review of the large catfish fisheries in the upper Amazon and the stock depletion of piraíba (Brachyplatystoma filamentosumLichtenstein). Reviews in Fish Biology and Fisheries 14:403–414.

Pi-Yun Chen, Neng-Sheng Pai, Guan-Yu Chen, and Hua-Jui Kuang. 2015. Design and implementation of a speech controlled omnidirectional robot using a DTW-based recognition algorithm. Page 279*in* Teen-Hang Meen, Stephen D. Prior, and Arte Donald Kin-Tak Lam, editors.Applied System Innovation: Proceedings of the 2015 International Conference on Applied Systems Innovation. First edition. CRC Press - Taylor & Francis, Osaka, Japan.

Pikitch, E. K., P. Doukakis, L. Lauck, P. Chakrabarty, and D. L. Erickson. 2005. Status, trends and management of sturgeon and paddlefish fisheries. Fish and Fisheries 6:233–265.

Pirker, L. E. M. 2001. Determinação da idade e crecimento da Piramutaba Brachyplatystoma vaillantii (Valenciennes, 1840) (Siluriformes: Pimilodidae) capturada no estuário Amazônico. Universidade Federal do Pará/Museo Paraense Emílio Goeldi.

Pirker, L. E. M. 2008. Morfometria e Descrição de Otólitos Dourada (Bracyplaystoma rousseauxii) (Castelnau, 1855) e de Piramutaba (B. vaillantii) (Valenciennes, 1840)(Siluriformes: Pimolodidae) e Verificação de Anéis de Crescemento em Otólitos de Juvenis de Dourada e de Pirimut. Museu Paraense Emílio Goeldi - Universidade Federal Do Pará.

Poiani, K. a., B. D. Richter, M. G. Anderson, and H. E. Richter. 2000. Biodiversity Conservation at Multiple Scales: Functional Sites, Landscapes, and Networks. BioScience 50:133.

Pompeu, P. S., A. A. Agostinho, and F. M. Pelicice. 2012. Existing and Future Challenges : The Concept of Successful Fish Passage in South America. River Research and Applications 512:504–512.

Potts, W. T. W., and P. P. Rudy. 1969. WATER BALANCE IN THE EGGS OF THE ATLANTIC SALMON SALMO SALAR. J. Exp. Biol 50:223–337.

Queiroz, M. M. A., A. M. C. Horbe, P. Seyler, and C. A. V. Moura. 2009. Hidroquímica do rio Solimões na região entre Manacapuru e Alvarães: Amazonas - Brasil. Acta Amazonica 39:943–952.

Rabenhorst, D. A., E. J. Farrell, D. H. Jameson, T. D. Linton, Jr., and J. A. Mandelman. 1990. Complementary visualization and sonification of multi-dimensional data. Pages 147–153Proceedings of the SPIE conference on Extracting Meaning from Complex Data: Processing, Display, Interaction.

Rakthanmanon, T., B. Campana, A. Mueen, G. Batista, B. Westover, Q. Zhu, J. Zakaria, and E. Keogh. 2012a. Searching and mining trillions of time series subsequences under dynamic time warping. Page 262Proceedings of the 18th ACM SIGKDD international conference on Knowledge discovery and data mining - KDD '12. ACM Press, New York, New York, USA.

Rakthanmanon, T., B. Campana, A. Mueen, G. Batista, B. Westover, Q. Zhu, J. Zakaria, and E. Keogh. 2012b. Data Mining a Trillion Time Series Subsequences Under Dynamic Time Warping. Pages 3047–3051*in* Fancesca Rossi, editor. Proceedings of

the Twenty-Third International Joint Conference on Artificial Intelligence. AAAI Press, Palo Alto, California, Beijing, China.

Randall, R., M. Healey, and J. Dempson. 1987. Variability in length of freshwater residence of salmon, trout, and char. Am. Fish. Soc. Symp:27–41.

Ratanamahatana, C., and E. Keogh. 2004. Everything you know about dynamic time warping is wrong. Pages 22–25Third Workshop on Mining Temporal and Sequential Data.

Regonda, S. K., B. Rajagopalan, M. Clark, J. Pitlick, S. K. Regonda, B. Rajagopalan, M. Clark, and J. Pitlick. 2005. Seasonal Cycle Shifts in Hydroclimatology over the Western United States. Journal of Climate 18:372–384.

Reznick, D. N., and C. K. Ghalambor. 2001. The population ecology of contemporary adaptations: what empirical studies reveal about the conditions that promote adaptive evolution. Genetica 112:183–198.

Rieman, B. E., D. L. Myers, and R. L. Nielsen. 1994. Use of Otolith Microchemistry to Discriminate *Oncorhynchus nerka* of Resident and Anadromous Origin. Canadian Journal of Fisheries and Aquatic Sciences 51:68–77.

Robertson, B. L., J. Middleton, and J. Hegg. 2015. Multi-Channel Spatial Sonification of Chinook Salmon Migration Patterns in the Snake River Watershed. Proceedings of the 12th International Conference on Sound and Music Computing 1:497–502.

Rombough, P. J., and E. T. Garside. 1982. Cadmium toxicity and accumulation in eggs and alevins of atlanticsalmon Salmo salar. Can. J. Zool. 60:2006–2014.

Rosenberg, D. M., P. Mccully, and C. M. Pringle. 2000. Global-Scale Environmental Effects of Hydrological Alterations: Introduction. BioScience 50:746.

Ruckelshaus, M. H., P. Levin, J. B. Johnson, and P. M. Kareiva. 2002. The Pacific salmon wars: what science brings to the challenge of recovering species. Annual review of ecology and systematics 33:665–706.

Ruttenberg, B. I. et al. 2005. Elevated evels of trace elements in cores of otoliths and their potential for use as natural tags. Marine Ecology Progress Series 297:273–281.

Sagar, J., A. Borde, L. Johnson, C. Corbett, J. Morace, K. Macneale, W. Temple, J. Mason, R. Kaufman, V. Cullinan, S. Zimmerman, R. Thom, P. Wright, P. M. Chittaro, O. Olsen, S. Sol, D. Teel, G. Ylitalo, and N. Jahns. 2013. Ecosystem Monitoring Program : Juvenile Salmon Ecology in Tidal Wetlands of the Lower Columbia River Estuary. Page Prepared by the Lower Columbia Estuary Partnership for the Bonneville Power Administration. Portland, OR.

Sakoe, H., and S. Chiba. 1978. Dynamic Programming Algorithm Optimization for Spoken Word Recognition. IEEE Transactions on Acoustics, Speech, and Signal Processing 26:43–49.

Sakurai, Y., Y. Matsubara, and C. Faloutsos. 2015. Mining and Forecasting of Big Time-series Data. Pages 929–922Proceedings of the 2015 ACM SIGMOD International Conference on Management of Data. ACM Press, New York, New York, USA.

Salvador, S., and P. Chan. 2007. FastDTW : Toward Accurate Dynamic Time Warping in Linear Time and Space. Intelligent Data Analysis 11:561–580.

Santos, R. V., F. Sondag, G. Cochonneau, C. Lagane, P. Brunet, K. Hatting, and J. G. S. Chaves. 2013. Source area and seasonal 87 Sr/ 86 Sr variations in rivers of the Amazon basin. Hydrological Processes:n/a-n/a.

Sarda-Espinosa, A. 2017a. dtwclust: Time Series Clustering Along with Optimizations for the Dynamic Time Warping Distance. CRAN (https://cran.r-project.org/).

Sarda-Espinosa, A. 2017b. Comparing Time-Series Clustering Algorithms in R Using the dtwclust Package.

Satterthwaite, W. H., M. P. Beakes, E. M. Collins, D. R. Swank, J. E. Merz, R. G. Titus, S. M. Sogard, and M. Mangel. 2009. Steelhead life history on California's central coast: insights from a state-dependent model. Transactions of the American Fisheries Society 138:532–548.

Satterthwaite, W. H., S. A. Hayes, J. E. Merz, S. M. Sogard, D. M. Frechette, and M. Mangel. 2012. State-Dependent Migration Timing and Use of Multiple Habitat Types in Anadromous Salmonids. Transactions of the American Fisheries Society 141:781–794.

Schaffler, J. J., T. J. Miller, and C. M. Jones. 2014. Spatial and Temporal Variation in Otolith Chemistry of Juvenile Atlantic Menhaden in the Chesapeake Bay. Transactions of the American Fisheries Society 143:1061–1071.

Schindler, D. E., J. B. Armstrong, and T. E. Reed. 2015. The portfolio concept in ecology and evolution. Frontiers in Ecology and the Environment 13:257–263.

Schindler, D. E., R. Hilborn, B. Chasco, C. P. Boatright, T. P. Quinn, L. A. Rogers, and M. S. Webster. 2010. Population diversity and the portfolio effect in an exploited species. Nature 465:609–612.

Schlicht, E. 1985. Isolation and Aggregation in Economics. Springer-Verlag Berlin Heidelberg, Berlin, Heidelberg.

Schuett, J. H., and B. N. Walker. 2013. Measuring comprehension in sonification tasks that have multiple data streams. Page ACM International Conference Proceeding Series. Piteå, Sweden.

Scrucca, L., M. Fop, T. B. Murphy, and A. E. Raftery. 2016. mclust 5: Clustering, Classification and Density Estimation Using Gaussian Finite Mixture Models. The R Journal 8:289–317.

Secor, D. H. 2010. Is otolith science transformative? New views on fish migration. Environmental Biology of Fishes 89:209–220.

Secor, D. H., J. M. Dean, and E. H. Laban. 1991a. Manual for otolith removal and preparation for microstructural examination 1:85.

Secor, D. H., J. M. Dean, and E. H. Laban. 1991b. Manual for otolith removal and preparation for microstructural examination. Electric Power Research Institute; Belle W. Baruch Institute for Marine Biology and Coastal Research.

Secor, D. H., and L. A. Kerr. 2009. Lexicon of life cycle diversity in diadromous and other fishes. Challenges for diadromous fishes in a dynamic global environment, American Fisheries Society Symposium 69 69:537–556.

Shippentower, G. E., C. B. Schreck, and S. A. Heppell. 2011. Who's Your Momma? Recognizing Maternal Origin of Juvenile Steelhead Using Injections of Strontium

Chloride to Create Transgenerational Marks. Transactions of the American Fisheries Society 140:1330–1339.

Shrimpton, J. M., K. D. Warren, N. L. Todd, C. J. McRae, G. J. Glova, K. H. Telmer, and a D. Clarke. 2014. Freshwater movement patterns by juvenile Pacific salmon Oncorhynchus spp. before they migrate to the ocean: Oh the places you'll go! Journal of fish biology 85:987–1004.

Sioli, H. 1956. As aguas da regiao do alto Rio Negro [Biologia aquatica; Fisica da agua; Quimica da agua; Hidrogeologia; Hidrografia; Amazonia; Brasil]. Boletim Técnico Instituto Agronômico do Norte 32:117–155.

Stathopoulos, V., V. Zamora-Gutiérrez, K. E. Jones, and M. Girolami. 2014. Bat Call Identication with Gaussian Process Multinomial Probit Regression and a Dynamic Time Warping Kernel. 17th International Conference on Artificial Intelligence and Statistics (AISTATS, JMLR: W&CP 33:913–921.

Stearns, S. C. 1989. Trade-offs in life-history evolution. Functional Ecology 3:259–268.

Steel, E. A., A. Tillotson, D. A. Larsen, A. H. Fullerton, K. P. Denton, and B. R. Beckman. 2012. Beyond the mean: The role of variability in predicting ecological effects of stream temperature on salmon. Ecosphere 3:art104.

Stevens, D. E., and L. W. Miller. 1983. Effects of River Flow on Abundance of Young Chinook Salmon, American Shad, Longfin Smelt, and Delta Smelt in the Sacramento-San Joaquin River System. North American Journal of Fisheries Management 3:425–437.

Stewart, D. C., S. J. Middlemas, and a. F. Youngson. 2006. Population structuring in Atlantic salmon (Salmo salar): evidence of genetic influence on the timing of smolt migration in sub-catchment stocks. Ecology of Freshwater Fish 15:552–558.

Stone, R. 2007. The last of the leviathans. Science 316:1684.

Syphard, A. D., and J. Franklin. 2004. Spatial aggregation effects on the simulation of landscape pattern and ecological processes in southern California plant communities. Ecological Modelling 180:21–40.

Tan, L. N., A. Alwan, G. Kossan, M. L. Cody, and C. E. Taylor. 2015. Dynamic time warping and sparse representation classification for birdsong phrase classification using limited training dataa). The Journal of the Acoustical Society of America 137:1069–1080.

Tang, K. S., K. F. Man, S. Kwong, and Q. He. 1996. Genetic algorithms and their applications. IEEE Signal Processing Magazine 13:22–37.

Tavener, B. 2012, September 25. New Dams Planned for Heart of Amazon. The Rio Times. Hawthorne, New York.

Taylor, E. B. B. 1990. Environmental correlates of life-history variation in juvenile chinook salmon, Oncorhynchus tshawytscha (Walbaum). Journal of Fish Biology 37:1–17.

Theil, H. 1954. Linear aggregation of economic relations, Vol 3. Pages 233–235Review of Economics and Statistics. MIT Press, Cambridge, MA.

Thériault, V., D. Garant, L. Bernatchez, and J. J. Dodson. 2007. Heritability of life-history tactics and genetic correlation with body size in a natural population of brook charr (Salvelinus fontinalis). Journal of Evolutionary Biology 20:2266–2277.

Thorpe, J. E., and N. B. Metcalfe. 1998. Is smolting a positive or a negative developmental decision? Aquaculture 168:95–103.

Thorrold, S. R., C. M. Jones, S. E. Campana, J. W. McLaren, and J. W. H. Lam. 1998. Trace element signatures in otoliths record natal river of juvenile American shad (Alosa sapidissima). Limnology and Oceanography:1826–1835.

Thorrold, S. R., G. P. Jones, S. Planes, and J. A. Hare. 2006. Transgenerational marking of embryonic otoliths in marine fishes using barium stable isotopes. Canadian Journal of Fisheries and Aquatic Sciences 63:1193–1197.

Tiao, G. C., and W. S. Wei. 1976. Effect of Temporal Aggregation on the Dynamic Relationship of Two Time Series Variables. Source: Biometrika Biometrikka 63:513–523.

Tiffan, K. F., and W. P. Connor. 2012. Seasonal Use of Shallow Water Habitat in the Lower Snake River Reservoirs by Juvenile Fall Chinook Salmon. Walla Walla District, Walla Walla, WA.

Tiffan, K. F., J. M. Erhardt, and S. J. St. John. 2014. Prey Availability, Consumption, and Quality Contribute to Variation in Growth of Subyearling Chinook Salmon Rearing in Riverine and Reservoir Habitats. Transactions of the American Fisheries Society 143:219–229.

Tiffan, K. F., T. J. Kock, W. P. Connor, R. K. Steinhorst, and D. W. Rondorf. 2009. Behavioural thermoregulation by subyearling fall (autumn) Chinook salmon Oncorhynchus tshawytscha in a reservoir. Journal of fish biology 74:1562–79.

Tockner, K., M. Pusch, J. Gessner, and C. Wolter. 2011. Domesticated ecosystems and novel communities: challenges for the management of large rivers. Ecohydrology & Hydrobiology 11:167–174.

Tormene, P., T. Giorgino, S. Quaglini, and M. Stefanelli. 2009. Matching incomplete time series with dynamic time warping: an algorithm and an application to post-stroke rehabilitation. Artificial Intelligence in Medicine 45:11–34.

Tsukamoto, K., and T. Arai. 2001. Facultative catadromy of the eel Anguilla japonica between freshwater and seawater habitats. Marine Ecology Progress Series 220:265–276.

Tufte, E. 2001. The Visual Display of Quantitative Information. Second edition. Graphics Press, Cheshire, CT.

Turner, S. M., K. E. Limburg, and E. P. Palkovacs. 2015. Can different combinations of natural tags identify river herring natal origin at different levels of stock structure ? Canadian Journal of Fisheries and Aquatic Sciences 72:845–854.

USGS. 1996. GTOPO30 30-Arc-Second Elevation Data Set of South America. United States Geological Survey, Sioux Falls, South Dakota.

USGS. 1999. Geologic Map of the Amazon Region. United States Geological Survey, Denver, Colorado.

Veinott, G., P. A. H. Westley, C. F. Purchase, and L. Warner. 2014. Experimental evidence simultaneously confirms and contests assumptions implicit to otolith microchemistry research. Canadian Journal of Fisheries and Aquatic Sciences 71:356.

Volk, E. C., A. Blakley, S. L. Schroder, and S. M. Kuehner. 2000. Otolith chemistry reflects migratory characteristics of Pacific salmonids: using otolith core chemistry to distinguish maternal associations with sea and freshwaters. Fisheries Research 46:251–266.

Waite, E. M., G. P. Closs, J. Kim, B. Barry, A. Markwitz, and R. Fitzpatrick. 2008. The strontium content of roe collected from spawning brown trout Salmo trutta L. reflects recent otolith microchemistry. Journal of Fish Biology 72:1847–1854.

Walker, B. N., and M. A. Nees. 2011. Theory of Sonification. Pages 9–39*in* T. Hermann, A. Hunt, and J. G. Neuhoff, editors.The Sonification Handbook. Logos-Verlag.

Walther, B. D., T. Dempster, M. Letnic, and M. T. McCulloch. 2011. Movements of diadromous fish in large unregulated tropical rivers inferred from geochemical tracers. PloS one 6.

Walther, B. D., and K. E. Limburg. 2012. The use of otolith chemistry to characterize diadromous migrations. Journal of Fish Biology 81:796–825.

Walther, B. D., and S. R. Thorrold. 2006. Water, not food, contributes the majority of strontium and barium deposited in the otoliths of a marine fish. Marine Ecology Progress Series 311:125–130.

Walther, B. D., and S. R. Thorrold. 2010. Limited diversity in natal origins of immature anadromous fish during ocean residency. Canadian Journal of Fisheries and Aquatic Sciences 67:1699–1707.

Walther, B. D., S. R. Thorrold, and J. E. Olney. 2008. Geochemical Signatures in Otoliths Record Natal Origins of American Shad. Transactions of the American Fisheries Society 137:57–69.

Walther, G.-R., E. Post, P. Convey, A. Menzel, C. Parmesan, T. J. C. Beebee, J.-M. Fromentin, O. Hoegh-Guldberg, and F. Bairlein. 2002. Ecological responses to recent climate change. Nature 416:389–395.

Wang, G. J., C. Xie, F. Han, and B. Sun. 2012. Similarity measure and topology evolution of foreign exchange markets using dynamic time warping method: Evidence from minimal spanning tree. Physica A: Statistical Mechanics and its Applications 391:4136–4146.

Waples, R. S., A. Elz, B. D. Arnsberg, J. R. Faulkner, J. J. Hard, E. Timmins-Schiffman, and L. K. Park. 2017. Human-mediated evolution in a threatened species? Juvenile life-history changes in Snake River salmon. Evolutionary Applications.

Waples, R. S., R. P. Jones Jr, B. R. Beckman, and G. A. Swan. 1991. Status review for Snake River fall chinook salmon. NOAA Technical Memorandum NMFS N/NWC-201, Seattle, Washington.

Ware, C. 2004. Information visualization: perception for design. First edition. Elsevier, San Francisco.

Warren-Myers, F., T. Dempster, P. G. Fjelldal, T. Hansen, and S. E. Swearer. 2015. Immersion during egg swelling results in rapid uptake of stable isotope markers in salmonid otoliths. Canadian Journal of Fisheries and Aquatic Sciences 72:722–727.

Webster, M. S., P. P. Marra, S. M. Haig, S. Bensch, and R. T. Holmes. 2002. Links between worlds: unraveling migratory connectivity. Trends in Ecology & Evolution 17:76–83.

Wei, W. W. S. 1979. Some Consequences of Temporal Aggregation in Seasonal Time Series Models. Pages 433–448*in* Arnold Zellner, editor.Seasonal Analysis of Economic Time Series. NBER.

Weideman, H. J., Z. M. Jablons, J. Holmberg, K. Flynn, J. Calambokidis, R. B. Tyson, J. B. Allen, R. S. Wells, K. Hupman, K. Urian, and C. V. Stewart. 2017. Integral Curvature Representation and Matching Algorithms for Identification of Dolphins and Whales. arXive.

Wenger, S. J., D. J. Isaak, C. H. Luce, H. M. Neville, K. D. Fausch, J. B. Dunham, D. C. Dauwalter, M. K. Young, M. M. Elsner, B. E. Rieman, A. F. Hamlet, and J. E. Williams. 2011. Flow regime, temperature, and biotic interactions drive differential declines of trout species under climate change. Proceedings of the National Academy of Sciences of the United States of America 108:14175–80.

Wenger, S. J., C. H. Luce, A. F. Hamlet, D. J. Isaak, and H. M. Neville. 2010. Macroscale hydrologic modeling of ecologically relevant flow metrics. Water Resources Research 46.

Wilcove, D. S., and M. Wikelski. 2008. Going, going, gone: is animal migration disappearing. PLoS biology 6:e188.

Wilder, S. M., D. Raubenheimer, and S. J. Simpson. 2016. Moving beyond body condition indices as an estimate of fitness in ecological and evolutionary studies. Functional Ecology 30:108–115.

Williams, J. G., R. W. Zabel, R. S. Waples, J. A. Hutchings, and W. P. Connor. 2008. Potential for anthropogenic disturbances to influence evolutionary change in the life history of a threatened salmonid. Evolutionary Applications 1:271–285.

Winemiller, K. O. 2005. Life history strategies , population regulation , and implications for fisheries management. Canadian Journal of Fisheries and Aquatic Sciences 885:872–885.

Wolkovich, E. M., B. I. Cook, K. K. McLauchlan, and T. J. Davies. 2014. Temporal ecology in the Anthropocene. Ecology Letters 17:1365–1379.

Wong, P. C., H.-W. Shen, C. R. Johnson, C. Chen, and R. B. Ross. 2012. Visualization Viewpoints The Top 10 Challenges in Extreme-Scale Visual Analytics. Computer Graphics and Appplications 32:63–67.

Woodcock, S. H., C. A. Grieshaber, and B. D. Walther. 2013. Dietary transfer of enriched stable isotopes to mark otoliths, fin rays, and scales. Canadian Journal of Fisheries and Aquatic Sciences 70:1–4.

Xu, D., X. Wu, Y.-L. Chen, and Y. Xu. 2014. Online Dynamic Gesture Recognition for Human Robot Interaction. Journal of Intelligent and Robotic Systems: Theory and Applications 77:583–596.

Yamada, S. B., and T. J. Mulligan. 1987. Marking Nonfeeding Salmonid Fry with Dissolved Strontium. Canadian Journal of Fisheries and Aquatic Sciences 44:1502–1506.

Zabel, R., K. Haught, and P. Chittaro. 2010. Variability in fish size/otolith radius relationships among populations of Chinook salmon. Environmental biology of fishes 89:267–278.

Zabel, R. W., and J. G. Williams. 2008. Selective mortality in chinook salmon: What is the role of human disturbance?

Zimmerman, C. E. 2005. Relationship of otolith strontium-to-calcium ratios and salinity: experimental validation for juvenile salmonids. Canadian Journal of Fisheries and Aquatic Sciences 62:88–97.

Appendix A: Human and Animal Protocol Approvals

The use of animals in this study was submitted to the University of Idaho Animal Care and Use Committee in protocol 2012-122. The proposal was reviewed and it was found that "no activities that require animal care and use were identified," per email communication from Campus Veterinarian Brad Williams, DVM on Friday, July 13th, 2012.

Authorization was granted for the perceptual survey in chapter 5 from the Eastern Washington University Institutional Review Board for Human Subjects Research on November 10th, 2016. The submitted protocol "Human subjects protocol HS-5155 *Perceptual Survey: Sonifications for Pacific Northwest Salmon Migration Data*" was reviewed and determined to be exempt from further review according to federal regulations for the Protection of Human Subjects under CFR Title 45, Part 46.101(b)(1-6).

Further authorization was granted by the University of Idaho Institutional Review Board on April 26th, 2017. The submitted project number 17-080, "*Perceptual Survey: Sonifications for Pacific Northwest Salmon Migration Data*" was reviewed and certified as exempt under category 2, 4 at 45 CFR 46.101(b)(2-4).